Quantifying sediment source contributions in contrasted agricultural catchments (Uruguay River, Southern Brazil)

Rafael Ramon

Thèse de doctorat

NNT : 2021UPASJ009

Quantifying sediment source contributions in contrasted agricultural catchments (Uruguay River, Southern Brazil)

Quantification des sources de sédiments dans des bassins cultivés contrastés (Fleuve Uruguay, sud du Brésil)

Thèse de doctorat de l'université Paris-Saclay et de l'Universidade Federal do Rio Grande do Sul

École doctorale n° 579 : Sciences mécaniques et énergétiques, matériaux et géosciences (SMEMAG)
Spécialité de doctorat : Terre solide : géodynamique des enveloppes supérieures, paléobiosphères
Unité de recherche : Université Paris-Saclay, CNRS, CEA, UVSQ, Laboratoire des sciences du climat et de l'environnement, 91191, Gif-sur-Yvette, France.
Référent : Université de Versailles-Saint-Quentin-en-Yvelines

Thèse présentée et soutenue à Paris-Saclay, le 05/07/2021, par

Rafael RAMON

Composition du Jury

Christine HATTÉ Directrice de recherche CEA, Université Paris Saclay – LSCE	Présidente
Christine ALEWELL Professeur, Université de Basel	Rapporteur & Examinatrice
Ricardo Hugo VELASCO Professeur, Université National de San Luis	Rapporteur & Examinateur
Jean Paolo Gomes MINELLA Professeur, Université Federal de Santa Maria	Examinateur
Carlos Gustavo TORNQUIST Professeur, Université Federal du Rio Grande do Sul	Examinateur

Direction de la thèse

Olivier EVRARD Chargé de recherche CEA, Université Paris-Saclay – LSCE	Directeur de thèse
Tales TIECHER Professeur, Université Federal du Rio Grande do Sul	Directeur de thèse

FEDERAL UNIVERSITY OF RIO GRANDE DO SUL
GRADUATE PROGRAM IN SOIL SCIENCE
PARIS-SACLAY UNIVERSITY
DOCTORAL SCHOOL IN MECHANICS, ENERGY, MATTER AND GEOLOGICAL SCIENCES

Quantifying sediment source contributions in contrasted agricultural catchments (Uruguay River, Southern Brazil)

Thesis presented to the Soil Science Postgraduate Program of Federal University of Rio Grande do Sul and to the Doctoral School of Science in Mechanics, Energy, Matter and Geosciences of Paris-Saclay University as a prerequisite to obtain the title of *Doctor in Soil Science* and *Docteur en terre solide: géodynamique des enveloppes supérieures, paléobiosphère*, respectively.

Rafael Ramon

Porto Alegre, RS, Brazil
July 2021

“Have no fear of perfection, you will never reach it.”

(Salvador Dalí)

“You cannot hope to build a better world without improving the individuals. To that end, each of us must work for his own improvement and, at the same time, share a general responsibility for all humanity, our particular duty being to aid those to whom we think we can be most useful.”

(Marie Curie)

Dedico à minha família.

ACKNOWLEDGMENTS

AGRADECIMENTOS

REMERCIEMENTS

First of all, I would like to thank everyone who helped me in any way with the development of this thesis.

Agradeço aos meus orientadores Tales Tiecher e Olivier Evrard, pela orientação, confiança, companheirismo, amizade, incentivo e por ter oportunizado para mim essa experiência única de formação doutoral com dupla diplomação.

Agradeço a Universidade Federal do Rio Grande do Sul pela formação cientifica e pessoal, de forma gratuita e com altíssima qualidade.

Agradeço ao Programa de Pós-Graduação em Ciência do Solo e todo seu corpo docente e técnico pelos ensinamentos, apoio e formação durante o curso de doutorado.

Je remercie l'Université de Paris-Saclay et l'Ecole Doctorale « Sciences mécaniques et énergétiques, matériaux et Géosciences » pour la formation scientifique.

Je remercie le Laboratoire des Sciences du Climat et de l'Environnement pour son soutien et son hospitalité durant mon séjour en France.

Agradeço às agências brasileiras financiadoras desta tese: ao Conselho Nacional de Pesquisa – CNPq pela bolsa de doutorado no Brasil; a Coordenação de Aperfeiçoamento de Pessoal de Nível Superior – CAPES pela bolsa no período no exterior concedida via projeto CAPESCOFECUB No. 88887.196234/2018-00; a Financiadora de Estudos e Projetos – FINEP e Fundação de Amparo à Pesquisa do Estado do Rio Grande do Sul – FAPERGS pelo projeto "Mais Água" e PRONEX n° 008/2009; a Fundação Agrisus – Agricultura Sustentável pelo financiamento do projeto 2920/20; ao projeto NEXUS Pampa, na pessoa do coordenador Vicente Celestino Silveira pelo financiamento das atividades desenvolvidas na Bacia Hidrográfica do Rio Ibirapuitã.

Je remercie les organismes de recherche français, le Centre national de la recherche scientifique – CNRS et le Commissariat à l'énergie atomique et aux énergies alternatives – CEA.

Agradeço ao grupo IRGEB pelo apoio técnico e pessoal nas atividades de laboratório e no dia-a-dia do laboratório. Agradeço especialmente ao Carlos Eduardo

Linhares, Lucas Aquino e Jacques K. Carvalho pelo auxilio nas atividades de campo. Também agradeço a Gabriela Naibo pela parceria nas modelagens de espectroscopia.

Je remercie tous les collègues de l'équipe GEDI pour leur soutien au laboratoire, en particulier Irène Lefèvre et Olivier, ainsi que tous les autres pour les bons déjeuners à la cantine, avec toujours un bon café à la fin. Je remercie particulièrement Pierre-Alexis Chaboche, mon collègue de bureau, chimarrão et café, ainsi que Virginie Sellier qui nous rendait visite quotidiennement dans notre bureau pour de bonnes conversations.

Agradeço aos colegas e amigos da Universidade Federal de Santa Maria, em especial ao professor Jean Minella por dar todo suporte para os trabalhos de campo. Agradeço aos colegas do grupo GIPHES, em especial ao Felipe Bernardi (grande parceiro de coletas no Alegrete), Dinis Deuschle, Alexandre Schlesner, Fabio Schneider, Alice Dambros que também auxiliaram nas atividades de campo.

Agradeço à CPRM e toda sua equipe nas campanhas de monitoramento no Rio Ibirapuitã.

I thank Patrick Laceby for your support with modelling and data analysis, as well as for your patience and great contributions reviewing the articles. Certainly your support was fundamental to the progress of this work.

Agradeço ao Jean Moura Bueno pelo seu suporte com a modelagem dos dados de espectroscopia.

Agradeço imensamente ao suporte oferecido pelos alunos, professores e técnicos do Instituto Federal Farroupilha – campus Alegrete, em especial ao bolsista do projeto Antônio Augusto Marquez, Vinício Bordignon e Prof. Tadeu Tiecher.

Agradeço ao professor Danilo Rheinheimer por ceder um espaço para dormir nas idas para o laboratório em Poitiers, assim como pelo suporte no laboratório no Brasil.

Je suis immensément reconnaissant au Professeur Laurent Caner pour m'avoir donné accès à l'équipement pour les analyses de spectroscopie diffuse à l'Université de Poitiers, ainsi qu'à tous les techniciens qui m'ont aidé dans les activités de laboratoire.

Je remercie le Professeur Sylvain Huon pour son soutien pour l'analyse de la composition de la matière organique et pour l'hospitalité à Sorbonne Université.

Agradeço aos colegas da Maison du Brésil, pelo companheirismo em refeições, festas, viagens, conversas e todas experiências maravilhosas que vivemos juntos.

Agradeço com todo meu coração a minha família pelo apoio e incentivo aos estudos desde o início, por ter dado suporte às minhas decisões, por ter compreendido minhas ausências e por todo amor incondicional.

Agradeço a minha noiva, Cláudia Barros, pela sua parceria como pesquisadora e muitas vezes colega nos trabalhos científicos, mas também pelo amor, carinho e atenção de sempre no convívio diário.

Agradeço especialmente a Moa, que se juntou a nós no último e mais difícil período de elaboração desta tese, acredito muito que você surgiu para nos dar força, compartilhar amor e carinho neste período complicado de pandemia, homme office e finalização da tese. Com isso deixo a dica: ADOTE um amiguinho/amiguinha, sua saúde irá agradecer.

Merci encore une fois à tous ceux qui ont contribué à l'élaboration de cette thèse et qui ont fait partie d'une étape aussi importante de ma vie, vous aurez ma gratitude éternelle.

Mais uma vez, a todos e todas que contribuíram para o desenvolvimento desta tese e que fizeram parte desta fase tão importante da minha vida, o meu eterno agradecimento.

Muito obrigado!

Merci beaucoup!

Thank you very much!

Thesis title:

Quantifying sediment source contributions in contrasted agricultural catchments (Uruguay River, Southern Brazil)

Candidate:

Eng. Agr. Msc. Rafael Ramon

Advisors:

Tales Tiecher (UFRGS, Brazil)

Olivier Evrard (Univ. Paris-Saclay, France)

Abstract

Intensification of water erosion by agricultural activities is one of the main causes of soil degradation in subtropical regions. In addition to the on-site negative impacts observed in cropland, the excess of surface runoff increases the transfer of sediments and contaminants to water bodies, resulting in environmental, economic and social deleterious effects. The objective of this thesis is to develop and apply original sediment source fingerprinting techniques in two tributaries of the Uruguay River Basin with contrasting conditions in terms of geology, land use, management, and soil types, representative of those found in the drainage area (266,132 km^2). The Conceição River catchment (804 km^2) is located in upper parts of the Uruguay River Basin. This catchment is representative of the basaltic plateau, where deep Ferralsols rich in clay and iron oxides predominate, and are cultivated for soybean, corn and cereals production or covered with pastures for dairy farming. In contrast, the Ibirapuitã River catchment (5,943 km^2) is representative of the sandstone plateau. With a predominance of shallow Regosols and sandy Acrisols more sensitive to degradation, it is mainly occupied by native grasslands of the Brazilian Pampa Biome with extensive cattle ranching, although irrigated rice fields are also found in lowlands. Moreover, a rapid increase in the surface area cultivated with soybean in this catchment has been observed in the last twenty years. Soil samples were collected to characterize land use-based sediment sources and suspended sediment was sampled at the outlet of these catchments using different strategies. All samples were analyzed for a panel of properties. Their geochemical composition, diffuse reflectance spectroscopy properties, radionuclide activities and magnetic susceptibility were determined to provide a set of potential tracing parameters. Magnetic and diffuse reflectance spectroscopy analyses were also carried out on

sediment samples collected on the main stream of the Uruguay River, downstream of its confluence with both representative tributaries. Results of sediment source contribution are consistent with field observations. However, as catchment area and source number increase, more uncertainty is observed. Surface sources (pasture and cropland) were indicated as the main source of suspended sediment in the Conceição catchment, contributing with approximately 50%. Stream banks provided the second main source of fine bed sediment, contributing with approximately 35%. Cropland was also found to provide the main source in the Ibirapuitã catchment, contributing 32% of the sediment despite occupying only 9.5% of the total catchment area, followed by subsurface sources (stream bank and gully) with 29%. Unpaved roads and native grassland provided lower contributions (24 and 15%, respectively) in Ibirapuitã catchment. These results indicate that the soil conservation practices used in these catchments are not enough to prevent soil erosion in cropland. Moreover, agricultural activities may enhance erosion and sediment delivery to the river systems, causing soil impoverishment and contamination of water resources. Finally, through the comparison of sediment properties of both tributary catchments, this thesis provided – to our knowledge – the first insights into the contribution of both contrasting geomorphologic regions to the main Uruguay River. The sediment samples collected in the bottom deposits of the Uruguay River, had similar characteristics as the suspended sediment of the Ibirapuitã River, indicating the Pampa region as the main likely source. Despite the associated uncertainties, these results further increase the current concerns regarding the ongoing land use changes observed in the Pampa biome. Appropriate soil conservation practices should therefore be urgently applied in agricultural areas of this region to reduce soil erosion and sediment delivery to the river systems.

Título da tese:

Quantificação das fontes de sedimentos em duas bacias hidrográficas contrastantes (Rio Uruguai, Sul do Brasil)

Candidato:

Eng. Agr. Msc. Rafael Ramon

Orientadores:

Tales Tiecher (UFRGS, Brasil)

Olivier Evrard (Univ. Paris-Saclay, França)

Resumo

A intensificação da erosão hídrica pelas atividades agrícolas é uma das principais causas da degradação do solo em regiões subtropicais. Além dos impactos negativos observados na lavoura, o excesso de escoamento superficial aumenta a transferência de sedimentos e contaminantes para os corpos d'água, resultando em efeitos deletérios ambientais, econômicos e sociais. O objetivo desta tese é desenvolver e aplicar técnicas originais de traçagem das fontes de sedimentos em dois tributários da bacia do rio Uruguai com condições contrastantes em termos de geologia, uso do solo, manejo e tipos de solo, representativas das encontradas na área de drenagem (266.132 km^2). A bacia hidrográfica do Rio Conceição (804 km^2) está localizada na porção superior da Bacia do Rio Uruguai. Esta bacia é representativa do planalto basáltico, onde predominam os Ferralsols profundos ricos em argila e óxidos de ferro, e são cultivados para a produção de soja, milho e cereais ou cobertos com pastagens para a produção leiteira. Em contraste, a bacia hidrográfica do Rio Ibirapuitã (5.943 km^2) é representativa da planície de arenito. Com predominância de Regosols rasos e Acrisols arenosos mais sensíveis à degradação, é ocupada principalmente por pastagens nativas do Bioma Pampa brasileiro com pecuária extensiva, embora os campos de arroz irrigados também sejam encontrados em terras baixas. Além disso, nos últimos vinte anos, observou-se um rápido aumento da superfície cultivada com soja nesta bacia hidrográfica. Amostras de solo foram coletadas para caracterizar as fontes de sedimentos baseados no uso do solo e sedimentos em suspensão foram amostrados na saída destas bacias utilizando diferentes estratégias. Todas as amostras foram analisadas para um painel de propriedades. Sua composição geoquímica, propriedades de espectroscopia de reflexão difusa, atividades de radionuclídeos e suscetibilidade magnética foram determinadas para fornecer um conjunto de parâmetros traçadores potenciais. Também foram realizadas análises por

espectroscopia de reflexão difusa e suscetibilidade magnéticas em amostras de sedimentos coletadas no Rio Uruguai, a jusante da confluência com ambos os tributários representativos. Os resultados da contribuição das fontes de sedimentos são consistentes com as observações de campo. Entretanto, à medida que a área de captação e o número de fontes aumentam, mais incerteza é observada. As fontes superficiais (pastagens e lavouras) foram indicadas como a principal fonte de sedimentos em suspensão na bacia hidrográfica do Rio Conceição, contribuindo com aproximadamente 50%. Os bancos do canal de drenagem foram a segunda fonte principal de sedimentos em suspensão, contribuindo com aproximadamente 35%. As lavouras também foram indicadas como a principal fonte na bacia do Ibirapuitã, contribuindo com 32% do sedimento, apesar de ocupar apenas 9,5% da área total da bacia, seguida pelas fontes subsuperficiais (bancos do canal de drenagem e voçorocas) com 29%. Estradas não pavimentadas e campos nativos proporcionaram contribuições menores (24 e 15%, respectivamente) na bacia hidrográfica do Ibirapuitã. Estes resultados indicam que as práticas de conservação do solo utilizadas nestas bacias não são suficientes para evitar a erosão do solo nas lavouras. Além disso, as atividades agrícolas podem aumentar a erosão e a entrega de sedimentos aos sistemas fluviais, causando empobrecimento do solo e contaminação dos recursos hídricos. Finalmente, através da comparação das propriedades dos sedimentos de ambas as bacias tributárias, esta tese forneceu - ao nosso conhecimento - os primeiros conhecimentos sobre a contribuição de ambas as regiões geomorfológicas contrastantes para o Rio Uruguai. As amostras de sedimento coletadas no fundo do rio Uruguai, apresentaram características semelhantes às do sedimento em suspensão do rio Ibirapuitã, indicando a região do Pampa como a provável fonte principal. Apesar das incertezas associadas, estes resultados aumentam ainda mais as atuais preocupações com as mudanças no uso do solo observadas no bioma Pampa. Portanto, práticas apropriadas de conservação do solo devem ser urgentemente aplicadas em áreas agrícolas desta região para reduzir a erosão do solo e a entrega de sedimentos aos sistemas fluviais.

Titre de la These:

Quantification des sources de sédiments dans des bassins cultivés contrastés (Fleuve Uruguay, sud du Brésil)

Candidate:

Eng. Agr. Msc. Rafael Ramon

Advisors:

Tales Tiecher (UFRGS, Brazil)

Olivier Evrard (Univ. Paris-Saclay, France)

Résumé

L'intensification de l'érosion hydrique par les activités agricoles constitue l'une des principales causes de dégradation des sols dans les régions subtropicales. En plus des impacts négatifs observés à l'amont, l'excès de ruissellement accroît le transfert de sédiments et de contaminants vers les masses d'eau. L'objectif de cette étude est de développer des techniques originales de traçage des sources de sédiments dans deux affluents-type du fleuve Uruguay présentant des conditions contrastées en termes de géologie, d'utilisation des terres, de gestion et de types de sols, représentatifs de ceux que l'on trouve dans la zone de drainage (266 132 km^2). Le bassin de la rivière Conceição (804 km^2) est représentatif du plateau basaltique où prédominent les Ferralsols profonds riches en argile et en oxydes de fer, où sont cultivés le soja, le maïs, les céréales et où on trouve des pâturages pour l'élevage laitier. Au contraire, le bassin de la rivière Ibirapuitã (5 943 km^2) est représentatif du plateau gréseux où prédominent les Regosols et Acrisols plus sensibles à la dégradation, les prairies indigènes utilisées pour l'élevage bovin extensif prédominent, bien que l'on trouve également des rizières irriguées dans les plaines alluviales. Des échantillons de sol ont été prélevés pour caractériser les sources de sédiments liées à l'utilisation des terres. Des échantillons de sédiments en suspension ont été collectés à l'exutoire de ces bassins versants en utilisant différentes stratégies. Tous ces échantillons ont été analysés avec plusieurs techniques. Leur composition géochimique, leurs propriétés de spectroscopie de réflectance diffuse, leurs activités en radionucléides et la susceptibilité magnétique ont été déterminées afin de fournir un ensemble de paramètres de traçage potentiels. Des analyses magnétiques et de spectroscopie ont également été réalisées sur des échantillons de sédiments collectés sur le cours principal du fleuve Uruguay, en aval de la confluence avec les deux affluents représentatifs. Les résultats de la contribution des sources de sédiments sont cohérents

avec les observations sur le terrain. Cependant, plus la superficie du bassin versant et le nombre de sources augmentent, plus les incertitudes sont importantes. Les sources superficielles (pâturages et terres cultivées) ont été indiquées comme la principale source de sédiments dans le bassin de Conceição, avec environ 50% d'apports. Les berges ont fourni, quant à elles, la seconde source de sédiments, avec une contribution d'environ 35%. Les terres cultivées se sont également avérées être la principale source de sédiments dans le bassin d'Ibirapuitã, fournissant 32% des sédiments bien qu'elles n'occupent que 9,5% de la surface totale du bassin, suivies par les sources de subsurface (berges et ravines) avec 29%. Les routes et les prairies indigènes ont fourni, au contraire, des contributions bien plus faibles (24 et 15%, respectivement). Ces résultats indiquent que les activités agricoles peuvent augmenter l'érosion et l'apport de sédiments dans les systèmes fluviaux, provoquant l'appauvrissement des sols et la contamination des ressources en eau. Enfin, en comparant les propriétés des sédiments des deux affluents-type, cette thèse a fourni - à notre connaissance – la première estimation de la contribution de ces deux régions géomorphologiques contrastées aux sédiments du fleuve Uruguay. Les échantillons de sédiments collectés dans le lit du fleuve Uruguay présentaient des caractéristiques similaires à celles des sédiments en suspension du fleuve Ibirapuitã, ce que indique que la Pampa en constitue la source principale. Malgré les incertitudes associées, ces résultats renforcent les préoccupations actuelles en lien avec les changements d'utilisation des terres observés dans la Pampa. Il est donc urgent de mettre en œuvre des stratégies de conservation des sols dans les zones agricoles de cette région afin de réduire l'érosion des sols et l'apport de sédiments aux systèmes fluviaux.

LIST OF FIGURES

LIST OF TABLES

LIST OF CONTENTS

1 INTRODUCTION

Water erosion intensified by agricultural activities is one of the main factors of soil degradation in subtropical regions (Golosov and Walling, 2019). The increase of soil erosion by human activities can generate several negative impacts on the environment. On-site, erosion reduces the productive potential of soils as a consequence of nutrient, water and soil losses, which are accelerated in the absence of conservation practices (Bertol et al., 2017; Londero et al., 2018; Ramos et al., 2019). Off-site, the excess of runoff and erosion increases the transfer of sediment and contaminants to water bodies, causing the siltation and the eutrophication of rivers and reservoirs (Bennett et al., 2001). At the same time, rivers supply the main source of water for large urban centres along with a potential source of energy for electric power generation. Thus, any action carried out in a river catchment will have direct and/or indirect consequences for the society as a whole (Boardman et al., 2019; Telles et al., 2011).

Studies conducted at the river catchment scale provide information that relate all these impacts, since the river integrates all the processes that occur in its drainage area, receiving and transporting the sediments and contaminants generated further upstream (Lloyd et al., 2019; Minella et al., 2014a). During the last decade, several studies have been carried out in river catchments of southern Brazil to assess the impact of agriculture on water resources. In the framework of long-term monitoring programmes carried out in river catchments such as Arvorezinha catchment (Minella et al., 2017b, 2014b), the Guaporé River (Le Gall et al., 2017; Tiecher et al., 2017c; Zafar et al., 2016), and the Conceição River (Tiecher et al., 2018), it was found that croplands provide the main source of sediment and contaminants due to the absence or the inadequate implementation of soil conservation practices for surface runoff control.

Recently, siltation and eutrophication of the reservoir of the Salto Grande Hydroelectric Power Plant built in 1980 on the Uruguay River have been reported by technicians and engineers who manage the dam, as it has accumulated large quantities of sediments presumably produced in the agricultural land areas located to the northwest and southwest of Rio Grande do Sul (RS), the western part of Santa Catarina State (SC), forests and grasslands of north-eastern Argentina, and paddy fields and grasslands of northern Uruguay. The Uruguay River basin drains most of the RS state territory (57% of the total area), where land use and occupation are dominated by agricultural, livestock

and agro-industrial activities (Figure 1). At the same time, the Uruguay basin drains about 50% of the territory of SC, including its entire western region, in which intensive farming, with high population and industrial densities predominate across the catchments of the Peixe River and the Chapecó River. Currently, despite the concerns associated with water quality, there is a lack of quantitative information on the amount of sediment accumulated in the Salto Grande reservoir, which potentially reduces the lifetime of the reservoir. Information regarding the potential sources supplying this material is also lacking.

The study of erosion processes and sediment transfer in sub-basins that drain into the Uruguay River is a way to understand the fragility of distinct economically significant regions for Brazil. Regions with distinct physiographic characteristics that drain into the Uruguay River are affected by processes of sediment generation and transfer that are still unknown. The understanding of these phenomena at the catchment scale can help to design specific conservationist farming strategies for each of the regions. Besides that, the identification of the main regions contributing with sediment and contaminants to the Uruguay River will assist in directing efforts to the regions with the greatest problems. Therefore, this thesis aims to characterize the main sediment transfer processes and to quantify the contribution of each sediment source across the Uruguay River basin, which covers an area of 365,000 km^2, 57% of which is located in the Brazilian territory, 31% in Uruguay and 12% in Argentina. As a first step, the current thesis dissertation will focus on improving our understanding of the processes of erosion and sediment transfer in the Brazilian part of this river basin. To this end, the main erosion and sediment transfer processes will be investigated in two tributaries of the Uruguay River, representing the two main contrasting geomorphological regions. More specifically, it seeks to evaluate the impact of land use and management on sediment transfer processes, making a critical evaluation of the natural and anthropogenic factors involved. In addition, this thesis will deal with methodological questions regarding the technique for identifying sediment sources, with an emphasis on the differences occurring when implementing different types of tracers in homogeneous or heterogeneous catchments, in terms of soil type, parental material and land use.

This thesis is related to two main research projects that aim to assess the impact of agricultural land use and management on water quality, energy and food production capacity, which provided financial support for field and laboratory activities. The most

recent project (NEXUS Pampa Biome) address the so-called MCTI/CNPq N° 20/2017 action - Nexus II: Research and Development in Integrated and Sustainable Actions for the Guarantee of Water, Energy and Food Security in the Pampa, Pantanal and Atlantic Forest Biomes, which is entitled "Livestock production systems in the Ibirapuitã River Catchment and their relationship with water and energy in food production", under the coordination of Professor Dr. Vicente C. P. Silva of the Federal University of Santa Maria. The investigations carried out in the Ibirapuitã River catchment presented in this doctoral project contribute to meet the demands of this large project linked to ensuring water, energy and food security, discussing the impact of soil degradation by erosion on food production and the availability and quality of water.

The second project, initiated in 2014 and extended until 2018, is a cooperation project between Brazilian universities and French research institutions of the CAPES/COFECUB program (Call 19/2014, nº 870/15). The project entitled "Use of radionuclides and geochemistry in soils and sediments to quantify erosion rates and identify sediment and pollutant sources in agricultural catchments to support the development of soil conservation measures", coordinated by Professor Dr. Jean Paolo Gomes Minella of the Federal University of Santa Maria and by Dr. Olivier Evrard of the Laboratory of Climate and Environmental Sciences (LSCE) supervised by the National Scientific Research Center (CNRS) of France, the French Atomic Energy Commission (CEA) and the University of Versailles/Paris-Saclay. The current doctoral thesis fits in the continuation of studies related to the CAPES/COFECUB project already carried out in the Conceição river catchment. Together with the studies to be carried out in the Ibirapuitã River catchment, we will explore in more details the techniques developed for identifying the sources of sediment and improve these methods for implementing them in regions with limited information on soil and sediment characteristics, starting as an initial step to understand the main sources of sediment contributing to such a large river basin as that of the Uruguay River. Besides this, this CAPES/COFECUB project granted my fourteen months' doctoral stay in France (November 2018 – December 2019).

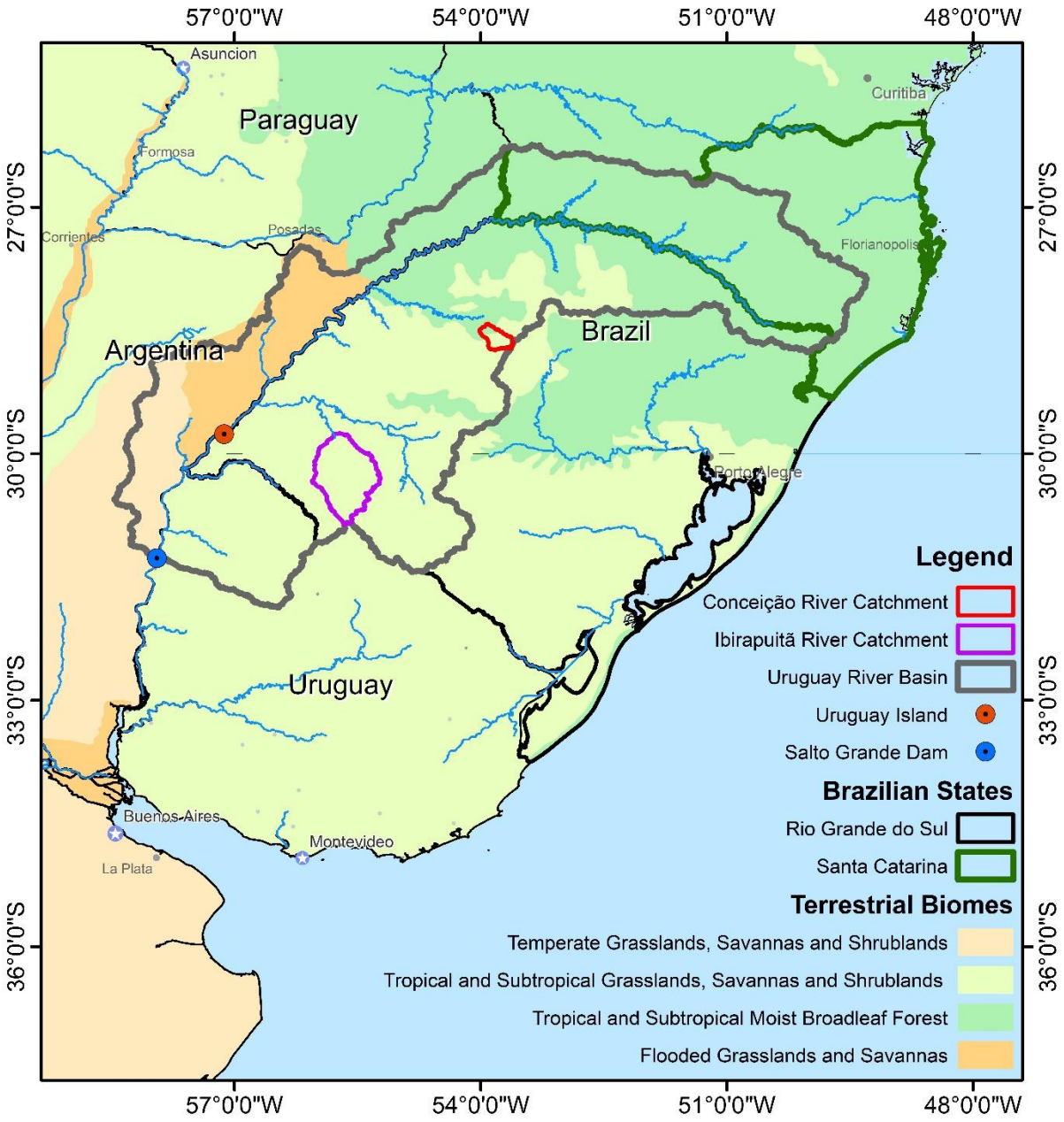

Figure 1.1. Uruguay River basin and the studied tributaries – Conceição River and Ibirapuitã River catchments.

The doctoral thesis document is organized in six chapters. Before them, an overall literature review about the soil erosion processes at the catchment scale and the previous knowledge is presented. It is followed by the section detailing the research hypothesis, the objectives and the materials and methods. After these, a chapter detailing each specific study is developed, including a meta-analysis of the sediment fingerprinting studies that used geochemical composition as potential tracers.

2 BACKGROUND: LITERATURE REVIEW

A literature review was carried out seeking to address basically three aspects related to the sediment dynamics in a river catchment and their relationship with changes in land use and management under different geomorphological contexts. First, the relationship between erosion processes and their impacts on society is discussed. Then, the effect of changes in land use and management and the geomorphological features of the river catchment on sediment dynamics is discussed. Finally, the sediment tracing technique and the main problems associated with the method that will be addressed in this study are discussed.

2.1 The context of soil erosion and its on-site and off-site impacts

Currently, the global demand for raw materials and food has increased the price of commodities, such as soybean, encouraging the development of agriculture in environmentally fragile areas, which associated with the occurrence of extreme weather events, has accelerated erosion processes (Marengo, 2012). Under this scenario, the challenge will be to produce food for 9 billion people, a number that should be reached by the middle of this century (Godfray et al., 2010). According to these authors, producing food in a sustainable manner, reducing greenhouse gas emissions and conserving water supplies, currently in decline, is a great challenge to achieve the millennium development goal of ending hunger (UNDP, 2003). Soil erosion has been considered as a threat for supplying food, fibre, and fuel production in the next years (Lal, 2007; Pimentel, 2006). In addition, the concerns of society have increased in recent years, especially regarding the quality and availability of water (Boholm and Prutzer, 2017), as extreme dry or wet events, with either water deficit or the occurrence of floods, have happened more frequently (Rogger et al., 2017). Thus, we thereby highlighted two of the soil functions – namely the support for plant growth and a regulator of water flows – illustrating that this resource is more than ever an essential component in ensuring food production and the supply of high quality water (Weil and Brady, 2016).

The absence of soil conservation practices has reduced the natural capacity of soils to fulfil their functions. In general, erosion rates are higher than those of soil formation. The time required to form one centimeter of soil can vary from 500 to 1000 years in tropical wet-dry climate (Evans, 2020), while this same amount of soil can be lost during

a single rainfall event. In an assessment of the impact of human activities on soil degradation, based on studies conducted in the United States, Nearing et al. (2017) found that erosion rates in cultivated soils reach 6.7 Mg ha^{-1} $year^{-1}$, while under natural conditions these rates do not exceed 1.9 Mg ha^{-1} $year^{-1}$. In the Brazilian Cerrado region, the removal of natural vegetation has increased erosion rates from 0.1 Mg ha^{-1} $year^{-1}$ under natural conditions to 12.4 Mg ha^{-1} $year^{-1}$ (Oliveira et al., 2015). In a meta-analysis of studies conducted on erosion plots in Brazil, Anache et al. (2017) found that the average soil losses observed under different cultivation systems and land uses can range from 0.1 Mg km^{-2} $year^{-1}$ (under native fields and pastures in southern Brazil) to 136.0 Mg km^{-2} $year^{-1}$ under conventional cropland in the north-eastern region of the country. Although most cultivated fields in Brazil are under no-till, soil erosion continues to be one of the main agents of soil degradation (Guerra et al., 2014).

The climatic and geological diversity of Brazil results in a great diversity of soil types, and consequently, each location has a specific land use and management capacity. However, the improper occupation of naturally fragile soils or their inadequate management, both through agricultural activities and urbanization, can generate environmental, social and economic costs that are estimated to several billions of dollars per year (Dechen et al., 2015; Hernani et al., 2002). Some studies have sought to quantify the costs of erosion both "on-site" (where erosion occurs) and "off-site" (sites affected by sediment originating from upper catchment parts). In an estimate of on-site costs in Brazil, relative to losses of nutrients such as P, K, Ca and Mg, Dechen et al. (2015) estimated a cost of about US$ 1.3 billion per year, considering only nutrient losses, without taking into account the replacement costs, where the soil losses were estimated to be approximately 616.5 million tons per year. This calculation took into account the area occupied by annual crops by different soil preparation systems, based on data from the 2006 agricultural census, as published by Llanillo et al. (2013). Some off-site costs of erosion in Brazil were taken into account in a study carried out by Hernani et al. (2002), considering the loss and replacement of nutrients, water treatment, replacement of reservoirs, greenhouse gas emissions, among others, annual costs of around US$ 10.59 billion were estimated (approximately 69% internal/on-site and 31% external/off-site). As an example given by Hernani et al. (2002), according to Derpsch et al. (1991), in 1982, about 12.5 million tons of sediment were deposited in the Itaipu dam. Of this amount, considering only the sediments from the state of Paraná (4.8 million tons), it is estimated

a loss of the main nutrients, N, P, K, Ca and Mg corresponding to a value of US$ 419 million per year. In a way, on-site costs are relatively easy to estimate, however, off-site costs require a much broader approach, taking into account technical engineering, social and environmental aspects, which is particularly difficult to accurately assess.

Some of the off-site erosion costs can be more easily calculated based on available datasets, such as the costs estimated by Evrard et al. (2007) related to road cleaning, infrastructure repair, assistance to population, dredging of river canals, based on Disaster Fund databases. However, there are several costs related to environmental impacts, the silting up of river channels and reservoirs, the contamination of water resources by excessive agrochemical waste, floods and droughts, and the destruction of roads, among others that are not taken into account. The same applies to on-site costs. Alfsen et al. (1996) has taken a broad approach to estimate the local costs of erosion in Nicaragua, but found that these are still uncertain results, as the impacts range from the loss of soil productive potential to the impacts on the agricultural market and migrations between rural and urban areas. In a review on soil erosion, Boardman (2006) points out that in most cases, we do not really know the severity of the problem associated with erosion. There is a need to identify erosion hotspots based not only on on-site effects, but also on off-site impacts.

Other social and environmental impacts due to erosion are difficult to calculate, although based on the data already collected, it is possible to verify that there is an urgent need to implement practices to mitigate erosion processes and control the surface runoff. Investment in prevention is a benefit to society as a whole and not just to landowners. Public policies are essential to encourage the adoption of conservation practices, and it is important to develop tools that can help to collaborate to use resources in a sustainable way, justifying the relevance of research on soil erosion.

2.2 Sediment discharge monitoring to understand the erosion processes in the catchment scale

Soil management, geomorphological features and climate control erosion processes and sediment transfers in the catchments. Thus, monitoring the variability of sediment yield, flow and concentration of contaminants, is a strategy to quantify the effects of land use and management, together with climate change, on water resources at the river catchment scale (Li et al., 2009; Minella et al., 2009b). Monitoring provides

quantitative information regarding the sediment transfer processes. However, to better understand the erosion process, complementary techniques such as hydrological modelling of erosion and tracing of sediment sources are essential.

In a long-term monitoring study conducted in a small rural catchment with intensive agriculture on fragile landscapes (i.e. the Arvorezinha catchment, 1,2 km^2), Minella et al. (2017) found that the implementation of conservation practices reduced erosion rates significantly. The inclusion of conservation practices in tobacco fields reduced sediment yield by approximately 70% compared to the period without conservation practices, and cropland areas were identified as the main source of sediment. Through hydro-sedimentary monitoring and mathematical modelling at the Conceição River catchment (804 km^2), Didoné et al. (2017) found that erosion rates have increased in recent years due to inadequate soil management, with sediment yields reaching the order of 36 to 260 t km^{-2} $year^{-1}$ in predominantly agricultural catchments in southern Brazil. Using techniques to identify sediment sources, Tiecher et al. (2018) found that current soil conservation techniques, where no-tillage is implemented in southern Brazil without complementary practices to control surface runoff, have not been efficient in controlling erosion in cropland fields used for grain production. About 50% of the sediment yield in the Conceição River catchment, in the northwest of Rio Grande do Sul state, originate from agricultural areas (cropland and pastures). Another 50% of the sediment comes from drainage channels, which can be the result of excess runoff, because in no-till areas, the straw deposited on the soil surface may be efficient to control soil loss, but not water excess. Consequently, this water, which will inexorably need to satisfy its sediment transport capacity, ends up causing erosion in the drainage channels, as it was also already observed in the Arvorezinha catchment by Minella et al. (2009). These are some examples of how river catchment scale studies help in understanding erosion and sediment transfer processes.

Studies combining watershed monitoring and the identification of sediment sources conducted in Brazil have concentrated on the country' southern region (Table 2.1). Of the seventeen river catchments studied in Brazil that applied the technique of identifying sediment sources, ten are located in the State of Rio Grande do Sul. Outside of this state, Franz et al. (2014) sought to identify sediment sources in the Paranoá Lake catchment and the Riacho Fundo sub-catchment in the Federal District. Batista et al. (2018) and Lima et al. (2020) worked in the Ingaí River catchment and Rio Grande

catchment, respectively, in Minas Gerais state. Lately, another study was developed in Pernambuco, Northeast Brazil, seeking to quantify the source contributions in a large catchment and in a sub-catchment to understand the scale dependency in sediment sources (Amorin et al., 2021). Almost all river catchments already studied in Brazil are predominantly agricultural areas, with the exception of the Dilúvio stream catchment, which is located in the metropolitan region of Porto Alegre, and Lake Paranoá, which receives a large contribution from urban areas.

Table 2.1. Sediment fingerprinting studies in Brazil.

Catchments studied	Authors	Year	Catchment area (km^2)	Location
Lajeado Ferreira Creek - Arvorezinha	(Clarke and Minella, 2016; Minella et al., 2009a, 2008a, 2007, 2004; Tiecher et al., 2021, 2019, 2017a, 2016, 2015)	2008-2021	1.23	Arvorezinha, RS
Agudo	(Minella et al., 2007)	2007	1.68	Agudo, RS
Dilúvio Creek	(Poleto et al., 2009)	2009	0.83	Viamão, RS
Alvorada Settlement 1	(Tiecher et al., 2017b)	2017	1.4	Júlio de Castilhos, RS
Alvorada Settlement 2	(Tiecher et al., 2017b, 2014)	2014-2017	0.8	Júlio de Castilhos, RS
Vacacaí-Mirim	(Miguel et al., 2014a, 2014b)	2014	20	Santa Maria, RS
Guaporé River	(Le Gall et al., 2017; Tiecher et al., 2017c)	2017	2030	Guaporé, RS
Terra Dura Forest	(Rodrigues et al., 2018)	2018	0.98	Eldorado do Sul, RS
Conceição River	(Tiecher et al., 2018)	2018	804	Ijuí, RS
Eucalyptus catchment	(Valente et al., 2020)	2018	0.83	São Gabriel, RS
Grassland catchment	(Valente et al., 2020)	2018	1.1	São Gabriel, RS
Paranoá Lake	(Franz et al., 2014)	2014	950	Brasília, DF
Riacho Fundo	(Franz et al., 2014)	2014	224	Brasília, DF
Ingaí River	(Batista et al., 2018)	2018	1200	Ingaí, MG
Posses Catchment	(Bispo et al., 2020)	2020	12	Extrema, MG
Upper Grande River Catchment	(Lima et al., 2020)	2020	0.8 and 1.75	Lavras, MG
Goiana Catchment	(Farias Amorim et al., 2021)	2021	2857	PB

Abbreviations: RS – Rio Grande do Sul State, DF – Distrito Federal State, MG – Minas Gerais State and PB – Pernambuco State.

The studies of erosion processes associated with different land uses in river catchments in the state of Rio Grande do Sul (RS) were mostly concentrated on the basaltic plateau and its borders, where clay soils from basalt of the Serra Geral Formation predominate (Figure 2.1). In these catchments, small family farms predominate, with land use for grain production and intensive cattle ranching. The main sources of sediment

in these catchments are grain production areas, unpaved roads and drainage channels. In the Guaporé River catchment, cropland areas provide the main source of sediment (78%), followed by drainage channels (20%) and unpaved roads (2%) (Tiecher et al., 2017c). In the Conceição River catchment, drainage channels provide the most important source of sediment, contributing more than 55% of the total sediment produced, while cropland fields contribute approximately 45%, based on sediment samples collected by time integrated suspended sediment samplers (Tiecher et al., 2018). In smaller river catchments, such as Arvorezinha, cropland contributes approximately 57% of sediments, followed by unpaved roads that contribute 23% and the stream channel 20% (Minella et al., 2008b; Tiecher et al., 2017a). In the Vacacaí-Mirim Stream catchment, in the central region of the state, unpaved roads become the main sources of sediment, contributing up to 80% of the sediments depending on the sediment sampling period (Miguel et al., 2014). From these studies, it is clear that a large variability of source contributions is found depending on the river catchment, which can be attributed to different land uses, relief, management measures, but also to different sampling designs or catchment scales.

In addition to the studies developed in the basaltic plateau region and its borders, three other studies were developed on catchments located in the southern half of the RS state, where geomorphological conditions and main land uses are distinct. Among them, one of the first sediment fingerprinting studies in Brazil was developed in the urban catchment of the Dilúvio Stream, where Poleto et al. (2009) verified that there is a large variability in the contribution of each sediment source during individual rainfall events. The variability in the contributions of paved and unpaved roads, and the drainage channel itself, shows that the method of sediment fingerprinting is very sensitive to the period of sample collection. The second study is that conducted in the Terra Dura Forest catchment, which is located in the region of the central depression of RS and which is planted with eucalyptus forests, where soils have a sandy texture developed on a bedrock of intrusive igneous material. In this catchment, the drainage channels provide the main sources of fine and coarse sediment, as the instability of the stream channels increase the processes of landslides (Rodrigues et al., 2018). Another recent study was carried out in two small paired catchments, one occupied with native grassland and the other with eucalyptus forests, over granites of the central depression of RS, where channel banks were identified as the main sediment source (Valente et al., 2020). In both studies, a high uncertainty was associated with the sediment source contributions obtained for certain

sediment samples, which was attributed to the small number of tracers available (Poleto et al., 2009) and also the low discrimination between potential sources by the selected tracers (Rodrigues et al., 2018; Valente et al., 2020).

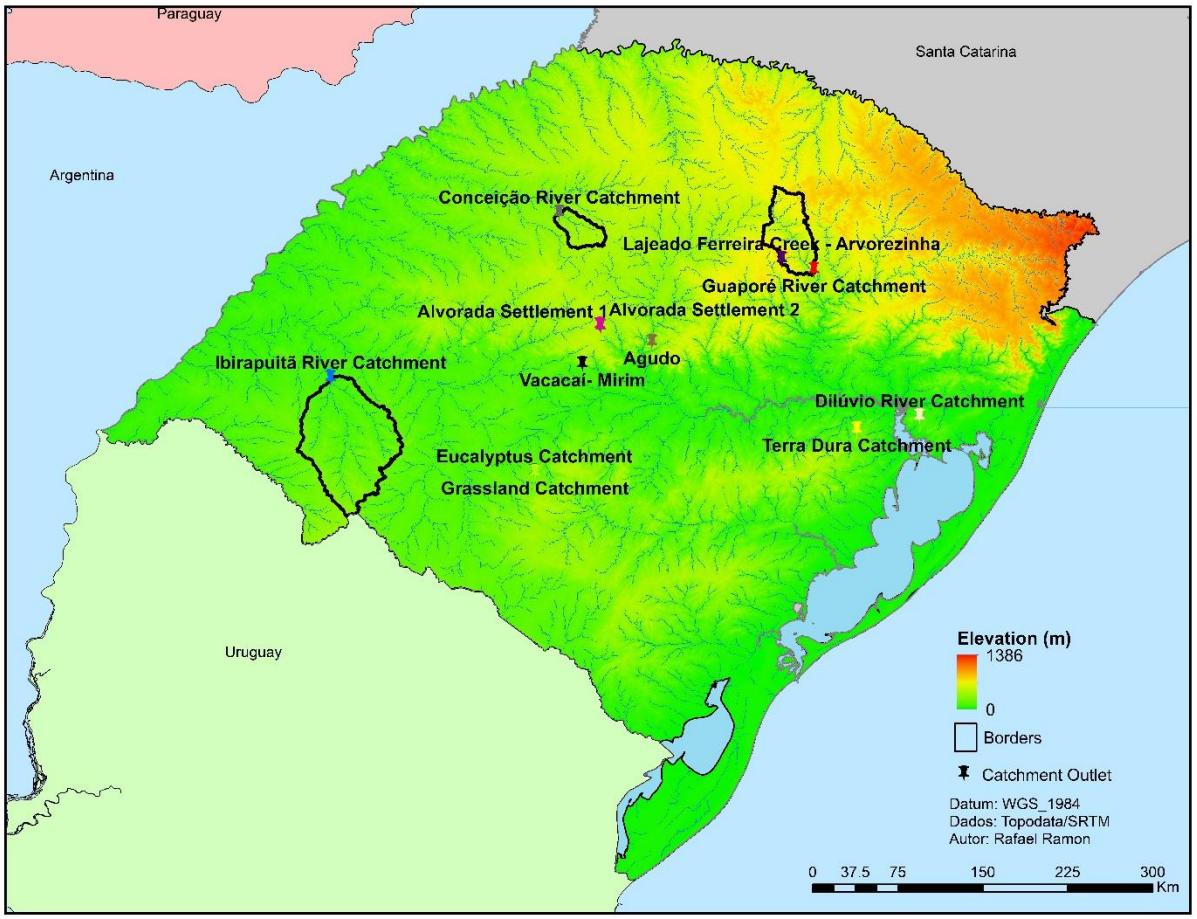

Figure 2.1. Location of the sediment fingerprinting studies conducted in the Rio Grande do Sul State.

Monitoring studies involving the identification of sediment sources in southern Brazil have been mostly conducted in catchments where clayey soils developed on basalt material and where intensive agricultural production is dominant. However, an extensive area of agricultural production in the state of RS is found in the Pampa biome, where the land is occupied predominantly with native grasslands for extensive livestock production, rice production and more recently with an increase of the surface area devoted to soybean production and eucalyptus plantations (Roesch et al., 2009). The study of Silveira et al. (2017) shows that in 15 years (2000 to 2015), the annual cropland areas in the Pampa biome increased by 57%. The soils of this region have a high susceptibility to erosion and land degradation processes, where soils originating from sedimentary rocks and less weathered soils derived from volcanic rocks occur

(EMBRAPA, 2013). The predominantly sandy soils show a low resistance to erosion processes, which makes them very sensitive to degradation. Similarly, the low stability of drainage channels results in their high sensitivity to erosion, generating large quantities of sediment available for subsequent transportation. In addition, the current expansion of soybean and cultivated forest production areas without land conservation practices at the expense of native grasslands may increase the erosion processes, which may lead to a state of irreversible degradation over the short term, as in the case of sandy areas that have already been formed in the region (Roesch et al., 2009). At the same time, the high content of carbon naturally stocked in natural grasslands, can be reduced to less than 50% following their conversion into cropland without the implementation of effective soil conservation practices (Guo and Gifford, 2002; Pillar et al., 2012).

Therefore, the analysis of sediment flows, as well as the identification of the main sources of sediment in environmentally fragile areas, are crucial for the public managers, to identify the main areas where active erosion occurs, which should be prioritized in the allocation of resources for implementing conservation practices (Koiter et al., 2013b). However, more research still needs to be conducted to optimize the methods of identification of sediment sources and enable the application of this technique in this particular region. This is a demand for the technique to move from being just a research tool to being a management and control tool that could be inserted into regulatory programs for controlling soil and water quality (Mukundan et al., 2012).

2.3 Challenges associated with the sediment fingerprinting technique under different environmental conditions

The need to quantify the contribution of sediment sources in river catchments to guide the implementation of practices capable of reducing the delivery and impact of sediment excess in rivers, reservoirs and lakes, has encouraged the development of techniques for identifying sediment sources (Collins et al., 2017a). An increase in the number of studies applying or developing this technique has been reported since the first studies carried out in the mid-1970s (Walling, 2013). The technique of sediment fingerprinting is based on two main assumptions stating (i) that the various potential sources of sediment can be discriminated by the analysis of different diagnostic properties and (ii) that the sediment collected in the river preserve the properties of their

sources, allowing through the comparison of these properties to estimate the importance of each potential source (Walling et al., 1993).

The first approaches to identify sediment sources originate from the 1970s (Klages et al., 1975; Wall and Wilding, 1976; Walling et al., 1979), seeking to calculate the contribution of different diffuse sources of sediment in river catchments in a rather qualitative way. Subsequently, an important advance in the identification of sediment sources was the use of multiple combined properties to estimate quantitatively the proportion with which each source contributes to each individual sediment sample (Collins et al., 1997; Walling et al., 1993; Yu and Oldfield, 1989). In one of the first articles published on the identification of sediment sources, Klages et al. (1975) used mineralogy to infer on the main tributary catchments as sediment sources. At the same time, Wall and Wilding (1976) used mineralogy combined with some geochemical elements to differentiate surface sources from subsurface material, a discrimination also explored later by Walling et al. (1979), although using magnetic properties, in order to design a more robust methodology for the identification of sources that was not destructive, with a low cost technique that required a small amount of samples.

Currently, the most consolidated tracing properties are the geochemical composition and the contents in fallout radionuclides, such as ^{210}Pb, ^{137}Cs and ^{7}Be (Evrard et al., 2016; Huisman and Karthikeyan, 2012; Minella et al., 2008b). Other properties such as geogenic radionuclides (^{238}U, ^{232}Th, ^{40}K) (Evrard et al., 2013; Sellier et al., 2020a), stable isotopes of hydrogen, carbon and nitrogen (δ^{2}H, δ^{15}N and δ^{13}C) (Hancock and Revill, 2013; Stewart et al., 2015), geochemical isotope composition (^{87}Sr/^{86}Sr) (Le Gall et al., 2016), ultra-violet-visible spectra (UV) and infrared spectroscopy (Poulenard et al., 2012; Tiecher et al., 2015), colour parameters derived from UV, magnetic susceptibility (Foster et al., 2007), rare earth elements (Habibi et al., 2019), plant pollen (Brown et al., 2008), soil enzymes (Nosrati et al., 2011), organic compounds (Cooper et al., 2015), carbon and nitrogen contents (Evrard et al., 2013), were also used in previous studies.

The application of each type of tracer is variable according to the objective of each study, the financial resources and tools available in each laboratory. Fallout radionuclides, for example, are very efficient for differentiating surface sources from subsurface sources (Walling and Woodward, 1992; Wilkinson et al., 2009), despite their high analytical cost. Accordingly, ^{137}Cs is strongly adsorbed to the surface soil particles after its atmospheric deposition, so that the highest concentrations of ^{137}Cs in sediment

samples will be attributed to surface sources (He and Walling, 1996; Parsons and Foster, 2011). Geochemical tracers, major, trace and rare earth elements, are related to the geological substrate, but may also have been transformed during the soil formation and weathering processes, or by the addition of fertilizers, manure, and other residues, and, therefore, have the potential to discriminate between different soil types and land uses (Collins et al., 2010c). Mineral magnetic properties, which are sensitive to soil formation processes and contaminations, are a low-cost alternative and have the potential to discriminate between different soil parental materials (Rowntree et al., 2017). The stable isotopic signature ($\delta^{13}C$) of specific organic compounds (CSSI) combined with conventional geochemical composition have been useful to identify sources under specific crops (Blake et al., 2012; Gibbs, 2008), but they are relatively expensive analyses and dependent of historical data of past vegetation in the sources (Hirave et al., 2019). Reiffarth et al. (2019) showed that biomarkers are strongly dependent on environmental conditions and a high variability is expected both in space and time, making sampling methods one of the main challenges when using CSSI. Recently, diffuse reflectance spectroscopy has proven to be an efficient low cost and quick tool to characterize and identify potential sediment sources in catchments (Martínez-Carreras et al., 2010b; Tiecher et al., 2017a).

In addition to estimating the contribution of each source according to the land use and management, it is possible to obtain information on the spatial contribution, considering tributary catchments as sources, or even considering different types of soil as source materials (Evrard et al., 2011; Haddadchi et al., 2015). Maher et al. (2009) used magnetic properties of the sand fraction of sediments in a large catchment covering 130,000 km^2 in Australia, seeking to identify the respective contributions of the main tributary sub-catchments of the Burdekin River catchment. In the study of Maher et al. (2009), it was possible to identify the contribution of each sub-catchment by means of their magnetic properties, which are directly related to mineralogy, magnetic domain state, composition and morphology of the source material, preserving the properties from its sources in host silicate particles. This approach allows to identify which regions have the greatest erosion problems and contribute with the greatest amount of sediments, even allowing to infer about the effect of the catchment geomorphology of each tributary river catchment or their main land uses.

As the size of the river catchment increases, the complexity of the processes involved increases as well and, consequently, the identification of the sources may become less assertive, requiring a greater care with the details of the technique (Koiter et al., 2013a). Large deposition zones in the catchment, or even the occurrence of reservoir deposits, can alter the transference and properties of sediments, causing a selectivity in particle size, where larger particles tend to deposit while finer particles are transported over greater distances (Bainbridge et al., 2014). In addition, sediment properties may change their physical and chemical properties from their source, according to the environmental conditions and processes involved. In general, the average particle size decreases due to disaggregation and abrasion, and selectivity may occur during the different stages of the erosion process (Koiter et al., 2013b). Consequently, the need to apply correction factors regarding particle size and organic matter content, as well as conservative tests, are issues widely discussed in the literature and they require attention (Koiter et al., 2013b; Sherriff et al., 2015). According to the review made by Laceby et al. (2017), each tracer property has different concentrations or values according to the particle size or specific surface area. Therefore, for each river catchment, these properties tend to be different, resulting in different optimal sets of tracers for each case.

The complexity of quantifying the erosion process at the river catchment scale is due to the large number of factors that interfere with the disaggregation, transport and deposition of sediments. Among these, the physical characteristics of soils and sediments are one of the main parameters evaluated for understanding the process, since they interfere in the ability to form aggregates and resist to the impact of rainfall, in its transportability on the hillside and rivers, and in its ability to transport nutrients and contaminants (Beuselinck et al., 1998; Horowitz, 1991; Walling and Woodward, 2000). The particle size directly influences the erodibility of soils. On the one hand, clay particles have a higher binding energy with the substrate around them, resulting in a greater power of aggregation and resistance to detachment processes, but they are easily transported. The coarse sand particles, on the other hand, have a greater capacity to resist to the transportation processes due to their larger size and weight, but they show a lower resistance to detachment. Silt-sized particles and fine sand are more susceptible to be disintegrated and transported, due to their small size and low reactive power in relation

to the clay fraction, hindering the formation of aggregates (Bradford et al., 1992; Morgan, 2005; Torri and Poesen, 1992).

Consequently, the concentration of tracer properties (geochemical composition, radionuclides, TOC) tends to be dependent on the transported particle size (Horowitz and Elrick, 1987). The concentration of trace elements associated with the physical properties such as size and specific surface area of sediment are widely studied (Parizanganeh, 2007; Ujević et al., 2000; Wei et al., 2015), since these are key physical parameters controlling the adsorption of chemical elements (Adiyiah et al., 2014; Xiao et al., 2013). The concentration of trace elements has an inverse relationship with the particle size and with the specific surface area, which are the most important physical factors in relation to the concentration of trace elements in suspended sediments (Horowitz, 1991). This relationship is due to the fact that there is a need for exposure of reactive surfaces to allow the adsorption of ions to particle surfaces. The main mechanism of interaction of the elements is the adsorption, which can occur with or without the exchange of cations, which should not be confounded with absorption, which involves the penetration of the element in the mineral or an inner-sphere complex. Therefore, the selectivity between the geochemical properties and the granulometry may be different for each element, depending on how it is incorporated in the sediment (being part of the mineral structure or adsorbed) (Laceby et al., 2017).

The majority of sediment fingerprinting studies have selected the fraction smaller than 63 μm, to eliminate the effect of the particle size when comparing the properties in the sediments with those of the potential sources (Collins et al., 1997; Wilson et al., 2011). The same fraction was used in a previous study already conducted in the Conceição River catchment (Tiecher et al., 2018), which is valid, since the average diameter of suspended sediments transported during rainfall events are less than 20 μm (Kochem, 2014).

The knowledge of the relative importance of each component of the sediment yield (i.e. suspended sediment and bedload) by means of conventional monitoring is fundamental to define the sediment source fingerprinting strategy. Suspended sediments are usually the finest fraction, while bedload is mainly composed of coarse sediments. Therefore, the selection of the particle size fraction adopted in a sediment fingerprinting approach should take into account the main particle size transported in the system (Laceby et al., 2017). However, tracing coarse sediment sources remains a challenge, since most tracer properties rely on the adsorption to the finest soil particles that are

chemically reactive. Therefore, the technique of sediment fingerprinting needs to be adapted in order to find the best strategies for sediment tracing in the Uruguay River basin where soils are heterogeneous. Protocols of the fingerprinting technique need to be verified, such as the number of potential sources, the spatial distribution of sources based on the main tributaries, sediment sampling and the selection of the most appropriate tracers for this basin (Haddadchi et al., 2015). Through improving our understanding of the sediment fluxes in the geomorphological contrasting environments of the Uruguay River basin, it will be possible to obtain substantial knowledge advances in our knowledge of sediment dynamics in such a large catchment.

2.4 References

Adiyiah, J., Acheampong, M.A., Ansa, E.D.O., Kelderman, P., 2014. Grain-Size Analysis and Heavy Metals Distribution in Sediment Fractions of Lake Markermeer in the Netherlands 1. Int. J. Environ. Sci. Toxicol. Res. 2, 160–167.

Alfsen, K.H., De Franco, M.A., Glomsrød, S., Johnsen, T., 1996. The cost of soil erosion in Nicaragua. Ecol. Econ. 16, 129–145. https://doi.org/10.1016/0921-8009(95)00083-6

Anache, J.A.A., Wendland, E.C., Oliveira, P.T.S., Flanagan, D.C., Nearing, M.A., 2017. Runoff and soil erosion plot-scale studies under natural rainfall: A meta-analysis of the Brazilian experience. CATENA 152, 29–39. https://doi.org/10.1016/j.catena.2017.01.003

Bainbridge, Z.T., Lewis, S.E., Smithers, S.G., Kuhnert, P.M., Henderson, B.L., Brodie, J.E., 2014. Fine-suspended sediment and water budgets for a large, seasonally dry tropical catchment: Burdekin River catchment, Queensland, Australia. Water Resour. Res. 50, 9067–9087. https://doi.org/10.1002/2013WR014386

Batista, P.V.G., Laceby, J.P., Silva, M.L.N., Tassinari, D., Bispo, D.F.A., Curi, N., Davies, J., Quinton, J.N., 2018. Using pedological knowledge to improve sediment source apportionment in tropical environments. J. Soils Sediments. https://doi.org/10.1007/s11368-018-2199-5

Bennett, E.M., Carpenter, S.R., Caraco, N.F., 2001. Human Impact on Erodable Phosphorus and Eutrophication: A Global Perspective. Bioscience 51, 227. https://doi.org/10.1641/0006-3568(2001)051[0227:HIOEPA]2.0.CO;2

Bertol, I., Luciano, R.V., Bertol, C., Bagio, B., 2017. Nutrient and Organic Carbon Losses,

Enrichment Rate, and Cost of Water Erosion. Rev. Bras. Ciência do Solo 41, 1–15. https://doi.org/10.1590/18069657rbcs20160150

Beuselinck, L., Govers, G., Poesen, J., Degraer, G., Froyen, L., 1998. Grain-size analysis by laser diffractometry: comparison with the sieve-pipette method. CATENA 32, 193–208. https://doi.org/10.1016/S0341-8162(98)00051-4

Bispo, D.F.A., Batista, P.V.G., Guimarães, D.V., Silva, M.L.N., Curi, N., Quinton, J.N., 2020. Monitoring land use impacts on sediment production: a case study of the pilot catchment from the Brazilian program of payment for environmental services. Rev. Bras. Ciência do Solo 44, 1–15. https://doi.org/10.36783/18069657rbcs20190167

Blake, W.H., Ficken, K.J., Taylor, P., Russell, M.A., Walling, D.E., 2012. Tracing crop-specific sediment sources in agricultural catchments. Geomorphology 139–140, 322–329. https://doi.org/10.1016/j.geomorph.2011.10.036

Boardman, J., 2006. Soil erosion science: Reflections on the limitations of current approaches. CATENA 68, 73–86. https://doi.org/10.1016/j.catena.2006.03.007

Boardman, J., Vandaele, K., Evans, R., Foster, I.D.L., 2019. Off-site impacts of soil erosion and runoff: Why connectivity is more important than erosion rates. Soil Use Manag. 35, 245–256. https://doi.org/10.1111/sum.12496

Boholm, Å., Prutzer, M., 2017. Experts' understandings of drinking water risk management in a climate change scenario. Clim. Risk Manag. 16, 133–144. https://doi.org/10.1016/j.crm.2017.01.003

Bradford, J.M., Truman, C.C., Huang, C., 1992. Comparison of three measures of resistance of soil surface seals to riandrop splash. Soil Technol. 5, 47–56.

Brown, A.G., Carpenter, R.G., Walling, D.E., 2008. Monitoring the fluvial palynomorph load in a lowland temperate catchment and its relationship to suspended sediment and discharge. Hydrobiologia 607, 27–40. https://doi.org/10.1007/s10750-008-9364-6

Clarke, R.T., Minella, J.P.G., 2016. Evaluating sampling efficiency when estimating sediment source contributions to suspended sediment in rivers by fingerprinting. Hydrol. Process. 30, 3408–3419. https://doi.org/10.1002/hyp.10866

Collins, A.L., Pulley, S., Foster, I.D.L., Gellis, A., Porto, P., Horowitz, A.J., 2017. Sediment source fingerprinting as an aid to catchment management: A review of the current state of knowledge and a methodological decision-tree for end-users. J. Environ. Manage. 194, 86–108. https://doi.org/10.1016/j.jenvman.2016.09.075

Collins, A.L., Walling, D.E., Leeks, G.J.L., 1997. Source type ascription for fluvial suspended

sediment based on a quantitative composite fingerprinting technique. Catena 29, 1–27. https://doi.org/10.1016/S0341-8162(96)00064-1

Collins, A.L., Zhang, Y., Walling, D.E., Grenfell, S.E., Smith, P., 2010. Tracing sediment loss from eroding farm tracks using a geochemical fingerprinting procedure combining local and genetic algorithm optimisation. Sci. Total Environ. 408, 5461–5471. https://doi.org/10.1016/j.scitotenv.2010.07.066

Cooper, R.J., Pedentchouk, N., Hiscock, K.M., Disdle, P., Krueger, T., Rawlins, B.G., 2015. Apportioning sources of organic matter in streambed sediments: An integrated molecular and compound-specific stable isotope approach. Sci. Total Environ. 520, 187–197. https://doi.org/10.1016/j.scitotenv.2015.03.058

Dechen, S.C.F., Telles, T.S., Guimarães, M. de F., De Maria, I, C., Maria, I.C. De, 2015. Perdas e custos associados à erosão hídrica em função de taxas de cobertura do solo. Bragantia 74, 224–233. https://doi.org/10.1590/1678-4499.0363

Derpsch, R., Roth, C.H., Sidiras, N., Kopke, U., 1991. Controle da erosão no Paraná, Brasil: Sistemas de cobertura do solo, plantio direto e preparo conservacionista do solo, GTZ/IAPAR. Deutsche Gesellschaft fur Technische Zusammenarbeit, Eschborn [Alemanha].

Didoné, E.J., Minella, J.P.G., Evrard, O., 2017. Measuring and modelling soil erosion and sediment yields in a large cultivated catchment under no-till of Southern Brazil. Soil Tillage Res. 174, 24–33. https://doi.org/10.1016/j.still.2017.05.011

EMBRAPA, 2013. Sistema brasileiro de classificação de Solos (SiBCS), 3ª Ed. ed. EMBRAPA, Brasília.

Evans, D.L., 2020. New insights into the rates of soil formation and their contribution to our understanding of soil lifespans. Lancaster University.

Evrard, O., Bielders, C.L., Vandaele, K., van Wesemael, B., 2007. Spatial and temporal variation of muddy floods in central Belgium, off-site impacts and potential control measures. Catena 70, 443–454. https://doi.org/10.1016/j.catena.2006.11.011

Evrard, O., Laceby, J.P., Huon, S., Lefèvre, I., Sengtaheuanghoung, O., Ribolzi, O., 2016. Combining multiple fallout radionuclides (137Cs, 7Be, 210Pbxs) to investigate temporal sediment source dynamics in tropical, ephemeral riverine systems. J. Soils Sediments 16, 1130–1144. https://doi.org/10.1007/s11368-015-1316-y

Evrard, O., Navratil, O., Ayrault, S., Ahmadi, M., Némery, J., Legout, C., Lefèvre, I., Poirel, A., Bonté, P., Esteves, M., 2011. Combining suspended sediment monitoring and

fingerprinting to determine the spatial origin of fine sediment in a mountainous river catchment. Earth Surf. Process. Landforms 36, 1072–1089. https://doi.org/10.1002/esp.2133

Evrard, O., Poulenard, J., Némery, J., Ayrault, S., Gratiot, N., Duvert, C., Prat, C., Lefèvre, I., Bonté, P., Esteves, M., 2013. Tracing sediment sources in a tropical highland catchment of central Mexico by using conventional and alternative fingerprinting methods. Hydrol. Process. 27, 911–922. https://doi.org/10.1002/hyp.9421

Farias Amorim, F., Jacques Agra Bezerra da Silva, Yuri, Cabral Nascimento, R., Jacques Agra Bezerra da Silva, Ygor, Tiecher, T., Williams Araújo do Nascimento, C., Paolo Gomes Minella, J., Zhang, Y., Ram Upadhayay, H., Pulley, S., Collins, A.L., 2021. Sediment source apportionment using optical property composite signatures in a rural catchment, Brazil. CATENA 202, 105208. https://doi.org/10.1016/j.catena.2021.105208

Foster, I.D.L., Boardman, J., Keay-Bright, J., 2007. Sediment tracing and environmental history for two small catchments, Karoo Uplands, South Africa. Geomorphology 90, 126–143. https://doi.org/10.1016/j.geomorph.2007.01.011

Franz, C., Makeschin, F., Weiß, H., Lorz, C., 2014. Sediments in urban river basins: Identification of sediment sources within the Lago Paranoá catchment, Brasilia DF, Brazil – using the fingerprint approach. Sci. Total Environ. 466–467, 513–523. https://doi.org/10.1016/j.scitotenv.2013.07.056

Gibbs, M.M., 2008. Identifying Source Soils in Contemporary Estuarine Sediments: A New Compound-Specific Isotope Method. Estuaries and Coasts 31, 344–359. https://doi.org/10.1007/s12237-007-9012-9

Godfray, H.C.J., Beddington, J.R., Crute, I.R., Haddad, L., Lawrence, D., Muir, J.F., Pretty, J., Robinson, S., Thomas, S.M., Toulmin, C., 2010. Food Security: The Challenge of Feeding 9 Billion People. Science (80-.). 327, 812–818. https://doi.org/10.1126/science.1185383

Golosov, V.N., Walling, D.E., 2019. Erosion and sediment problems: global hotspots. Paris, France.

GUERRA, A.J.T., FULLEN, M.A., JORGE, M.C.O., ALEXANDRE, S.T., 2014. Erosão e Conservação de Solos no Brasil. Anuário do Inst. Geociências - UFRJ 37_1, 81–91. https://doi.org/10.11137/2014_1_81_91

Guo, L.B., Gifford, R.M., 2002. Soil carbon stocks and land use change : a meta analysis.

Glob. Chang. Biol. 345–360. https://doi.org/10.1046/j.1354-1013.2002.00486.x

Habibi, S., Gholami, H., Fathabadi, A., Jansen, J.D., 2019. Fingerprinting sources of reservoir sediment via two modelling approaches. Sci. Total Environ. 663, 78–96. https://doi.org/10.1016/j.scitotenv.2019.01.327

Haddadchi, A., Olley, J., Pietsch, T., 2015. Quantifying sources of suspended sediment in three size fractions. J. Soils Sediments 15, 2086–2100. https://doi.org/10.1007/s11368-015-1196-1

Hancock, G.J., Revill, A.T., 2013. Erosion source discrimination in a rural Australian catchment using compound-specific isotope analysis (CSIA). Hydrol. Process. 27, 923–932. https://doi.org/10.1002/hyp.9466

He, Q., Walling, D.E., 1996. Interpreting particle size effects in the adsorption of 137Cs and unsupported 210Pb by mineral soils and sediments. J. Environ. Radioact. 30, 117–137. https://doi.org/10.1016/0265-931X(96)89275-7

Hernani, L.C., Freitas, P.L., Pruski, F.F., Maria, I.C. de, Castro Filho, C., Landers, J.C., 2002. A erosão e seu impacto, in: Manzatto, C. V., Freitas Júnior, E., Peres, J.R.R. (Eds.), Uso Agrícola Dos Solos Brasileiros. Embrapa Solos, Rio de Janeiro, pp. 47–60.

Hirave, P., Wiesenberg, G.L.B., Birkholz, A., Alewell, C., 2019. Understanding the effects of early degradation on isotopic tracers: implications for sediment source attribution using compound-specific isotope analysis (CSIA). Biogeosciences Discuss. 1–18. https://doi.org/10.5194/bg-2019-205

Horowitz, A.J., 1991. A Primer on Sediment-Trace Element Chemistry. U.S.G.S. Open-File Rep. 2nd Editio, 136 (2 fiche).

Horowitz, A.J., Elrick, K.A., 1987. The relation of stream sediment surface area, grain size and composition to trace element chemistry. Appl. Geochemistry 2, 437–451. https://doi.org/10.1016/0883-2927(87)90027-8

Huisman, N.L.H., Karthikeyan, K.G., 2012. Using radiometric tools to track sediment and phosphorus movement in an agricultural watershed. J. Hydrol. 450–451, 219–229. https://doi.org/10.1016/j.jhydrol.2012.05.007

Klages, M.G., Hsieh, Y.P., Logan, L.D., Forest, G.N., States, U., Service, F., Hsieh, Y.P., Uoiversity, M.S., 1975. Suspended Solids Carried by the Gallatin River of Southwestern Montana: II. Using Mineralogy for Inferring Sources1. J. Environ. Qual. 4, 68. https://doi.org/10.2134/jeq1975.00472425000400010016x

Kochem, M.L., 2014. Características granulométricas, carbono, nitrogênio e frações de

fósforo em sedimentos durante eventos chuva-vazão em bacias hidrográficas no Rio Grande do Sul, Brasil. Universidade Federal de Santa Maria, Santa Maria, RS.

Koiter, A.J., Lobb, D.A., Owens, P.N., Petticrew, E.L., Tiessen, K.H.D.D., Li, S., 2013a. Investigating the role of connectivity and scale in assessing the sources of sediment in an agricultural watershed in the Canadian prairies using sediment source fingerprinting. J. Soils Sediments 13, 1676–1691. https://doi.org/10.1007/s11368-013-0762-7

Koiter, A.J., Owens, P.N., Petticrew, E.L., Lobb, D.A., 2013b. The behavioural characteristics of sediment properties and their implications for sediment fingerprinting as an approach for identifying sediment sources in river basins. Earth-Science Rev. 125, 24–42. https://doi.org/10.1016/j.earscirev.2013.05.009

Laceby, J.P., Evrard, O., Smith, H.G., Blake, W.H., Olley, J.M., Minella, J.P.G., Owens, P.N., 2017. The challenges and opportunities of addressing particle size effects in sediment source fingerprinting: A review. Earth-Science Rev. 169, 85–103. https://doi.org/10.1016/j.earscirev.2017.04.009

Lal, R., 2007. Anthropogenic Influences on World Soils and Implications to Global Food Security. Adv. Agron. 93, 69–93. https://doi.org/10.1016/S0065-2113(06)93002-8

Le Gall, M., Evrard, O., Dapoigny, A., Tiecher, T., Zafar, M., Minella, J.P.G., Laceby, J.P., Ayrault, S., 2017. Tracing Sediment Sources in a Subtropical Agricultural Catchment of Southern Brazil Cultivated With Conventional and Conservation Farming Practices. L. Degrad. Dev. 28, 1426–1436. https://doi.org/10.1002/ldr.2662

Le Gall, M., Evrard, O., Foucher, A., Laceby, J.P., Salvador-Blanes, S., Thil, F., Dapoigny, A., Lefèvre, I., Cerdan, O., Ayrault, S., 2016. Quantifying sediment sources in a lowland agricultural catchment pond using 137Cs activities and radiogenic 87Sr/86Sr ratios. Sci. Total Environ. 566–567, 968–980. https://doi.org/10.1016/j.scitotenv.2016.05.093

Li, Z., Liu, W., Zhang, X., Zheng, F., 2009. Impacts of land use change and climate variability on hydrology in an agricultural catchment on the Loess Plateau of China. J. Hydrol. 377, 35–42. https://doi.org/10.1016/j.jhydrol.2009.08.007

Lima, P.L.T., Silva, M.L.N., Quinton, J.N., Armstrong, A., Inda, A.V., Batista, P.V.G., Poggere, G.C., Curi, N., 2020. Tracing the origin of reservoir sediments using magnetic properties in Southeastern Brazil. Semin. Agrar. 41, 847–864. https://doi.org/10.5433/1679-0359.2020v41n3p847

Llanillo, R.F., Telles, T.S., Soares Júnior, D., Pelinni, T., 2013. Tillage systems on annual crops in Brazil: figures from the 2006 Agricultural Census. Semin. Ciências Agrárias 34, 3691. https://doi.org/10.5433/1679-0359.2013v34n6Supl1p3691

Lloyd, C.E.M., Johnes, P.J., Freer, J.E., Carswell, A.M., Jones, J.I., Stirling, M.W., Hodgkinson, R.A., Richmond, C., Collins, A.L., 2019. Determining the sources of nutrient flux to water in headwater catchments: Examining the speciation balance to inform the targeting of mitigation measures. Sci. Total Environ. 648, 1179–1200. https://doi.org/10.1016/J.SCITOTENV.2018.08.190

Londero, A.L., Minella, J.P.G., Deuschle, D., Schneider, F.J.A., Boeni, M., Merten, G.H., 2018. Impact of broad-based terraces on water and sediment losses in no-till (paired zero-order) catchments in southern Brazil. J. Soils Sediments 18, 1159–1175. https://doi.org/10.1007/s11368-017-1894-y

Maher, B.A., Watkins, S.J., Brunskill, G., Alexander, J., Fielding, C.R., 2009. Sediment provenance in a tropical fluvial and marine context by magnetic "fingerprinting" of transportable sand fractions. Sedimentology 56, 841–861. https://doi.org/10.1111/j.1365-3091.2008.00999.x

Marengo, J.A., 2012. Mudanças climáticas, condições meteorológicas extremas e eventos climáticos no Brasil, in: Mudanças Climáticas e Eventos Extremos No Brasil. Fundação Brasileira para o Desenvolvimento Sustentável - FDBS, pp. 4–19.

Martínez-Carreras, N., Krein, A., Udelhoven, T., Gallart, F., Iffly, J.F., Hoffmann, L., Pfister, L., Walling, D.E., 2010. A rapid spectral-reflectance-based fingerprinting approach for documenting suspended sediment sources during storm runoff events. J. Soils Sediments 10, 400–413. https://doi.org/10.1007/s11368-009-0162-1

Miguel, P., Dalmolin, R.S.D., Pedron, F. de A., Moura-Bueno, J.M., Tiecher, T., 2014. Identificação de fontes de produção de sedimentos em uma bacia hidrográfica de encosta. Rev. Bras. Cienc. do Solo 38, 585–598. https://doi.org/10.1590/S0100-06832014000200023

Minella, J.P.G., Clarke, R.T., Merten, G.H., Walling, D.E., 2008a. Sediment source fingerprinting : testing hypotheses about contributions from potential sediment sources. IAHS-AISH Publ. 31–37.

Minella, J.P.G., Merten, G.H., Barros, C.A.P. de, Ramon, R., Schlesner, A., Clarke, R.T., Moro, M., Dalbianco, L., 2017a. Long-term sediment yield from a small catchment in southern Brazil affected by land use and soil management changes. Hydrol. Process.

https://doi.org/10.1002/hyp.11404

Minella, J.P.G., Merten, G.H., Clarke, R.T., 2009a. Método “fingerprinting” para identificação de fontes de sedimentos em bacia hidrográfica rural. Rev. Bras. Eng. Agrícola e Ambient. 13, 633–638. https://doi.org/10.1590/S1415-43662009000500017

Minella, J.P.G., Merten, G.H., Clarke, R.T., 2004. Identification of sediment sources in a small rural drainage basin, in: Sediment Transfer through the Fluvial System (Proceedings of a Symposium Held in Moscow, August 2004). IAHS Press, Moscow, pp. 44–51.

Minella, J.P.G., Merten, G.H., Reichert, J.M., Santos, D.R. dos, 2007. Identificação e implicações para a conservação do solo das fontes de sedimentos em bacias hidrográficas. Rev. Bras. Ciência do Solo 31, 1637–1646. https://doi.org/10.1590/S0100-06832007000600039

Minella, J.P.G., Merten, G.H., Walling, D.E., Reichert, J.M., 2009b. Changing sediment yield as an indicator of improved soil management practices in southern Brazil. CATENA 79, 228–236. https://doi.org/10.1016/j.catena.2009.02.020

Minella, J.P.G., Merten, G.H.G.H., Barros, C.A.P. de, Ramon, R., Schlesner, A., Clarke, R.T.R.T., Moro, M., Dalbianco, L., 2017b. Long-term sediment yield from a small catchment in southern Brazil affected by land use and soil management changes. Hydrol. Process. 17, 10803. https://doi.org/10.1002/hyp.11404

Minella, J.P.G., Walling, D.E., Merten, G.H., 2014a. Establishing a sediment budget for a small agricultural catchment in southern Brazil, to support the development of effective sediment management strategies. J. Hydrol. 519, 2189–2201. https://doi.org/10.1016/j.jhydrol.2014.10.013

Minella, J.P.G., Walling, D.E., Merten, G.H., 2014b. Establishing a sediment budget for a small agricultural catchment in southern Brazil, to support the development of effective sediment management strategies. J. Hydrol. 519, 2189–2201. https://doi.org/10.1016/j.jhydrol.2014.10.013

Minella, J.P.G., Walling, D.E., Merten, G.H., 2008b. Combining sediment source tracing techniques with traditional monitoring to assess the impact of improved land management on catchment sediment yields. J. Hydrol. 348, 546–563. https://doi.org/10.1016/j.jhydrol.2007.10.026

Morgan, R.P.C., 2005. Soil Erosion & Conservation, 3º Edition. ed. Blackwell Publishing

Ltd.

Mukundan, R., Walling, D.E., Gellis, A.C., Slattery, M.C., Radcliffe, D.E., 2012. Sediment Source Fingerprinting : Transforming From a Research Tool To a Management Tool 1. JAWRA J. Am. Water Resour. Assoc. 48, 1241–1257. https://doi.org/10.1111/j.1752-1688.2012.00685.x

Nearing, M.A., Xie, Y., Liu, B., Ye, Y., 2017. Natural and anthropogenic rates of soil erosion. Int. Soil Water Conserv. Res. 5, 77–84. https://doi.org/10.1016/j.iswcr.2017.04.001

Nosrati, K., Govers, G., Ahmadi, H., Sharifi, F., Amoozegar, M.A., Merckx, R., Vanmaercke, M., 2011. An exploratory study on the use of enzyme activities as sediment tracers: biochemical fingerprints? Int. J. Sediment Res. 26, 136–151. https://doi.org/10.1016/S1001-6279(11)60082-6

Oliveira, P.T.S., Nearing, M.A., Wendland, E., 2015. Orders of magnitude increase in soil erosion associated with land use change from native to cultivated vegetation in a Brazilian savannah environment. Earth Surf. Process. Landforms 40, 1524–1532. https://doi.org/10.1002/esp.3738

Parizanganeh, A., 2007. Grain size effect on trace metals in contamined sediments along the iranian coast of the Caspian Sea. 12th World Lake Conf. 329–336.

Parsons, A.J., Foster, I.D.L., 2011. What can we learn about soil erosion from the use of 137Cs? Earth-Science Rev. 108, 101–113. https://doi.org/10.1016/j.earscirev.2011.06.004

Pillar, V., Tornquist, C., Bayer, C., 2012. The southern Brazilian grassland biome: soil carbon stocks, fluxes of greenhouse gases and some options for mitigation. Brazilian J. Biol. 72, 673–681. https://doi.org/10.1590/S1519-69842012000400006

Pimentel, D., 2006. Soil Erosion: A Food and Environmental Threat. Environ. Dev. Sustain. 8, 119–137. https://doi.org/10.1007/s10668-005-1262-8

Poleto, C., Merten, G.H., Minella, J.P.G., 2009. The identification of sediment sources in a small urban watershed in southern Brazil: An application of sediment fingerprinting. Environ. Technol. 30, 1145–1153. https://doi.org/10.1080/09593330903112154

Poulenard, J., Legout, C., Némery, J., Bramorski, J., Navratil, O., Douchin, A., Fanget, B., Perrette, Y., Evrard, O., Esteves, M., 2012. Tracing sediment sources during floods using Diffuse Reflectance Infrared Fourier Transform Spectrometry (DRIFTS): A case study in a highly erosive mountainous catchment (Southern French Alps). J. Hydrol. 414–415, 452–462. https://doi.org/10.1016/j.jhydrol.2011.11.022

Ramos, M.C., Lizaga, I., Gaspar, L., Quijano, L., Navas, A., 2019. Effects of rainfall intensity and slope on sediment, nitrogen and phosphorous losses in soils with different use and soil hydrological properties. Agric. Water Manag. 226, 105789. https://doi.org/10.1016/j.agwat.2019.105789

Reiffarth, D.G., Petticrew, E.L., Owens, P.N., Lobb, D.A., 2019. Spatial differentiation of cultivated soils using compound-specific stable isotopes (CSSIs) in a temperate agricultural watershed in Manitoba, Canada. J. Soils Sediments 19, 3411–3426. https://doi.org/10.1007/s11368-019-02406-3

Rodrigues, M.F., Reichert, J.M., Burrow, R.A., Flores, E.M.M., Minella, J.P.G., Rodrigues, L.A., Oliveira, J.S.S., Cavalcante, R.B.L., 2018. Coarse and fine sediment sources in nested watersheds with eucalyptus forest. L. Degrad. Dev. 29, 2237–2253. https://doi.org/10.1002/ldr.2977

Roesch, L.F., Vieira, F., Pereira, V., Schünemann, A.L., Teixeira, I., Senna, A.J., Stefenon, V.M., 2009. The Brazilian Pampa: A Fragile Biome. Diversity 1, 182–198. https://doi.org/10.3390/d1020182

Rogger, M., Agnoletti, M., Alaoui, A., Bathurst, J.C., Bodner, G., Borga, M., Chaplot, V., Gallart, F., Glatzel, G., Hall, J., Holden, J., Holko, L., Horn, R., Kiss, A., Quinton, J.N., Leitinger, G., Lennartz, B., Parajka, J., Peth, S., Robinson, M., Salinas, J.L., Santoro, A., Szolgay, J., Tron, S., Viglione, A., 2017. Land use change impacts on floods at the catchment scale: Challenges and opportunities for future research. Water Resouces Res. 53, 5209–5219. https://doi.org/10.1002/2017WR020723.Received

Rowntree, K.M., van der Waal, B.W., Pulley, S., 2017. Magnetic susceptibility as a simple tracer for fluvial sediment source ascription during storm events. J. Environ. Manage. 194, 54–62. https://doi.org/10.1016/j.jenvman.2016.11.022

Sellier, V., Navratil, O., Laceby, J.P., Allenbach, M., Lefèvre, I., Evrard, O., 2020. Investigating the use of fallout and geogenic radionuclides as potential tracing properties to quantify the sources of suspended sediment in a mining catchment in New Caledonia, South Pacific. J. Soils Sediments 20, 1112–1128. https://doi.org/10.1007/s11368-019-02447-8

Sherriff, S.C., Franks, S.W., Rowan, J.S., Fenton, O., Ó'hUallacháin, D., 2015. Uncertainty-based assessment of tracer selection, tracer non-conservativeness and multiple solutions in sediment fingerprinting using synthetic and field data. J. Soils Sediments 15, 2101–2116. https://doi.org/10.1007/s11368-015-1123-5

Silveira, V.C.P., González, J.A., Fonseca, E.L. da, 2017. Land use changes after the period commodities rising price in the Rio Grande do Sul State, Brazil. Ciência Rural 47, 1–7. https://doi.org/10.1590/0103-8478cr20160647

Stewart, H.A., Massoudieh, A., Gellis, A., 2015. Sediment source apportionment in Laurel Hill Creek, PA, using Bayesian chemical mass balance and isotope fingerprinting. Hydrol. Process. 29, 2545–2560. https://doi.org/10.1002/hyp.10364

Telles, T.S., de Fátima Guimarães, M., Dechen, S.C.F., 2011. Os custos da erosão do solo. Rev. Bras. Cienc. do Solo 35, 287–298. https://doi.org/10.1590/S0100-06832011000200001

Tiecher, T., Caner, L., Minella, J.P.G., Bender, M.A., dos Santos, D.R., 2016. Tracing sediment sources in a subtropical rural catchment of southern Brazil by using geochemical tracers and near-infrared spectroscopy. Soil Tillage Res. 155, 478–491. https://doi.org/10.1016/j.still.2015.03.001

Tiecher, T., Caner, L., Minella, J.P.G., Evrard, O., Mondamert, L., Labanowski, J., Rheinheimer, D. dos S., 2017a. Tracing Sediment Sources Using Mid-infrared Spectroscopy in Arvorezinha Catchment, Southern Brazil. L. Degrad. Dev. 28, 1603–1614. https://doi.org/10.1002/ldr.2690

Tiecher, T., Caner, L., Minella, J.P.G., Pellegrini, A., Capoane, V., Rasche, J.W.A., Schaefer, G.L., Rheinheimer, D. dos S., 2017b. Tracing sediment sources in two paired agricultural catchments with different riparian forest and wetland proportion in southern Brazil. Geoderma 285, 225–239. https://doi.org/10.1016/j.geoderma.2016.10.008

Tiecher, T., Caner, L., Minella, J.P.G., Santos, D.R. dos, 2015. Combining visible-based-color parameters and geochemical tracers to improve sediment source discrimination and apportionment. Sci. Total Environ. 527–528, 135–149. https://doi.org/10.1016/j.scitotenv.2015.04.103

Tiecher, T., Minella, J.P.G., Caner, L., Evrard, O., Zafar, M., Capoane, V., Le Gall, M., Santos, D.R. dos, 2017c. Quantifying land use contributions to suspended sediment in a large cultivated catchment of Southern Brazil (Guaporé River, Rio Grande do Sul). Agric. Ecosyst. Environ. 237, 95–108. https://doi.org/10.1016/j.agee.2016.12.004

Tiecher, T., Minella, J.P.G., Evrard, O., Caner, L., Merten, G.H., Capoane, V., Didoné, E.J., dos Santos, D.R., 2018. Fingerprinting sediment sources in a large agricultural catchment under no-tillage in Southern Brazil (Conceição River). L. Degrad. Dev. 29, 939–951.

https://doi.org/10.1002/ldr.2917

Tiecher, T., Minella, J.P.G., Miguel, P., Alvarez, J.W.R., Pellegrini, A., Capoane, V., Ciotti, L.H., Schaefer, G.L., dos Santos, D.R., 2014. Contribuição das fontes de sedimentos em uma bacia hidrográfica agrícola sob plantio direto. Rev. Bras. Cienc. do Solo 38, 639–649. https://doi.org/10.1590/S0100-06832014000200028

Tiecher, T., Moura-Bueno, J.M., Caner, L., Minella, J.P.G.P.G., Evrard, O., Ramon, R., Naibo, G., Barros, C.A.P. de, Silva, Y.J.A.B., Amorim, F.F., Rheinheimer, D.S., 2021. Improving the quantification of sediment source contributions using different mathematical models and spectral preprocessing techniques for individual or combined spectra of ultraviolet–visible, near- and middle-infrared spectroscopy. Geoderma 384, 114815. https://doi.org/10.1016/j.geoderma.2020.114815

Tiecher, T., Ramon, R., Laceby, J.P., Evrard, O., Minella, J.P.G., 2019. Potential of phosphorus fractions to trace sediment sources in a rural catchment of Southern Brazil: Comparison with the conventional approach based on elemental geochemistry. Geoderma 337. https://doi.org/10.1016/j.geoderma.2018.11.011

Torri, D., Poesen, J., 1992. The effect of soil surface slope on raindrop detachment. Catena 19, 561–578. https://doi.org/10.1016/0341-8162(92)90053-E

Ujević, I., Odžak, N., Barić, A., Ujevic, I., Odzak, N., Baric, a., 2000. Trace metal accumulation in different grain size fractions of the sediments from a semi- enclosed bay heavily contaminated by urban and industrial wastewaters. Water Res. 34, 3055–3061. https://doi.org/10.1016/S0043-1354(99)00376-0

UNDP, 2003. DEVELOPMENT REPORT 2003 Millennium Development, Human Development.

Valente, M.L., Reichert, J.M., Legout, C., Tiecher, T., Cavalcante, R.B.L., Evrard, O., 2020. Quantification of sediment source contributions in two paired catchments of the Brazilian Pampa using conventional and alternative fingerprinting approaches. Hydrol. Process. 34, 2965–2986. https://doi.org/10.1002/hyp.13768

Wall, G.J., Wilding, L.P., 1976. Mineralogy and Related Parameters of Fluvial Suspended Sediments in Northwestern Ohio1. J. Environ. Qual. 5, 168. https://doi.org/10.2134/jeq1976.00472425000500020012x

Walling, D.E., 2013. The evolution of sediment source fingerprinting investigations in fluvial systems. J. Soils Sediments 13, 1658–1675. https://doi.org/10.1007/s11368-013-0767-2

Walling, D.E., Peart, M.R., Oldfield, F., Thompson, R., 1979. Suspended sediment sources identified by magnetic measurements. Nature 281, 110–113. https://doi.org/0028-0836/79/370110-04$01.00

Walling, D.E., Woodward, J.C., 2000. Effective particle size characteristics of fluvial suspended sediment transported by lowland British rivers. Role Eros. Sediment Transp. Nutr. Contam. Transf. 129–139.

Walling, D.E., Woodward, J.C., 1992. Use of radiometric fingerprints to derive information on suspended sediment sources. Eros. Sediment TrnsRiver Basinspr Monit. Program. 153–164.

Walling, D.E., Woodward, J.C., Nicholas, A.P., 1993. A multi-parameter approach to fingerprinting suspended-sediment, in: Tracers in Hydrology. IAHS Publ. 215, Yokohama, pp. 329–338.

Wei, M., Chen, J., Sun, Z., Lv, C., Cai, W., 2015. Distribution of Heavy Metals in Different Size Fractions of Agricultural Soils Closer to Mining Area and its Relationship to TOC and Eh, in: Proceedings of the World Congress on New Technologies (NewTech 2015). pp. 1–6.

Weil, R.R., Brady, N.C., 2016. The nature and properties of soils, 15th editi. ed. Pearson Education.

Wilkinson, S.N.N., Wallbrink, P.J.J., Hancock, G.J.J., Blake, W.H.H., Shakesby, R.A.A., Doerr, S.H.H., 2009. Fallout radionuclide tracers identify a switch in sediment sources and transport-limited sediment yield following wildfire in a eucalypt forest. Geomorphology 110, 140–151. https://doi.org/10.1016/j.geomorph.2009.04.001

Wilson, H., Cruse, R., Burras, L., 2011. A method to adapt watershed-scale sediment fingerprinting techniques to small-plot runoff experiments. J. Soil Water Conserv. 66, 323–328. https://doi.org/10.2489/jswc.66.5.323

Xiao, Y., Zhu, X.L., Cheng, H.K., Li, K.J., Lu, Q., Liang, D.F., 2013. Characteristics of phosphorus adsorption by sediment mineral matrices with different particle sizes. Water Sci. Eng. 6, 262–271. https://doi.org/10.3882/j.issn.1674-2370.2013.03.003

Yu, L., Oldfield, F., 1989. A multivariate mixing model for identifying sediment source from magnetic measurements. Quat. Res. 32, 168–181. https://doi.org/10.1016/0033-5894(89)90073-2

Zafar, M., Tiecher, T., de Castro Lima, J.A.M., Schaefer, G.L., Santanna, M.A., dos Santos, D.R., 2016. Phosphorus seasonal sorption-desorption kinetics in suspended sediment in

response to land use and management in the Guaporé catchment, Southern Brazil. Environ. Monit. Assess. 188, 643. https://doi.org/10.1007/s10661-016-5650-3

3 HYPOTHESIS

The land use change in the Pampa biome region and the absence of effective land conservation practices in agricultural areas in the Southern Brazilian plateau region, make agricultural cropland areas the main source of suspended sediments in the Uruguay River basin.

4 AIM AND OBJECTIVES

4.1 Aim

Quantify sediment source contribution in two contrasting tributaries of the Uruguay River basin, which differ mainly in terms of soil types and land uses.

4.2 Objectives

Calculate the contribution of multiple sources of sediment in a ~~large~~ catchment (804 km^2) with highly weathered and homogeneous soils of the plateau region of Rio Grande do Sul state.

Quantify the contribution of potential sediment sources from a representative catchment of the Pampa Biome (5,943 km^2), assessing the impact of recent land use change.

Identify and analyse the signature of the sediments collected in the Uruguay River, comparing with those of the representative tributaries of the two main regions that are found in the basin, and propose directions for future studies of sediment source tracing in such large river basins (242,000 km^2).

5 MATERIALS AND METHODS

5.1 Study catchments

This study will be carried out in two tributary catchments of the Uruguay River, representative of two contrasting geomorphological regions of the southern region of Brazil. The Uruguay River is one of the largest rivers in the southern region of South America, draining an area of approximately 242,000 km^2 (considering the Salto Grande Hydroelectric Plant as the outlet of the catchment), with 70% of its area located in southern Brazil, 20% in Argentina and 10% in Uruguay (Figure 1.1). On the one hand, land use in the catchment is predominantly agricultural, with intensive agricultural production in the states of Rio Grande do Sul (RS-Brazil) and Santa Catarina (SC-Brazil), where small farms (<50 ha) predominate in the more undulating relief regions (with dairy crops, intensive poultry and pig farming, natural and cultivated forests), while larger properties (mostly <100 ha) are located in flatter areas (with dominant soybean, corn and wheat productions). Similar conditions are also observed in the northernmost portion of the Argentinian side, in the Atlantic biome, where land use is predominantly occupied by plantations of *mate*, tea, and also eucalyptus plantations. On the other hand, in the southwestern regions of RS and northern Uruguay, large properties are predominant (>100 ha). In general, in these regions, most of the areas are occupied with pasture for extensive ranching and irrigated rice production in the plains, with an increased soybean production in the region during the last few years. The southernmost part of the Argentinian side comprises the flooded grasslands and savannahs, an extremely flat region, with hydromorphic soils where pastures and planted forests for the extraction of wood and cellulose are predominant.

Along the course of the Uruguay River and its tributaries, there are approximately 44 dams, which are predominantly used for electric power generation, while some reservoirs are used for water abstraction for basic sanitation. These dams are located in the upper portion of the Uruguay River basin, where the relief is more mountainous and allows for a more effective use of the potential river energy, with the exception of the Salto Grande Hydroelectric Power Plant dam, which is the most downstream dam of the basin, located in the flattest portion of the basin. Therefore, the two study sites were

chosen because they represent two very contrasting regions and the main geomorphological features of the Uruguay River basin, which have a high environmental, economic and social significance.

5.2 Conceição River catchment

The Conceição River catchment is located on the southern plateau in the state of Rio Grande do Sul, with an area of approximately 804.3 km^2 (Figure 5.1). The catchment outlet is located next to the monitoring point number 75200000 of the National Water Agency (ANA) (28°27'22" S, 53°58'24" O) in the municipality of Ijuí. According to the Köppen classification, the climate is Cfa type, humid subtropical without a defined dry season, with an average precipitation of 1900 to 2200 mm per year and an average temperature of approximately 18°C (Alvares et al., 2013). This catchment is representative of the basalt plateau region of the Serra Geral Formation, where the main soil classes found are the Ferralsols (80%), Nitosols (18%) and Acrisols (2%), rich in iron oxides and kaolinite, with the Ferralsols being the most widespread soil type in the catchment (Figure 5.1a). Small areas from the Tupanciretã Formation, which are remnants of the Botucatu Formation amidst the volcanic spills of the Serra Geral Formation, are also found. The relief of the region is characterized by gentle slopes (6-9%) at the top and moderate or steep slopes (10-14%) near the drainage channels, with altitude ranging from 270 to 480 m a.s.l. In this catchment, the main land use is cropland for grain production and dairy farming, where inadequate soil management has resulted in high erosion rates (Didoné et al., 2015b). The main land use is cropland (82%) mainly cultivated with soybean (*Glycine max*) under no-tillage system in the summer and wheat (*Triticum aestivum*) for grain production, oat (*Avena sativa* and *Avena strigosa*) and ryegrass (*Lolium multiflorum*) for dairy cattle feed or soil cover during the winter. However, inadequate soil management in these areas has resulted in high erosion rates in the last decades (Didoné et al., 2019, 2015a). Pastures (grassland, pasture and mosaics of agriculture and pasture, according to the Mapbiomas classification), mainly used for cattle raising, cover 12% of the total surface area, whereas forest is found on only 5% of the surface (Figure 5.1b). In the Conceição River catchment, the pasture area obtained from Mapbiomas, includes both perennial and temporary pastures, although only perennial pastures were sampled in this study site.

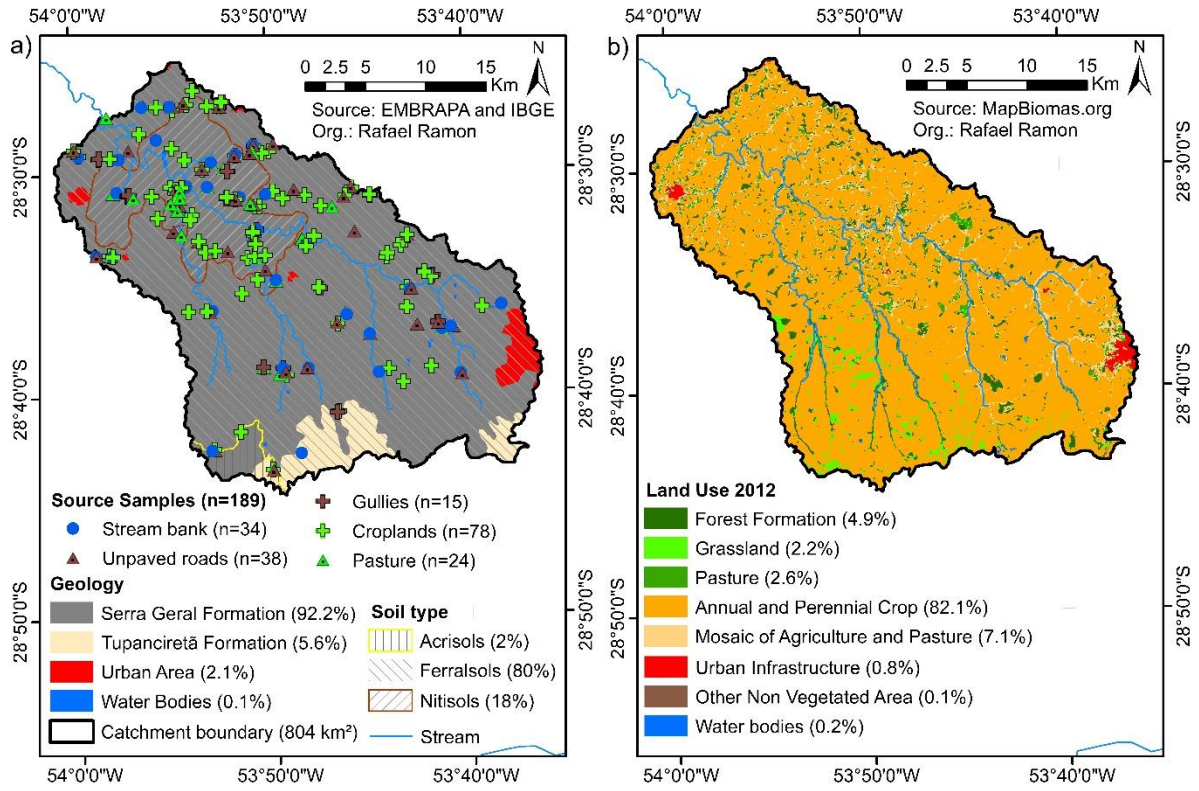

Figure 5.1. Soil types and geology of the Conceição River catchment (a) and land use map of 2012 based on the classification of the MapBiomas database (b).

5.3 Ibirapuitã River catchment

The Ibirapuitã River catchment is located in the extreme south of Brazil and is representative of the southern grassland region, typical of the Pampa biome, covering approximately 7975 km^2. The outlet of the studied catchment is located next to monitoring point number 76750000 of ANA (28°27'22" S, 53°58'24" O) in the municipality of Alegrete (5943 km^2), representing 75% of the total area of the Ibirapuitã catchment. According to the Köppen classification, the climate is Cfa type, humid subtropical without a defined dry season, with an average precipitation of 1,600 to 1,900 mm per year and an average temperature of 17°C (Alvares et al., 2013). The altitude of the catchment is comprised between 70 and 370 m a.s.l., and the elevations above 280 meters are located in the headwaters of the catchment, near the border between Brazil and Uruguay and represent less than 15% of the catchment area. Approximately 90% of the catchment area has slopes of less than 15%, and the slopes decrease in the northern direction, varying from 2 to 5% in the lower Ibirapuitã region. Land use is predominantly occupied by native grasslands with extensive livestock activity (81%) (Figure 5.2),

although as in the whole Pampa region, it tends to be increasingly occupied by soybean production areas. The catchment is composed of three sub-catchments. The (i) Ibirapuitã Environmental Protection Area subcatchment (EPA), which is an environmental protection area controlled by the Chico Mendes Institution of Biodiversity Conservation (ICMBio) from the National Ministry of the Environment, where native grasslands (85%) and natural forests (10%) predominate. Located in the central portion of the Ibirapuitã River catchment, the EPA subcatchment has an area of 3196 km^2, where the main soil types are Regosols in the upper half and Acrisols in the lower half, from basalts of the Serra Geral formation (Fácies Alegrete) and sandstones/silts of the Botucatu formation (Fácies Gramado, Caxias and Guará), respectively. The (ii) Pai-Passo Stream subcatchment covers approximately 1043 km^2, and it is mainly occupied by native grassland (83%) areas with extensive livestock on shallow Regosols originating from basalt (Fácies Alegrete), and paddy fields for irrigated rice production (10%) located in the lower and flat positions of the landscape, where Planosols and Vertisols occur. The (iii) Caverá Stream subcatchment covers approximately 1455 km^2, and it is the tributary catchment with the higher percentage of cropland (irrigated rice and soybean) and cultivated pastures (15%), where the native grassland (73%) has been converted into cropland on deeper soils, predominantly Acrisols originating from sandstones of the Botucatu formation (Figure 5.3).

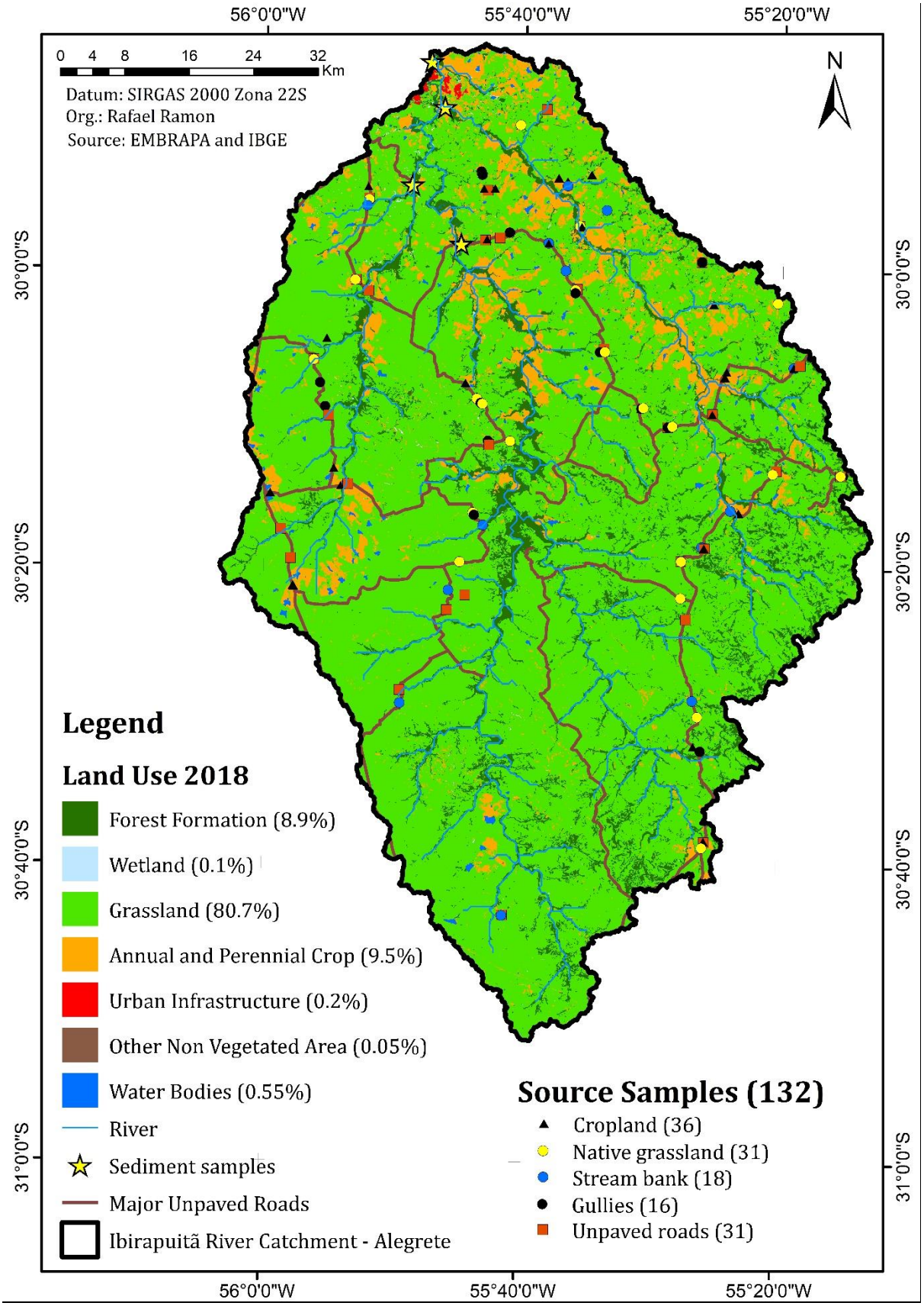

Figure 5.2. Land uses and location of the source samples collected in the Ibirapuitã River catchment.

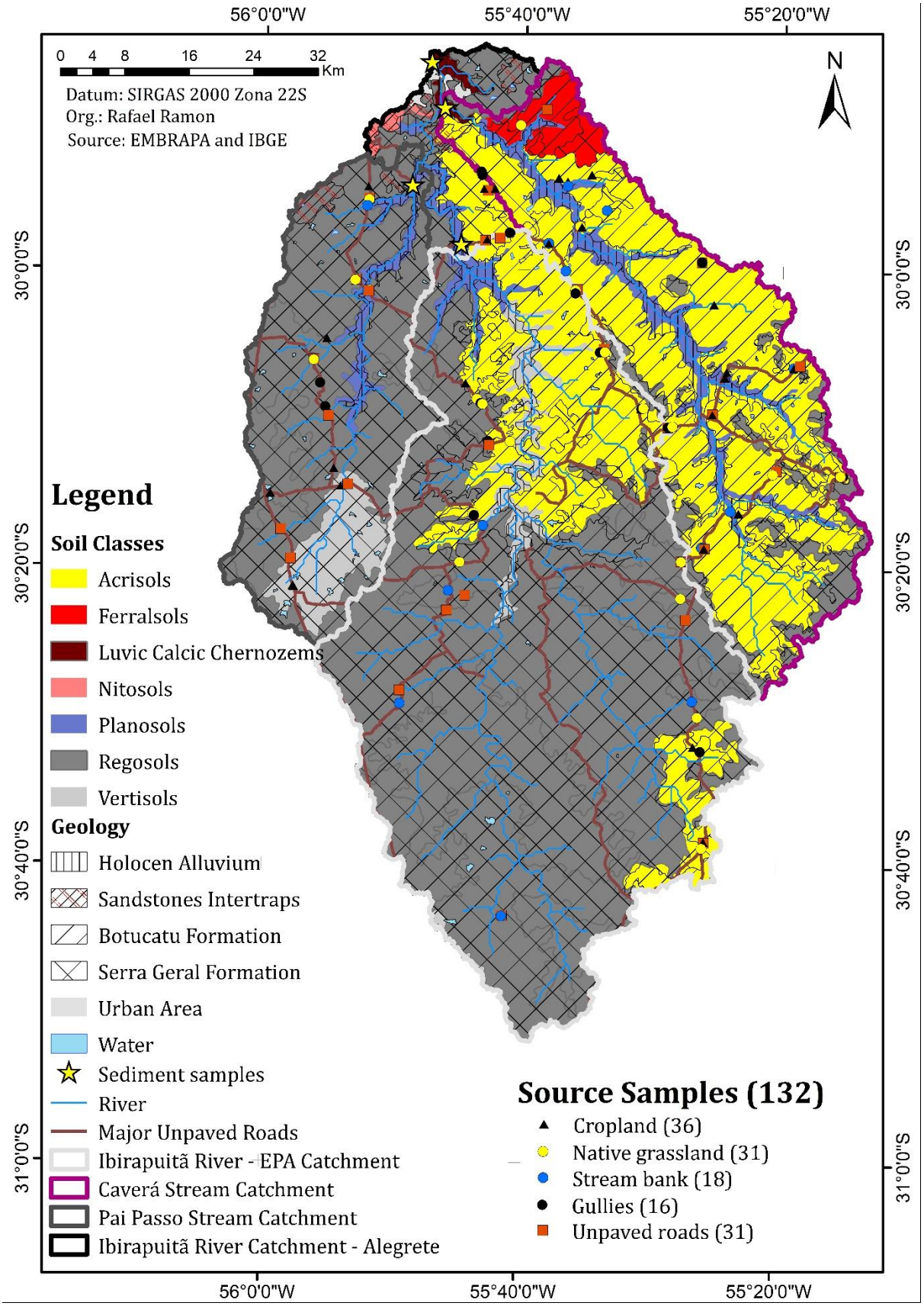

Figure 5.3. Soil types, geology and sediment sampling points of the Ibirapuitã River catchment.

5.4 Sediment source sampling

The potential sediment sources were chosen during reconnaissance campaigns, where the main components of the landscape showing potential for sediment contribution were identified. For the Conceição River catchment, sediment source samples collected by Tiecher (2015) in 2012 were used in this study, distributed among croplands (n = 77), unpaved roads (n = 38), stream banks (n = 34), gullies (n = 14) and permanent pastures (n = 24).

In the Ibirapuitã River catchment, soil samples from potential sources were collected at representative areas that showed active erosion and that were connected to the drainage network, following the same principle adopted by Tiecher (2015). Care was taken to avoid those sites that have accumulated sediment originating from other sources, not to collect transiting material. In the surface sources, soil from the upper 0-2 cm layer was collected, as this layer is the most likely to be eroded and transported to the waterways. In the subsurface sources, samples were collected at the edge of the drainage channels at exposed sites sensitive to erosion. For each composite source sample, around 10 sub-samples were collected within a radius of approximately 50 meters, mixed in a bucket and approximately 500 grams of material were stored. The source samples sites were selected in order to cover all the soil types and the variability in slope positions, as well as the three main tributary catchments. Samples were taken during the winter period in 2018 under the following land uses and erosion features: croplands and cultivated pastures (n = 28), paddy fields (n = 8), native grasslands (n = 31), unpaved roads (n = 31), stream banks (n = 18) and erosion channels (n = 16).

5.5 Sediment sampling

For sediment characterization and quantification of suspended sediment fluxes, sediment samples were collected using different strategies, in order to have enough material for subsequent analyses. Three methods were used:

i. Time integrated suspended sediment sampler (TISS) - The sampler designed by Phillips et al. (2000) consists in a plastic tube of 75 mm of diameter and 80 cm length, which has a small inlet and outlet tubes (4 mm of diameter) in the extreme edges, which allows the suspended sediment to enter, reducing the flow velocity and allow the sediment to deposit

inside the tube based on the principle of sedimentation. The equipment is submerged for a certain period of time integrating the sediments from different rainfall events, in which the eroded material of the catchment is mobilized under different conditions of transport and energy, and consequently consists of contrasted physical, chemical and mineralogical characteristics. The samples were collected during intervals of 2 to 3 months, varying according to the records of rainfall events.

ii. Storm event samples (Event) - Samples collected during storm events were collected at the outlet, where a large volume of water (50 to 200 litters) was collected at different stages of the rainfall-runoff event to evaporate the water and have enough material to perform the analyses.

iii. Fine bed sediment samples (FBS) – in the Conceição River, samples were collected with a suction device in the bottom of the river. Multiple samples collected in different positions of the river bed close to the outlet composed each individual sample. According to Horowitz et al. (2012), fine sediment (<63 μm) deposited in the first centimetres of the river bed can be used as a surrogate to quantify the concentration of chemicals in suspended sediment.

iv. Flood deposits (FD) – sediment deposited in the flooding area after a storm event were collected along the Ibirapuitã River. Care was taken to sample only material that was deposited by the previous major rainfall event.

For the Conceição River catchment, sediment samples already collected by Tiecher (2015) were used, where more information related to the samples can be found. Sediment samples collected by TISS, Event and FBS methods were taken at the outlet of the catchment in the period of March of 2011 to January of 2013. Samples were also collected during the period of 2017 to 2019, however the samples could not be used in this thesis due to the different analytical methods used.

In the Ibirapuitã River catchment, suspended sediment samples were collected during rainfall events that resulted in increased water discharge and sediment yield at the main outlet. Samples were collected in duplicates, where one was used for sediment concentration analysis and the other, with a greater volume, was collected to accumulate enough sediment for subsequent physical and chemical analyses. A second method used was the TISS that were installed in the three main sub-catchments of the Ibirapuitã River

(Pai-Passo Stream, Caverá Stream and the Ibirapuitã-EPA catchment) and at the main outlet (Figure 5.4).

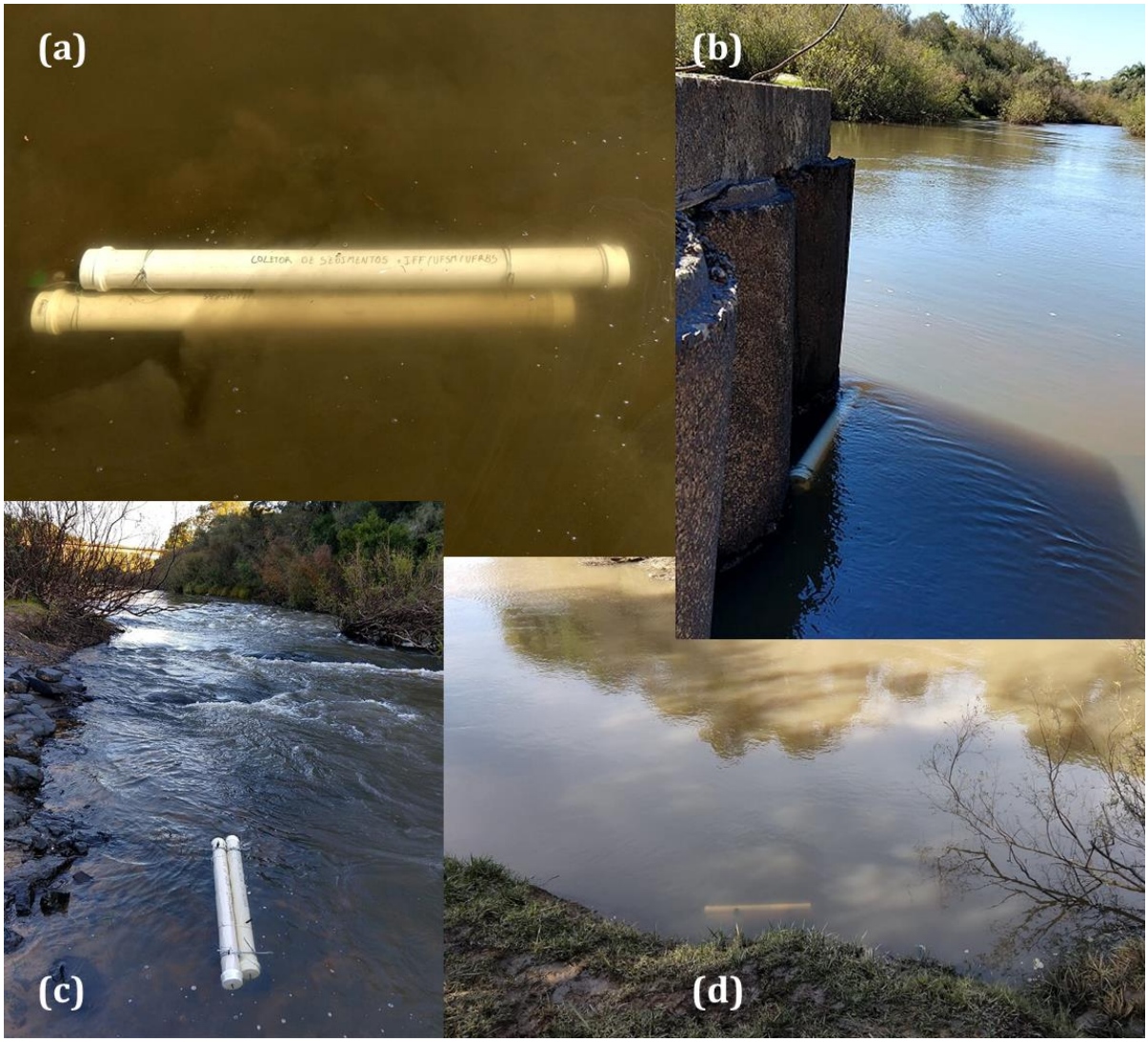

Figure 5.4. TISS installed at the Ibirapuitã River catchment outlet (a), Caverá Stream outlet (b), Ibirapuitã APA outlet (c) and Pai Passo Stream outlet (d). Source: the author.

Figure 5.5. Suspended sediment sampling to determine the concentration during a monitoring campaign made in collaboration with the National Water Agency service provider, the Brazilian Geological Service (CPRM) (a); Event sampling in the Ibirapuitã River during a storm event, sample taken with a bucket to obtain larger volumes (b) and for suspended sediment concentration collected with a US-D49 sampler (d); Suspended sediment sampling in the Conceição River before a storm event using a US-D49 on a bridge (c). Source: the author (a, c), Paulo C. Ramon (b), Antônio A. Marquez (d).

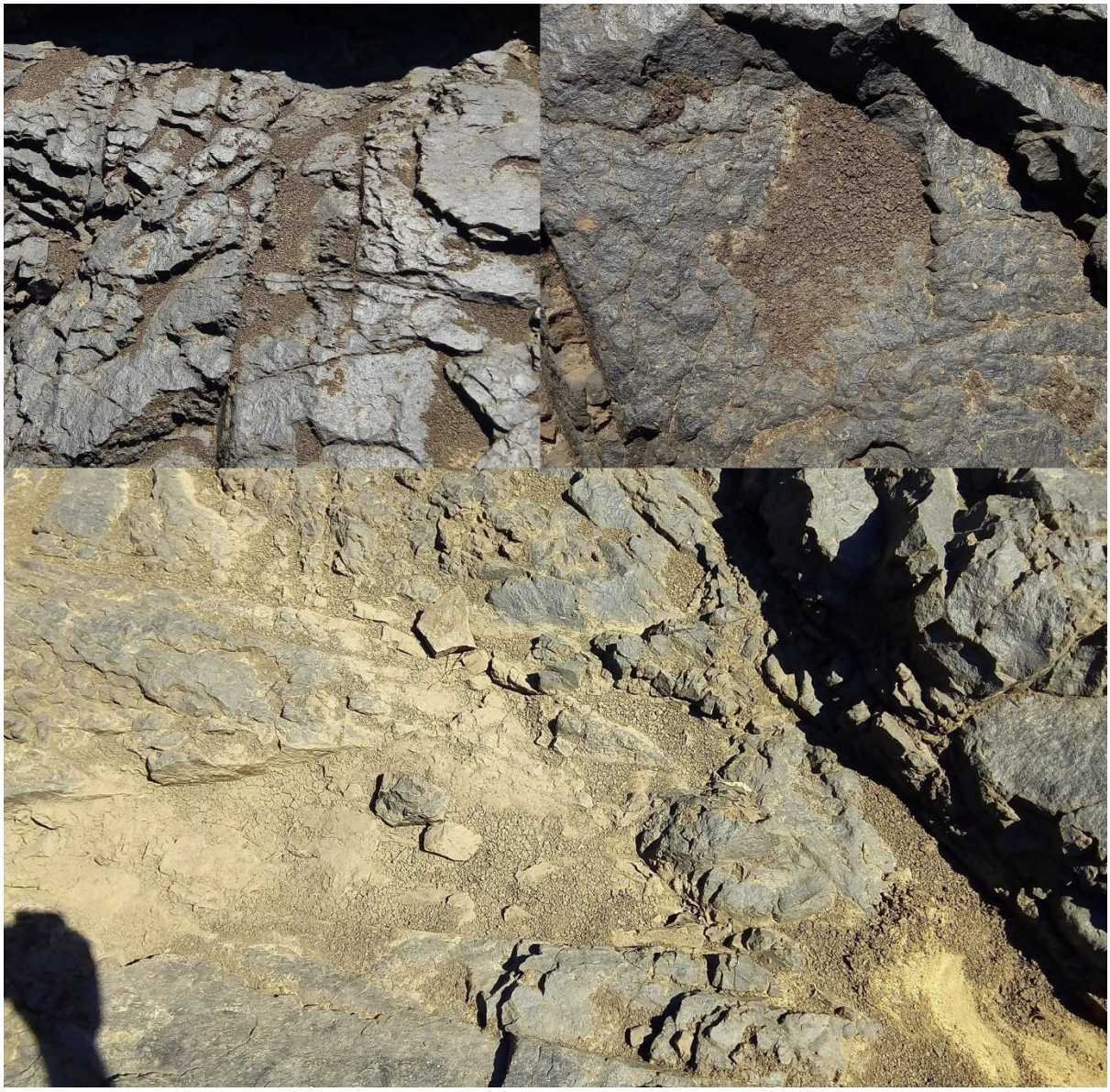

Figure 5.6. Flood deposit after a storm event in the outlet of the Ibirapuitã River. Source: Felipe Bernardi and Antônio A. Marquez.

In addition to the samples collected in the two tributaries (Conceição and Ibirapuitã), samples were collected from a sediment profile located on an island of the Uruguay River, situated downstream of the municipality of Uruguaiana, on the border with Argentina. Samples were collected in 5 cm layers down to a depth of 50 cm, and at 10 cm intervals down to a depth of 1 meter. These samples were used to make a first characterization of the sediment samples from the Uruguay River and compare them to the samples from the tributaries.

Figure 5.7. Sediment sampling in a deposit within an island of the Uruguay River. Source: the author.

5.6 Soils and sediment analysis

5.6.1 Sample preparation

Source and sediment samples were oven-dried at 45°C and gently disaggregated using pestle and mortar and sieved with a 2.0 mm mesh to remove gravels and coarse material. Soil source and sediment samples were divided into two parts, one preserved as <2.0 mm and the other sieved to 63 μm prior to the laboratory analysis in order to compare similar grain-size fractions for conducting the sediment fingerprinting approach (Koiter et al., 2013b; Laceby et al., 2017).

5.6.2 Biogeochemical analysis

For the Conceição River catchment samples, the biogeochemical tracers evaluated were total organic carbon (TOC) estimated by wet oxidation ($K_2Cr_2O_7$ + H_2SO_4) and the total concentration of several elements (Al, Ba, Be, Ca, Co, Cr, Cu, Fe, K, La, Li, Mg, Mn, Na, Ni, P, Sr, Ti, V, and Zn) using Inductively Coupled Plasma Optical Emission Spectrometry

after microwave-assisted digestion with concentrated HCl and HNO_3 (ratio 3:1) for 9.5 min at 182 °C.

For the Ibirapuitã river catchment, TOC, total nitrogen (TN), $\delta^{13}C$ and $\delta^{15}N$ isotope ratios were measured using continuous flow isotope ratio mass spectrometry (EA-IRMS). After sieving, the samples were hand-ground with a pestle and mortar to obtain a fine and homogeneous powder and weighted in tin capsules. A tyrosine laboratory standard was inserted after each successive 4 soil or sediment samples. X-ray diffraction analyses were performed to certify the absence of carbonates in representative samples from each source.

5.6.3 Magnetic susceptibility analysis

Samples from the Conceição, Ibirapuitã and Uruguay Rivers were analysed for magnetic susceptibility. Two grams of each sample were used to measure the magnetic susceptibility in a Bartington MS2B Dual Frequency sensor, with three readings for each sample in high (4.7 kHz) and low frequency (0.47 kHz) modes to obtain the mass specific magnetic susceptibility for high (χ_{HF} – $m^3\ kg^{-1}$) and low frequency (χ_{LF} – $m^3\ kg^{-1}$) (Mullins, 1977). Furthermore, the percentage of frequency dependent susceptibility (χ_{fd}) was calculated according to the Equation 1 (Dearing et al., 1996), which indicates the presence of viscous grains lying at the stable single domain/superparamagnetic boundary and their delayed response to the magnetizing field (Yu and Oldfield, 1989).

$$\chi_{fd}(\%) = 100 \times \left[\frac{(\chi_{LF} - \chi_{HF})}{\chi_{LF}}\right] \quad (1)$$

5.6.4 Radionuclide analyses

Samples for the Ibirapuitã and Uruguay Rivers were analysed for radionuclides. Fallout (^{7}Be, ^{137}Cs and ^{210}Pb) radionuclide activities were measured by gamma spectrometry using low-background high-purity germanium detectors (Canberra/Ortec). Between 10 to 20 grams of samples were weighted into polyethylene containers and sealed airtight and analysed on a detector installed into a lead-protected shield. Measurements were taken overnight (typically for 85,000 – 90,000 s) to optimise counting statistics. The fallout radionuclides ^{210}Pb, ^{7}Be and ^{137}Cs were obtained from the counts at 46.5 keV, 477.6 keV and 661.6 keV, respectively. The unsupported or excess

lead-210 ($^{210}Pb_{xs}$) was calculated by subtracting the supported activity from the total ^{210}Pb activity using two ^{238}U daughters, i.e. ^{214}Pb (average count at 295.2 and 351.9 keV) and ^{214}Bi (609.3 keV). Radionuclide activities were decay-corrected to the sampling date.

5.6.5 Ultra-violet-visible, near and mid infrared diffuse reflectance analysis

5.6.5.1 Ultra-violet-visible diffuse reflectance analysis

Samples from the Conceição and Ibirapuitã Rivers were analysed for ultra-violet-visible (UV). The diffuse reflectance spectra in the UV wavelengths (200 to 800 nm, with 1 nm step) were measured for each powdered sample using a Cary 5000 UV-NIR spectrophotometer (Varian, Palo Alto, CA, USA) at room temperature. Samples were added into the sample port and care was taken to avoid differences in sample packing and smoothness of the surface. $BaSO_4$ was used as a 100% reflectance standard.

Twenty-four colour parameters were calculated from the ultraviolet-visible spectra following the colorimetric models described in detail by Viscarra Rossel et al. (2006), which are based on the Munsell HVC, RGB, the decorrelation of RGB data, CIELAB and CIELUV Cartesian coordinate systems, three parameters from the HuterLab colour space model and two indices (coloration – CI and saturation index – SI). First, the colour coefficients XYZ based on the colour-matching functions defined by the International Commission on Illumination - CIE (CIE, 1931) were calculated, where X and Z are the virtual components of the primary spectra and Y represents the brightness. The XYZ tristimulus were standardised with values corresponding to the Standard Illuminant D65 white point for 10 Degree Standard Observer (X = 94.8110; Y = 100.00; Z = 107.304), then transformed into the Munsel HVC, RGB, CIELAB and CIELUV Cartesian coordinate systems using the equations from CIE (1978). Three parameters from the HunterLab (HunterLab, 2015) colour space model, and two indices (coloration - CI and saturation index - SI) (Pulley et al., 2018) were calculated as well. In total, 27 colourimetric parameters were derived from the spectra of potential source and sediment samples (L, L*, a, a*, b, b*, C*, h, RI, x, y, z, u*, v*, u', v', Hvc, hVc, hvC, R, G, B, HRGB, IRGB, SRGB, CI and SI).

Three other parameters were calculated from the second derivative curves of remission functions in the visible range of soil and sediment samples, which displayed three major absorption bands at short wavelengths commonly attributed to Fe-oxides (Caner et al., 2011; Fritsch et al., 2005; Kosmas et al., 1984; Scheinost et al., 1998). The

first band (A1, ~430 nm) corresponds to the single electron transition of goethite (Gt), whereas the two others correspond to the electron pair transition for goethite (A2, ~480 nm) and for hematite (Hm) (A3, ~520 nm), respectively (Figure B1). The band intensity is estimated from the amplitude between a minimum and the nearby maximum at its lower energy side. The amplitudes of the three bands (A1, A2 and A3) are positively correlated with the contents of Gt and Hm (Fritsch et al., 2005). A1 and A3 are commonly used to assess the content of Gt and Hm, respectively, and the relative proportions of hematite in Fe oxides (Hr) are estimated by applying the equation Hr (%) = Hm/(Hm+Gt). The band intensities were measured from the amplitude between each band minimum and its nearby maximum at higher wavelength.

5.6.5.2 Fourier Transform Infrared Spectroscopy analysis

Fourier Transform Infrared (FTIR) spectroscopy analyses were carried out in the range of near (NIR) and mid infrared (MIR) wavelengths (10000 – 4000 cm^{-1} and 4000 – 400 cm^{-1}, respectively) for the Conceição and Ibirapuitã River samples. NIR spectra was measured using a Nicolet 26700 FTIR spectrometer (Waltham, Massachusetts, USA) in diffuse reflectance mode with an integrating sphere with an internal InGaAs detector with 2 cm^{-1} resolution and with 100 co-added scans per spectrum. MIR spectra were measured using a Nicolet 510-FTIR spectrometer (Thermo Electron Scientific, Madison, WI, USA) in reflection mode with a 2 cm^{-1} resolution and with 100 co-added scans per spectrum. The spectrometer was continuously purged with dry CO_2 depleted air. For both analyses, care was taken when adding a sample into the sample port to avoid differences in sample packing and smoothness of the surface. Resulting data were collected and converted into 1 nm resolution using the Omnic software supplied by the spectrometer manufacturer (Thermo-Nicolet, USA).

Table 5.1. Summary with the types of samples collected and analyses performed on each of them.

Sampling site	Sampling strategy	Analyses						
		Biogeochemical		Diffuse reflectance			Radionuclide	Magnetic susceptibility
		Geochemical elements	Organic matter composition	UV	NIR	MIR		
Conceição River - Outlet	Source samples	x	x[1]	x	x	x		x
	TISS	x	x[1]	x	x	x		x
	FBS	x	x[1]	x	x	x		x
	Event			x	x	x		
Ibirapuitã River - Outlet	Source samples		x	x	x		x	x
	TISS		x	x	x		x	x
	FD		x	x	x		x	x
	Event		x	x	x		x	
Ibirapuitã River - EPA catchment outlet	TISS		x	x	x		x	x
	FD		x	x	x		x	x
Ibirapuitã River - Caverá catchment outlet	TISS		x	x	x		x	x
Ibirapuitã River - Pai-Passo catchment outlet	TISS		x	x	x		x	x
Uruguay River	Sediment deposit				x		x	x

[1]Total organic carbon only; UV - Ultra-violet-visible; NIR - Near Infrared; MIR - Mid Infrared; TISS - Time Integrated Suspended Sediment; FBS - Fine-bed Sediment; FD - Flood Deposit; Event – samples collected during rainfall-runoff events.

5.7 Sediment source discrimination and apportionment

Two different methodologies for the sediment source discrimination and apportionment were applied. The first one, where the approaches were based on discrete variables (geochemical, magnetic, radionuclides and UV derived parameters), a classical method based on a three-step procedure to selected the best set of variables was applied: i) a range test; ii) the Kruskal-Wallis *H* test (KW *H* test); and iii) a linear discriminant function analysis (LDA). The best set of variables selected by the LDA were then included in the mixing model (Collins et al., 2010a). In the second method, multivariate models were calibrated with the spectral data of artificial mixtures with known proportions from each source and used to predict the source contributions to the sediment samples (Brosinsky et al., 2014; Poulenard et al., 2009).

In the range test for discrete variables, sediment concentration or values lying outside the range of the sources were excluded. Three methods were tested: i) the values observed in the sediment samples should lie within the minimum and maximum values observed in the sources; ii) the average values ± one standard deviation for the sediment samples should remain within the average ± on standard deviation of each individual source; and iii) the sediment median values ± the 25th or 75th percentiles should be comprised within the range defined as the median values ± the 25th or 75th percentiles of the source (IQR). The KW *H* test was performed to test the null hypothesis ($p < 0.05$) that the sources belong to the same population. The variables that provided significant discrimination between sources were analysed with a forward stepwise LDA ($p < 0.1$) in order to reduce the number of variables to a minimum that maximizes source discrimination (Collins et al., 2010b). The statistical analyses were performed with R software (R Development Core Team, 2017) and more details on the model can be found in Batista et al. (2018).

The source contributions were estimated by minimizing the sum of squared residuals (SSR) of the mass balance un-mixing model:

$$SSR = \sum_{i=1}^{n} \left(\left(C_i - \left(\sum_{s=1}^{m} P_s S_{si} \right) \right) / C_i \right)^2 \quad (2)$$

where n is the number of variables/elements used for modelling, C_i is the concentration of the element i in the target sediment, m is the number of sources, P_s is the optimized

relative contribution of source *s*, and S_{si} is the concentration of element *i* in the source *s*. Optimization constraints were set to ensure that source contributions were non-negative and that their sum equalled 1. The un-mixing model was solved by a Monte Carlo simulation with 2500 iterations. More information about model settings and compilation can be found in Batista et al. (2018).

For the second method based on multivariate spectral models, artificial mixtures with known proportion of each source have to be prepared to calibrate and validate the models. Samples of each source were mixed in equal proportions in order to prepare a single sample representative for the corresponding source. The reference samples of each source were then mixed with different weight proportions to obtain different source material ratios to calibrate the multivariate models and for validation of the mixing model results. The UV, NIR and MIR spectra were obtained for each mixture and the corresponding weight contribution of each sediment source were analysed by multivariate models (e.g. partial least square regression – PLSR and support vector machine – SVM). The model fitted from the spectra with known proportions was used to estimate the contribution of each source to the sediment samples (Poulenard et al., 2012; Tiecher et al., 2017a). The model accuracy was evaluated by the coefficient of determination (R^2) and the mean square root of the prediction error (RMSE).

5.8 References

Alvares, C.A., Stape, J.L., Sentelhas, P.C., de Moraes Gonçalves, J.L., Sparovek, G., 2013. Köppen's climate classification map for Brazil. Meteorol. Zeitschrift 22, 711–728. https://doi.org/10.1127/0941-2948/2013/0507

Batista, P.V.G., Laceby, J.P., Silva, M.L.N., Tassinari, D., Bispo, D.F.A., Curi, N., Davies, J., Quinton, J.N., 2018. Using pedological knowledge to improve sediment source apportionment in tropical environments. J. Soils Sediments. https://doi.org/10.1007/s11368-018-2199-5

Brosinsky, A., Foerster, S., Segl, K., Kaufmann, H., 2014. Spectral fingerprinting: sediment source discrimination and contribution modelling of artificial mixtures based on VNIR-SWIR spectral properties. J. Soils Sediments 14, 1949–1964. https://doi.org/10.1007/s11368-014-0925-1

Collins, A.L., Walling, D.E., Webb, L., King, P., 2010a. Apportioning catchment scale sediment sources using a modified composite fingerprinting technique

incorporating property weightings and prior information. Geoderma 155, 249–261. https://doi.org/10.1016/j.geoderma.2009.12.008

Collins, A.L., Zhang, Y., Walling, D.E., 2010b. Apportioning sediment sources in a grassland dominated agricultural catchment in the UK using a new tracing framework. Sediment Dyn. a Chang. Futur. 337, 68–75.

Dearing, J.A., Dann, R.J.L., Hay, K., Lees, J.A., Loveland, P.J., Maher, B.A., Grady, K.O., Survey, S., Mk, B., 1996. Frequency-dependent susceptibility measurements of environmental materials. Geophys. J. Int. 228–240.

Didoné, E.J., Gomes Minella, J.P., Andres Schneider, F.J., Londero, A.L., Lefèvre, I., Evrard, O., 2019. Quantifying the impact of no-tillage on soil redistribution in a cultivated catchment of Southern Brazil (1964–2016) with 137Cs inventory measurements. Agric. Ecosyst. Environ. 284, 106588. https://doi.org/10.1016/j.agee.2019.106588

Didoné, E.J., Minella, J.P.G., Merten, G.H., 2015a. Quantifying soil erosion and sediment yield in a catchment in southern Brazil and implications for land conservation. J. Soils Sediments 15, 2334–2346. https://doi.org/10.1007/s11368-015-1160-0

Didoné, E.J., Paolo, J., Minella, J.P.G., Merten, G.H., 2015b. Quantifying soil erosion and sediment yield in a catchment in southern Brazil and implications for land conservation Quantifying soil erosion and sediment yield in a catchment in southern Brazil and implications for land conservation. https://doi.org/10.1007/s11368-015-1160-0

Horowitz, A.J., Stephens, V.C., Elrick, K.A., Smith, J.J., 2012. Concentrations and annual fluxes of sediment-associated chemical constituents from conterminous US coastal rivers using bed sediment data. Hydrol. Process. 26, 1090–1114. https://doi.org/10.1002/hyp.8437

Koiter, A.J., Owens, P.N., Petticrew, E.L., Lobb, D.A., 2013. The behavioural characteristics of sediment properties and their implications for sediment fingerprinting as an approach for identifying sediment sources in river basins. Earth-Science Rev. 125, 24–42. https://doi.org/10.1016/j.earscirev.2013.05.009

Laceby, J.P., Evrard, O., Smith, H.G., Blake, W.H., Olley, J.M., Minella, J.P.G., Owens, P.N., 2017. The challenges and opportunities of addressing particle size effects in sediment source fingerprinting: A review. Earth-Science Rev. 169, 85–103. https://doi.org/10.1016/j.earscirev.2017.04.009

Mullins, C.E., 1977. Magnetic Susceptibility of the Soil and Its Significance in Soil Science

– a Review. J. Soil Sci. 28, 223–246. https://doi.org/10.1111/j.1365-2389.1977.tb02232.x

Poulenard, J., Legout, C., Némery, J., Bramorski, J., Navratil, O., Douchin, A., Fanget, B., Perrette, Y., Evrard, O., Esteves, M., 2012. Tracing sediment sources during floods using Diffuse Reflectance Infrared Fourier Transform Spectrometry (DRIFTS): A case study in a highly erosive mountainous catchment (Southern French Alps). J. Hydrol. 414–415, 452–462. https://doi.org/10.1016/j.jhydrol.2011.11.022

Poulenard, J., Perrette, Y., Fanget, B., Quetin, P., Trevisan, D., Dorioz, J.M., 2009. Infrared spectroscopy tracing of sediment sources in a small rural watershed (French Alps). Sci. Total Environ. 407, 2808–2819. https://doi.org/10.1016/j.scitotenv.2008.12.049

R Development Core Team, 2017. R: a language and environment for statistical computing.

Tiecher, T., 2015. Fingerprinting sediment sources in agricultural catchments in Southern Brazil. Universidade Federal de Santa Maria.

Tiecher, T., Caner, L., Minella, J.P.G., Evrard, O., Mondamert, L., Labanowski, J., Rheinheimer, D. dos S., 2017. Tracing Sediment Sources Using Mid-infrared Spectroscopy in Arvorezinha Catchment, Southern Brazil. L. Degrad. Dev. 28, 1603–1614. https://doi.org/10.1002/ldr.2690

Yu, L., Oldfield, F., 1989. A multivariate mixing model for identifying sediment source from magnetic measurements. Quat. Res. 32, 168–181. https://doi.org/10.1016/0033-5894(89)90073-2

6 Chapter 1. Sediment fingerprinting using geochemical tracers: a global meta-analysis

6.1 Introduction

The sediment tracing technique has been used in several studies around the world to identify the main sources of sediment and indicate where efforts to control soil erosion processes should be concentrated (Collins et al., 2017a). Soil erosion has been considered as a risk to ensure food, fibre and energy production in the future, but also as a potential source of diffuse pollution. Soil erosion studies have increased significantly in recent years. According to a FAO report recently published (FAO, 2019), in the last 3 years (2016-2018) the number of published articles on soil erosion was greater than that released during the entire 20th century (5698 articles published between 1931 and 1999), with 7348 articles published, according to a survey using the Web of Science database. Studies on sediment fingerprinting also increased sharply in the last three decades, providing a lot of information about the sediment dynamics at the catchment scale. According to a review of Walling (2013), the number of articles reporting sediment source investigations increased exponentially from the first studies carried out in the 1970s to 2013, where around 50 studies were accounted for the year 2013 only. More recently, Collins et al. (2020) published a bibliographic review discussing the main themes related to sediment source fingerprinting and showed that the number of articles on this subject continue to increase. According to this more recent bibliometric review based on a search in the Web of Science and Google Scholar, an average of 31 articles per year have been published in the period between 2013 and 2019.

Notwithstanding, according to Poesen (2017), additional studies are still needed to understand the human impacts on soil erosion, mainly in large catchments or at the regional scale, in order to analyse the links between soil erosion and its off-site effects (Boardman et al., 2019). Therefore, to identify and diagnose the problems associated with the transfer of sediments, nutrients and contaminants to water resources have gained scientific relevance and their sources need to be quantified (Mukundan et al., 2012; Owens and Xu, 2011).

Sediment fingerprinting studies have been developed for identifying the main erosion problems, to understand the erosion processes and their impacts at the river

catchment scale, and for directing solutions to the origin of the problems. There is no defined methodology that can be applied in all cases and in any environment, since the properties of soils and sediments vary according to the natural processes of formation (parent material, climate, relief, living organisms and time), which requires specific tracers or research designs (Collins et al., 2020; Motha et al., 2002). Although there is no single methodology, several premises of the method must be met, including that: i) the tracers must be conservative, i.e., the values of a certain parameter must lie within the limits defined by their variability observed in the sources or vary in a predictable way; ii) the parameters used must have a discrimination potential between at least two sources; and iii) the tracer values in the sediment must be linearly additive in relation to its sources (Haddadchi et al., 2013). Accordingly, attempts to trace sediments may be risky, since investment in high-cost and time-consuming analyses may not be efficient in discriminating between the potential sources observed or may not meet the method's premises.

Therefore, several types of parameters have been tested as tracer variables, among them parameters based on magnetic properties (Black et al., 1965; Slattery et al., 1995), fallout radionuclides (Collins et al., 2001; Evrard et al., 2016; Gaspar et al., 2013; Porto et al., 2014; Walling and Quine, 1992), colour and spectral properties (Barthod et al., 2015; Martínez-Carreras et al., 2010c, 2010b, 2010a; Pulley et al., 2018; Tiecher et al., 2015), mineralogy (Motha et al., 2003), geochemical elements (Lamba et al., 2015; Tiecher et al., 2018), organic matter composition (TOC, TN, $\delta^{15}N$ and $\delta^{13}C$) (Blake et al., 2012; Brandt et al., 2018; Fox and Papanicolaou, 2007; Minella et al., 2008b; Sloto et al., 2012).

Fallout radionuclides (^{137}Cs, $^{210}Pb_{xs}$, ^{7}Be) are the most consolidated tracers, as they are considered to be the most reliable and accurate tracers to calculate the contribution of surface and subsurface sediment sources, especially for ^{137}Cs (Evrard et al., 2016; Wallbrink and Murray, 1993). Subsequently, the second classic set of tracers for sediment tracing is the geochemical composition, usually used as a reference to validate other alternative tracer results (Martínez-Carreras et al., 2010c; Tiecher et al., 2016). This type of tracer allows the evaluation of a large number of parameters, usually analysed by means of multi-elemental techniques such as inductively coupled plasma mass spectrometry (ICP-OES/MS) or X-ray fluorescence (XRF). Geochemistry has been pointed out by the review of Collins et al. (2020) as the most used set of tracers in fingerprinting

studies, followed by radionuclides. The variability of the factors controlling the concentration of certain elements, allows differentiating contrasted parent materials for example, which controls the basic geochemical composition of soil and sediments, but also differentiates land uses, since different processes of formation, positions in the landscape, uses of fertilizers among others, may modify the chemical composition of the soil.

Accordingly, different environmental conditions may lead to a specific set of geochemical tracers being more efficient for each study. Because of this complexity involving the use of geochemical tracers, to the best of our knowledge, there is no indication in the literature on what would be the most appropriate chemical elements for tracing sediment sources. However, it is possible that specific chemical properties of certain elements, based on their ionic potential for example, may increase the probability of these being effective in discriminating between sediment sources. Therefore, the purpose of this chapter is to identify which geochemical tracers are more commonly selected to discriminate between potential sediment sources based on a review of a set of articles published in scientific journals and to identify trends related to the chemical elements being more frequently selected. Furthermore, another objective is to analyse the statistical procedures used to select the potential tracers, and identify the relationships between the tracers selected, the statistical methods used and the study designs.

6.2 Methodology

6.2.1 Review strategy

This review was conducted with the objective of compiling sediment fingerprinting articles that incorporated the geochemical composition in the potential suite of tracers used to discriminate between potential sediment sources and analyse those that were selected in each study, according to the different methods applied. The search was performed in English in the Web of Science (WoS) database with the following conditions: TOPIC: ("sediment fingerprint*") AND TOPIC: ("soil erosion") OR TOPIC: ("sediment trac*") AND TOPIC: ("soil erosion") OR TOPIC: ("sediment source*") AND TOPIC: ("soil erosion"). The search was conducted in November 2019, resulting in a set of 374 articles and 14 reviews about the subject of interest. The articles were

systematically reviewed to remove all those which have not met the following criteria: include geochemical tracers; consider agricultural areas, tributaries or geological material as potential sources; apply a quantitative sediment fingerprinting approach; and being published before 2017, included. Articles cited in the 388 articles which were not individually covered by the previous web search were also included in order to expand the number of publications compiled, to satisfy the demand of this systematic review. As a result, after a screening according to the established criteria, a total of 111 articles were retained which used geochemical tracers, but only 88 articles presented all the information required for further analyses.

6.2.2 Data base and analysis

The information collected from the retained articles was organized in a spreadsheet in which the bibliometric data was collected as well the data of interest for the meta-analysis. The main information collected from each article was: bibliometric information (authors, title, year of publication, journal), catchment under study, geographical position, surface area of the catchment, types and number of sediment sources, number of samples to characterize the sources, type of sediment samples, number of sediment samples, particle size fraction of interest, correction factors applied, tracers evaluated, statistical tests and tracers selected at each stage (conservative test, mean test and discriminant analysis), percentage of samples correctly classified by the discriminant analysis and the type of mixing model used. Some of the articles used more than one sediment fingerprinting approach. An approach is considered as a sediment fingerprinting procedure which is applied to an individual catchment using a determined set of tracers, a given statistical procedure and a specific mixing model. As an example, if in one publication, the authors tested different sets of tracers in the same catchment, each test was considered as an individual approach. Overall, 111 publications and 463 approaches have been reviewed, each of which considered at least geochemical elements as tracers, and from those, only 88 articles and 310 approaches met all the criteria to be included in the final meta-analysis.

The list of geochemical tracers identified is: Ag, Al, Al_{di}, Al_{di+py}, Al_{ox}, Al_{py}, As, Au, B, Ba, Be, Bi, Br, Ca, Cd, Ce, Cl, Co, Cr, Cs, Cu, Dy, Er, Eu, Fe, Fe_{di}, Fe_{di+py}, Fe_{ox}, Fe_{py}, Ga, Gd, Ge, H, Hf, Hg, Ho, In, Ir, K, La, Li, Lu, Mg, Mn, Mn_{di}, Mn_{di+py}, Mn_{ox}, Mn_{py}, Mo, Na, Nb, Nd, Ni, Os, P, P_{in}, P_{or}, Pb, Pd, Pr, Pt, Rb, Re, Rh, Ru, S, Sb, Sc, Se, Si, Sm, Sn, Sr, Ta, Tb, Te, Th, Ti, Tl, Tm,

TN, TOC, TS, U, V, W, Y, Yb, Zn and Zr. The Al, Fe and Mn quantified by different chemical extraction (organic – or, inorganic – in, oxalate extractable – ox, dithionite extractable – di, pyrophosphate extractable – py) methods were included as their elemental form, since both fractions were analysed in the same articles. The selected elements in each step of the sediment fingerprinting approach (range test, mean test or selected to be included in the model by a discriminant function analysis) were evaluated according to their chemical characteristics.

6.3 Results and discussion

6.3.1 Literature overview

The first sediment fingerprinting studies using geochemical elements were published in 1986 and 1988 by Peart and Walling (1986, 1988). The authors used the content of Mn and P content, some Fe fractions, and the C/N ratio as potential tracers to quantify the contribution of two sources using a simple mixing model in two British catchments. Until 2001, all the fingerprinting studies evaluated in the current meta-analysis (n=13) were developed in England, by the team of Professor Walling. The same authors developed studies in Zambia and Scotland (n=4), in the following years until 2003. In 2003 and 2004, the first sediment fingerprinting approach using geochemical elements conducted by other research groups were developed in Australia by Krause et al. (2003) and in Brazil by Minella et al. (2004). Then, sediment fingerprinting studies using geochemical elements have been widely developed in other countries around the world as shown in Figure 6.1, although most of them continued to be developed in the UK. Several fingerprinting studies have been conducted in the USA as well. According to the survey done in the WoS, the largest number of studies was developed in this country (Figure 6.2). This is likely mainly due to the wide river monitoring network available and the obligation to make data publicly available in this country.

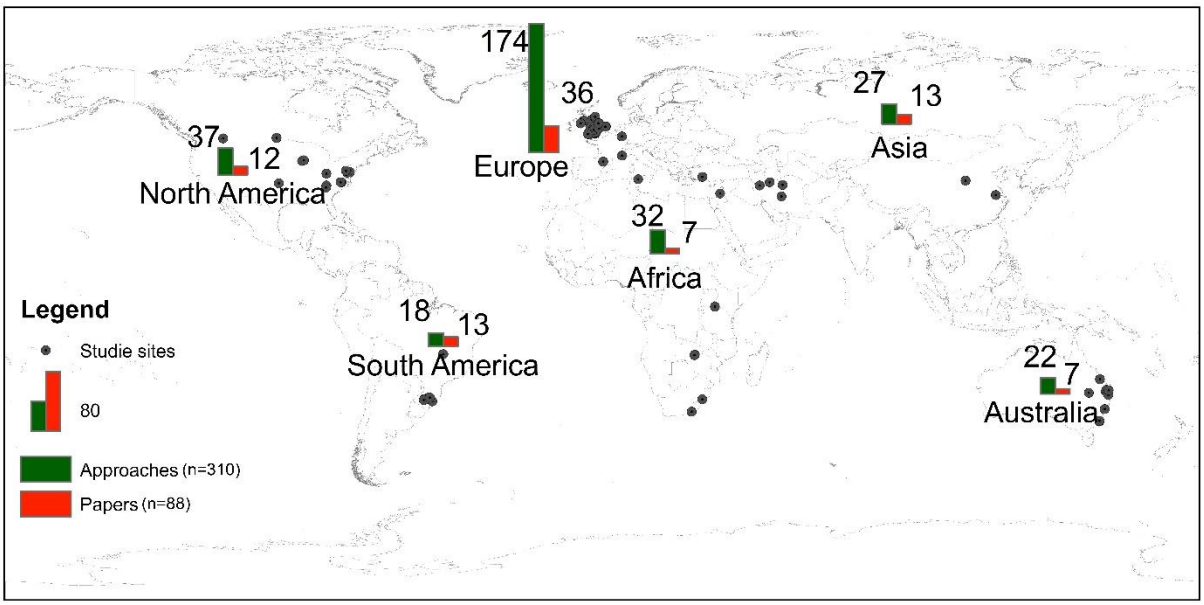

Figure 6.1. Distribution of sediment fingerprinting studies that used geochemical tracers around the world, based on the number of scientific articles (n=88) and the approaches (n=310) used.

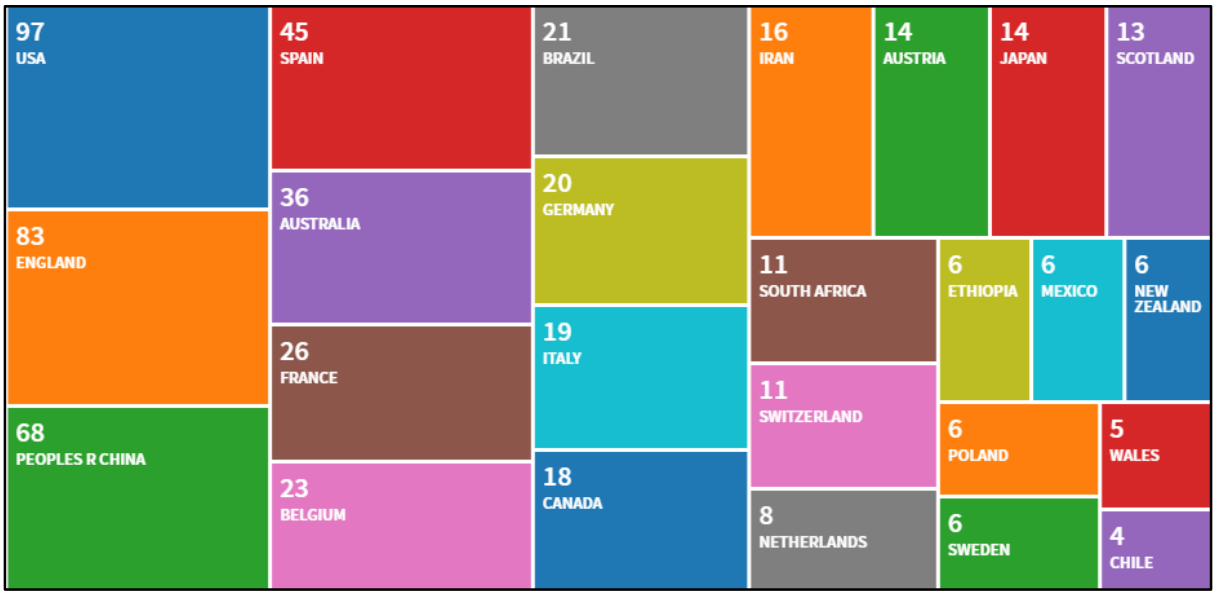

Figure 6.2. Number of sediment fingerprinting studies by country according to the search made on WoS.

The number of fingerprinting studies using geochemical tracers has increased exponentially, mainly in the last 15 years, as shown in Figure 6.4. However, these numbers remain low when they are compared to those of the sediment tracing studies using all types of tracers, i.e. 388 publications according to the search made using WoS (Figure 6.3). This search results differ slightly from the estimation of Walling (2013), who found approximately 500 articles published until 2013. The results are highly dependent on the restrictions made with the search terms and the article availability on scientific

web search engines. As an example, the first three articles referred to by Walling (2013) published in 1986 and 1988 were not detected in the search on WoS (Figure 6.3), and they were manually included in our search (Figure 6.4).

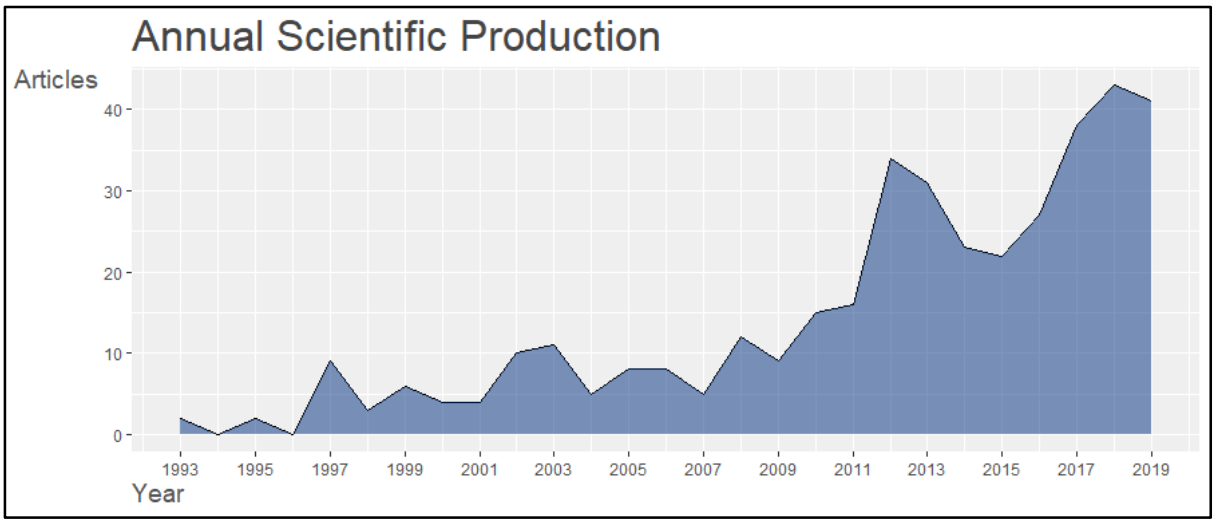

Figure 6.3. Number of scientific articles published each year based on the WoS search (n=388).

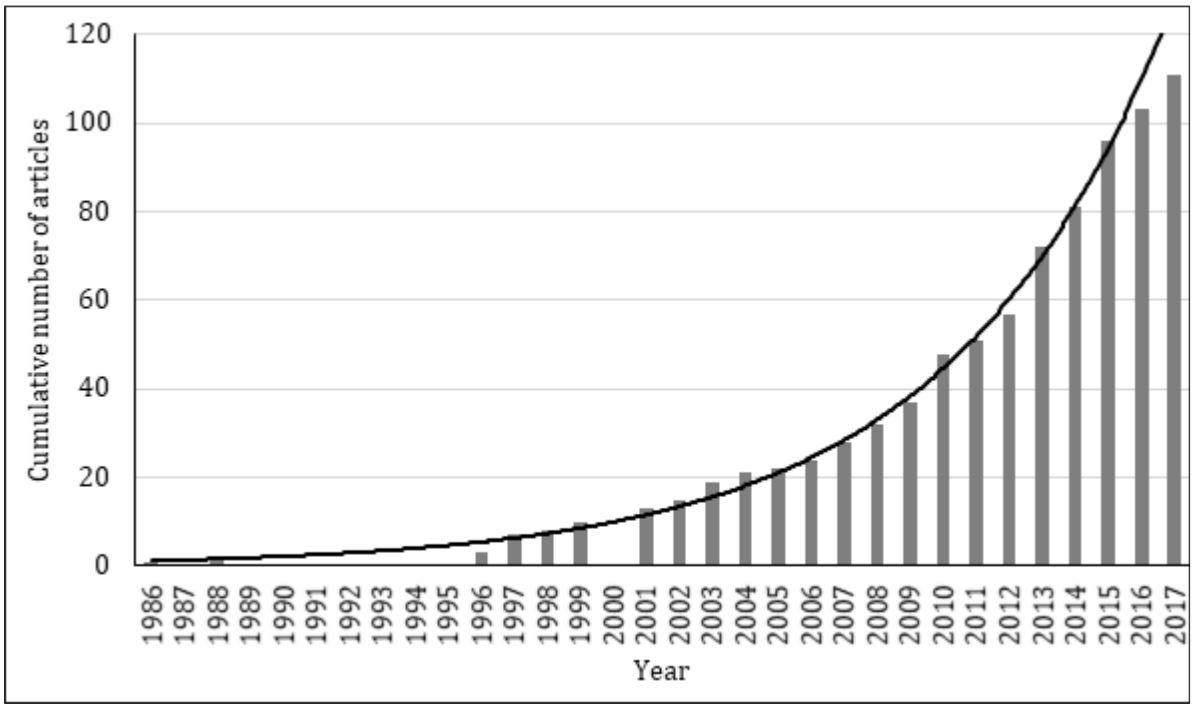

Figure 6.4. Cumulative distribution of the final set of 111 reviewed articles – making use of geochemical tracers – with time.

The list of authors who published the most over time is presented in Figure 6.5. Professor Desmond Walling, a pioneer in sediment tracing, followed by his former PhD students Willian Blake and Adrian Collins, have remained the leading researchers in the

field over time, according to the search performed using WoS (Figure 6.5). However, the result is only an approximation, since the search could not cover all the sediment fingerprinting studies as mentioned earlier.

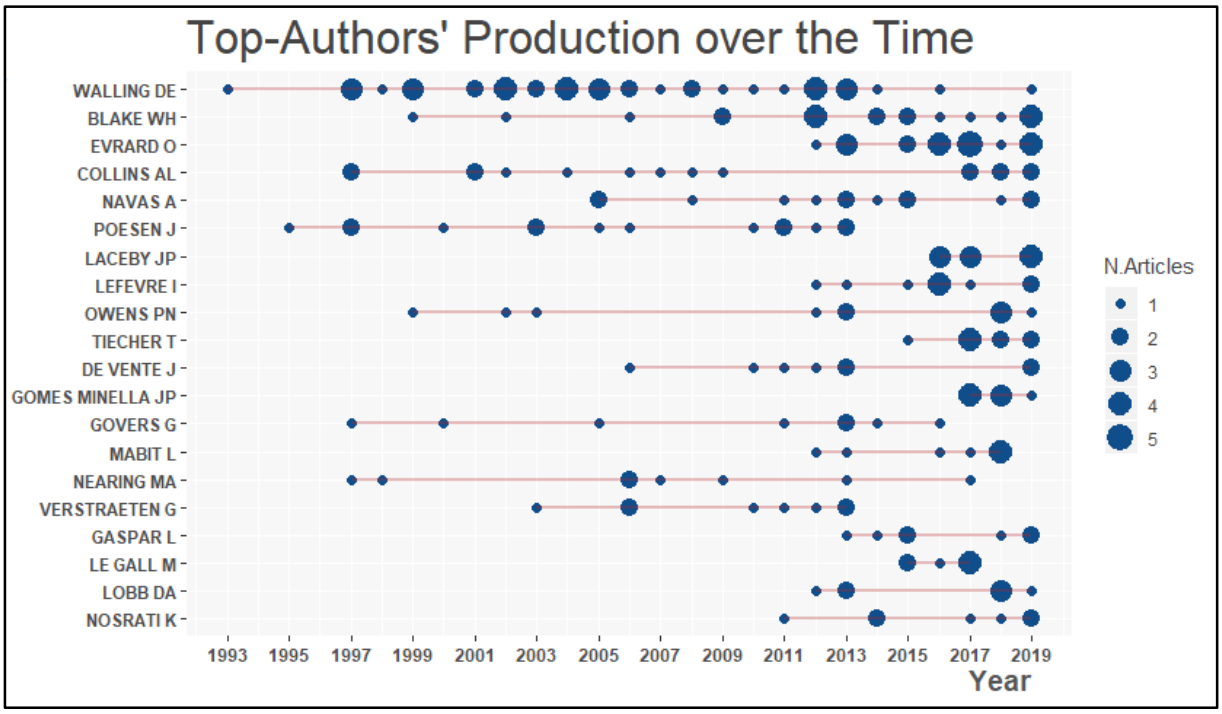

Figure 6.5. Top 20 authors' production over the time according to the search on WoS (n=374).

6.3.2 Methodological aspects

The tracer selection in the classical sediment fingerprinting approach based on discrete variables, usually follows a three-step procedure, including: (i) a conservative range test, (ii) a non-parametric test (Mann-Whitney *U*-test or Kruskal–Wallis *H*-test), and (iii) a discriminant function analysis (DFA) or a principal component analysis (PCA) (Collins et al., 2010a). In the conservative range test, it is verified whether the value observed in the sediment variables lies within the range observed for the sources. If it falls out of the source range, it is removed from the following steps. In the second step, the purpose of the non-parametric test is to check the null hypothesis that the sources belong to the same population: if a variable differs statistically for each source, it can be used as a tracer. The third step is to determine the minimum number of tracers that maximizes the discrimination among the sources, defining the set of tracers to enter in the mixing model. The most commonly used parameter to verify the efficiency of a set of tracers in maximizing the discrimination between sources, is the percentage of correctly reclassified samples according to their source group (SCC), obtained from the DFA. This

parameter was used in this study to verify the impact of the different versions of the method on the quality of the discrimination between the sources achieved by the selected tracers.

From all the articles revised, only 60% (n=186) applied a conservative test to verify whether the values observed in the sediment samples fitted within the range found in the sources, which is one of the main prerequisites of the sediment fingerprinting method. Surprisingly, the studies that used a conservative test showed lower percentage of source samples correctly classified (90.7% for those with mean test and 86.3% without mean test) compared to studies that did not use a conservative test (95.1.7% for those with mean test and 90.6% without mean test) (Figure 6.6a). This may be a result of the greater discard of potential tracers when using the conservative test. For example, in a study of Smith and Blake (2014) in two of the catchments studied in England, 50% of the tracers were discarded from the analysis because they did not present conservative characteristics, resulting in SCC below 76% due to restricted number that enter in the model. For other catchments that had a larger number of tracers available, SCC was higher than 92%. Similar results were also described by Manjoro et al. (2017), where many tracers where not conservative and the optimum fingerprints resulted in SCC below 72%. On the other hand, when tracers are not discarded by the conservative test, a larger number of potential tracers can reach the final stage of the discriminant analysis, thus resulting in greater percentage of source samples correctly classified. It is important to note, however, that this does not mean that the modelling results will be better, since there is a risk of running the models with tracers with high degree of uncertainty.

Another important point that should be highlighted is that the conservativity tests vary greatly among studies. There are records that consider tracers as conservative when the tracers value falls within the median ±one median absolute deviation (Pulley et al., 2015a), or when they fit into the range of the sources (Laceby et al., 2015; Mukundan et al., 2010; Palazón and Navas, 2017), bi-plots (Pulley et al., 2015b), based on evidence of enrichement (Martínez-Carreras et al., 2010b), interquartile range (Batista et al., 2018), among others. As already stated by Collins et al. (2020), it is necessary to evaluate a way to standardise the methods for applying the technique in order to have more robust results.

The use of mean test as one of the steps in the tracer selection resulted in correct classification of sources higher (93%) than when no mean test was used (87%) to

selected potential tracers (Figure 6.6). Although the discriminant analysis can be performed with all the potential tracers analyzed, the results obtained in the present study clearly demonstrate that there is a significant gain in the correct classification of the sources when the mean test is used as a prerequisite in fingerprinting studies.

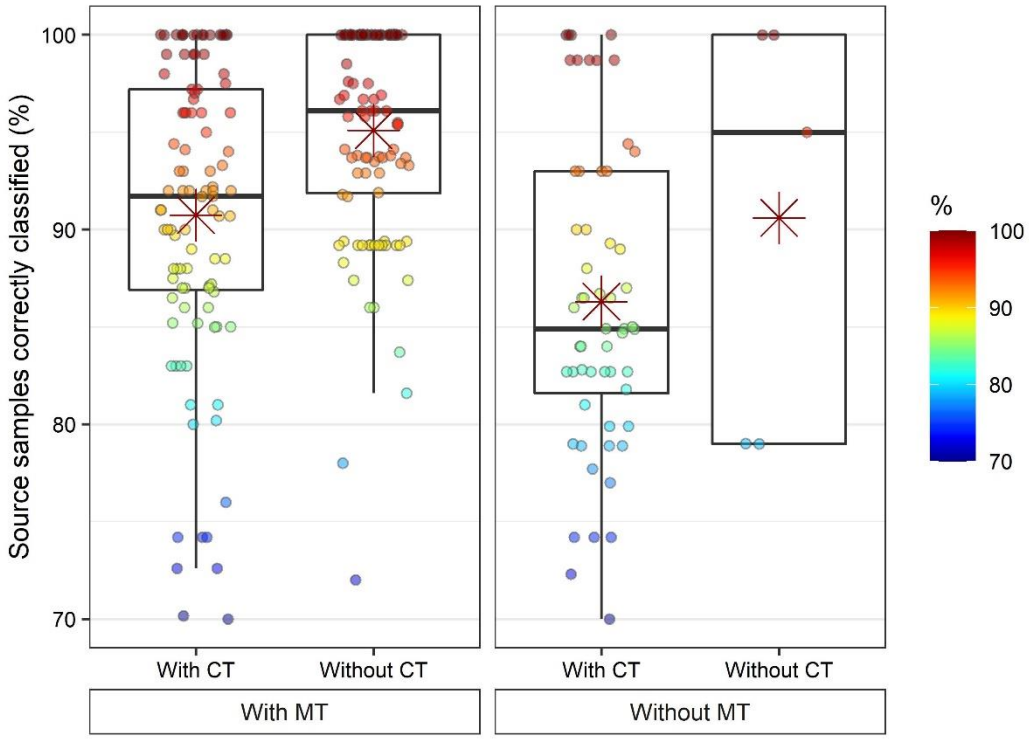

Figure 6.6. Source samples correctly classified by the discriminant analysis in studies using or not conservative test (CT) and using or not mean test (MT) as a prerequisite for tracer selection.

Another important factor is the adequate characterization of the sediment sources. As the size of the catchment increases, there is an increase in the heterogeneity of the sources as well as in the variability within each individual source, which requires a larger number of samples to properly characterize them (Collins et al., 2017b; Pulley et al., 2017). Besides that, the different catchment size can play a role in the selection of the potential tracers, since the increased distance between the sediment and its sources increases the probability of the sediment undergoing chemical and physical disturbances during its transit (Koiter et al., 2013b). The combined analysis of the literature shows that when the catchment size is smaller than 10 km^2, there is a slightly better reclassification of the sources by the DFA (Figure 6.7 and Figure 6.9). It would also be expected that the discriminatory power of potential sources decreases with the increase in the catchment area and with the increase in the number of potential sources of sediment considered.

However, no clear tendency of discrimination and number of potential sources considered was observed (Figure 6.8).

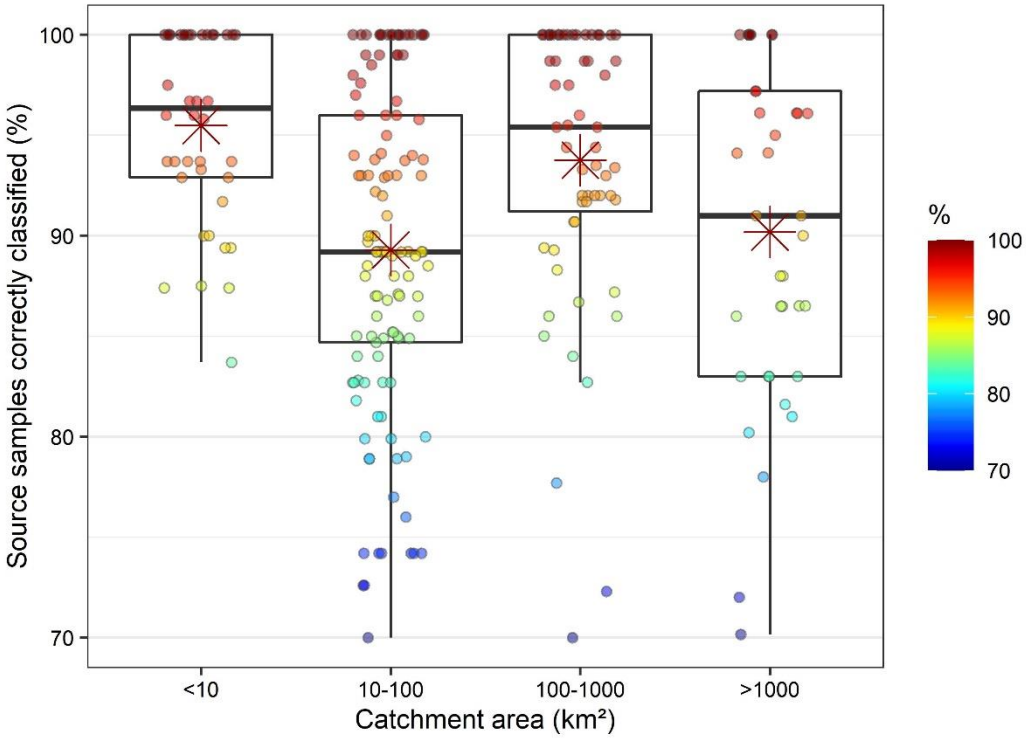

Figure 6.7. Percentage of source samples correctly classified according to the catchment size.

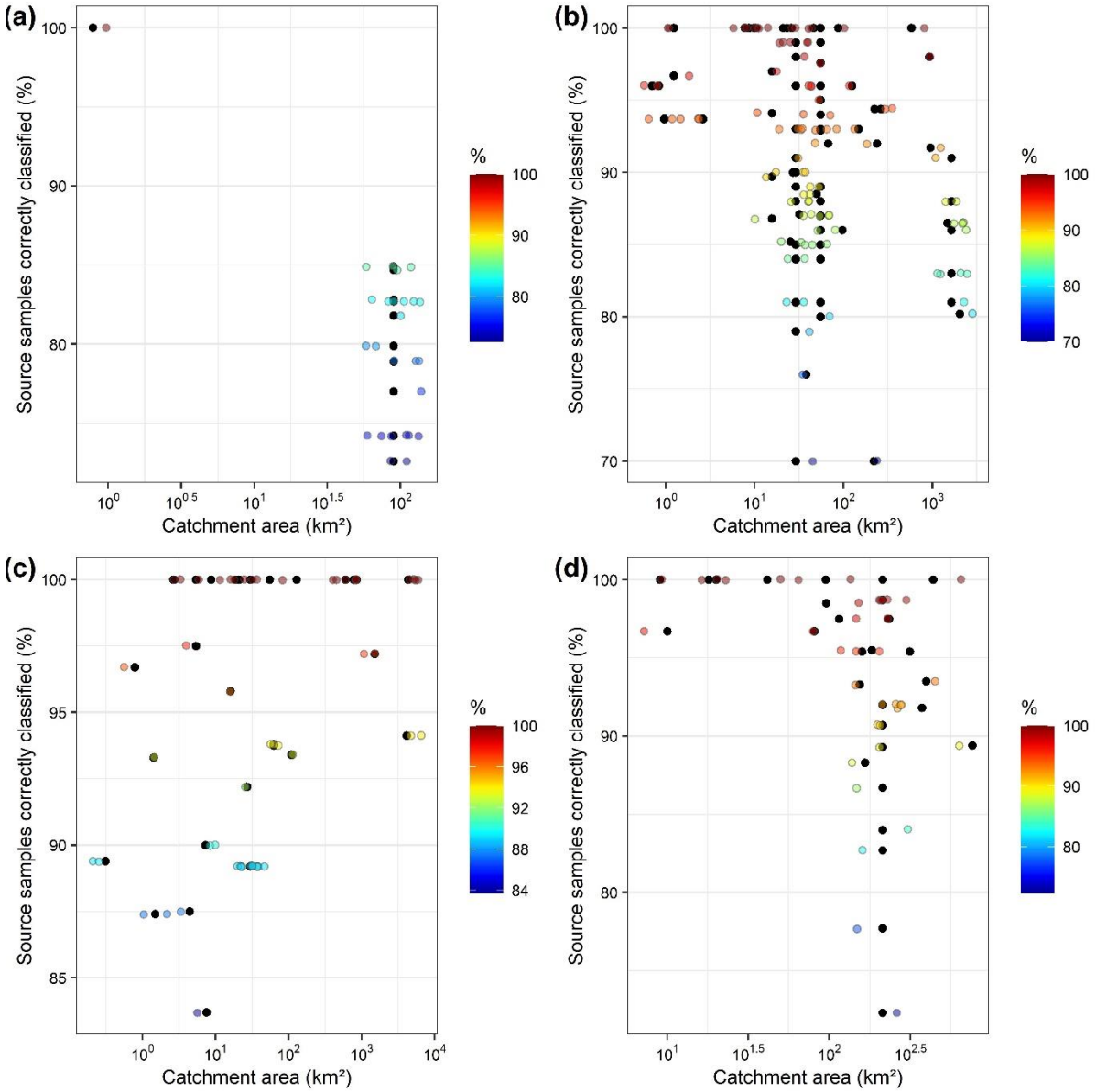

Figure 6.8. Bi-plot between catchment area and percentage of source samples correctly classified for the studies with two sources (a), three sources (b), four sources (c) and more than four sources (d).

Besides the size of the catchment, the ability of geochemical tracers to discriminate potential sources of sediment may be affected by the density of samples collected in the catchment. Interestingly, we observed a threshold where fingerprinting studies using a minimum of 10 samples per km^2 resulted in a percentage of source samples correctly classified always higher than 90% (

Figure 6.9). In fingerprinting studies with more than 90% of source samples correctly classified, it is possible to obtain good modelling results with low uncertainty (Haddadchi et al., 2014; Laceby and Olley, 2015). However, when sampling density is lower than 0.5 samples/km^2 there is a wide range of source samples correctly classified (70-100%), with approximately half of the cases ranging from 90 to 100%, and half

ranging from 70 to 90%. Moreover, the sample density between 0.5-10 samples/km² results in intermediate discrimination. Therefore, studies using low sample density are more likely to obtain low discrimination between sources, transferring great uncertainty to the final results, and therefore should be avoided.

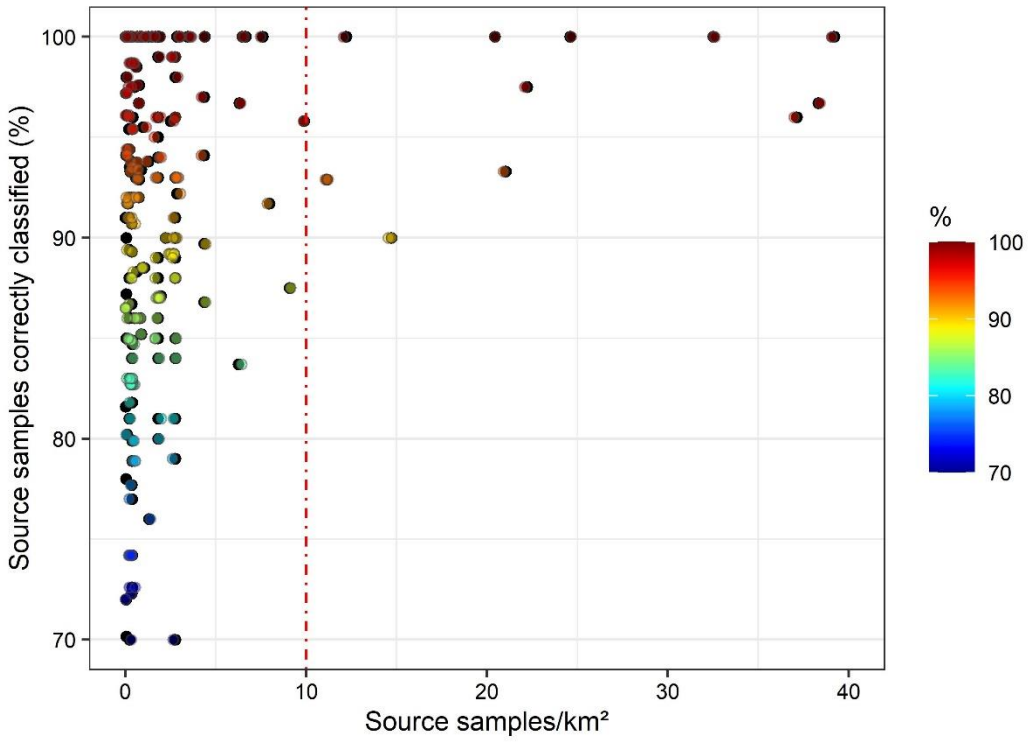

Figure 6.9. Source sample density and percentage of the source samples correctly reclassified by the DFA.

In order to compare similar source and sediment particle sizes, restricting the analyses to a particular particle size fraction is a common practice in sediment tracing studies (Laceby et al., 2017). In addition, considering the sorting of sediment particle size by erosion and transport processes, as well as potential biogeochemical transformations, correction factors based on the organic carbon content and particle size are often applied. Although particle size remains a matter of debate on which a greater attention is suggested (Laceby et al., 2017), the results obtained demonstrate that there is no clear relationship between the particle size used and the correct discrimination of sediment sources (Fig. 6.9a). However, it is possible to verify that the "standard" granulometry (<0.063 mm) used in fingerprinting studies, is the one with the greatest variation. That occurs because commonly the particle size is selected without a detailed prior analysis of the granulometry of the sediment in the river network. Of the 310 approaches, in 232

(75%) the particle size fraction <0.063 mm was used for the analyses, making it the most used in sediment fingerprinting studies (Figure 6.10). Others have used the fractions < 0.010 (n=1), < 0.053 (n=4), < 0.15 (n=7), < 2 mm (n=16) and in 14 approaches, the fraction considered was not informed. In these last cases, the correct classification of the source samples showed lower variation compared to the fraction <0.063 mm.

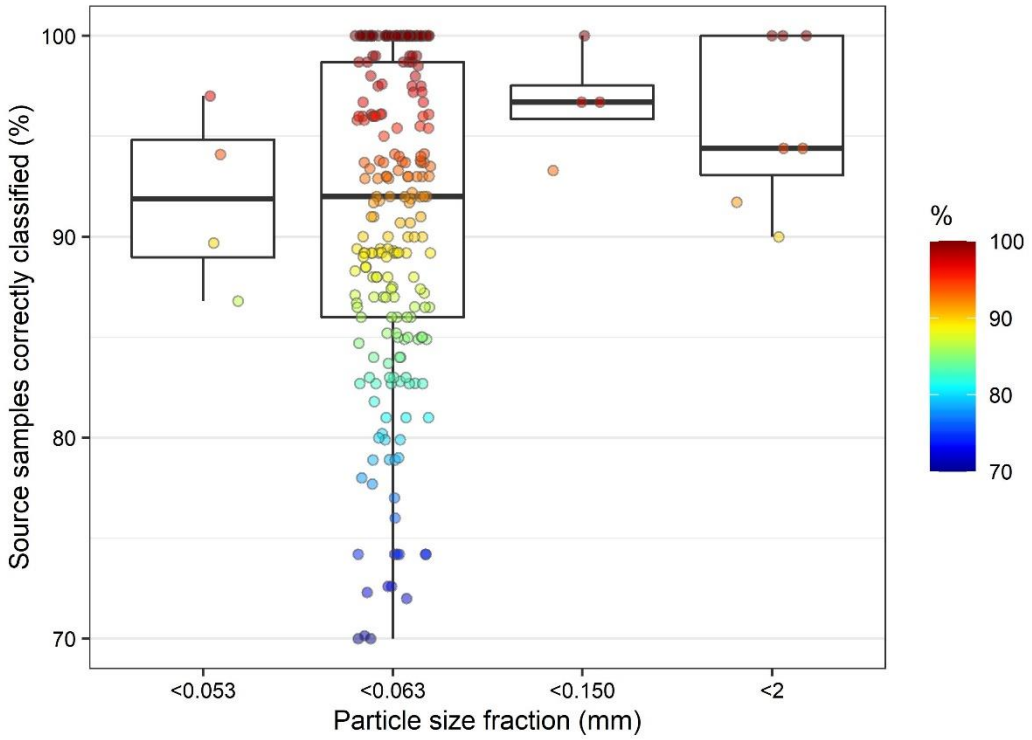

Figure 6.10. Percentage of source samples correctly classified according to the particle size fraction used in the approach.

Particle size corrections or organic matter correction factors were applied in 77% of the approaches (Figure 6.11). No significant effect on the SCC was observed depending on the correction factors. The median of SCC for the cases in which correction factors were not applied was only slightly lower.

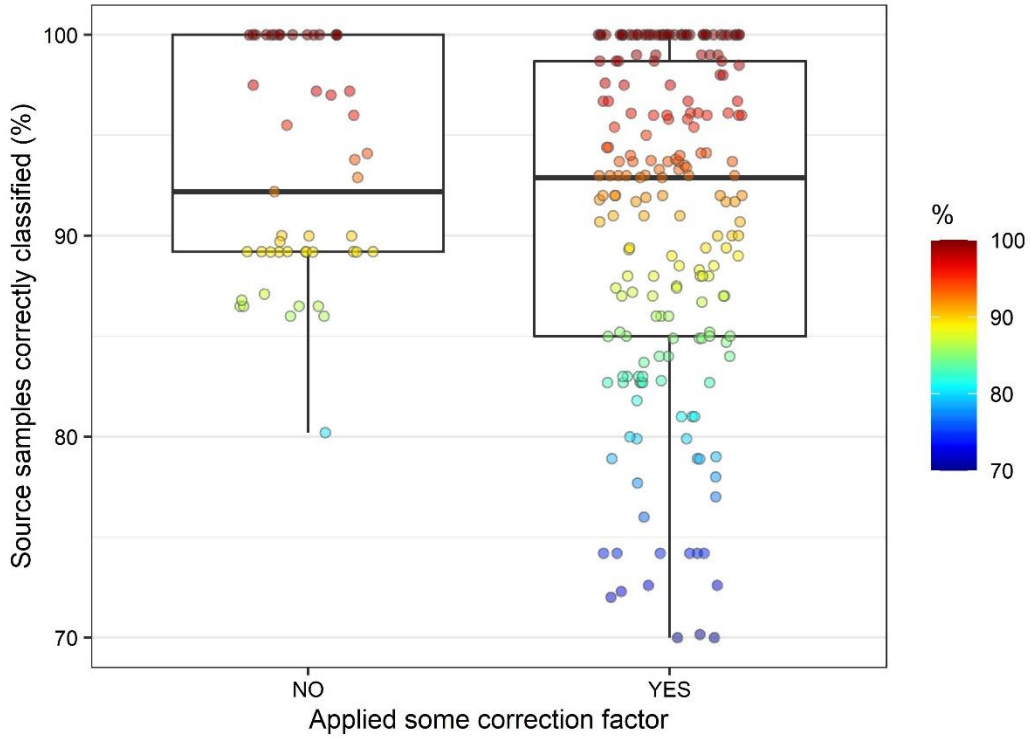

Figure 6.11. Percentage of source samples correctly classified depending whether particle size or organic carbon correction factors were applied.

6.3.3 Geochemical elements as sediment source tracers

In total, 68 chemical elements were tested as potential tracers, as listed in section 6.2.2. Figure 6.12 shows the number of publications in which each element was analysed as a potential tracer. The most frequently used elements, considering the number of articles where they appear as potential tracers, are highlighted in blue and most of them belong to the group of semi-metals of the 4th period of the periodic table, like Mn, Fe, Zn and Cu. Alkaline and alkaline earth metals are also often considered as potential tracers, like Mg, Na, K and Ca. These elements are more commonly measured in laboratories, reason that may explain their higher frequency in tracing studies.

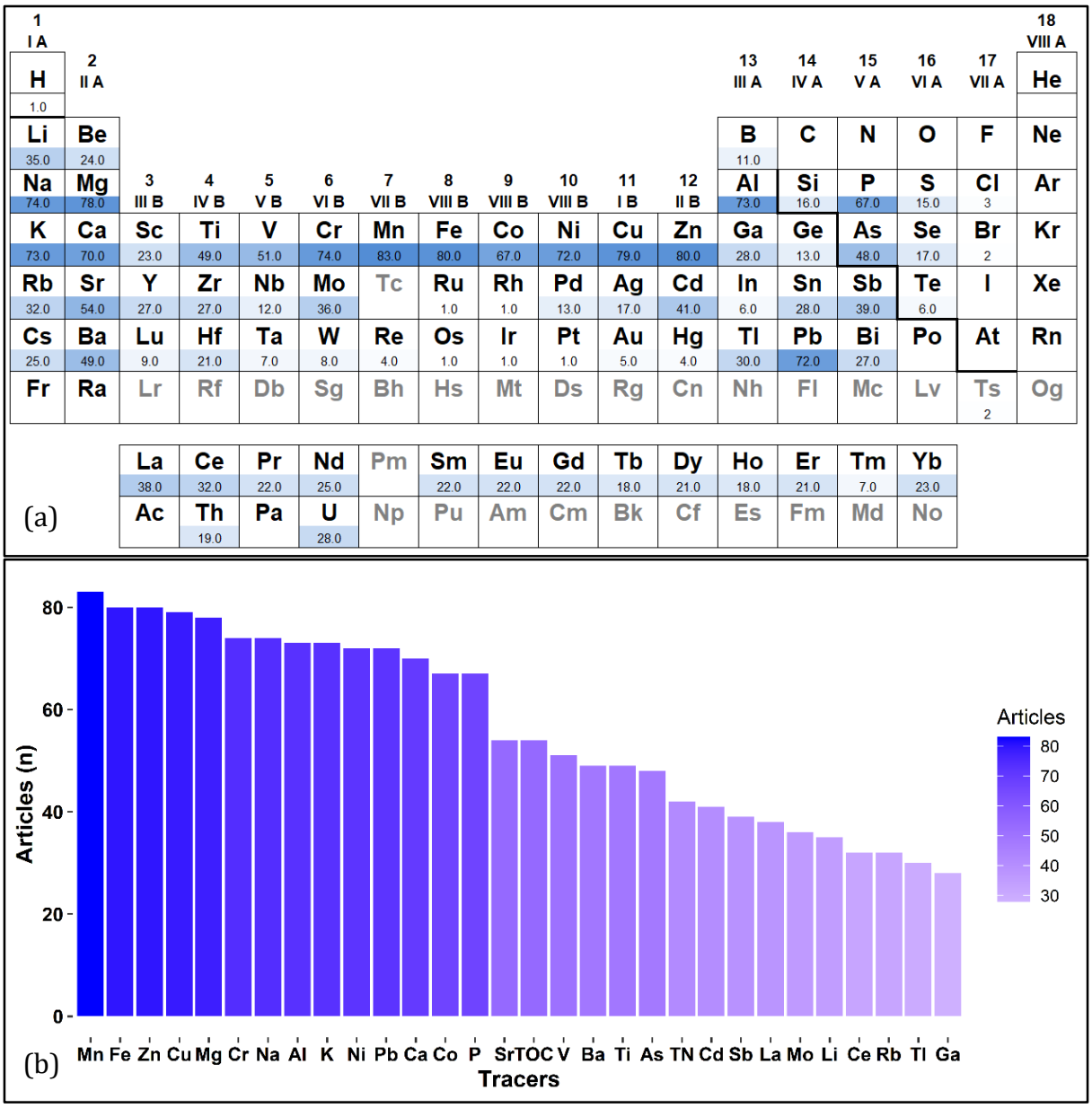

Figure 6.12. Number of articles in which each element was analysed. Distribution according to the periodic table (a) and ranked according to the frequency (b).

The concentration in these elements was mainly determined by ICP-MS after an *aqua regia* acid digestion (n=212, 68% of the approaches). In 28 approaches, the element concentration was determined by X-ray fluorescence and in 67 approaches, multiple analytical methods were applied depending on the elements of interest. The proportion of studies with which each element behaves conservatively did not follow their frequency analysis. Rare earth and semi-metal elements of the 5th period presented a higher percentage of cases in which they were conservative (Figure 6.13). Elements that are bound to the matrix of the soil, are more strongly adsorbed (e.g. Ti, V) as well as rare earth

elements (eg. Y, La, Ce), and have more chance to behave conservatively (Collins et al., 2020).

Phosphorus and TOC were the least conservative elements (approximately 20% of cases only). Similar results were found for some alkaline and alkaline earth metals (Ca, Mg and K), although other elements of these groups are among the most conservative reported in the literature (Ba and Rb). These results may be an effect of the anthropization of soils in the studied catchments, as COT, P, Ca, Mg and K are directly influenced by the use and management of the soil, being added via fertilizers in many cases (P, Ca, Mg and K). The enrichment/depletion of these elements with some land uses can be an excellent tracer of these sources (Tiecher et al., 2021; Minella et al., 2007), but when the use of agricultural land is not a target source, it results in non-conservativeness of these elements.

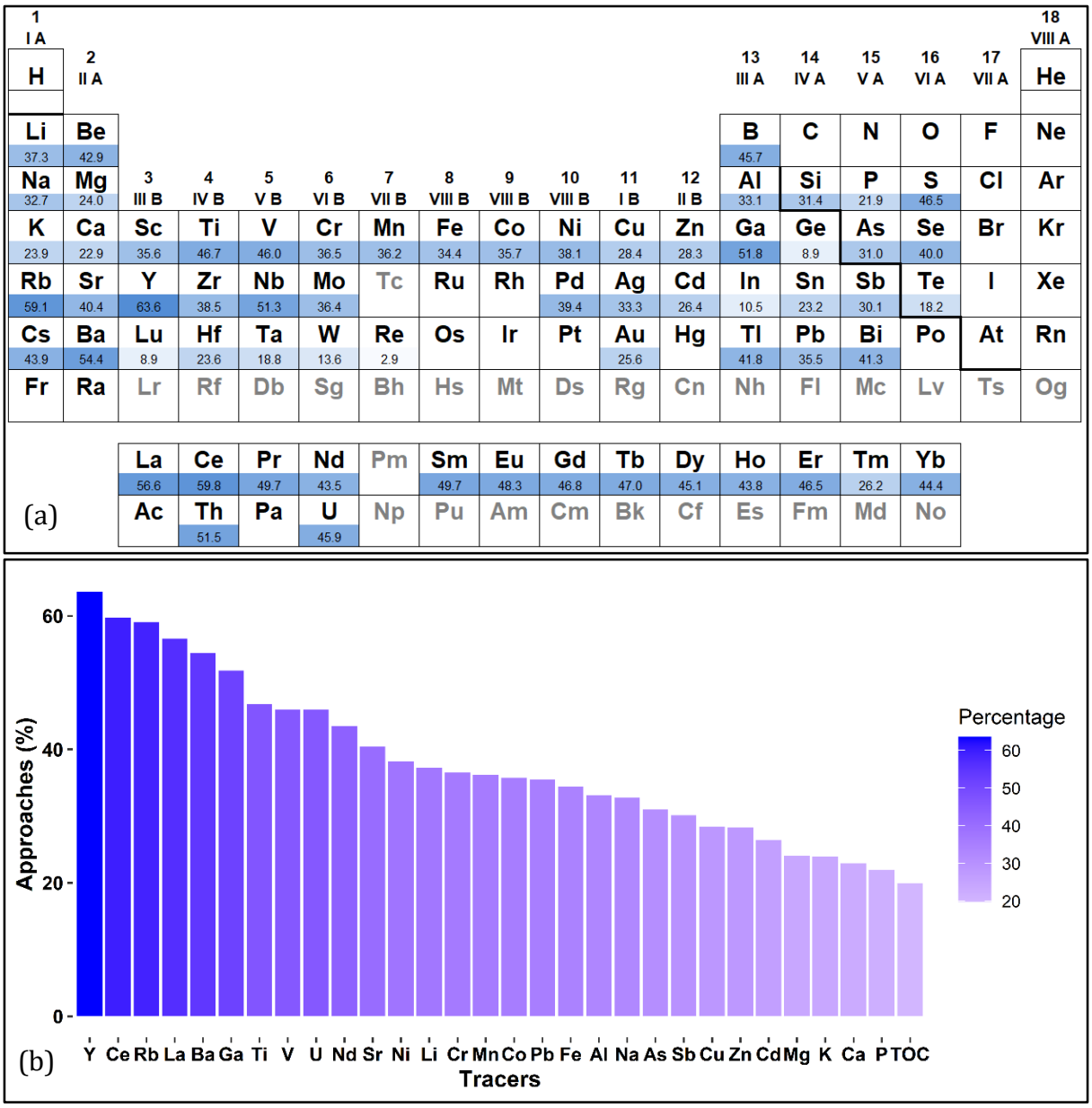

Figure 6.13. Percentage of approval in the conservative test related to the number of approaches in which they were considered as potential tracers. Distribution according to the periodic table (a) and ranked according to the frequency (b).

Some REE elements of the lanthanide group, U and Th of actinides, alkaline and alkaline earth metals from the 5th and 6th period (Rb, Sr, Cs, Ba), Y and Se are among the elements that were the most often selected by the DFA, proportionally to the number of articles in which they were analysed (Figure 6.14). Macro elements that are found in higher concentrations in soils such as Ca, Na, K, Mg, P and S, are the elements that were the less often selected. The latter are found naturally in soils, but many of them are added in large quantities via fertilizers in agricultural areas to replace what is exported with agricultural products. Consequently, the dynamics of the latter in the landscape is even

more variable than that of minor elements, which are directly linked to the natural composition of the source material, for example.

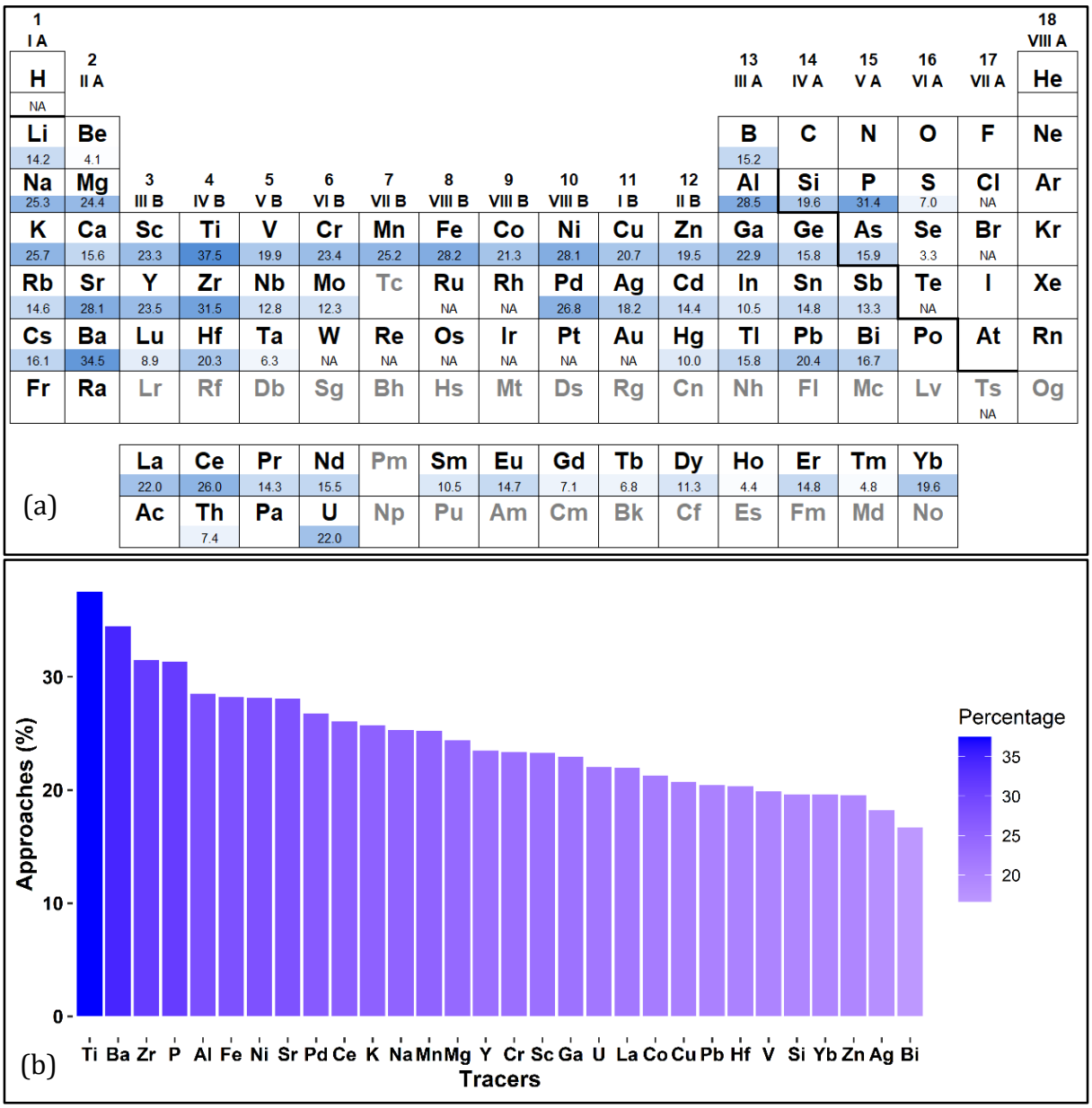

Figure 6.14. Percentage of approval in the conservative test related to the number of articles in which they were selected by the DFA for the final model. Distribution according to the periodic table (a) and ranked according to the frequency (b).

6.4 Conclusions

This meta-analysis show that the number of studies related to sediment fingerprinting are increasing every year. The conventional approach considering geochemical composition as tracer is still widely used and their efficiency is highly variable according to each study case. It was verified that the standard three steps method of selecting tracer variables has some variations which can affect the

discrimination between sources and consequently the accuracy of the modelling results. Based on that, a better definition of a procedure to be followed is needed in order to have more robust results for any application of the method. Further meta-analyses that assess method uncertainties in already published articles may help to have some direction in defining a standard approach. Geochemical elements that are bound to the soil matrix, has greater potential to show conservative behaviour and to be able to discriminate between potential sources. However, a process based selection of the potential tracers should be taken into account according to the potential sources considered and also the catchment characteristics.

6.5 References

Barthod, L.R.M., Liu, K., Lobb, D.A., Owens, P.N., Martínez-Carreras, N., Koiter, A.J., Petticrew, E.L., McCullough, G.K., Liu, C., Gaspar, L., 2015. Selecting Color-based Tracers and Classifying Sediment Sources in the Assessment of Sediment Dynamics Using Sediment Source Fingerprinting. J. Environ. Qual. 44, 1605. https://doi.org/10.2134/jeq2015.01.0043

Batista, P.V.G., Laceby, J.P., Silva, M.L.N., Tassinari, D., Bispo, D.F.A., Curi, N., Davies, J., Quinton, J.N., 2018. Using pedological knowledge to improve sediment source apportionment in tropical environments. J. Soils Sediments. https://doi.org/10.1007/s11368-018-2199-5

Black, C.A., Evans, D.D., Ensminger, L.E., White, J.L., Clark, F.E., 1965. Part 1: Physical and Mineralogical Properties, Including Statistics of Measurement and Sampling, in: Black, C.A. (Ed.), Methods of Soil Analysis. American Society of Agronomy, pp. 128–151.

Blake, W.H., Ficken, K.J., Taylor, P., Russell, M.A., Walling, D.E., 2012. Tracing crop-specific sediment sources in agricultural catchments. Geomorphology 139–140, 322–329. https://doi.org/10.1016/j.geomorph.2011.10.036

Boardman, J., Vandaele, K., Evans, R., Foster, I.D.L., 2019. Off-site impacts of soil erosion and runoff: Why connectivity is more important than erosion rates. Soil Use Manag. 35, 245–256. https://doi.org/10.1111/sum.12496

Brandt, C., Benmansour, M., Walz, L., Nguyen, L.T., Cadisch, G., Rasche, F., 2018. Integrating compound-specific δ13C isotopes and fallout radionuclides to retrace land use type-specific net erosion rates in a small tropical catchment exposed to intense land use

change. Geoderma 310, 53–64. https://doi.org/10.1016/j.geoderma.2017.09.008

Collins, A.L., Blackwell, M., Boeckx, P., Chivers, C.A., Emelko, M., Evrard, O., Foster, I., Gellis, A., Gholami, H., Granger, S., Harris, P., Horowitz, A.J., Laceby, J.P., Martinez-Carreras, N., Minella, J.P.G., Mol, L., Nosrati, K., Pulley, S., Silins, U., da Silva, Y.J., Stone, M., Tiecher, T., Upadhayay, H.R., Zhang, Y., 2020. Sediment source fingerprinting: benchmarking recent outputs, remaining challenges and emerging themes, Journal of Soils and Sediments. Journal of Soils and Sediments. https://doi.org/10.1007/s11368-020-02755-4

Collins, A.L., Pulley, S., Foster, I.D.L., Gellis, A., Porto, P., Horowitz, A.J., 2017a. Sediment source fingerprinting as an aid to catchment management: A review of the current state of knowledge and a methodological decision-tree for end-users. J. Environ. Manage. 194, 86–108. https://doi.org/10.1016/j.jenvman.2016.09.075

Collins, A.L., Pulley, S., Foster, I.D.L., Gellis, A., Porto, P., Horowitz, A.J., 2017b. Sediment source fingerprinting as an aid to catchment management: A review of the current state of knowledge and a methodological decision-tree for end-users. J. Environ. Manage. 194, 86–108. https://doi.org/10.1016/j.jenvman.2016.09.075

Collins, A.L., Walling, D.E., Sichingabula, H.M., Leeks, G.J.L., 2001. Using 137 Cs measurements to quantify soil erosion and redistribution rates for areas under different land use in the Upper Kaleya River basin , southern Zambia 299–323.

Collins, A.L., Walling, D.E., Webb, L., King, P., 2010. Apportioning catchment scale sediment sources using a modified composite fingerprinting technique incorporating property weightings and prior information. Geoderma 155, 249–261. https://doi.org/10.1016/j.geoderma.2009.12.008

Evrard, O., Laceby, J.P., Huon, S., Lefèvre, I., Sengtaheuanghoung, O., Ribolzi, O., 2016. Combining multiple fallout radionuclides (137Cs, 7Be, 210Pbxs) to investigate temporal sediment source dynamics in tropical, ephemeral riverine systems. J. Soils Sediments 16, 1130–1144. https://doi.org/10.1007/s11368-015-1316-y

FAO, 2019. Soil erosion: the gratest challenge for sustainable soil management. Licence: CC BY-NC-SA 3.0 IGO, Rome.

Fox, J.F., Papanicolaou, A.N., 2007. The use of carbon and nitrogen isotopes to study watershed erosion processes. J. Am. Water Resour. Assoc. 43, 1047–1064. https://doi.org/10.1111/j.1752-1688.2007.00087.x

Gaspar, L., Navas, A., Walling, D.E., Machín, J., Gómez Arozamena, J., 2013. Using 137Cs and

210Pbex to assess soil redistribution on slopes at different temporal scales. CATENA 102, 46–54. https://doi.org/10.1016/j.catena.2011.01.004

Haddadchi, A., Olley, J., Laceby, J.P., 2014. Accuracy of mixing models in predicting sediment source contributions. Sci. Total Environ. 497–498, 139–152. https://doi.org/10.1016/j.scitotenv.2014.07.105

Haddadchi, A., Ryder, D.S., Evrard, O., OLLEY, J., 2013. Sediment fingerprinting in fluvial systems: review of tracers, sediment sources and mixing models. Int. J. Sediment Res. 28, 560–578. https://doi.org/10.1016/S1001-6279(14)60013-5

Koiter, A.J., Owens, P.N., Petticrew, E.L., Lobb, D.A., 2013. The behavioural characteristics of sediment properties and their implications for sediment fingerprinting as an approach for identifying sediment sources in river basins. Earth-Science Rev. 125, 24–42. https://doi.org/10.1016/j.earscirev.2013.05.009

Krause, A.K., Franks, S.W., Kalma, J.D., Loughran, R.J., Rowan, J.S., 2003. Multi-parameter fingerprinting of sediment deposition in a small gullied catchment in SE Australia. Catena 53, 327–348. https://doi.org/10.1016/S0341-8162(03)00085-7

Laceby, J.P., Evrard, O., Smith, H.G., Blake, W.H., Olley, J.M., Minella, J.P.G., Owens, P.N., 2017. The challenges and opportunities of addressing particle size effects in sediment source fingerprinting: A review. Earth-Science Rev. 169, 85–103. https://doi.org/10.1016/j.earscirev.2017.04.009

Laceby, J.P., McMahon, J., Evrard, O., Olley, J., 2015. A comparison of geological and statistical approaches to element selection for sediment fingerprinting. J. Soils Sediments 15, 2117–2131. https://doi.org/10.1007/s11368-015-1111-9

Laceby, J.P., Olley, J., 2015. An examination of geochemical modelling approaches to tracing sediment sources incorporating distribution mixing and elemental correlations. Hydrol. Process. 29, 1669–1685. https://doi.org/10.1002/hyp.10287

Lamba, J., Karthikeyan, K.G.G., Thompson, A.M.M., 2015. Apportionment of suspended sediment sources in an agricultural watershed using sediment fingerprinting. Geoderma 239, 25–33. https://doi.org/10.1016/j.geoderma.2014.09.024

Manjoro, M., Rowntree, K., Kakembo, V., Foster, I., Collins, A.L., 2017. Use of sediment source fingerprinting to assess the role of subsurface erosion in the supply of fine sediment in a degraded catchment in the Eastern Cape, South Africa. J. Environ. Manage. 194, 27–41. https://doi.org/10.1016/j.jenvman.2016.07.019

Martínez-Carreras, N., Krein, A., Gallart, F., Iffly, J.F., Pfister, L., Hoffmann, L., Owens, P.N.,

2010a. Assessment of different colour parameters for discriminating potential suspended sediment sources and provenance: A multi-scale study in Luxembourg. Geomorphology 118, 118–129. https://doi.org/10.1016/j.geomorph.2009.12.013

Martínez-Carreras, N., Krein, A., Udelhoven, T., Gallart, F., Iffly, J.F., Hoffmann, L., Pfister, L., Walling, D.E., 2010b. A rapid spectral-reflectance-based fingerprinting approach for documenting suspended sediment sources during storm runoff events. J. Soils Sediments 10, 400–413. https://doi.org/10.1007/s11368-009-0162-1

Martínez-Carreras, N., Udelhoven, T., Krein, A., Gallart, F., Iffly, J.F., Ziebel, J., Hoffmann, L., Pfister, L., Walling, D.E., 2010c. The use of sediment colour measured by diffuse reflectance spectrometry to determine sediment sources: Application to the Attert River catchment (Luxembourg). J. Hydrol. 382, 49–63. https://doi.org/10.1016/j.jhydrol.2009.12.017

Minella, J.P.G., Merten, G.H., Clarke, R.T., 2004. Identification of sediment sources in a small rural drainage basin, in: Sediment Transfer through the Fluvial System (Proceedings of a Symposium Held in Moscow, August 2004). IAHS Press, Moscow, pp. 44–51.

Minella, J.P.G., Walling, D.E., Merten, G.H., 2008. Combining sediment source tracing techniques with traditional monitoring to assess the impact of improved land management on catchment sediment yields. J. Hydrol. 348, 546–563. https://doi.org/10.1016/j.jhydrol.2007.10.026

Motha, J.A., Wallbrink, P.J., Hairsine, P.B., Grayson, R.B., 2003. Determining the sources of suspended sediment in a forested catchment in southeastern Australia. Water Resour. Res. 39, n/a-n/a. https://doi.org/10.1029/2001WR000794

Motha, J.A., Wallbrink, P.J., Hairsine, P.B., Grayson, R.B., 2002. Tracer properties of eroded sediment and source material. Hydrol. Process. 16, 1983–2000. https://doi.org/10.1002/hyp.397

Mukundan, R., Radcliffe, D.E., Ritchie, J.C., Risse, L.M., McKinley, R.A., 2010. Sediment Fingerprinting to Determine the Source of Suspended Sediment in a Southern Piedmont Stream. J. Environ. Qual. 39, 1328. https://doi.org/10.2134/jeq2009.0405

Mukundan, R., Walling, D.E., Gellis, A.C., Slattery, M.C., Radcliffe, D.E., 2012. Sediment Source Fingerprinting : Transforming From a Research Tool To a Management Tool 1. JAWRA J. Am. Water Resour. Assoc. 48, 1241–1257. https://doi.org/10.1111/j.1752-1688.2012.00685.x

Owens, P.N., Xu, Z., 2011. Recent advances and future directions in soils and sediments research. J. Soils Sediments 11, 875–888. https://doi.org/10.1007/s11368-011-0406-8

Palazón, L., Navas, A., 2017. Variability in source sediment contributions by applying different statistic test for a Pyrenean catchment. J. Environ. Manage. 194, 42–53. https://doi.org/10.1016/j.jenvman.2016.07.058

Peart, M., Walling, D.E., 1988. Techniques for establishing suspended sediment sources in two drainage basins in Devon, UK: a comparative assessment. Sediment Budgets. IAHS Publ. 269–280.

Peart, M.R., Walling, D.E., 1986. Fingerprinting sediment source: The examples of a drainage basion in Devon, UK 41–56.

Poesen, J., 2017. Soil erosion in the Anthropocene: research needs. Earth Surf. Process. Landforms 84, 64–84. https://doi.org/10.1002/esp.4250

Porto, P., Walling, D.E., Capra, A., 2014. Using 137Cs and 210Pbex measurements and conventional surveys to investigate the relative contributions of interrill/rill and gully erosion to soil loss from a small cultivated catchment in Sicily. Soil Tillage Res. 135, 18–27. https://doi.org/10.1016/j.still.2013.08.013

Pulley, S., Foster, I., Antunes, P., 2015a. The application of sediment fingerprinting to floodplain and lake sediment cores: assumptions and uncertainties evaluated through case studies in the Nene Basin, UK. J. Soils Sediments 15, 2132–2154. https://doi.org/10.1007/s11368-015-1136-0

Pulley, S., Foster, I., Collins, A.L., 2017. The impact of catchment source group classification on the accuracy of sediment fingerprinting outputs. J. Environ. Manage. 194, 16–26. https://doi.org/10.1016/j.jenvman.2016.04.048

Pulley, S., Rowntree, K., Foster, I., 2015b. Conservatism of mineral magnetic signatures in farm dam sediments in the South African Karoo: the potential effects of particle size and post-depositional diagenesis. J. Soils Sediments 15, 2387–2397. https://doi.org/10.1007/s11368-015-1265-5

Pulley, S., Van der Waal, B., Rowntree, K., Collins, A.L., 2018. Colour as reliable tracer to identify the sources of historically deposited flood bench sediment in the Transkei, South Africa: A comparison with mineral magnetic tracers before and after hydrogen peroxide pre-treatment. CATENA 160, 242–251. https://doi.org/10.1016/j.catena.2017.09.018

Slattery, M.C., Burt, T.P., Walden, J., 1995. The application of mineral magnetic measurements to quantify within-storm variations in suspended sediment sources. Geography.

Sloto, R.A., Gellis, A.C., Galeone, D.G., 2012. Total nitrogen and suspended-sediment loads and identification of suspended-sediment sources in the Laurel Hill Creek Watershed, Somerset County, Pennsylvania, Water Years 2010–11: Scientific Investigations Report 2012–5250.

Smith, H.G., Blake, W.H., 2014. Sediment fingerprinting in agricultural catchments: A critical re-examination of source discrimination and data corrections. Geomorphology 204, 177–191. https://doi.org/10.1016/j.geomorph.2013.08.003

Tiecher, T., Caner, L., Minella, J.P.G., Bender, M.A., dos Santos, D.R., 2016. Tracing sediment sources in a subtropical rural catchment of southern Brazil by using geochemical tracers and near-infrared spectroscopy. Soil Tillage Res. 155, 478–491. https://doi.org/10.1016/j.still.2015.03.001

Tiecher, T., Caner, L., Minella, J.P.G., Santos, D.R. dos, 2015. Combining visible-based-color parameters and geochemical tracers to improve sediment source discrimination and apportionment. Sci. Total Environ. 527–528, 135–149. https://doi.org/10.1016/j.scitotenv.2015.04.103

Tiecher, T., Minella, J.P.G., Evrard, O., Caner, L., Merten, G.H., Capoane, V., Didoné, E.J., dos Santos, D.R., 2018. Fingerprinting sediment sources in a large agricultural catchment under no-tillage in Southern Brazil (Conceição River). L. Degrad. Dev. 29, 939–951. https://doi.org/10.1002/ldr.2917

Wallbrink, P.J., Murray, A.S., 1993. Use of fallout radionuclides as indicators of erosion processes. Hydrol. Process. 7, 297–304. https://doi.org/10.1002/hyp.3360070307

Walling, D.E., 2013. The evolution of sediment source fingerprinting investigations in fluvial systems. J. Soils Sediments 13, 1658–1675. https://doi.org/10.1007/s11368-013-0767-2

Walling, D.E., Quine, T., 1992. The use of caesium-137 measurements in soil erosion surveys. Eros. sediment Transp. Monit. Program. River Basins 143–152.

7 Chapter 2. Combining spectroscopy and magnetism with geochemical tracers to improve the discrimination of sediment sources in a homogeneous subtropical catchment

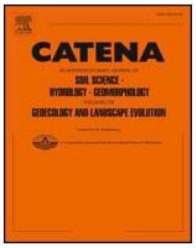

Rafael Ramon[a,b,*], Olivier Evrard[b], J. Patrick Laceby[c], Laurent Caner[d], Alberto V. Inda[e], Cláudia A.P. de Barros[e], Jean P.G. Minella[f], Tales Tiecher[e]

[a] Graduate Program in Soil Science, Federal University of Rio Grande do Sul, Bento Gonçalves Ave., 91540-000 Porto Alegre, RS, Brazil[1]

[b] Laboratoire des Sciences et de l'Environnement, UMR 8212 (CEA/CNRS/UVSQ), 91 191 Gif-sur-Yvette Cedex (France), Université Paris-Saclay, France[1]

[c] Alberta Environment and Parks, 3535 Research Rd NW, T2L 2K8, Calgary, Alberta, Canada

[d] IC2MP-HydrASA UMR, Université de Poitiers, Poitiers, France

[e] Department of Soil Science, Federal University of Rio Grande do Sul, Bento Gonçalves Ave. 7712, 91540-000 Porto Alegre, RS, Brazil[1]

[f] Department of Soil Science, Federal University of Santa Maria, Roraima Ave. 1000, 97105-900 Santa Maria, RS, Brazil

[1] Interdisciplinary Research Group On Environmental Biogeochemistry – IRGEB.

https://doi.org/10.1016/j.catena.2020.104800
Received 30 March 2020; Received in revised form 16 July 2020; Accepted 17 July 2020

7.1 Introduction

The sustainable production of food, fiber and fuel remains limited by soil erosion. Despite the vast knowledge accumulated about soil erosion, it remains a significant global environmental issue that is one of the main causes of soil degradation worldwide. In this context, Southern Brazil has one of the highest erosion rates in the world (Borrelli et al., 2017) due to the relief characteristics along with intense and erosive rainfall (Ramon et al., 2017). In particular, rainfall erosivity is expected to increase ~10% in Southern Brazil by 2040 (Almagro et al., 2017).

Although field research programs are an essential tool to understand the impacts of human activities and climate changes on natural resources (Poesen, 2017), in Brazil they have been employed only relatively recently compared to other regions of the world such as the United States or Europe (Melo et al., 2020). In this scenario of limited hydrological and geomorphological understanding, it is important to identify the main

sediment sources (Collins et al., 2017) to guide decision-makers in the efficient allocation of limited public resources available to mitigate soil erosion and sediment production.

The sediment fingerprinting technique has been increasingly used in catchments worldwide to quantify the relative source contributions to river sediment (Walling, 2013). The method offers an effective way to calculate the contribution of diffuse sources of sediment and contaminants, providing useful information to focus efforts on controlling major soil erosion problems (Niu et al., 2019; Nosrati and Collins, 2019; Torres Astorga et al., 2018; Uber et al., 2019). However, many challenges require further research with sediment source fingerprinting such as the selection of tracers to analyse and the grouping of the main sediment sources (Pulley et al., 2017b; Smith et al., 2015).

Sediment tracer properties need to be conservative and their signature from source to the river network must remain constant or vary predictably (Belmont et al., 2014; Laceby et al., 2017). Although it is known that the conservativeness of potential inorganic tracers is dependent on their chemical nature (e.g., alkali metals, transition metals, rare earth elements) and how they are bound to the sediment (e.g., sorbed onto sediment particles or matrix-bounded elements), there is still no consensus on the best approach to assess conservativeness.

Most studies typically evaluate conservativeness empirically through comparisons of concentration between sources and sediments, which in turns depend on the conservativeness test applied (Smith et al., 2018; Lizaga et al., 2020). Moreover, tracer conservativeness can also be dependent on the characteristics of the studied catchment and the sediment sources evaluated. Studying land use sources in homogeneous catchments may be much more challenging as any enrichment or depletion of a particular element during the erosion process can result in sediment concentrations varying outside the range of source values (Smith and Blake, 2014). To overcome conservativeness issues and increase the number of conservative tracers, physical characteristics such as colour, or related to mineralogical constitution, such as magnetism and parameters related to Fe oxides, that can be easily measured, may potentially maintain their conservativeness in these homogeneous catchments and be combined with other tracing parameters (Pulley et al., 2018).

In addition, tracer properties should ideally be low-cost, quick and easy to analyse, as characterizing a large number of samples is needed in order to be representative of the within-source variability, especially in large catchments. Furthermore, analyses that

require a low sample mass and are non-destructive are preferable, as in several environmental contexts, it can be difficult to collect large quantities of suspended sediment during fieldwork (Guzmán et al., 2013).

Geochemical composition of source and sediment samples is among the most used tracers for sediment fingerprinting worldwide (Koiter et al., 2013). Multiple geochemical analyses such as inductively coupled plasma (ICP) or X-ray fluorescence analyses result in high number of potential tracers, however they are not an option for research groups that do not have access to sophisticated equipment (e.g. ICP-OES or ICP-MS, microwave oven) or sufficient resources to afford such analysis.

Another option for tracing sediment sources are magnetic properties which have been widely used since the original sediment fingerprinting studies (Walling et al., 1979; Yu and Oldfield, 1989). Some measures like magnetic susceptibility can be easily measured with relatively basic equipment (Rowntree et al., 2017), increasing the number of tracers available for multiple sources contribution apportionment.

Moreover, spectroscopy data have been intensively investigated in the last decade as a low-cost, non-destructive and straightforward alternative method to provide tracer properties (Poulenard et al, 2009; Pulley et al., 2018). A variety of approaches have been used to incorporate spectroscopy analysis into sediment fingerprinting research (Legout et al., 2013; Martínez-Carreras et al., 2010b; Poulenard et al., 2012; Tiecher et al., 2017). Among them, the use of colour parameters and spectral features derived from ultraviolet-visible (UV) has shown to be promising because it can be used alone or incorporated into mathematical models together with geochemical tracers, radionuclides and others (Brosinsky et al., 2014a, 2014b, Tiecher et al., 2015). Ultra-violet derived parameters may therefore offer a strong potential for sediment tracing, although the proper classification of sources and the use of effective modelling strategies are required to obtain reliable results (Pulley et al., 2018).

An important question in sediment fingerprinting surrounds the proper identification of the potential sources of sediment to be incorporated into end-member mixing models. Reducing the number of sources considered based on their relevance in the study sites, or regrouping similar sources is a common practice in sediment fingerprinting studies. For instance, Pulley et al. (2015b) did not consider grassland as a source, since it occupied only a very low proportion of the catchment area and because it was not possible to discriminate between cultivated and grassland areas with the tracers

used. A similar decision was taken by Minella et al. (2004), where fallow areas could not be distinguished from pasture by the geochemical tracers used, and then they were combined, while channel banks and new fields were removed because there was not enough data to discriminate them, reducing the previous six sources to three.

In a previous study conducted in the Conceição River catchment in Southern Brazil, pastures were not considered as potential sources, since the geochemical tracers were not able to discriminate pastures from croplands and because they occupy only a low percentage of the total catchment surface area (Tiecher et al., 2018). Gullies were also not considered, as they are not commonly observed in the Conceição catchment, where rill erosion is much more widespread (Didoné et al., 2015). In this catchment, which consists of relatively homogeneous soil and geology, geochemical tracers were only able to correctly classify only 84% of the samples in their respective source groups (ie., cultivated sources, unpaved roads and streambanks) (Tiecher et al., 2018). The small difference in the elemental concentrations observed between the sources, because of intense weathering and leaching of most elements except Al and Fe, complicated their discrimination, requiring further studies and alternative tracers to increase the robustness of the results.

Here, the use of low-cost alternative parameters, including spectroscopy derivatives in the ultraviolet-visible range and magnetic parameters, in combination with geochemical tracers are investigated to provide an alternative approach that increases the discrimination between multiple land use sources. This research investigates the potential of six different sets of tracing parameters combing low cost and geochemical element traces to calculate the respective contributions of five potential sediment sources in a homogeneous catchment (Conceição River) in southern Brazil. This research contributes to the ongoing development of low-cost tracers, examining their efficacy in a complicated homogeneous tracing environment, that is representative of regions with extensive agricultural activities that contribute deleterious sediment loads degrading waterways worldwide.

7.2 Methodology

7.2.1 Study site

The Conceição River catchment is located on a basaltic plateau in the southern part of the Paraná Basin in the state of Rio Grande do Sul, and it covers an area of approximately 804 km^2 (Figure 7.1). According to Köppen's classification, the climate is classified as of Cfa type, humid subtropical without a defined dry season, with an average annual precipitation ranging between 1750 to 2000 mm per year and an average temperature of 18.6°C. This catchment is representative of the basaltic plateau region of the Serra Geral Formation (92%), where the soil classes found are Ferralsols (80%), Nitisols (18%) and Acrisols (2%), with a mineralogy dominated by iron oxides and kaolinite (Figure 7.2). These soils are very rich in clays, typically, the Ferralsols that predominate in this catchment have less than 10% of sand and clay content as high as 85% (Ramos et al., 2017). Small areas from the Tupanciretã Formation (6%), which are outcrops of the Botucatu Formation enclosed by volcanic spills of the Serra Geral Formation, are also found. The relief of the catchment is characterized by gentle slopes (6-9%) at the higher positions of the landscape and steeper slopes (10-14%) near the drainage channels, with altitudes ranging from 270 to 480 m a.s.l. The catchment outlet is located next to the monitoring point number 75200000 of the National Water Agency (ANA) (28°27'22" S, 53°58'24" O) in the municipality of Ijuí.

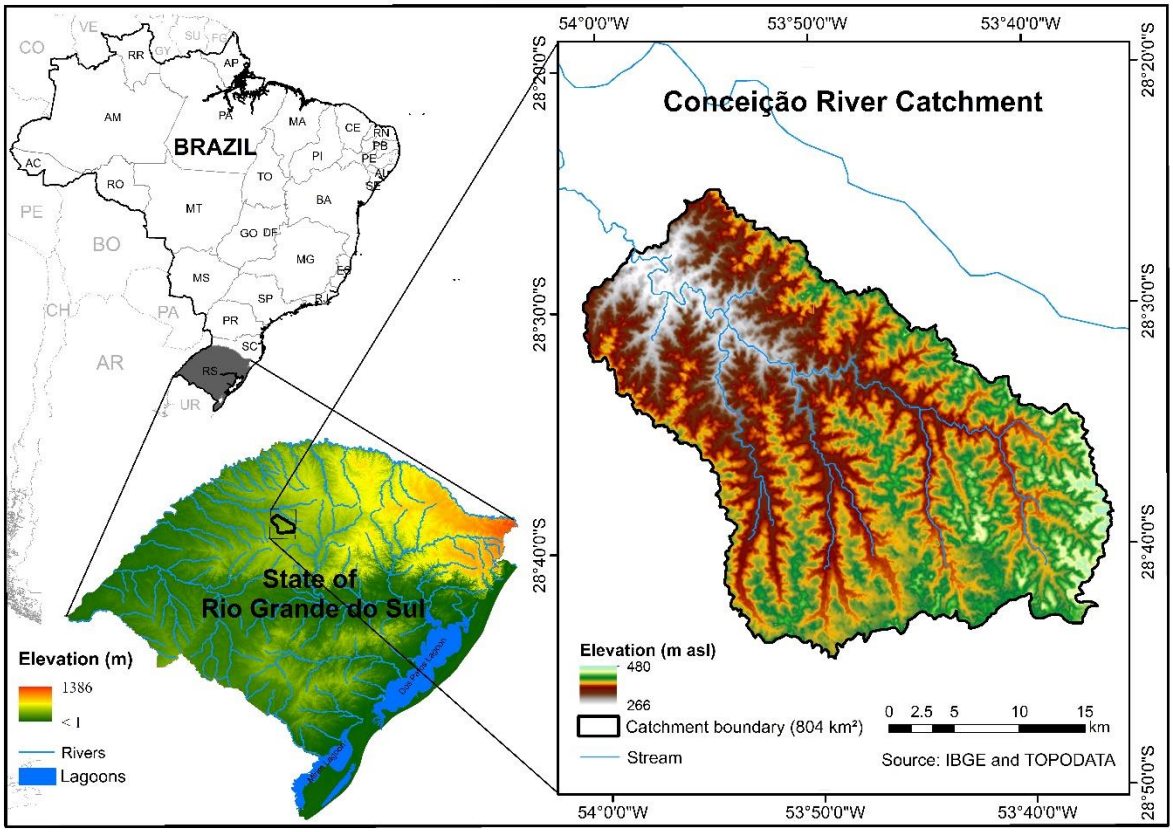

Figure 7.1. Location of the Conceição River catchment in Southern Brazil and digital elevation model.

The main land use is cropland (89%) mainly cultivated with soybean (*Glycine max*) under no tillage system in the summer and with wheat (*Triticum aestivum*) for grain production, oat (*Avena sativa* and *Avena strigosa*) and ryegrass (*Lolium multiflorum*) for dairy cattle feed or used as cover crops for protecting the soils during winter. However, inadequate soil management in these areas, without crop rotation, cover crops during the autumn and winter, and mechanical practices to control surface runoff, has resulted in high erosion rates during the last 60 years, even with the no-tillage system implemented during the last 30 years (Didoné et al., 2019, 2015). Grasslands and pasture, mainly used for cattle raising, cover 5% of the total surface area, whereas forest is found on only 5% of the surface. Approximately 1 to 2% of the area is occupied by non-vegetated areas, urban infrastructure and water bodies.

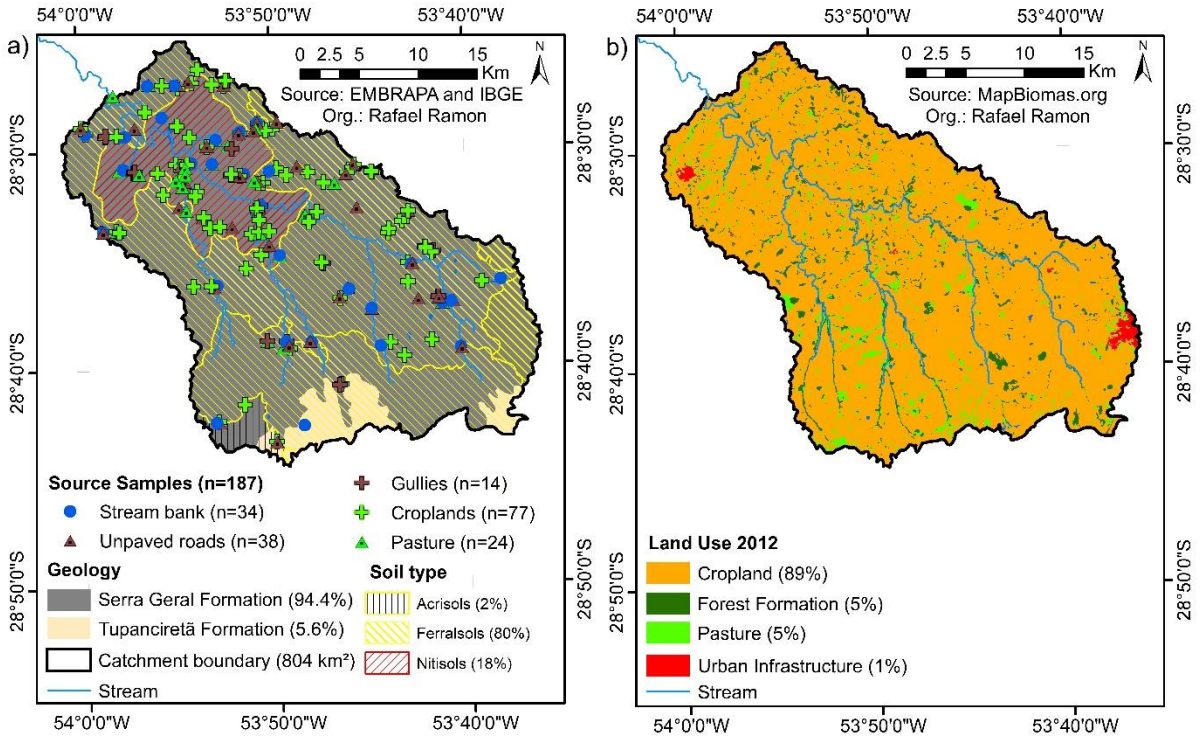

Figure 7.2. Lithological formations, soil types and source sample location (a); and land use map for the year 2012 (b).

7.2.2 Source and sediment sampling

Soil composite samples (n=187) were collected in areas representative of the potential sediment sources, which include cropland (n=77), pasture (which include grasslands and permanent pastures, n=24), unpaved road (n=38), stream bank (n=34) and gullies (n=14) (Figure 7.2). The source samples were taken from the surface layer (0 – 5 cm) of cropland and pasture (surface sources). In gully sites and stream bank samples were taken from the exposed sidewall avoiding the material of the most superficial layer (0-5 cm). The height exposed in the gullies sites and stream banks varies greatly, but as the soil below the surface layer is quite homogeneous in the Ferralsols of this catchment, the samples were collected in a representative manner throughout the exposed subsurface area. To characterize unpaved roads, samples were taken mainly in the roadsides where erosion is more evident, which in all cases correspond to the subsurface of the soil, always avoiding collecting transient materials from other potential sources. Care was taken to avoid those sites that have accumulated sediment originating from other sources. Around ten sub-samples were collected within a radius of approximately 50 m and mixed to prepare a composite sample, in order to obtain representative source material. Samples were taken at sites sensitive to erosion and connected to the stream

network, and attention was paid to cover all the range of soil types found in the catchment.

Eleven sediment samples were collected at the catchment outlet during the monitoring period (Appendix A). From these, eight samples are fine-bed sediment (FBS) collected in the bottom of the river with a suction device and three samples were collected with a time-integrated sediment sampler (TISS) designed according to Phillips et al. (2000). The period during which the TISS was sampled and the collection date of each FBS sample are detailed in Table 7.1.

Table 7.1.Sediment samples and their respective period of sampling.

ID	Sample Type	Collection period
S-1	FBS	02/03/2011
S-2	FBS	21/04/2011
S-3	FBS	21/05/2011
S-4	FBS	18/07/2011
S-5	FBS	18/10/2011
S-6	FBS	02/02/2012
S-7	FBS	24/03/2012
S-8	FBS	10/11/2012
S-9	TISS	02/03/2012 - 09/08/2012
S-10	TISS	17/08/2012 - 10/11/2012
S-11	TISS	10/11/2012 - 30/01/2013

FBS – fine bed sediments and TISS – time integrated sediment samples.

7.2.3 Source and sediment analyses

All samples were oven-dried (50°C), gently disaggregated using a pestle and mortar and dry-sieved to 63 μm to avoid particle size effects prior to further analysis (Koiter et al., 2013; Laceby et al., 2017).

7.2.3.1 Geochemical properties

A total of 20 geochemical elements were evaluated as potential tracers. The total concentration of Al, Ba, Be, Ca, Co, Cr, Cu, Fe, K, La, Li, Mg, Mn, Na, Ni, P, Sr, Ti, V, and Zn was determined using inductively coupled plasma optical emission spectrometry (ICP-OES) after microwave-assisted digestion with concentrated HCl and HNO_3 (ratio 3:1) for 9.5 min at 182 °C. This method was adapted from U.S. EPA (2007), as it was reported to provide satisfactory recovery for quantifying metal concentrations in soils (Chen and Ma, 2001; Da Silva et al., 2014). Total organic carbon (TOC), which was estimated by wet

oxidation ($K_2Cr_2O_7$ + H_2SO_4 - Walkley and Black, 1934), was included in the set of geochemical tracers.

7.2.3.2 Magnetic properties

Two grams of each sample were used to measure the magnetic susceptibility in a Bartington MS2B Dual Frequency sensor, with three readings for each sample at high (4.7 kHz) and low frequencies (0.47 kHz) to obtain the mass specific magnetic susceptibility for high (χ_{HF} – m^3 kg^{-1}) and low frequencies (χ_{LF} – m^3 kg^{-1}) (Mullins, 1977).

7.2.3.3 Ultraviolet-visible analysis and parameters calculation

The diffuse reflectance spectra in the ultraviolet-visible (UV) wavelengths (200 to 800 nm, with 1 nm step) were measured for each powdered sample using a Cary 5000 UV-NIR spectrophotometer (Varian, Palo Alto, CA, USA) at room temperature, using $BaSO_4$ as 100% reflectance standard. Twenty-two colour parameters were derived from the UV spectra following the colorimetric models described in details by Viscarra Rossel et al. (2006), which are based on the Munsell HVC, RGB, the decorrelation of RGB data, CIELAB and CIELUV Cartesian coordinate systems, three parameters from the HunterLab colour space model (HunterLab, 2015) and two indices (coloration – CI and saturation index – SI) (Pulley et al., 2018). In total, 27 colour metric parameters were derived from the spectra of source and sediment samples (L, L*, a, a*, b, b*, C*, h, RI, x, y, z, u*, v*, u', v', Hvc, hVc, hvC, R, G, B, HRGB, IRGB, SRGB, CI and SI). Three other parameters were calculated from the second derivative curves of remission functions in the visible range of soil and sediment samples, which displayed three major absorption bands at short wavelengths commonly assigned to Fe-oxides (Caner et al., 2011; Fritsch et al., 2005; Kosmas et al., 1984; Scheinost et al., 1998) (Appendix B).

7.2.4 Sediment source discrimination and apportionment

The selection of the discriminant tracers followed the classical three-step procedure, including: i) a range test; ii) the Kruskal-Wallis *H* test (KW *H* test); and iii) a linear discriminant function analysis (LDA) (Collins et al., 2010a). In the range test, variables with median ± the interquartile range (IQR, 25^{th} and 75^{th} percentiles) values of sediment samples lying outside the range of the sources were excluded (Batista et al., 2018). The KW *H* test was performed to test the null hypothesis ($p < 0.05$) that the sources belong to the same population. The variables that provided significant discrimination between sources were analysed with a forward stepwise LDA ($p < 0.1$) in order to reduce

the number of variables to a minimum that maximizes source discrimination (Collins et al., 2010b). The statistical analyses were performed with R software (R Development Core Team, 2017) and more details can be found in Batista et al. (2018).

The source contributions were estimated by minimizing the sum of squared residuals (SSR) of the mass balance un-mixing model. Optimization constraints were set to ensure that source contributions were non-negative and that their sum equalled 1. The un-mixing model was solved by a Monte Carlo simulation with 2500 iterations. More information about model settings and compilation can be found in Batista et al. (2018). Model uncertainties were evaluated based on the interquartile variation range of the predictions from the multiple interactions of the Monte Carlo simulation. The standard deviation (SD) of the Monte Carlo simulation results is calculated for each sediment sample and source.

In order to test the ability of magnetic (M) and ultraviolet-visible derived variables (UV) to discriminate between sediment sources, six approaches were tested to verify the contribution of each variable dataset. A first approach was carried out considering only geochemical variables (GEO) as potential tracers and the LDA and apportionment model results were compared to those obtained with geochemical tracers combined with M variables (GM), GEO plus UV (GUV), all variables together (GMUV) and UV variables alone. Finally, an approach was carried out considering only those "alternative" variables, involving M plus UV derived parameters (MUV).

7.3 Results

7.3.1 Selection of sediment tracers

All parameters were analysed individually to check their conservative behaviour and the property distribution in each group was evaluated using box plots. The interquartile range was more restrictive than the classical range test based on maximum and minimum values measured in the sources, resulting in a high number of tracers (70 %) removed by the range test (Table 7.2). From the 21 geochemical elements, only five behave conservatively (TOC, Be, Fe, K and P) . The set of 30 UV parameters included nine conservative properties (L*, x, L, a, b, v*, v', hVc, and B). Magnetic parameters, χ_{HF} and χ_{LF} were both conservative. It means that about 24, 30 and 100% of geochemical, UV parameters and magnetism tracers, respectively, behaved conservatively when applied

the IQR range test. If applied the classical range test, about 72, 97 and 100% of geochemical, UV parameters and magnetic tracers, respectively, behaved conservatively.

Table 7.2. Tracers removed by the conservative test.

Classical range test	IQR Approach
Co, V, Na, Ti, TOC, K, hvC	Al, Ba, Ca, Co, Cr, Cu, La, Li, Mg, Mn, Na, Ni, Sr, Ti, V, Zn, A1, A2, A3, a*, b*, CI, C*, G, h, HRGB, hvC, Hvc, IRGB, R, RI, SI, SRGB, u', u*, y, z

The KW H test was applied to all tracers, even to those that were not retained by the conservativity test. Only five tracers did not hold potential to discriminate between at least two potential sources (Cu, Ni, Fe, Na and A2 had $p > 0.1$) (Table 7.4). Among the parameters that were conservative and passed the KW H test, the combination of tracers that best discriminated between the sources was selected by the LDA, which are presented in Table 7.3.

Table 7.3. Selected tracers by the LDA for each tracer combination and the corresponding percentage of samples correctly classified (SCC).

Tracer combination	Tracers selected	% SCC
GEO	TOC, P, K	68.4%
UV	a, v*, v', b	59.4%
MUV	a, v*, v', b, χ_{HF}, χ_{LF}	60.4%
GUV	TOC, K, P, a, v*, b, L, L*	73.3%
GM	TOC, K, P, χ_{HF}, χ_{LF}	74.3%
GMUV	TOC, K, P, a, v*, b, L, L*	73.3%

G - geochemical tracers; UV – UV-VIS derived parameters; M - magnetic variables; SCC – Samples correctly classified.

When geochemical data were used as potential tracers, P, K and TOC were always selected as tracers. TOC and P are well correlated (Figure 7.3) and they have a higher concentration in the surface samples (24 g kg^{-1} and 445 mg kg^{-1}) than in the subsurface samples (11 g kg^{-1} and 300 mg kg^{-1}). The mean concentration of TOC and P found in the sediment (22 g kg^{-1} and 468 mg kg^{-1}) was close to that observed in the surface sources. K had no correlation with P and TOC, besides having higher concentrations in the surface sources (875 mg kg^{-1}). The K concentration in the sediments varied widely, with a standard deviation closer to the mean (397 ± 362 mg kg^{-1}), which makes this value similar to that found in subsurface sources (565 mg kg^{-1}). Potassium and P presented higher

concentrations in the cropland samples due to the addition of fertilizers for crop production. TOC presents higher concentrations in the pastures, which can be attributed to the permanent soil cover and the increase of below-ground biomass induced by well managed animal grazing (López-Mársico et al., 2015; Schuman et al., 1999; Tornquist et al., 2009). Iron was considered as conservative although it did not provide discrimination between sediment sources. This was somehow expected, since highly weathered soils have a high content of Fe oxides across the entire soil profile, making comparison of surface and subsurface sources very difficult. Beryllium was conservative, but its variation between sources was very low, presenting low potential for discrimination between sources (KW *H* test $p > 0.01$). Finally, the LDA selected only P, K and TOC as tracers for the GEO approach, which did not comply with the universal rule of the discriminant analysis for multiple groups, stating that the number of tracers must be at least equivalent to the number of groups (n) minus one (n-1) (Rencher, 2005). For this reason, the use of geochemical tracers alone was not modelled.

Table 7.4. Magnetic, geochemical and UV-VIS derived parameters concentrations in the potential sources and in sediment of the Conceição catchment, and results of the mean test.

Fingerprint property	Cropland	Pastures	Unpaved Road	Stream Banks	Gullies	Sources		Sediments	KW	
	Mean ± SD	Mean ± SD	Mean ± SD	Mean ± SD	Mean ± SD	Max	Min	Mean ± SD	p value	H value
n =	77	24	38	34	14	187		11		
χLF (10^{-6} m^3kg^{-1})	20.1 ± 8	15 ± 7.4	22 ± 8.7	11 ± 5.6	15.3 ± 9.3	42.7	1.7	14 ± 3	< 0.001	38.6
χHF (10^{-6} m^3kg^{-1})	18.4 ± 7.1	13.9 ± 6.8	19.4 ± 7.5	10.3 ± 5.2	13.7 ± 8	38.0	1.5	13.3 ± 3.1	< 0.001	36.7
TOC (g kg^{-1})	22 ± 4.6	25.9 ± 4.8	7.4 ± 4.6	15.7 ± 5.2	10.5 ± 5.9	36.3	1.5	22.4 ± 8.1	< 0.001	116.2
Ba (mg kg^{-1})	200.2 ± 84.6	209.7 ± 73.6	131.1 ± 79.4	215.1 ± 56.1	153.2 ± 72.2	500.4	46.1	261.9 ± 38.1	< 0.001	34.5
Be (mg kg^{-1})	3.7 ± 0.6	3.6 ± 0.7	3.5 ± 0.6	4 ± 0.6	3.5 ± 0.5	5.5	1.9	3.5 ± 0.6	0.010	13.2
Co (mg kg^{-1})	47 ± 21.6	53.3 ± 20.6	28.1 ± 18.8	59.6 ± 20.6	41.4 ± 30.5	118.8	2.6	88.5 ± 18.4	< 0.001	37.1
Cr (mg kg^{-1})	76.1 ± 19.1	77.8 ± 18.9	69.7 ± 14.5	79.8 ± 12.4	68.4 ± 26.3	146.4	39.4	88.4 ± 6.3	0.005	15.0
Cu (mg kg^{-1})	325.3 ± 66.8	306.3 ± 60.9	318.2 ± 73.1	335.2 ± 61.4	337.1 ± 77.5	568.2	139.3	303 ± 34	0.233	5.6
La (mg kg^{-1})	34.8 ± 10.1	31.8 ± 7.1	33.1 ± 10	37.6 ± 8.4	39.9 ± 7.5	66.8	15.8	30.6 ± 2.7	0.019	11.8
Li (mg kg^{-1})	56 ± 19.4	48.8 ± 22.2	73.1 ± 25.4	51.2 ± 12.4	63.2 ± 30.4	143.5	21.2	32.8 ± 3.5	< 0.001	24.4
Ni (mg kg^{-1})	50.1 ± 16.1	48.9 ± 12.8	53.3 ± 20.2	47.8 ± 11.9	41.7 ± 9.6	122.8	21.3	52.4 ± 2.3	0.240	5.5
Sr (mg kg^{-1})	23.9 ± 13	26.1 ± 11.8	13.7 ± 9.2	25.4 ± 8.6	22.4 ± 12.7	84.0	4.4	35 ± 5	< 0.001	55.2
V (mg kg^{-1})	365.3 ± 60.2	400.4 ± 70.4	299.7 ± 59.3	381.5 ± 60.4	309.5 ± 58.9	581.4	207.7	561.1 ± 87.5	< 0.001	48.9
Zn (mg kg^{-1})	13.8 ± 3.5	14.4 ± 3.5	12.2 ± 2.2	15.3 ± 3	11.9 ± 2.2	33.4	7.2	16.6 ± 2.8	< 0.001	25.7
Al (mg kg^{-1})	70578 ± 13882.3	59871.4 ± 11790.3	91786.4 ± 13002.7	61249.2 ± 10386.8	80320.9 ± 22155.4	113258.9	40415.3	50738.9 ± 4175.2	< 0.001	69.2
Ca (mg kg^{-1})	2140 ± 1204.3	2088.5 ± 1265.8	585.8 ± 904.3	1797.5 ± 838	1004.8 ± 1231	5423.2	0.0	3381 ± 697.6	< 0.001	67.1
Fe (mg kg^{-1})	92707.1 ± 12753.9	86542.5 ± 14868.8	89570.8 ± 11534.2	93838.2 ± 16710.6	90124.2 ± 9441.6	134108.4	48476.4	89629.6 ± 8526.4	0.219	5.7
K (mg kg^{-1})	928.9 ± 651.6	821.9 ± 679.9	697.1 ± 550.6	462.7 ± 384.7	535.3 ± 456.1	3392.3	79.7	397.5 ± 362	0.002	17.2
Mg (mg kg^{-1})	3142.8 ± 1591.8	3307.3 ± 1352.7	2182.8 ± 892.7	2985.9 ± 891	2875.6 ± 1712.4	8466.5	1239.0	3647.2 ± 360.6	< 0.001	26.9
Mn (mg kg^{-1})	1889 ± 580.1	2020.7 ± 746.1	1112.5 ± 546.1	2319.8 ± 1018.1	1739.7 ± 1039.4	5405.6	344.8	2880.2 ± 712.3	< 0.001	45.2
Na (mg kg^{-1})	77.4 ± 76.4	85.4 ± 71.1	78.2 ± 96.4	80.4 ± 35.8	60.6 ± 37.7	620.3	0.0	160.2 ± 170.7	0.163	6.5
P (mg kg^{-1})	486.9 ± 128.1	403.5 ± 66.2	300.8 ± 90.2	343.9 ± 147.7	256.2 ± 69.3	1104.6	59.7	467.7 ± 77.3	< 0.001	85.3
Ti (mg kg^{-1})	3091.8 ± 939	4176 ± 1045.5	2332.8 ± 738.8	3360.3 ± 931.3	2432.1 ± 678.6	6950.7	873.6	18662.4 ± 2472.2	< 0.001	49.2
L*	38.9 ± 3.3	38.3 ± 4.5	40.7 ± 4.8	41.2 ± 3.2	40.7 ± 5.7	52.5	23.8	37.1 ± 3.8	0.013	12.6

a*	16.4 ± 2.5	14.5 ± 2.7	21.5 ± 3.1	14.8 ± 2.5	17.3 ± 3.9	28.9	8.1	12.2 ± 1.5	< 0.001	72.1
b*	23.1 ± 2.2	21.6 ± 2.6	27.3 ± 3.2	24 ± 3.2	24.7 ± 4.2	36.7	15.4	21.5 ± 2.4	< 0.001	52.1
C*	28.4 ± 3.1	26.1 ± 3.6	34.7 ± 4.2	28.2 ± 3.8	30.2 ± 5.4	46.7	17.4	24.7 ± 2.8	< 0.001	60.8
h	54.7 ± 2.8	56.5 ± 3	51.9 ± 2.4	58.3 ± 2.9	55.4 ± 4	65.7	48.5	60.4 ± 1.2	< 0.001	69.0
x	0.4 ± 0	0.4 ± 0	0.5 ± 0	0.4 ± 0	0.4 ± 0	0.5	0.4	0.4 ± 0.006	< 0.001	56.1
y	0.4 ± 0	0.4 ± 0	0.4 ± 0	0.4 ± 0	0.4 ± 0	0.4	0.4	0.4 ± 0.005	< 0.001	42.5
z	0.2 ± 0	0.2 ± 0	0.2 ± 0	0.2 ± 0	0.2 ± 0	0.2	0.1	0.2 ± 0.007	< 0.001	54.7
L	32.6 ± 2.9	32.1 ± 3.9	34.2 ± 4.4	34.6 ± 2.9	34.3 ± 5.1	45.4	20.1	31.1 ± 3.3	0.013	12.7
a	12.5 ± 2.1	10.9 ± 2.3	16.9 ± 2.8	11.4 ± 2.1	13.4 ± 3.3	24.9	5.9	9 ± 1.4	< 0.001	69.2
b	12.3 ± 1.3	11.6 ± 1.6	14.2 ± 1.8	13.1 ± 1.7	13.3 ± 2.4	19.9	7.9	11.4 ± 1.5	< 0.001	37.6
u*	33.6 ± 4.8	29.9 ± 5.4	43.5 ± 6.3	32.1 ± 5.1	36 ± 7.8	62.3	17.9	26.4 ± 3.8	< 0.001	65.7
v*	21.8 ± 2.2	20.8 ± 2.8	24.7 ± 3	23.5 ± 3.1	23.5 ± 4.3	34.7	13.9	20.9 ± 2.8	< 0.001	32.8
u'	0.3 ± 0	0.3 ± 0	0.3 ± 0	0.3 ± 0	0.3 ± 0	0.3	0.2	0.3 ± 0	< 0.001	60.8
v'	0.5 ± 0	0.5 ± 0	0.5 ± 0	0.5 ± 0	0.5 ± 0	0.5	0.5	0.51 ± 0	< 0.001	65.4
RI	2.5 ± 1.5	3.5 ± 4.9	2.2 ± 1.2	1.8 ± 1	2.8 ± 4.1	25.8	0.5	3.1 ± 2.2	0.006	14.4
Hvc	163.7 ± 8.6	169.7 ± 9.7	152.3 ± 8.1	172.6 ± 8.1	164.2 ± 12.9	192.3	141.0	178.9 ± 3.3	< 0.001	71.5
hVc	23.4 ± 1.5	23.1 ± 2.1	24.2 ± 2.2	24.5 ± 1.4	24.3 ± 2.6	29.6	16.5	22.6 ± 1.7	0.013	12.7
hvC	30.0 ± 2.6	28.1 ± 3.1	35.2 ± 3.4	29.9 ± 3.0	31.6 ± 4.4	45.7	21.6	26.6 ± 2.6	< 0.001	60.8
R	193.5 ± 12.6	184.7 ± 14.0	216.1 ± 16.5	185.7 ± 12.3	196.8 ± 21.6	238.9	150.4	178.3 ± 4.9	< 0.001	60.2
G	74.8 ± 3.5	77.2 ± 3.6	68.7 ± 4.4	78.5 ± 3.2	74.5 ± 6.0	85.5	62.1	81 ± 1.1	< 0.001	70.2
B	34.2 ± 3.5	36.5 ± 4.1	28.1 ± 4.9	34.7 ± 4.2	32.8 ± 6.3	48.0	21.8	36.2 ± 1.9	< 0.001	53.5
HRGB	19.5 ± 4.1	16.7 ± 4.3	26.7 ± 5.2	15.8 ± 3.7	20.1 ± 6.9	34.1	7.5	13.1 ± 1.3	< 0.001	66.9
IRGB	100.8 ± 1.9	99.5 ± 2.2	104.3 ± 2.5	99.6 ± 1.9	101.3 ± 3.3	107.8	94.2	98.5 ± 0.8	< 0.001	60.2
SRGB	79.7 ± 8.0	74.1 ± 9.0	94.0 ± 10.6	75.5 ± 8.1	82.0 ± 13.8	108.3	51.2	71 ± 3.4	< 0.001	58.8
CI	0.44 ± 0.05	0.41 ± 0.05	0.52 ± 0.05	0.40 ± 0.04	0.45 ± 0.08	0.6	0.3	0.38 ± 0.02	< 0.001	64.7
SI	0.70 ± 0.04	0.67 ± 0.05	0.77 ± 0.05	0.68 ± 0.05	0.71 ± 0.08	0.8	0.5	0.66 ± 0.02	< 0.001	56.6
A1	0.003 ± 0.001	0.003 ± 0.002	0.004 ± 0.001	0.004 ± 0.002	0.004 ± 0.002	0.0	0.0	0.005 ± 0.001	< 0.001	19.9
A2	0.001 ± 0	0.001 ± 0.001	0.001 ± 0.001	0.001 ± 0.001	0.001 ± 0.001	0.0	0.0	0.002 ± 0.001	0.111	7.5
A3	0.002 ± 0.001	0.002 ± 0.001	0.003 ± 0.001	0.001 ± 0.001	0.002 ± 0.002	0.0	0.0	0.003 ± 0.001	< 0.001	51.0

SD – Standard Deviation

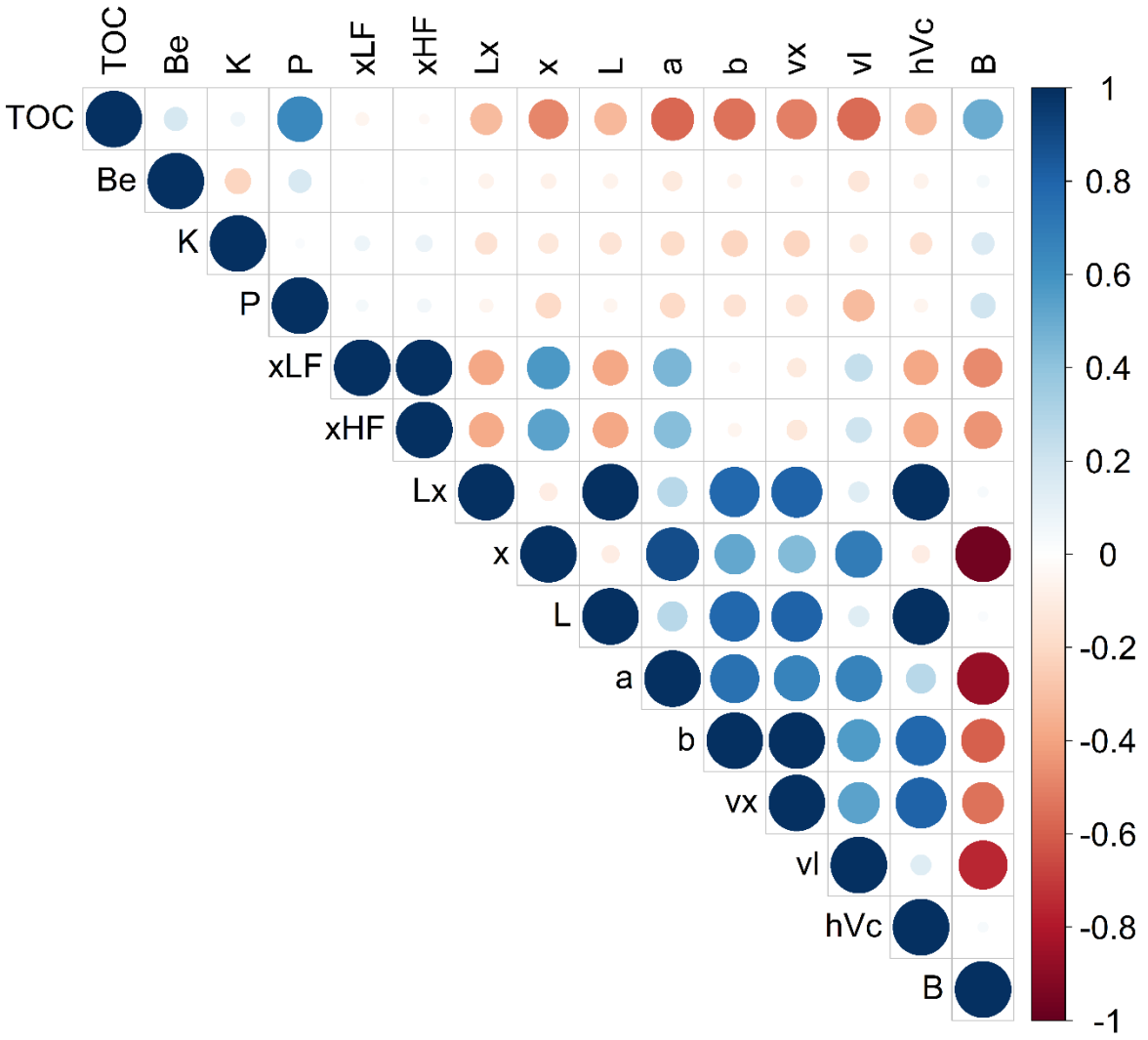

Figure 7.3. Correlation plot between variables that were approved in the conservativeness test and KW H test. The representation of the symbols " * " and " ' " used to differentiate the colour parameters was replaced by the letters "x" and "l" in the figure. xHF and xLF correspond to the magnetic parameters χ_{HF} and χ_{LF}, respectively.

In the approach using GEO and M parameters (GM), the LDA selected two magnetic parameters (χ_{LF}, χ_{HF}) and the three previously selected geochemical elements. The two M parameters were highly correlated (Figure 7.3) and they remained in the same cluster group of tracers, although they differed completely from the group of the other three geochemical elements (Figure 7.4). Therefore, the LDA kept the two M parameters, which improved the discrimination of the sources, resulting in 74.3% of SCC. The differences of magnetic susceptibility values between sources for the two magnetic parameters, χ_{LF} and

χ_{HF}, are similar, where unpaved roads presented higher values (22 x 10^{-6} and 19 x 10^{-6} m^3 kg^{-1}, respectively), followed by croplands, pastures, gullies and stream banks (Table 7.4). Sediment samples have magnetic susceptibility values (14 x 10^{-6} and 13 x 10^{-6} m^3 kg^{-1}, respectively) closer to those observed for pastures (15 x 10^{-6} and 14 x 10^{-6} m^3 kg^{-1}, respectively) and stream banks (11 x 10^{-6} and 10 x 10^{-6} m^3 kg^{-1}, respectively).

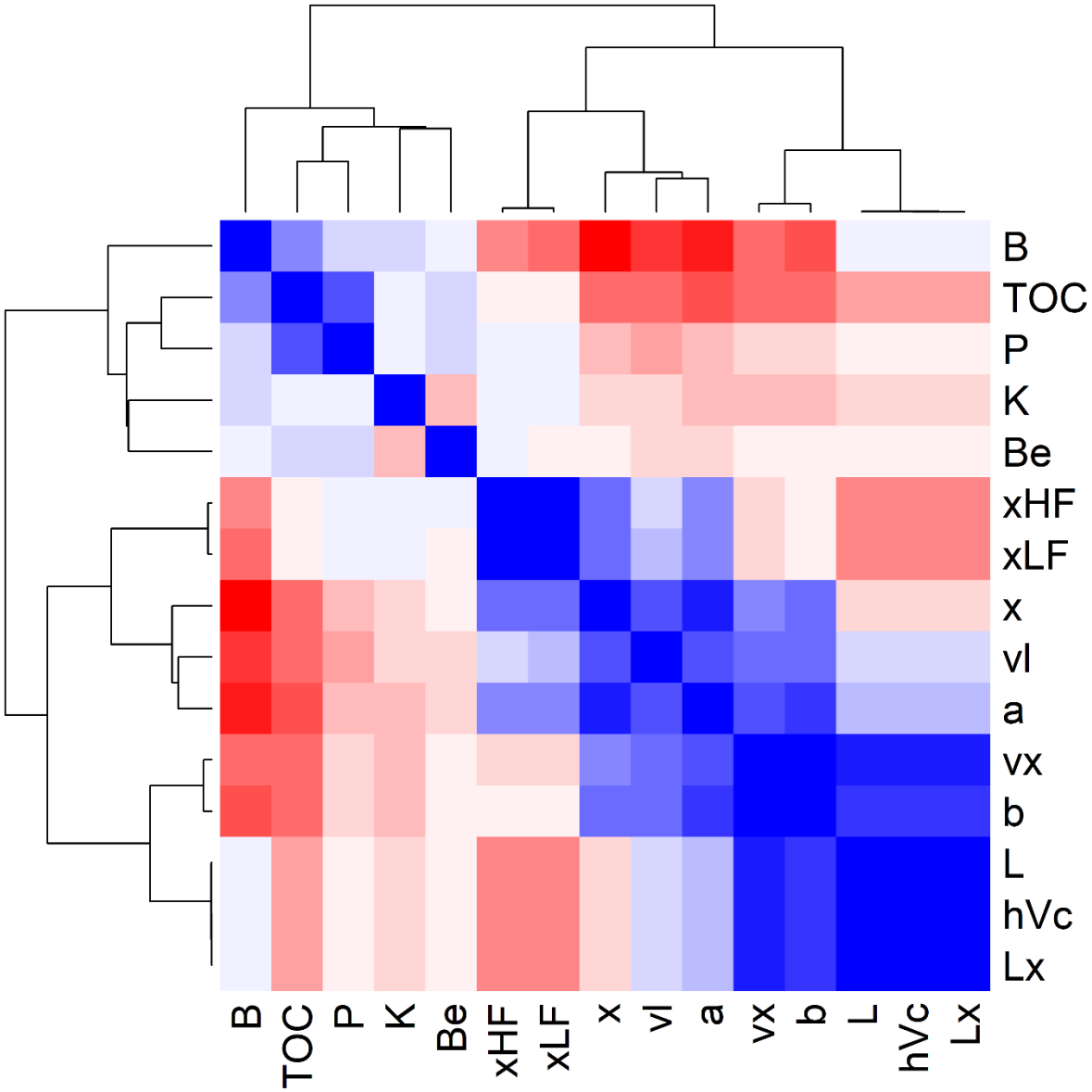

Figure 7.4. Heat map and dendrogram of the variables that were approved in the conservativeness test and KW H test. The representation of the symbols " * " and " ' " used to differentiate the colour parameters was replaced by the letters "x" and "l" in the figure.

The same parameters were selected for the combination of GEO and UV parameters (GUV) and the combination of GEO, UV and M parameters (GMUV). For the UV parameters, a, v*, b, L and L* were selected by the LDA, increasing the SCC to 73.3%, an increase of 4.9% compared to the use of GEO tracers alone. The parameter L and L*

are related to the variation between white and black colours, also considered as the luminosity index from HunterLab and CIELAB, respectively. Stream banks, gullies and unpaved roads, which are subsurface sources (mean of 34 and 41 for L and L*, respectively), had the highest values, which means that they have lighter colours than the surface sources (mean of 32 and 39 for L and L*, respectively). L and L* mean values for sediment samples (31 and 37, respectively) were lower than for all sources and closer to those found in surface sources. More positive values for *a* and *b* means that the colour is more red and yellow, respectively. Subsurface sources tend to be more red and yellow, as *a* and *b* values are higher in this material (13.9 and 13.5, respectively) than in surface sources (11.7 and 12.0, respectively). The mean values for sediments (9.0 and 11.4, respectively) were very close to those of the surface sources. The same behaviour was observed for the parameter v* (21.3 and 23.9 for surface and subsurface sources, respectively), which is the CIELUV colour space model derived parameter equivalent to the *a* from CIELAB.

When UV parameters were used individually, the percentage of SCC was the lowest among all the tested tracer combinations, with 59.4% of SCC. The UV parameters selected in this approach were a, v*, v' and b. Besides the other parameters selected in the other approaches, the parameter v' was selected in the UV approach, which is related to the chromacity coordinates u* and v* from the CIELUV model. When the UV and M parameters were combined, two M parameters were selected, but it did not improve the source classification by the DFA, increasing only by 1% the proportion of SCC. The reclassification of source samples by the LDA using the tracers selected in each approach is illustrated in the bi-plot graphs (Figure 7.5a,Figure 7.6a,Figure 7.7a and Figure 7.8a).

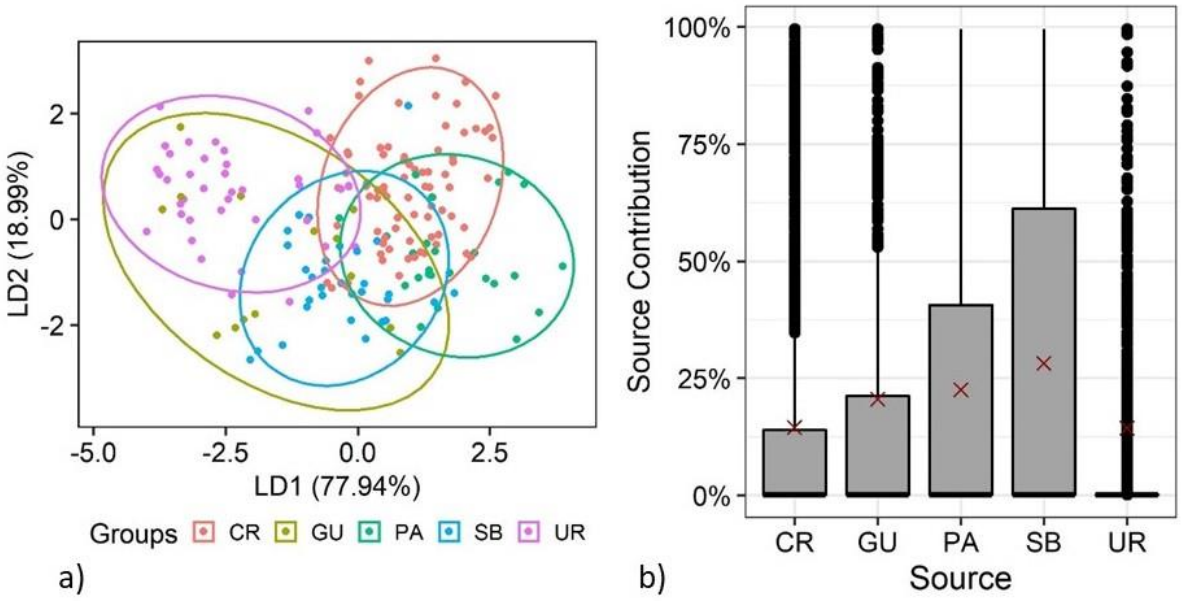

Figure 7.5. Approach considering only UV-VIS derived parameters – UV. a) Source reclassification by the LDA using the selected variables. b) Box plot with the source contributions. The red cross point represents the mean, the horizontal line inside the box represents the median, the lower and upper edges of the box represent the 25th and 75th percentiles, whiskers represent the 10th and 90th percentiles, and circles represent values greater than the 90th percentile.

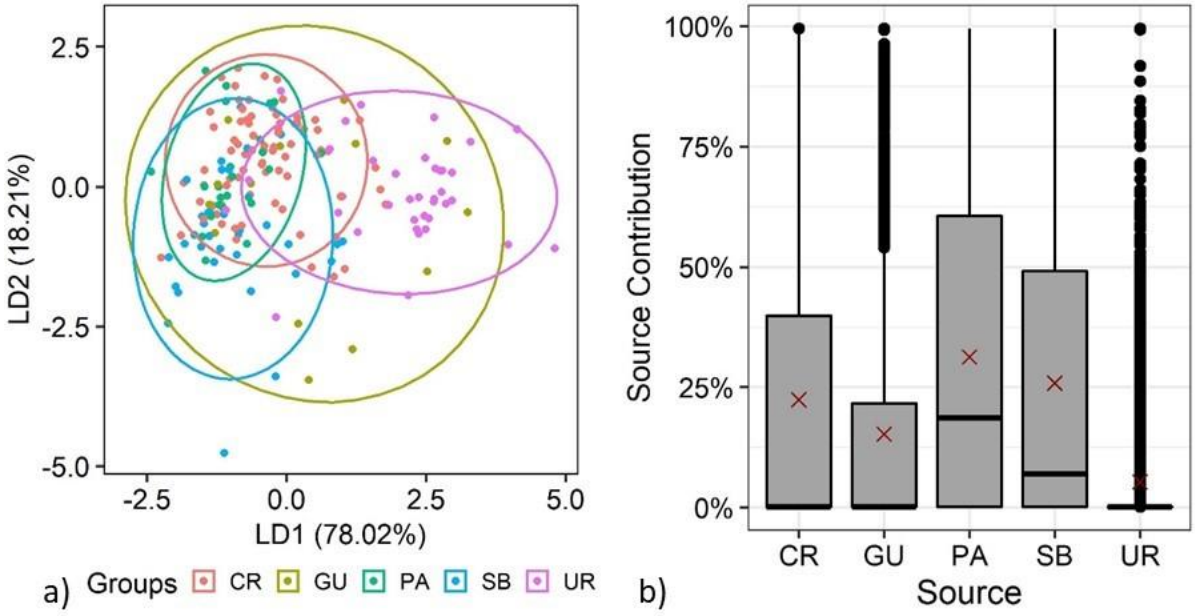

Figure 7.6. Approach considering the combination of UV and magnetic – MUV. a) Source reclassification by the LDA using the selected variables. b) Box plot with the source contribution. The red cross point represents the mean, the horizontal line inside the box represents the median, the lower and upper edges of the box represent the 25th and 75th percentiles, whiskers represent the 10th and 90th percentiles, and circles represent values greater than the 90th percentile.

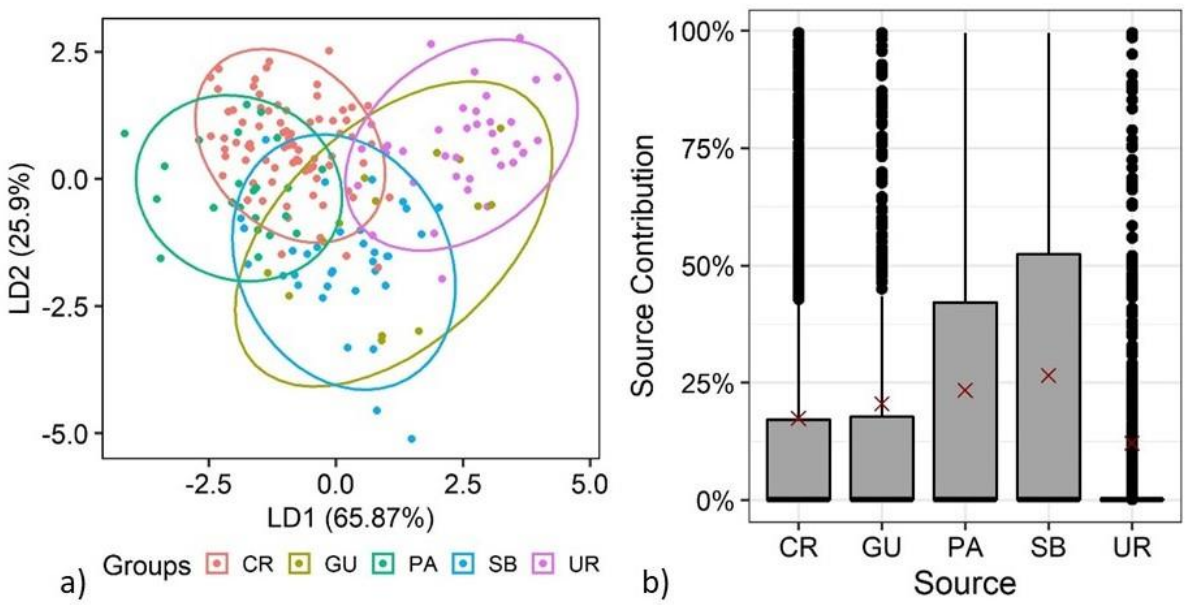

Figure 7.7. Approach considering the combination of GEO and UV parameters – GUV. a) Source reclassification by the LDA using the selected variables. b) Box plot with the source contribution. The red cross point represents the mean, the horizontal line inside the box represents the median, the lower and upper edges of the box represent the 25th and 75th percentiles, whiskers represent the 10th and 90th percentiles, and circles represent values greater than the 90th percentile.

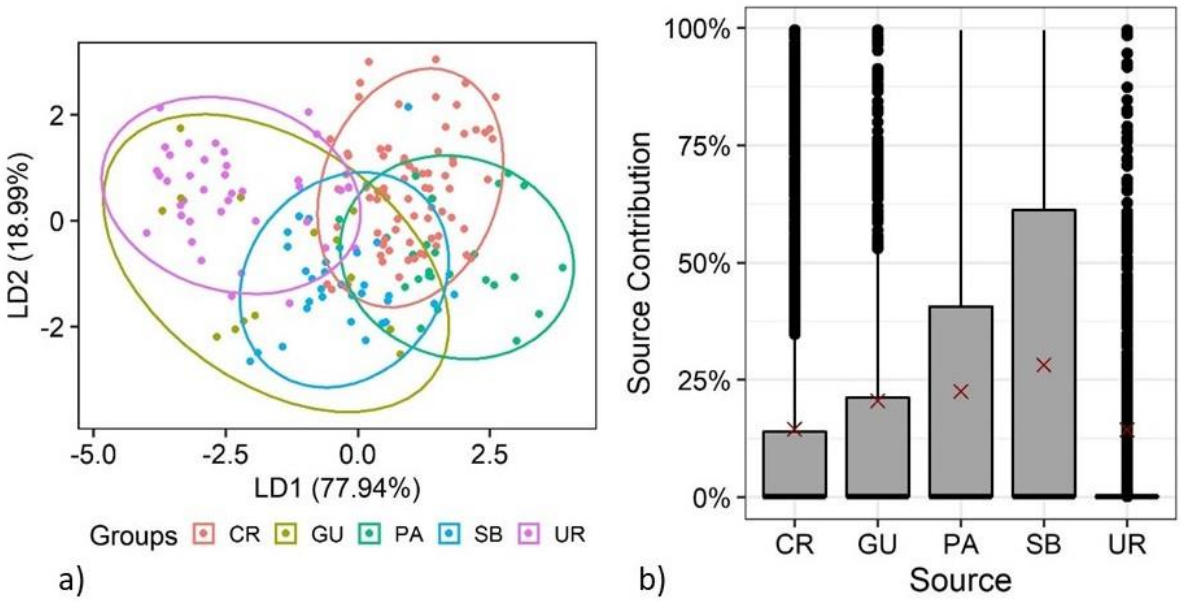

Figure 7.8. Approach considering the combination of geochemical and magnetic parameters – GM. a) Source reclassification by the LDA using the selected variables. b) Box plot with the source contribution. The red cross point represents the mean, the horizontal line inside the box represents the median, the lower and upper edges of the box represent the 25th and 75th percentiles, whiskers represent the 10th and 90th percentiles, and circles represent values greater than the 90th percentile.

7.3.2 Model results for each approach

According to the five approaches modelled (UV, MUV, GUV, GM and GMUV), not including the GEO only model as it had insufficient tracers for the number of sources, pasture had the highest sediment contribution for most approaches, except when geochemical tracers were combined with magnetic tracers, supplying sediment proportions ranging from 24 to 33%. Stream bank and cropland were the second and third sources in increasing order of contribution, with contributions ranging from 26 to 31% and 17 to 23%, respectively. Gullies were the fourth contributing source, with a sediment delivery proportion varying between 16 and 19%. Unpaved roads provided the lowest contribution to the river sediment, ranging from 2.6 to 12.2%. The mean relative contributions of each source did not vary significantly between approaches when the mean contributions for all sediment samples are compared, with the exception of unpaved roads, for which the UV approach led to different results (Table 7.5).

When sediment samples were separated according to the sampling strategy, significant differences between approaches were observed for cropland and unpaved roads for both sampling strategies (Table 7.5). Comparing the type of sediment samples, cropland had a higher contribution to TISS samples (16 to 39%) compared to FBS samples (15 to 25%). The contribution of pastures to TISS samples was even higher, ranging from 32 to 40%. Unpaved roads had a larger contribution to FBS samples (~10.5%) and contributed less to the TISS samples (~3.5%). For pasture and stream bank, significant differences between approaches were observed for FBS (19.9 to 33.2%) and TISS (16.8 to 31.8%) samples, respectively, while for gullies no difference was observed for any sampling strategy.

The differences in sediment source contributions are mainly observed between the approaches with only alternative tracers (UV and MUV) to those with geochemical parameters included. Figure 7.5b to 7.8b provide box plots demonstrating the variation in mean source contributions for all sediment samples when taking into account the 2500 Monte Carlo interactions results obtained for each approach. The large variations in source contributions obtained for each set of simulations resulted in a standard deviation (SD) that varied between 19 and 34% depending on the source considered (Table 7.5).

Table 7.5. Mean contribution and mean standard deviation of each source contribution for all target sediment samples and for individual sediment sampling strategies conducted in the Conceição River catchment.

	Approaches	CR (%)			GU (%)			PA (%)			SB (%)			UR (%)		
		Mean	TISS	FBS	Mean	TISS	FBS	Mean	TISS	FBS	Mean	TISS	FBS	Mean	TISS	FBS
Source contribution	UV	16.6a	16.5b	16.7ab	15.9a	15.6a	16.0a	33.6a	34.7a	33.2a	31.2a	31.8ab	31.0a	2.6b	1.5b	3.1b
	GM	17.8a	24.3ab	15.4b	19.2a	10.7a	22.4a	24.4a	36.3a	19.9b	26.4a	23.2ab	27.7a	12.2a	5.5a	14.7a
	GUV	19.9a	32.5a	15.1b	17.0a	7.3a	20.6a	26.7a	40.5a	21.5ab	26.3a	16.8b	29.9a	10.1a	2.9a	12.8a
	MUV	23.1a	17.6ab	25.2a	14.4a	15.8a	14.0a	31.1a	32.3a	30.6ab	26.4a	31.5a	24.6a	4.9ab	2.9a	5.7ab
	GMUV	19.6a	32.6a	14.8b	17.1a	7.2a	20.8a	26.4a	40.3a	21.2ab	26.6a	17.1ab	30.2a	10.2a	2.8a	13.0a
Standard deviation	UV	31.7	31.8	31.6	29.5	29.2	29.7	38.2	38.6	38.0	36.9	37.2	36.9	9.5	7.5	10.2
	GM	26.7	26.9	26.7	29.7	19.6	33.5	30.9	31.8	30.6	34.5	27.9	37.0	23.9	13.4	27.8
	GUV	28.2	29.4	27.8	28.3	15.5	33.0	31.8	31.2	32.1	34.4	23.7	38.4	22.0	9.0	26.9
	MUV	28.1	29.5	27.6	28.3	15.5	33.1	31.7	31.2	31.8	34.5	23.9	38.5	22.0	8.6	27.0
	GMUV	30.4	27.4	31.5	24.6	26.1	24.1	32.9	34.1	32.5	31.3	34.0	30.2	12.3	10.1	13.1

Means followed by the same letter in the columns do not differ statistically by the Kruskal-Wallis H-test at $p<0.05$. TISS = Time Integrated Sediment Sampler (n=3); FBS = Fine bed sediment samples from the river bottom (n=8); CR = Croplands; GU = Gullies, PA = Pastures; SB = Stream banks; and UR = Unpaved roads.

The sediment source contributions predicted by the five approaches were similar for the samples collected following the FBS sampling strategy, while the variation between approaches was higher for the TISS samples (Figure 7.9). Pasture provided the main source of TISS samples according to all approaches, contributing more than 32% of sediment, followed by cropland with more than 24%, with the exception of the approaches based on UV and MUV parameters, according to which cropland contributed only 16 and 18% of sediment, respectively. For the FBS samples, stream bank provided the main source of sediment, contributing more than 25% of the material delivered to the river, with the exception of the approaches based on UV and MUV parameters, according to which pasture was the main source of sediment, with 33 and 31%, respectively.

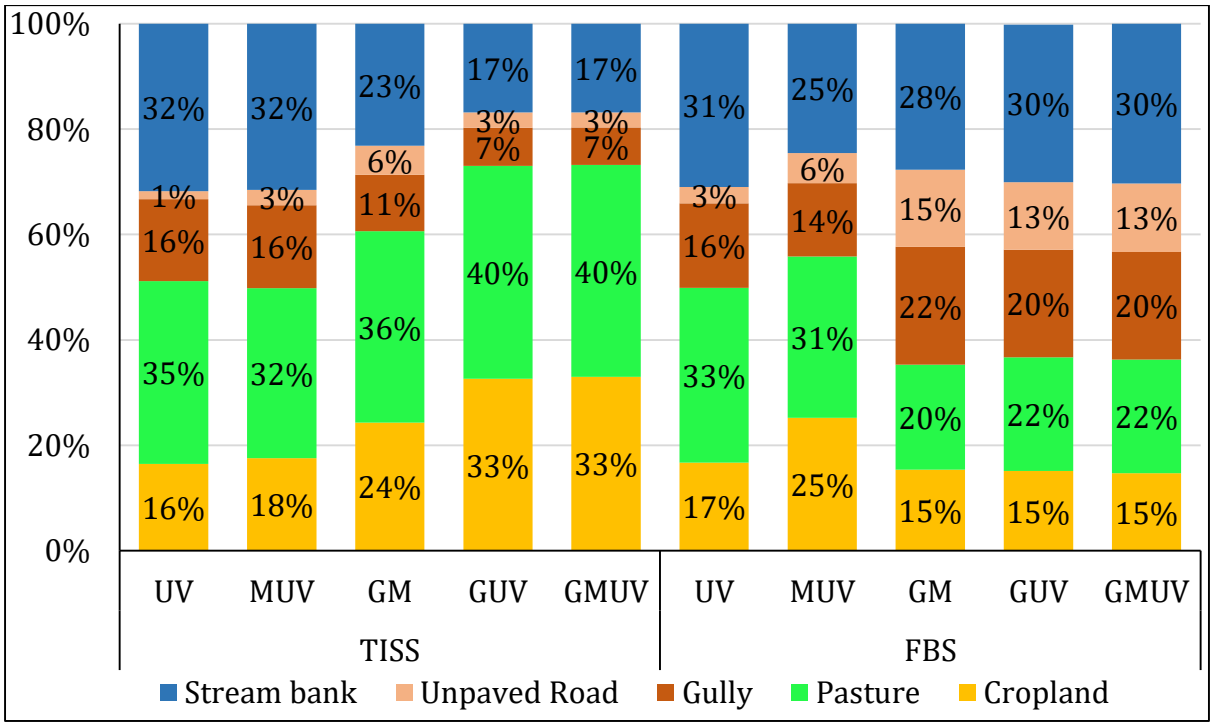

Figure 7.9. Mean contributions of each sediment source for the two types of sediment sampling strategies (TISS and FBS) and following the five approaches relying on different tracer combinations.

7.4 Discussion

7.4.1 Tracer selection and discrimination between sources

The conservative behaviour of a sediment property may vary according to different factors (e.g. physical, biochemical and geochemical), requiring an appropriate selection of those that do not suffer modifications from their sources to the sediment sampling site, avoiding uncertainties in the sediment fingerprinting technique (Koiter et al., 2013; Sherriff et al., 2015). There are different strategies to verify that a certain tracer

is conservative or not, such as the commonly used range test (Navratil et al., 2012; Palazón and Navas, 2017a; Smith and Blake, 2014), where the value of a given tracer measured in sediment must lie within the range of values observed in the sources. However, the statistical test chosen can select different tracers and, consequently, lead the final mixing model to provide different results (Gaspar et al., 2019). In addition, the conservatism test based on mathematical and statistical tests only cannot confirm that the tracer behaves conservatively (Collins et al., 2017b).

In the current research, the classical range test based on the maximum and minimum values found in the source samples indicated that 87% of the total variables were conservative, while with the IQR test, only 30% were considered to be conservative. The range test based on maximum and minimum values observed in the sources is less restrictive because, with this test, having only one extreme value for a source sample is sufficient to make the range wider. At the same time, if only one sediment sample has a value outside of the range, it is sufficient to remove the parameter from further analysis. This situation was observed for K and TOC, which were not retained after applying the minimum/maximum range test, because K was not detected in two sediment samples and TOC had a higher concentration in one sediment sample than in the sources, removing two of the three commonly best geochemical tracers used to discriminate potential sediment sources in agricultural catchments. The range test based on IQR proposed by Batista et al. (2018) provided more reasonable results, as it kept only those tracers for which the values measured in the target samples lied within the range found in the sources. Accordingly, it allowed keeping parameters that would have been removed otherwise because only one sediment sample was outside of the range of values measured in the sources. Future research considering the application of alternative conservativeness tests for this homogeneous catchment, such as bi-plots or more complex methods considering organic carbon and particle size dependency, may help to select the most appropriate tracers (Smith et al., 2018; Lizaga et al., 2020).

The potential of multiple sets of tracers to improve the discrimination between potential sources is clearly shown by the LDA biplot analysis. However, in none of the combinations tested, there was a clear distinction between potential source groups. According to the distribution of dots and ellipses, there is an overlap of groups, especially for the approaches UV and MUV. The combination of GEO with the other sets of tracers, M and UV, improved the discrimination between two groups: surface (pasture and

cropland) and subsurface sources (stream bank, unpaved road and gully). The lack of clear discrimination evident in the LDA biplots likely adds uncertainty to the model results.

The soils of the catchment are naturally poor in K and P, two of the main macronutrients essential for crop growth and productivity. The addition of fertilizers in croplands and pastures explains the higher concentration of these elements in surface sources, which differed significantly from those found in subsurface sources. The TOC concentration in the Ferralsols of the region is usually higher in the upper layer of the soil, due to the addition of carbon by the plant residues and roots, as observed in a study of Bortolon et al. (2011), where soil analyses had a mean concentration 1.5 times higher in the uppermost 10 cm of the soil compared to the 10-20 cm layer. Indeed, these three tracers (P, K and TOC) have great potential for tracing agricultural land uses. However, the three geochemical tracers selected in the current research (P, TOC and K) are usually removed from analysis in most sediment fingerprinting studies, as they are generally considered to be easily enriched or depleted during the erosion process (Palazón and Navas, 2017b; Smith and Blake, 2014). Even though, most studies end up discarding these elements without performing any range tests to assess their conservativeness. For example, in an evaluation of 60 studies that evaluated P as a potential tracer, only 27 of them applied a range test, and of these, P was conservative in 85% of cases (Tiecher et al., 2019). Moreover, this parameter was selected to model source contributions in 43% of the 60 sediment fingerprinting studies that were reviewed in Tiecher et al. (2019).

The transformation of the sediment composition during the erosion and river transport processes is variable depending on the study site considered. The TOC levels found in sediment samples collected in a previous study conducted in the Conceição River catchment (Tiecher et al., 2018) had a lower concentration in the target material compared to that found in the sources, while in the study of Pulley et al. (2015a) sediment was found to be enriched in TOC compared to potential sources. In catchments with strongly weathered soils rich in iron oxides, P is known to be mainly transported in particulate form in the rivers (Bender et al., 2018). This strong chemical adsorption to soil and sediment particles may preserve the P source signature during their transfer in river systems. The no-tillage farming that is main soil management system in the Conceição catchment in soils with a high content of clay and iron oxides may have induced the physico-chemical protection of C and P into micro aggregates (Six et al., 2002; Snyder

and Vázquez, 2005). TOC and P are highly correlated as shown in Figure 7.3, and the strong physical-chemical protection of these elements may support their conservative behaviour. Furthermore, the conservative behaviour of Fe demonstrates that the reduction from its solid state (oxides with Fe^{3+}) to the aqueous one (Fe^{2+}) is not an important process during sediment transport in this catchment, allowing the conservation of the source characteristics.

Soil organic carbon, water content, iron oxides and chemical composition are the main parameters responsible for the soil colour (Ben-dor et al., 1998). Although the TOC content had a low correlation with the colour parameters, this parameter can create a source of error in the colour indices, especially when there is a small colour difference between the potential sources (Pulley and Rowntree, 2016a). The soils of the Conceição River catchment are rich in iron oxides, mainly found as goethite and hematite, and colour parameters are closely linked to their respective content in the soils (Schaefer et al., 2008). The A3 index, which is related to the electron pair transition of hematite, have a strong correlation with most colour parameters (data not presented), highlighting the importance of iron oxides in defining the soils and sediment colours in this catchment. Hematite is responsible for the red colour of Ferralsols, while goethite is responsible for the brownish-reddish yellow colour of soils (Cornell and Schwertmann, 2003). The Hr index, which cannot be used in the mixing model because it is not linearly additive, represents the proportion of hematite in the pool of iron oxides (goethite + hematite). Although the soils in the region are predominantly red in colour, their content in goethite is higher than in hematite (Ramos et al., 2020). The Hr index had lower values in the stream banks compared to the other sources, since there is a greater tendency to form goethite in relief positions characterised by the accumulation of water, where ferrihydrite tends to dissolve and form goethite in its place (Schaefer et al., 2008).

Owing to the homogeneity of the soil types due to their intense chemical weathering found in the Conceição catchment, the difference in colour and iron oxide parameters between land uses (pastures and croplands) is very low. Differences between surface and subsurface sources tend to be more evident, since a difference in TOC and clay content is usually observed in this type of soils (Table 7.4) (Testoni et al., 2017). A similar observation is valid for magnetic parameters, which are closely related to the ferromagnetic properties of the soil, which are in turn mainly controlled by particle size and the nature of parent material (Pulley and Rowntree, 2016b). As the potential sources

evaluated are originated from very similar soil types and parent material in our catchment, M and UV parameters did not improve significantly the discrimination between land use-based sources.

In the same way as with the GEO parameters selected, UV and M likely provided stronger discrimination between surface and subsurface sources. When UV parameters were used in isolation, they were able to classify correctly almost 60% of the samples in their respective groups, which is not so different from the %SCC obtained with GEO tracers alone (68%), according to the LDA. This demonstrates the potential of UV and M tracers to provide a low-cost alternative to GEO tracers. Although UV parameters were not very effective alone in the current research, they have already been used successfully in other case studies (Evrard et al., 2019; Pulley et al., 2018).

The low conservativeness of the tracers tested may also be associated with particle size issues (Laceby et al., 2017). Owing to time and financial constraints it was not possible to conduct particle size analyses. Future studies should also consider assessing how particle size may affect conservativeness during erosion, transport and deposition processes in large river catchments. Furthermore, clay soils with high levels of iron oxides, as observed in the present catchment, often form strong stable microaggregates, during erosion process and transport processes, which may behave similarly to coarse particles (silt and sand) (Droppo et al, 2005). Future research should therefore investigate how microaggregates may also affect tracer conservativeness in sediment fingerprinting research in large scale catchments.

7.4.2 Mixing model results

The results of the mixing model are impacted by the relatively bad quality of the sediment source discrimination. The small difference in tracer signature observed within a given group (surface or subsurface) introduces high uncertainties in the mixing model (Pulley et al., 2017a). The mixing model results in a large IQR, which means that the uncertainty in the model predictions is high. However, the mean results are similar to those observed by Tiecher et al. (2018), who showed that surface sources provided the main source of suspended sediment collected following the TISS strategy, and subsurface sources, mainly stream bank, supplied the main source for FBS samples. The model results according to the different sets of tracers were consistent and there were no major differences between them. Although there is some correlation between the selected

parameters in each approach (Figure 7.3), the potential effect of this collinearity cannot be tested without artificial mixtures, which should be recommended for future research.

Pasture and cropland were poorly distinguished by the discriminant analysis. As a consequence, the mixing model predicted a larger contribution of pastures, which is not consistent with the situation observed in the catchment, where the percentage of land use occupied by pasture is much lower (maximum of 11.9%) and where soil erosion remains limited under this land use. Unpaved roads provided the source that contributed the least to sediment, as observed by Tiecher et al. (2018). Considering the mean source contributions obtained in the current research, they remained consistent with our overall understanding of the hydro-sedimentary behaviour of the catchment, although the high uncertainties associated with the model predictions limited the potential use that could be made of these calculated contributions (e.g. for catchment and river management). In that, the results of the current research strongly differed from those of Chen et al. (2019), who obtained a good discrimination between land uses using the geochemical composition in a catchment with similar geological conditions in the Three Gorges Dam Region, China. However, this study was conducted in two small catchments (0.78 and 0.46 km^2) with shallow (< 50 cm depth) and poorly developed soils with rock fragments, and land use management was also very different. Accordingly, this shows that considering the homogeneity of geological conditions is not sufficient to derive the tracer list as different pedogenic processes and land use mangement may impact the tracing properties.

The selection of tracers to be used in each study is generally defined by the constraints of financial resources and access to the analytical facilities (Collins et al., 2017a). However, the priority should be given to the physico-chemical basis supporting the potential sediment source. UV or M properties are often suggested as low cost tracers, but in a catchment with limited geological variability and intense chemical weathering such as under tropical conditions, their use is not straightforward. Indeed, soils had almost homogeneous chemical compositions and a reddish colour through the whole soil profile. Under these conditions, UV had low variability and does not provide a good tracer for discriminating land use-based sources. The need to add a set of different tracers in sediment fingerprinting studies is expected to increase as geological and soil type variability increases in the catchment, as well as the number of sources of interest increases.

As a consequence, the discrimination between the sources achieved in the current research remained low, and the modelling results uncertain. Furthermore, as observed by Haddadchi et al. (2013), mixing models may lead to different results depending on the input data. To avoid this problem, the use of tracers with >90% of SCC or the preparation of artificial mixtures for model validation should be systematically recommended in future sediment fingerprinting approaches. Indeed, there may simply be limitations to the efficacy of the sediment fingerprinting technique in catchments with homogeneous geology or soil types that can be found in many regions of the world, mainly under tropical climates where soils are highly weathered.

A significant proportion of the most productive soils around the world are found under these conditions, and this situation strengthens the need to develop new approaches to discriminate between these land use-based sources. Alternative tracers such as environmental DNA (Foucher et al., 2020) and compound specific stable isotopes (CSSI) (Blake et al., 2012) may provide a powerful alternative to trace the contribution of specific land use sources to sediment. However, technical solutions allowing for the global application of these methods still need to be developed (Brandt et al., 2018; Evrard et al., 2019). Moreover, the application of these vegetation specific related tracers maybe even more challenging in large tropical catchments, characterised by transient and heterogeneous land uses which are often scarcely documented. Accordingly, their use in combination with more conventional tracers may provide a solution to provide consistent and reliable estimations of sediment source contributions to help achieving sustainable agricultural development goals in these regions.

7.5 Conclusions

The use of alternative tracers based on ultraviolet-visible spectra combined with geochemical parameters improved the sediment source discrimination in the Conceição River catchment. However, the low differences in source signatures observed in this study site resulted in high uncertainties associated with the model predictions, which is mainly due to the homogeneous soil types occurring in the catchment, which are highly weathered and which have a low variability between land uses, as well as between surface and subsurface sources. Furthermore, in such a homogeneous catchment, the low differences between sources observed for almost all the tested parameters increased the probability of sediments to lie outside of the range observed in the sources and to be

removed by the range/conservative tests, which further reduced the number of tracer options.

Magnetic, geochemical and ultraviolet-visible derived parameters have proven to be relatively ineffective for tracing land use-based sources in the Conceição River catchment. When using only one set of tracers, which does not provide a robust discrimination between the sources leading to low percentages of correctly classified samples by the LDA, the results of the model should be used with caution, since they are associated with large uncertainties. This study presents results that differ from those commonly observed in the literature, where additional tracers generally have positive results, showing that the sediment fingerprinting technique may not provide meaningful results in all situations. Tracers with a greater potential for land use discrimination, such as environmental DNA or CSSI, could provide an alternative for better understanding soil erosion processes in the Conceição River catchment and other similar homogeneous catchments worldwide. As such, future research should investigate the efficacy of these next generation tracers in increasingly difficult tracing environments with more attention to the potential impact of particle size on them.

7.6 References

Almagro, Andre, Almagro, André, Oliveira, P.T.S., Nearing, M.A., Hagemann, S., 2017. Projected climate change impacts in rainfall erosivity over Brazil Projected climate change impacts in rainfall erosivity over Brazil 0–12. https://doi.org/10.1038/s41598-017-08298-y

Anache, J.A.A., Wendland, E.C., Oliveira, P.T.S., Flanagan, D.C., Nearing, M.A., 2017. Runoff and soil erosion plot-scale studies under natural rainfall: A meta-analysis of the Brazilian experience. CATENA 152, 29–39. https://doi.org/10.1016/j.catena.2017.01.003

Batista, P.V.G., Laceby, J.P., Silva, M.L.N., Tassinari, D., Bispo, D.F.A., Curi, N., Davies, J., Quinton, J.N., 2018. Using pedological knowledge to improve sediment source apportionment in tropical environments. J. Soils Sediments. https://doi.org/10.1007/s11368-018-2199-5

Belmont, P., Willenbring, J.K., Schottler, S.P., Marquard, J., Kumarasamy, K., Hemmis, J.M., 2014. Toward generalizable sediment fingerprinting with tracers that are conservative and nonconservative over sediment routing timescales. J. Soils

Sediments 14, 1479–1492. https://doi.org/10.1007/s11368-014-0913-5

Ben-dor, E., Irons, J., Epema, G.F., 1998. Soil Reflectance, in: Rencz, A.N. (Ed.), Remote Sensing for the Earth Sciences. Manual of Remote Sensing. John Wiley & Sons, Ltd, New York, pp. 111–188.

Bender, M.A., dos Santos, D.R., Tiecher, T., Minella, J.P.G., de Barros, C.A.P., Ramon, R., 2018. Phosphorus dynamics during storm events in a subtropical rural catchment in southern Brazil. Agric. Ecosyst. Environ. 261. https://doi.org/10.1016/j.agee.2018.04.004

Blake, W.H., Ficken, K.J., Taylor, P., Russell, M.A., Walling, D.E., 2012. Tracing crop-specific sediment sources in agricultural catchments. Geomorphology 139–140, 322–329. https://doi.org/10.1016/j.geomorph.2011.10.036Boardman, J., Vandaele, K., Evans, R., Foster, I.D.L., 2019. Off-site impacts of soil erosion and runoff: Why connectivity is more important than erosion rates. Soil Use Manag. 35, 245–256. https://doi.org/10.1111/sum.12496

Bortolon, E.S.O., Mielniczuk, J., Tornquist, C.G., Lopes, F., Bergamaschi, H., 2011. Validation of the Century model to estimate the impact of agriculture on soil organic carbon in Southern Brazil. Geoderma 167–168, 156–166. https://doi.org/10.1016/j.geoderma.2011.08.008

Borrelli, P., Robinson, D.A., Fleischer, L.R., Lugato, E., Ballabio, C., Alewell, C., Meusburger, K., Modugno, S., Schütt, B., Ferro, V., Bagarello, V., Oost, K. Van, Montanarella, L., Panagos, P., 2017. An assessment of the global impact of 21st century land use change on soil erosion. Nat. Commun. 8, 2013. https://doi.org/10.1038/s41467-017-02142-7

Brandt, C., Dercon, G., Cadisch, G., Nguyen, L.T., Schuller, P., Linares, C.B., Santana, A.C., Golosov, V., Benmansour, M., Amenzou, N., Xinbao, Z., Rasche, F., 2018. Towards global applicability? Erosion source discrimination across catchments using compound-specific δ13C isotopes. Agric. Ecosyst. Environ. 256, 114–122. https://doi.org/10.1016/j.agee.2018.01.010

Brosinsky, A., Foerster, S., Segl, K., Kaufmann, H., 2014a. Spectral fingerprinting: sediment source discrimination and contribution modelling of artificial mixtures based on VNIR-SWIR spectral properties. J. Soils Sediments 14, 1949–1964. https://doi.org/10.1007/s11368-014-0925-1

Brosinsky, A., Foerster, S., Segl, K., López-Tarazón, J.A., Piqué, G., Bronstert, A., 2014b.

Spectral fingerprinting: characterizing suspended sediment sources by the use of VNIR-SWIR spectral information. J. Soils Sediments 14, 1965–1981. https://doi.org/10.1007/s11368-014-0927-z

Caner, L., Petit, S., Joussein, E., Fritsch, E., Herbillon, A.J., 2011. Accumulation of organo-metallic complexes in laterites and the formation of Aluandic Andosols in the Nilgiri Hills (southern India): similarities and differences with Umbric Podzols. Eur. J. Soil Sci. 62, 754–764. https://doi.org/10.1111/j.1365-2389.2011.01389.x

Chen, F., Wang, X., Li, X., Wang, J., Xie, D., Ni, J., Liu, Y., 2019. Using the sediment fingerprinting method to identify the sediment sources in small catchments with similar geological conditions. Agric. Ecosyst. Environ. 286, 106655. https://doi.org/10.1016/j.agee.2019.106655

Chen, M., Ma, L.Q., 2001. Comparison of Three Aqua Regia Digestion Methods for Twenty Florida Soils. Soil Sci. Soc. Am. J. 65, 491–499. https://doi.org/10.2136/sssaj2001.652491x

CIE, 1978. Commission Internationale d'Eclairage. Recommendations on Uniform Colour Spaces, Colour Difference Equations, Psychometrice Colour Terms. J. Oral Rehabil.

CIE, C.I. de l'Eclairage, 1931. Commission Internationale de l'Eclairage (CIE), in: CIE Proceedings. Cambridge University Press, Cambridge, UK.

Collins, A.L., Foster, I.D.L., Gellis, A.C., Porto, P., Horowitz, A.J., 2017a. Sediment source fingerprinting for informing catchment management: Methodological approaches, problems and uncertainty. J. Environ. Manage. 194, 1–3. https://doi.org/10.1016/j.jenvman.2017.03.026

Collins, A.L., Pulley, S., Foster, I.D.L., Gellis, A., Porto, P., Horowitz, A.J., 2017b. Sediment source fingerprinting as an aid to catchment management: A review of the current state of knowledge and a methodological decision-tree for end-users. J. Environ. Manage. 194, 86–108. https://doi.org/10.1016/j.jenvman.2016.09.075

Collins, A.L., Walling, D.E., Webb, L., King, P., 2010a. Apportioning catchment scale sediment sources using a modified composite fingerprinting technique incorporating property weightings and prior information. Geoderma 155, 249–261. https://doi.org/10.1016/j.geoderma.2009.12.008

Collins, A.L., Zhang, Y., Walling, D.E., 2010b. Apportioning sediment sources in a grassland dominated agricultural catchment in the UK using a new tracing framework. Sediment Dyn. a Chang. Futur. 337, 68–75.

Cornell, R.M., Schwertmann, U., 2003. The iron oxides. Structure, properties, reactions, occurences and uses, Second. ed. WILEY-VCH Verlag GmbH & Co. KGaA, Weinheim.

Da Silva, Y.J.A.B., Do Nascimento, C.W.A., Biondi, C.M., 2014. Comparison of USEPA digestion methods to heavy metals in soil samples. Environ. Monit. Assess. 186, 47–53. https://doi.org/10.1007/s10661-013-3354-5

Didoné, E.J., Gomes Minella, J.P., Andres Schneider, F.J., Londero, A.L., Lefèvre, I., Evrard, O., 2019. Quantifying the impact of no-tillage on soil redistribution in a cultivated catchment of Southern Brazil (1964–2016) with 137Cs inventory measurements. Agric. Ecosyst. Environ. 284, 106588. https://doi.org/10.1016/j.agee.2019.106588

Didoné, E.J., Minella, J.P.G., Merten, G.H., 2015. Quantifying soil erosion and sediment yield in a catchment in southern Brazil and implications for land conservation. J. Soils Sediments 15, 2334–2346. https://doi.org/10.1007/s11368-015-1160-0

Droppo, I.G., Nackaerts, K., Walling, D.E., Williams, N., 2005. Can flocs and water stable soil aggregates be differentiated within fluvial systems? CATENA 60, 1–18. https://doi.org/10.1016/j.catena.2004.11.002

EPA, U.S., 2007. "Method 3051A (SW-846): Microwave Assisted Acid Digestion of Sediments, Sludges, and Oils," Revision 1. Washington, D.C.

Evrard, O., Durand, R., Foucher, A., Tiecher, T., Sellier, V., Onda, Y., Lefèvre, I., Cerdan, O., Laceby, J.P., 2019. Using spectrocolourimetry to trace sediment source dynamics in coastal catchments draining the main Fukushima radioactive pollution plume (2011–2017). J. Soils Sediments. https://doi.org/10.1007/s11368-019-02302-w

Evrard, O., Laceby, J.P., Ficetola, G.F., Gielly, L., Huon, S., Lefèvre, I., Onda, Y., Poulenard, J., 2019. Environmental DNA provides information on sediment sources: A study in catchments affected by Fukushima radioactive fallout. Sci. Total Environ. 665, 873–881. https://doi.org/10.1016/j.scitotenv.2019.02.191

FAO, 2019. Soil erosion: the gratest challenge for sustainable soil management. Licence: CC BY-NC-SA 3.0 IGO, Rome.

Foucher, A., Evrard, O., Ficetola, G.F., Gielly, L., Poulain, J., Giguet-Covex, C., Laceby, J.P., Salvador-Blanes, S., Cerdan, O., Poulenard, J., 2020. Persistence of environmental DNA in cultivated soils: implication of this memory effect for reconstructing the dynamics of land use and cover changes. Sci. Rep. 10, 1–12. https://doi.org/10.1038/s41598-020-67452-1

Fritsch, E., Morin, G., Bedidi, A., Bonnin, D., Balan, E., Caquineau, S., Calas, G., 2005. Transformation of haematite and Al-poor goethite to Al-rich goethite and associated yellowing in a ferralitic clay soil profile of the middle Amazon Basin (Manaus, Brazil). Eur. J. Soil Sci. 56, 575–588. https://doi.org/10.1111/j.1365-2389.2005.00693.x

Gaspar, L., Blake, W.H., Smith, H.G., Lizaga, I., Navas, A., 2019. Testing the sensitivity of a multivariate mixing model using geochemical fingerprints with artificial mixtures. Geoderma 337, 498–510. https://doi.org/10.1016/j.geoderma.2018.10.005

Guzmán, G., Quinton, J.N., Nearing, M.A., Mabit, L., Gómez, J.A., 2013. Sediment tracers in water erosion studies: Current approaches and challenges. J. Soils Sediments 13, 816–833. https://doi.org/10.1007/s11368-013-0659-5

Haddadchi, A., Ryder, D.S., Evrard, O., OLLEY, J., 2013. Sediment fingerprinting in fluvial systems: review of tracers, sediment sources and mixing models. Int. J. Sediment Res. 28, 560–578. https://doi.org/10.1016/S1001-6279(14)60013-5

Hatfield, J.L., Sauer, T.J., Cruse, R.M., 2017. Soil : The Forgotten Piece of the Water , Food , Energy Nexus, 1st ed, Advances in Agronomy. Elsevier Inc. https://doi.org/10.1016/bs.agron.2017.02.001

HunterLab, 2015. The basics of color perception and measurement [WWW Document]. URL https://www.hunterlab.com/basics-of-color-theory.pdf?r=false (accessed 7.9.19).

Jia, L., Zhao, W., Zhai, R., Liu, Y., Kang, M., Zhang, X., 2019. Regional differences in the soil and water conservation efficiency of conservation tillage in China. Catena 175, 18–26. https://doi.org/10.1016/j.catena.2018.12.012

Koiter, A.J., Owens, P.N., Petticrew, E.L., Lobb, D.A., 2013. The behavioural characteristics of sediment properties and their implications for sediment fingerprinting as an approach for identifying sediment sources in river basins. Earth-Science Rev. 125, 24–42. https://doi.org/10.1016/j.earscirev.2013.05.009

Kosmas, C.S., Curi, N., Bryant, R.B., Franzmeier, D.P., 1984. Characterization of iron oxide minerals by second-derivative visible spectroscopy. Soil Sci. Soc. Am. J. 48, 401–405. https://doi.org/10.2136/sssaj1984.03615995004800020036x

Laceby, J.P., Evrard, O., Smith, H.G., Blake, W.H., Olley, J.M., Minella, J.P.G., Owens, P.N., 2017. The challenges and opportunities of addressing particle size effects in sediment source fingerprinting: A review. Earth-Science Rev. 169, 85–103. https://doi.org/10.1016/j.earscirev.2017.04.009

Lal, R., 2007. Anthropogenic Influences on World Soils and Implications to Global Food Security. Adv. Agron. 93, 69–93. https://doi.org/10.1016/S0065-2113(06)93002-8

Legout, C., Poulenard, J., Nemery, J., Navratil, O., Grangeon, T., Evrard, O., Esteves, M., 2013. Quantifying suspended sediment sources during runoff events in headwater catchments using spectrocolorimetry. J. Soils Sediments 13, 1478–1492. https://doi.org/10.1007/s11368-013-0728-9

Lizaga, I., Latorre, B., Gaspar, L., Navas, A., 2020. Consensus ranking as a method to identify non-conservative and dissenting tracers in fingerprinting studies. Sci. Total Environ. 720, 137537. https://doi.org/10.1016/j.scitotenv.2020.137537

López-Mársico, L., Altesor, A., Oyarzabal, M., Baldassini, P., Paruelo, J.M., 2015. Grazing increases below-ground biomass and net primary production in a temperate grassland. Plant Soil 392, 155–162. https://doi.org/10.1007/s11104-015-2452-2

Martínez-Carreras, N., Krein, A., Gallart, F., Iffly, J.F., Pfister, L., Hoffmann, L., Owens, P.N., 2010a. Assessment of different colour parameters for discriminating potential suspended sediment sources and provenance: A multi-scale study in Luxembourg. Geomorphology 118, 118–129. https://doi.org/10.1016/j.geomorph.2009.12.013

Martínez-Carreras, N., Udelhoven, T., Krein, A., Gallart, F., Iffly, J.F., Ziebel, J., Hoffmann, L., Pfister, L., Walling, D.E., 2010b. The use of sediment colour measured by diffuse reflectance spectrometry to determine sediment sources: Application to the Attert River catchment (Luxembourg). J. Hydrol. 382, 49–63. https://doi.org/10.1016/j.jhydrol.2009.12.017

Melo, D.C.D., Anache, J.A.A., Almeida, C. das N., Coutinho, J. V., Ramos Filho, G.M., Rosalem, L.M.P., Pelinson, N.S., Ferreira, G.L.R.A., Schwamback, D., Calixto, K.G., Siqueira, J.P.G., Duarte-Carvajalino, J.C., Jhunior, H.C.S., Nóbrega, J.D., Morita, A.K.M., Leite, C.M.C., Guedes, A.C.E., Coelho, V.H.R., Wendland, E., 2020. The big picture of field hydrology studies in Brazil. Hydrol. Sci. J. 0, 1. https://doi.org/10.1080/02626667.2020.1747618

Minella, J.P.G., Merten, G.H., Clarke, R.T., 2004. Identification of sediment sources in a small rural drainage basin, in: Sediment Transfer through the Fluvial System (Proceedings of a Symposium Held in Moscow, August 2004). IAHS Press, Moscow, pp. 44–51.

Mullins, C.E., 1977. Magnetic Susceptibility of the Soil and Its Significance in Soil Science – a Review. J. Soil Sci. 28, 223–246. https://doi.org/10.1111/j.1365-

2389.1977.tb02232.x

Navratil, O., Evrard, O., Esteves, M., Legout, C., Ayrault, S., Némery, J., Mate-Marin, A., Ahmadi, M., Lefèvre, I., Poirel, A., Bonté, P., 2012. Temporal variability of suspended sediment sources in an alpine catchment combining river/rainfall monitoring and sediment fingerprinting. Earth Surf. Process. Landforms 37, 828–846. https://doi.org/10.1002/esp.3201

Niu, B., Zhang, X., Qu, J., Liu, B., Homan, J., Tan, L., An, Z., 2019. Using multiple composite fingerprints to quantify source contributions and uncertainties in an arid region. J. Soils Sediments. https://doi.org/10.1007/s11368-019-02424-1

Nosrati, K., Collins, A.L., 2019. Investigating the importance of recreational roads as a sediment source in a mountainous catchment using a fingerprinting procedure with different multivariate statistical techniques and a Bayesian un-mixing model. J. Hydrol. 569, 506–518. https://doi.org/10.1016/j.jhydrol.2018.12.019

Palazón, L., Navas, A., 2017a. Variability in source sediment contributions by applying different statistic test for a Pyrenean catchment. J. Environ. Manage. 194, 42–53. https://doi.org/10.1016/j.jenvman.2016.07.058

Palazón, L., Navas, A., 2017b. Variability in source sediment contributions by applying different statistic test for a Pyrenean catchment. J. Environ. Manage. 194, 42–53. https://doi.org/10.1016/j.jenvman.2016.07.058

Phillips, J.M., Russell, M.A., Walling, D.E., 2000. Time-integrated sampling of fluvial suspended sediment: A simple methodology for small catchments. Hydrol. Process. 14, 2589–2602. https://doi.org/10.1002/1099-1085(20001015)14:14<2589::AID-HYP94>3.0.CO;2-D

Pimentel, D., 2006. Soil Erosion: A Food and Environmental Threat. Environ. Dev. Sustain. 8, 119–137. https://doi.org/10.1007/s10668-005-1262-8

Poesen, J., 2017. Soil erosion in the Anthropocene: research needs. Earth Surf. Process. Landforms 84, 64–84. https://doi.org/10.1002/esp.4250

Poulenard, J., Legout, C., Némery, J., Bramorski, J., Navratil, O., Douchin, A., Fanget, B., Perrette, Y., Evrard, O., Esteves, M., 2012. Tracing sediment sources during floods using Diffuse Reflectance Infrared Fourier Transform Spectrometry (DRIFTS): A case study in a highly erosive mountainous catchment (Southern French Alps). J. Hydrol. 414–415, 452–462. https://doi.org/10.1016/j.jhydrol.2011.11.022

Pulley, S., Foster, I., Antunes, P., 2015a. The uncertainties associated with sediment

fingerprinting suspended and recently deposited fluvial sediment in the Nene river basin. Geomorphology 228, 303–319. https://doi.org/10.1016/j.geomorph.2014.09.016

Pulley, S., Foster, I., Antunes, P., 2015b. The application of sediment fingerprinting to floodplain and lake sediment cores: assumptions and uncertainties evaluated through case studies in the Nene Basin, UK. J. Soils Sediments 15, 2132–2154. https://doi.org/10.1007/s11368-015-1136-0

Pulley, S., Foster, I., Collins, A.L., 2017a. The impact of catchment source group classification on the accuracy of sediment fingerprinting outputs. J. Environ. Manage. 194, 16–26. https://doi.org/10.1016/j.jenvman.2016.04.048

Pulley, S., Rowntree, K., 2016a. The use of an ordinary colour scanner to fingerprint sediment sources in the South African Karoo. J. Environ. Manage. 165, 253–262. https://doi.org/10.1016/j.jenvman.2015.09.037

Pulley, S., Rowntree, K., 2016b. Stages in the life of a magnetic grain: Sediment source discrimination, particle size effects and spatial variability in the South African Karoo. Geoderma 271, 134–143. https://doi.org/10.1016/j.geoderma.2016.02.015

Pulley, S., Van Der Waal, B., Collins, A.L., Foster, I.D.L., Rowntree, K., 2017b. Are source groups always appropriate when sediment fingerprinting? The direct comparison of source and sediment samples as a methodological step. River Res. Appl. 33, 1553–1563. https://doi.org/10.1002/rra.3192

Pulley, S., Van der Waal, B., Rowntree, K., Collins, A.L., 2018. Colour as reliable tracer to identify the sources of historically deposited flood bench sediment in the Transkei, South Africa: A comparison with mineral magnetic tracers before and after hydrogen peroxide pre-treatment. CATENA 160, 242–251. https://doi.org/10.1016/j.catena.2017.09.018

R Development Core Team, 2017. R: a language and environment for statistical computing.

Ramon, R., Minella, J.P.G., Merten, G.H., de Barros, C.A.P., Canale, T., 2017. Kinetic energy estimation by rainfall intensity and its usefulness in predicting hydrosedimentological variables in a small rural catchment in southern Brazil. CATENA 148, 176–184. https://doi.org/10.1016/j.catena.2016.07.015

Ramos, P.V., Indaa, A.V., Barrón, V., Siqueira, D.S., Júnior, J., Teixeira, D.D.B., 2020. Color in subtropical brazilian soils as determined with a Munsell chart and by diffuse

reflectance spectroscopy. Catena 193, 1–26. https://doi.org/10.1016/j.catena.2020.104609

Rencher, A.C., 2005. A Review Of "Methods of Multivariate Analysis, Second Edition." IIE Trans. 37, 1083–1085. https://doi.org/10.1080/07408170500232784

Rowntree, K.M., van der Waal, B.W., Pulley, S., 2017. Magnetic susceptibility as a simple tracer for fluvial sediment source ascription during storm events. J. Environ. Manage. 194, 54–62. https://doi.org/10.1016/j.jenvman.2016.11.022

Schaefer, C.E.G.R., Fabris, J.D., Ker, J.C., 2008. Minerals in the clay fraction of Brazilian Latosols (Oxisols): a review. Clay Miner. 43, 137–154. https://doi.org/10.1180/claymin.qw2008.043.1.11

Scheinost, A.C., Chavernas, A., Barrón, V., Torrent, J., 1998. Use and limitations of second-derivative diffuse reflectance spectroscopy in the visible to near-infrared range to identify and quantify Fe oxide minerals in soils. Clays Clay Miner. 46, 528–536. https://doi.org/10.1346/CCMN.1998.0460506

Schuman, G.E., Reeder, J.D., Manley, J.T., Hart, R.H., Manley, W.A., 1999. Impact of grazing management on the carbon and nitrogen balance of a mixed-grass rangeland. Ecol. Appl. 9, 65–71. https://doi.org/10.1890/1051-0761(1999)009[0065:IOGMOT]2.0.CO;2

Sherriff, S.C., Franks, S.W., Rowan, J.S., Fenton, O., Ó'hUallacháin, D., 2015. Uncertainty-based assessment of tracer selection, tracer non-conservativeness and multiple solutions in sediment fingerprinting using synthetic and field data. J. Soils Sediments 15, 2101–2116. https://doi.org/10.1007/s11368-015-1123-5

Six, J., Feller, C., Denef, K., Ogle, S.M., de Moraes, J.C., Albrecht, A., 2002. Soil organic matter, biota and aggregation in temperate and tropical soils - Effects of no-tillage. Agronomie 22, 755–775. https://doi.org/10.1051/agro:2002043

Smith, H.G., Blake, W.H., 2014. Sediment fingerprinting in agricultural catchments: A critical re-examination of source discrimination and data corrections. Geomorphology 204, 177–191. https://doi.org/10.1016/j.geomorph.2013.08.003

Smith, H.G., Evrard, O., Blake, W.H., Owens, P.N., 2015. Preface—Addressing challenges to advance sediment fingerprinting research. J. Soils Sediments 15, 2033–2037. https://doi.org/10.1007/s11368-015-1231-2

Smith, H.G., Karam, D.S., Lennard, A.T., 2018. Evaluating tracer selection for catchment sediment fingerprinting. J. Soils Sediments 18, 3005–3019.

https://doi.org/10.1007/s11368-018-1990-7

Snyder, V.A., Vázquez, M.A., 2005. STRUCTURE, in: Encyclopedia of Soils in the Environment. Elsevier, pp. 54–68. https://doi.org/10.1016/B0-12-348530-4/00533-6

Testoni, S.A., de Almeida, J.A., da Silva, L., Andrade, G.R.P., 2017. Clay mineralogy of Brazilian oxisols with shrinkage properties. Rev. Bras. Cienc. do Solo 41, 1–16. https://doi.org/10.1590/18069657rbcs20160487

Tiecher, T., Caner, L., Minella, J.P.G., Evrard, O., Mondamert, L., Labanowski, J., Rheinheimer, D. dos S., 2017. Tracing Sediment Sources Using Mid-infrared Spectroscopy in Arvorezinha Catchment, Southern Brazil. L. Degrad. Dev. 28, 1603–1614. https://doi.org/10.1002/ldr.2690

Tiecher, T., Caner, L., Minella, J.P.G., Santos, D.R. dos, 2015. Combining visible-based-color parameters and geochemical tracers to improve sediment source discrimination and apportionment. Sci. Total Environ. 527–528, 135–149. https://doi.org/10.1016/j.scitotenv.2015.04.103

Tiecher, T., Minella, J.P.G., Evrard, O., Caner, L., Merten, G.H., Capoane, V., Didoné, E.J., dos Santos, D.R., 2018. Fingerprinting sediment sources in a large agricultural catchment under no-tillage in Southern Brazil (Conceição River). L. Degrad. Dev. 29, 939–951. https://doi.org/10.1002/ldr.2917

Tiecher, T., Ramon, R., Laceby, J.P., Evrard, O., Minella, J.P.G., 2019. Potential of phosphorus fractions to trace sediment sources in a rural catchment of Southern Brazil: Comparison with the conventional approach based on elemental geochemistry. Geoderma 337, 1067–1076. https://doi.org/10.1016/j.geoderma.2018.11.011

Tornquist, C.G., Mielniczuk, J., Cerri, C.E.P., 2009. Modeling soil organic carbon dynamics in Oxisols of Ibirubá (Brazil) with the Century Model. Soil Tillage Res. 105, 33–43. https://doi.org/10.1016/j.still.2009.05.005

Torres Astorga, R., de los Santos Villalobos, S., Velasco, H., Domínguez-Quintero, O., Pereira Cardoso, R., Meigikos dos Anjos, R., Diawara, Y., Dercon, G., Mabit, L., 2018. Exploring innovative techniques for identifying geochemical elements as fingerprints of sediment sources in an agricultural catchment of Argentina affected by soil erosion. Environ. Sci. Pollut. Res. 25, 20868–20879. https://doi.org/10.1007/s11356-018-2154-4

Uber, M., Legout, C., Nord, G., Crouzet, C., Demory, F., Poulenard, J., 2019. Comparing alternative tracing measurements and mixing models to fingerprint suspended sediment sources in a mesoscale Mediterranean catchment.

van der Waal, B., Rowntree, K., Pulley, S., 2015. Flood bench chronology and sediment source tracing in the upper Thina catchment, South Africa: the role of transformed landscape connectivity. J. Soils Sediments 15, 2398–2411. https://doi.org/10.1007/s11368-015-1185-4

Viscarra Rossel, R.A., Minasny, B., Roudier, P., McBratney, A.B.B., 2006. Colour space models for soil science. Geoderma 133, 320–337. https://doi.org/10.1016/j.geoderma.2005.07.017

Walkley, A., Black, I.A., 1934. An examination of the Degtjareff Method for determining soil organic matter, and a proposed modification of the chromic acid titration method. Soil Sci. 37, 29–38. https://doi.org/10.1097/00010694-193401000-00003

Walling, D.E., 2013. The evolution of sediment source fingerprinting investigations in fluvial systems. J. Soils Sediments 13, 1658–1675. https://doi.org/10.1007/s11368-013-0767-2

Walling, D.E., Peart, M.R., Oldfield, F., Thompson, R., 1979. Suspended sediment sources identified by magnetic measurements. Nature 281, 110–113. https://doi.org/0028-0836/79/370110-04$01.00

Yu, L., Oldfield, F., 1989. A multivariate mixing model for identifying sediment source from magnetic measurements. Quat. Res. 32, 168–181. https://doi.org/10.1016/0033-5894(89)90073-2

Appendix A

The water discharge (Q) and suspended sediment concentration (SSC) was monitored at the catchment outlet using automatic equipment's that recorded the water level and turbidity every 10 min through a pressure water level sensor and a turbidimeter (Hydrological monitoring station Model SL-2000, Solar®, Brazil), respectively. The Q was calculated from the water level data using a rating curve. The turbidity sensor was properly calibrated with SSC measured data obtained from samples of the water and sediment mixture collected during rainfall-runoff events and in a daily based schedule used for determination of SSC in the laboratory. In the Figure A1 shows the Q and SCC data measured with the automatic equipment's are presented. The period covered by

each time integrated sediment samples (TISS) and the date that fine bed sediment samples (FBS) were collected (Table 7.1) are illustrated in the Figure 7.10. The first TISS (S-9) was installed after the harvesting of the summer crop season of 2011/2012, and the sample collected before to start the following summer crop season, having a sample which represents the winter period which had less intense rainfall. The second TISS sample (S-10), represents the period in which the soil is more susceptible to erosion processes due to the soil preparation and sowing process, which occurs together with the period of heavier rainfall (September to November). The third sampling period (S-11) represents the period in which the summer crops are stablished and the soil is more protected by the summer crops.

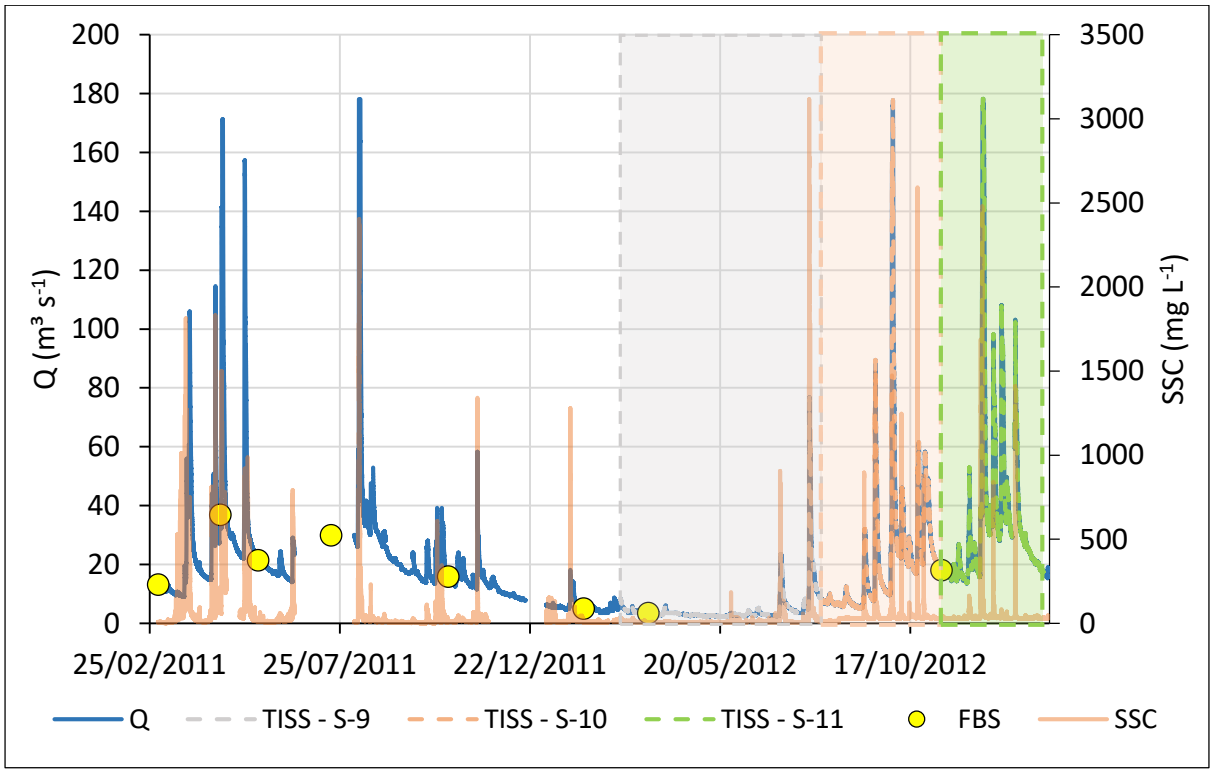

Figure 7.10. Water discharge (Q) and suspended sediment concentration (SSC) during the monitored period, sampling period of time integrated suspended sediment sampler (TISS) and sampling time of fine bed sediment samples (FBS).

Appendix B

Twenty-four colour parameters were calculated from the ultraviolet-visible spectra following the colorimetric models described in detail by Viscarra Rossel et al. (2006), which are based on the Munsell HVC, RGB, the decorrelation of RGB data, CIELAB and CIELUV Cartesian coordinate systems, three parameters from the HuterLab colour space model and two indices (coloration – CI and saturation index – SI). First, the colour

coefficients XYZ based on the colour-matching functions defined by the International Commission on Illumination - CIE (CIE, 1931) were calculated, where X and Z are the virtual components of the primary spectra and Y represents the brightness. The XYZ tristimulus were standardised with values corresponding to the Standard Illuminant D65 white point for 10 Degree Standard Observer (X = 94.8110; Y = 100.00; Z = 107.304), then transformed into the Munsel HVC, RGB, CIELAB and CIELUV Cartesian coordinate systems using the equations from CIE (1978). Three parameters from the HunterLab (HunterLab, 2015) colour space model, and two indices (coloration - CI and saturation index - SI) (Pulley et al., 2018) were calculated as well. In total, 27 colour metric parameters were derived from the spectra of potential source and sediment samples (L, L*, a, a*, b, b*, C*, h, RI, x, y, z, u*, v*, u', v', Hvc, hVc, hvC, R, G, B, HRGB, IRGB, SRGB, CI and SI).

Three other parameters were calculated from the second derivative curves of remission functions in the visible range of soil and sediment samples, which displayed three major absorption bands at short wavelengths commonly attributed to Fe-oxides (Caner et al., 2011; Fritsch et al., 2005; Kosmas et al., 1984; Scheinost et al., 1998). The first band (A1, ~430 nm) corresponds to the single electron transition of goethite (Gt), whereas the two others correspond to the electron pair transition for goethite (A2, ~480 nm) and for hematite (Hm) (A3, ~520 nm), respectively (Figure 7.11). The band intensity is estimated from the amplitude between a minimum and the nearby maximum at its lower energy side. The amplitudes of the three bands (A1, A2 and A3) are positively correlated with the contents of Gt and Hm (Fritsch et al., 2005). A1 and A3 are commonly used to assess the content of Gt and Hm, respectively, and the relative proportions of hematite in Fe oxides (Hr) are estimated by applying the equation Hr (%) = Hm/(Hm+Gt). The band intensities were measured from the amplitude between each band minimum and its nearby maximum at higher wavelength.

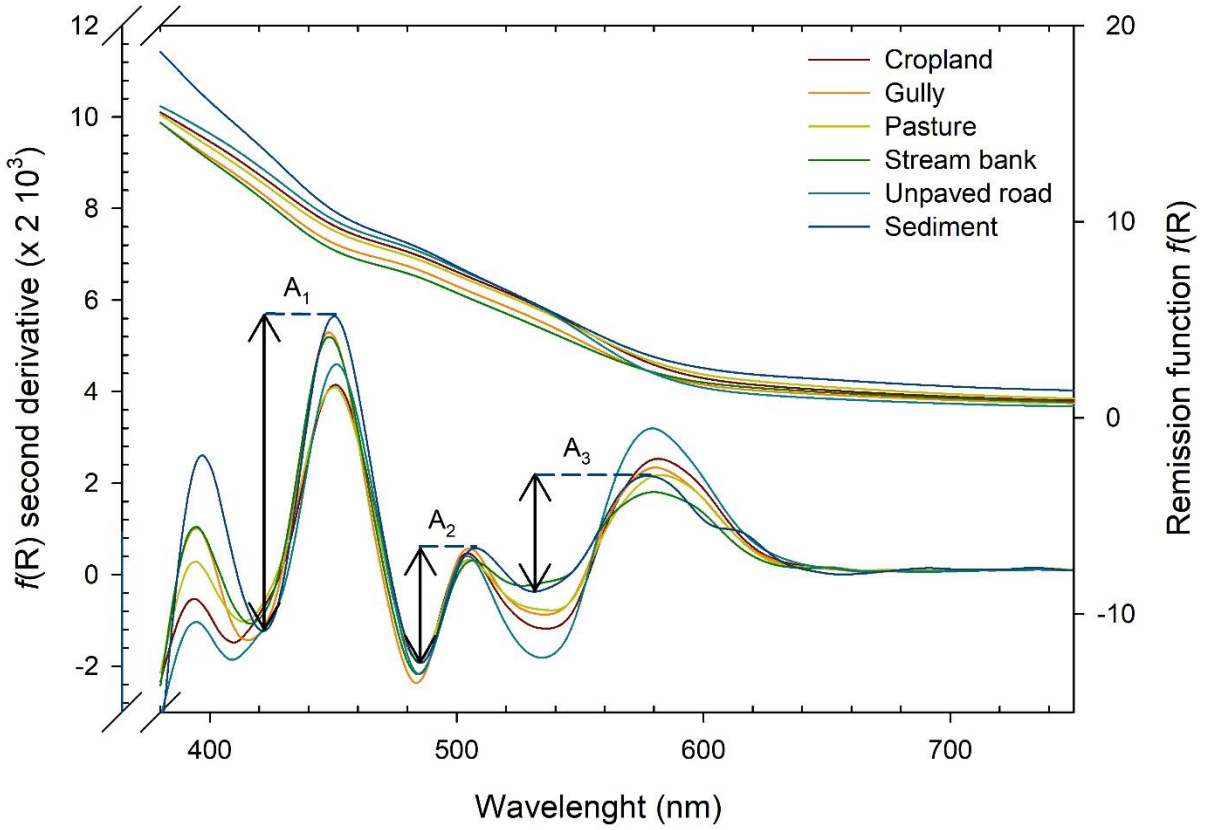

Figure 7.11. Second-derivative spectra of the remission function f(R) from visible diffuse reflectance spectroscopy showing the absorption bands (minima) of Fe-oxides in each land use and sediment samples mean spectra.

8 Chapter 3. Sediment sources tracing using different spectral ranges, multivariate models and spectral pre-processing techniques in a homogeneous subtropical catchment in Southern Brazil (Conceição River)

8.1 Introduction

The intensification of agriculture without conservationist management practices associated with the high rainfall erosivity observed in subtropical regions of Southern Brazil make the region a global water erosion hotspot (Golosov and Walling, 2019). Therefore, measures to control erosion processes need to be adequately designed to mitigate soil and water resource degradation. At the river catchment scale, identifying and quantifying the contribution of the main sources of sediment delivering material to the river system helps guiding the efforts to control erosion processes more effectively (Collins et al., 2017a).

Although monitoring studies of the impacts of human activity and climate change on natural resources (soil and water) are essential (Poesen, 2017), this type of research has remained scarce in Brazil (Melo et al., 2020). Conventional techniques for tracing the sources of sediments delivered to the river network using tracers such as radionuclides, stable isotopes of specific organic compounds, or even geochemical composition, are expensive and time-consuming methods.

In this context, the use of diffuse reflectance spectroscopy in the visible and infrared wavelengths has emerged as an alternative quantitative method, which is a physical measurement method that does not generate chemical residues, which requires only a small sample quantity for analysis and generates a large amount of information about the sample composition (Viscarra Rossel et al., 2006b). Spectroscopy data has already been used to derive parameters related to soil organic constituents and mineral composition (Farias Amorim et al., 2021), as well as colour parameters (Pulley et al., 2018; Sellier et al., 2020b; Tiecher et al., 2015) to be used as discrete variable tracers in mixture models. Another option is to use all spectra as a tracer by means of multivariate models. This method has already been used with success for predicting the contribution of sediment sources in contrasted catchments of Europe (Poulenard et al., 2012, 2009). In small catchments, it has already been proved to provide a satisfactory tool in Southern

Brazil as well (Tiecher et al., 2021, 2016), where the magnitude of the source contributions to sediment predicted by the alternative method based on spectroscopy data was similar to that obtained by the conventional method based on geochemical tracers.

However, in a context where soil types are homogeneous and more than two or three potential sediment sources may be found such as in the Conceição river catchment in Southern Brazil (Ramon et al., 2020), the combination of multiple spectral bands such as ultraviolet-visible (UV), near-infrared (NIR) and mid-infrared (MIR) may provide an alternative to improve the accuracy of model estimates. The use of multiple spectral ranges may improve the model performance due to the different types of information regarding the soil and sediment properties contained in each region of the spectra (Viscarra Rossel et al., 2006b). The UV spectra provide mainly information related to the organic matter and iron oxide content, while the MIR and NIR wavelength may provide information related to the presence of different minerals types and organic matter compounds, which together may result in a wide set of contrasted properties (Tiecher et al., 2021; Viscarra Rossel and Behrens, 2010). In addition, spectral pre-processing techniques for parametric and non-parametric multivariate models such as Partial Least Squares Regression (PLSR) and Support Vector Machine (SVM) can improve the accuracy of results by removing baseline shifts and enhancing spectral features. This strategy had already been applied successfully by Tiecher et al. (2021) in a small catchment (1.23 km^2) of Southern Brazil, where the SVM and PLSR associated with the first derivative of Savitzky-Golay spectral pre-processing offered the best results. However, this approach still needs to be tested and validated in larger and even more homogeneous catchments, especially when considering multiple sediment sources.

Therefore, the objective of the current chapter is to test and compare the performance of multiple multivariate models for estimating the contribution of sediment sources to the river network in an agricultural catchment using diffuse reflectance spectroscopy outputs as a set of potential fingerprints. In addition, our goal is to verify which spectral range and which pre-processing technique offer the best results for sediment source contribution predictions in a large catchment with highly weathered and homogeneous soils in Southern Brazil.

8.2 Methodology

8.2.1 Study site

The study was conducted in the Conceição River catchment (804 km^2), located in the northwest of the State of Rio Grande do Sul (Figure 8.1). According to the Köppen classification, the climate is classified as Cfa, humid subtropical without a defined dry season, with an average annual rainfall varying between 1750 and 2000 mm per year and an average temperature of 18.6°C. This catchment is representative of the basaltic plateau region of the Serra Geral Formation, where the main soil classes found are Ferralsols (80%), Nitisols (18%) and Acrisols (2%) (IUSS Working Group WRB, 2015), with a mineralogy dominated by iron oxides and kaolinite. The main land use is cropland (89%), mainly cultivated under no-tillage with soybeans (*Glycine max*) in summer and wheat (*Triticum aestivum*) for grain production, oats (*Avena sativa* and *Avena strigosa*) and ryegrass (*Lolium multiflorum*) for feeding dairy cattle or used as a cover crop to protect the soil during winter.

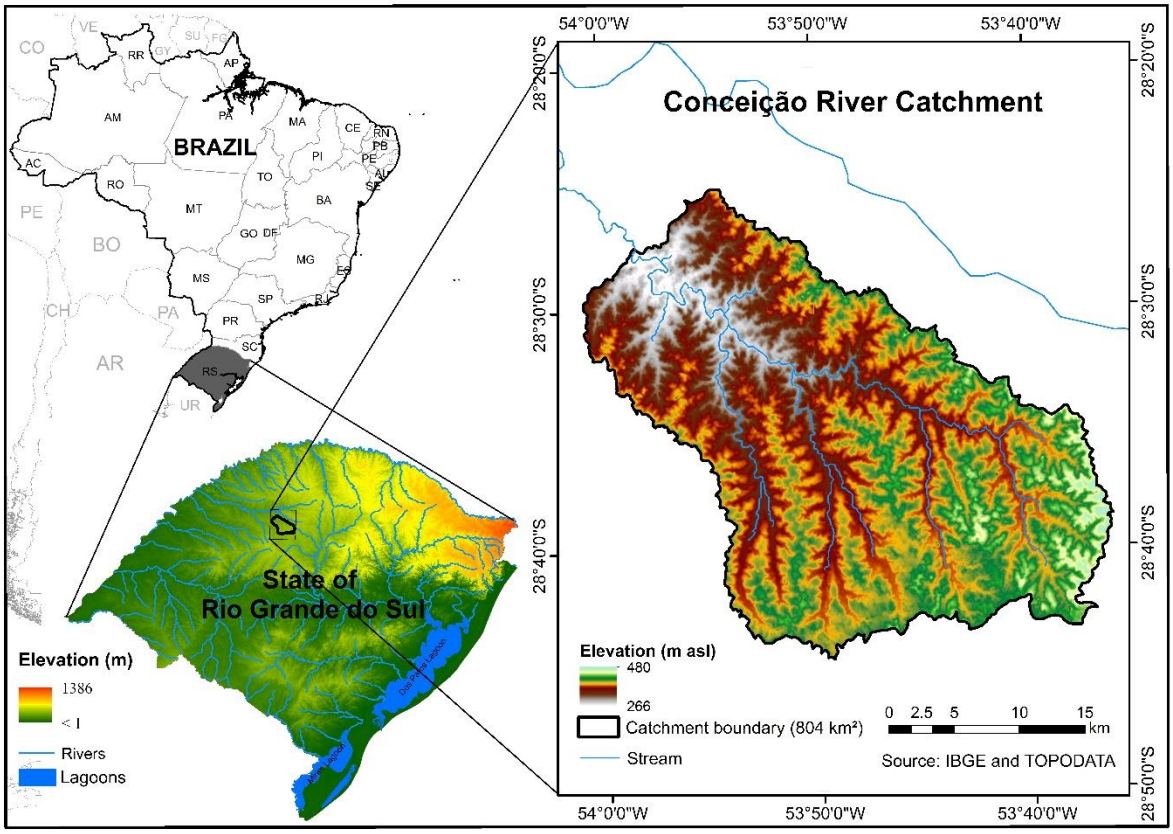

Figure 8.1. Location of the Conceição River catchment in Southern Brazil and digital elevation model.

The relief of the river catchment is characterised by gentle slopes (6-9%) at the highest positions of the landscape and steeper slopes (10-14%) near the drainage channels, with altitudes ranging from 270 to 480 m. The catchment outlet is located next to the monitoring point number 75,200,000 of the National Water Agency (ANA) (28°27'22" S, 53°58'24" O) in the county of Ijuí.

8.2.2 Source and sediment sampling

Soil composite samples (n=181) were collected in representative sites to characterize the four sediment sources, which include: cropland (n=78), stream bank (n=36), unpaved road (n=40) and pasture (n=27). Samples were collected from the topsoil layer (0-5 cm) of surface sources (cropland and pasture) (Figure 8.2). In stream banks, the samples were collected in the exposed sidewall avoiding the material from the uppermost layer. Samples of unpaved road were taken mainly in the roadsides where erosion is the most evident, which corresponds to the deeper layers of the soil. Moreover, this strategy avoids the sampling of material transiting from other sources before reaching the river network. For all source samples, around ten sub-samples were collected within a radius of approximately 50 m and well-mixed to prepare a composite sample representative of the area. Samples were collected at sites sensitive to erosion and connected to the stream network. A total of 44 sediment samples were collected from March 2011 to March 2013, which included suspended sediment samples collected by time integrating suspended sediment samplers (TISS) (n=8), fine sediment deposited on the riverbed (n=15) and suspended sediment samples collected in the water column during storm events (n=21).

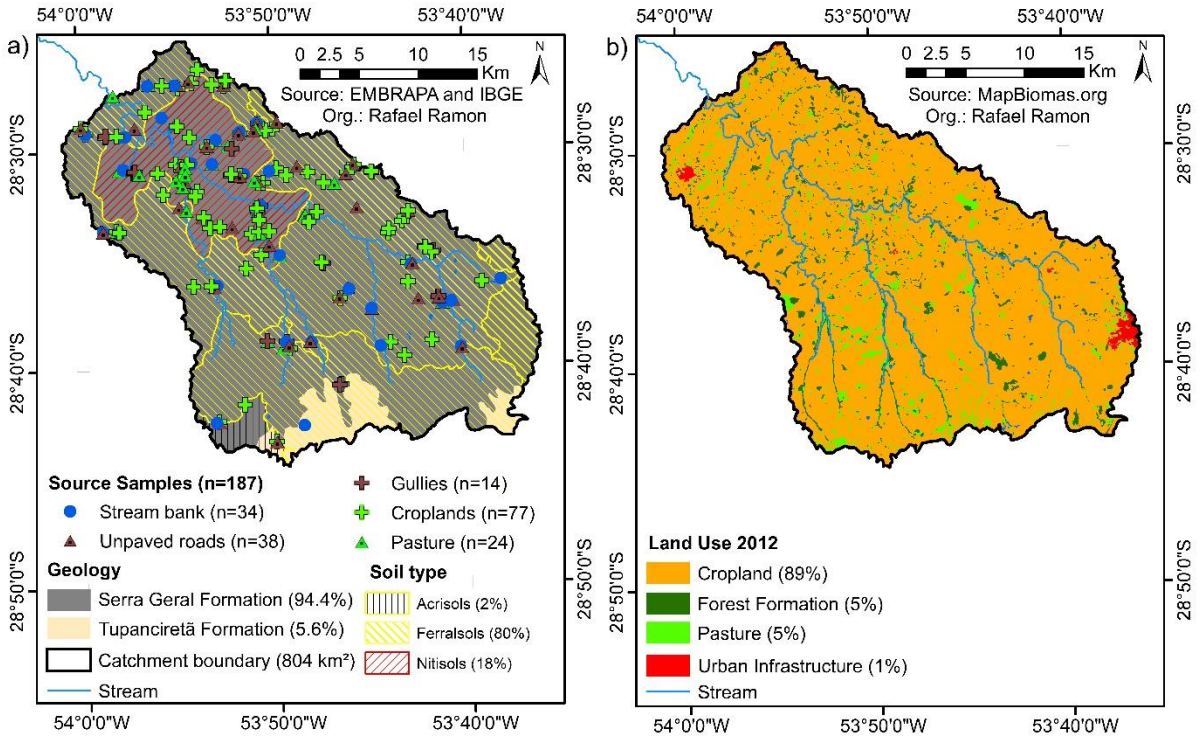

Figure 8.2. Lithological formations, soil types and source sample location (a); and land use map for the year 2012 (b).

8.2.3 Artificial mixtures and sediment analyses

Source and sediment samples were oven-dried at 50°C, gently disaggregated using a pestle and mortar and dry-sieved to 63 µm to avoid the particle size effect (Laceby et al., 2017).

8.2.3.1 Artificial mixtures of sediment sources

Equal proportions of the samples from each sediment source were mixed in the laboratory to prepare a single reference sample for each corresponding source (cropland, pasture, unpaved roads, and stream bank). Subsequently, these four reference samples were mixed in 97 different proportions from each source (Supplementary material). These mixtures were then used to calibrate the multivariate mathematical models used to estimate the respective source contributions to the sediment samples.

8.2.3.2 Spectral analyses

Diffuse reflectance spectral analyses were carried out in the ultraviolet–visible (UV, 200–800 nm with 1 nm step), near-infrared (NIR, 1000-2500 nm with 1 nm step) and mid-infrared wavelengths (MIR, 2500–25,000 nm with 5 nm step). UV spectrum were measured for each powdered sample using a Cary 5000 UV-NIR spectrophotometer (Varian, Palo Alto, CA, USA) at room temperature, using $BaSO_4$ as a 100% reflectance

standard. NIR spectra was measured using a Nicolet 26,700 FTIR spectrometer (Waltham, Massachusetts, USA) in diffuse reflectance mode with an integrating sphere and a InGaAs detector with 100 readings per spectrum. MIR spectra were measured with a Nicolet 510-FTIR (Thermo Electron Scientific, Madison, WI, USA) spectrometer in diffuse reflectance mode with 100 readings per spectrum. For MIR analysis, a direct current of air was used (dry and without CO_2) to eliminate CO_2 and water from the spectrometer in order not to interfere with scanning when obtaining the spectra.

8.2.4 Spectral pre-processing techniques and multivariate model calibration and validation

After the spectra acquisition, they were submitted to three different spectral pre-processing techniques to outline features of interest and reduce the physical variability due to light dispersion or systematic variations due to environmental and instrumental conditions (Barnes et al., 1989; Dotto et al., 2019). Standard Normal Variate (SNV), Detrend (DET) and Savitzky-Golay Derivate (SGD) pre-processing techniques were then compared to the raw spectra (RAW). The SNV normalize the spectral data to correct for light scatter. The DET allows to correct for wavelength dependent scattering effects, normalizing the spectral data. The SGD reduces the high frequency noise in the signal by smoothing properties and reducing the low frequency signal by differentiation. The SGD was applied with a first derivative using a first order polynomial and a 11 nm search window, where the latter window search was defined based on prior testing.

To develop the prediction models, a parametric multivariate model, the PLSR (method 'pls') (R pls package Mevik et al., 2016), and a non-parametric model, the SVM (method 'svmLinear') (R *e*1071 package Meyer et al., 2019), were used. PLSR are frequently used because of their simplicity, robustness, high performance and easy accessibility. In this method, the raw spectra are converted into latent variables to reduce the dimensionality and then implement multiple linear regressions between the measured spectra and the variable of interest. The SVM has the advantage of being able to model non-linear relations, since the latter are expected between spectral variables and organo-mineral components of the soil (Tiecher et al., 2021; Viscarra Rossel and Behrens, 2010). The models were calibrated and validated by cross-validation with 10 k-fold, using a random division into segments. The performance of the models in estimating the contribution from each source to sediment was evaluated by the following

quantification statistics of accuracy: coefficient of determination (R^2) and root mean square error of prediction (RMSE).

Moreover, the model performance was also compared based on the prediction results of source contributions in sediment samples. For this purpose, as suggested by Legout et al. (2013) and Tiecher et al. (2021), we considered that the closer the total sum of the source contributions in sediment samples is from 100%, the higher is the model performance. All pre-processing and data modelling was performed in R software (R Core Team, 2020). The statistical performance was compared with an ANOVA at a 5% significance level. When significant, the difference between the means of the multivariate model, the pre-processing technique and the spectral range combination means were evaluated by the Tukey test ($p<0.05$).

8.2.5 Building spectroscopy models for different sediment sources

Spectroscopic models were built considering three approaches. First, the models were calibrated for each one of the four potential sources considered (cropland, pasture, unpaved roads and stream bank). Previous studies conducted in the same catchment already indicated a high similarity of the soil properties under cropland and pasture (Ramon et al., 2020; Tiecher et al., 2018). For this reason and in order to avoid misclassification between these two surface/agricultural sources, they were grouped as surface sources in a second approach. Merging sources with similar characteristics is a method that has already been used in previous studies to have a greater reliability in model prediction (Poulenard et al., 2009). In addition, a third approach was tested grouping unpaved roads and stream banks into a subsurface source category. Accordingly, in that case, only two sources (i.e. surface and subsurface) were considered. This similarity between surface and subsurface sources in the Conceição River catchment was already observed in the previous chapter (Chapter 2). Even with the combination of different types of tracers, it was not possible to obtain a good discrimination between sources. Accordingly; the combination of similar sources offered an alternative to reduce the uncertainty in the model predictions.

Regardless the source considered, in total, 56 models were calibrated for each sediment source with the combination of two multivariate models (PLSR, and SVM), four spectra pre-processing techniques (RAW, SNV, DET, and SGD) and seven spectral ranges (UV, NIR, MIR, UV+NIR, UV+MIR, NIR+MIR, UV+NIR+MIR). Therefore, altogether, 504

models were constructed in the current research, considering four (n=224), three (n=168) and two (n=112) potential sources, respectively.

8.3 Results and Discussion

8.3.1 Multivariate model calibration

The three approaches with the combinations of multivariate models, spectral ranges and pre-processing techniques resulted in a total of 504 models. The statistical results of model calibrations are presented in Figure A 1, Figure A 2 and Figure A 3 for the approaches with four, three and two potential sources, respectively. These figures show the statistical values of RMSE and R^2 for each model constructed. The multivariate models, spectral pre-processing techniques and spectral ranges were compared statistically for each approach (4, 3 and 2 sources).

8.3.1.1 Effect of multivariate models

Overall, the SVM provided more accurate models compared to PLSR, as indicated by the higher R^2 and lower RMSE values obtained with SVM, regardless the number of sediment sources considered. The Table 8.1 show the statistical values obtained for each combination of multivariate models, pre-processing technique and spectral range. The PLSR provided the lower RMSE and the highest R^2 individual values for the three approaches. However, R^2 and RMSE varied widely depending on the source samples, the pre-processing technique and the spectral range considered. In contrast, the SVM model provided a lower variation in the associated R^2 and RMSE values, showing a better performance regardless the spectral range or pre-processing technique considered (average values of each approach: $R^2 > 0.97$ and RMSE < 4.14%) (Table 8.1). The SVM model manages to establish mathematical relationships to express non-linear correlations between the organo-mineral composition and the spectral behaviour of sediment and soil samples (Viscarra Rossel and Behrens, 2010; Wijewardane et al., 2016). Due to the ability and flexibility to handle non-linear relationships between spectra and soil/sediment properties, the SVM has been more appropriate for the calibration of large heterogeneous samples, providing better results than PLSR models (Araújo et al., 2014; Lucà et al., 2017; Tiecher et al., 2021). Based on the general statistical performance of the multivariate model calibration, the SVM was considered as the most robust model for the

prediction of sediment source contributions. The PLSR model also provided satisfactory validation statistical values, with R^2 values close to one and low RMSE values, as already observed in other studies (Legout et al., 2013; Ni et al., 2019). Since there is no consensus in the literature on how to define the best prediction models and the best pre-processing method, preliminary tests considering all the possible combinations is recommended, in particular in large and complex catchments with a higher number of potential sources (Tiecher et al., 2021).

8.3.1.2 Effect of pre-processing techniques

Among the tested pre-processing techniques, the SGD showed the lowest RMSE and the highest R^2 values for the SVM model (Table 8.1). Although the three pre-processing techniques (SGD, SNV and DET) resulted in models with similar accuracies, only the SGD technique was significantly better than the RAW spectra. Based on this result, the SGD was considered as the best pre-processing technique for SVM models. The opposite situation was observed for the PLSR model, where the SGD pre-processing technique resulted in the highest RMSE and the lowest R^2 values, even when compared to the RAW spectra (without spectra pre-processing). With the PLSR models, the SNV resulted in the lowest RMSE values. However, it did not differ significantly from the RAW spectra in all the approaches, and from other pre-processing techniques for the approaches considering four and two sources, respectively (Table 8.1). In the approach with three sources, the SNV was significantly different from the SGD pre-processing technique only. Tiecher et al. (2021) suggested that pre-processing techniques may have a greater potential to improve model calibration in larger catchments with soils showing homogeneous mineralogical compositions. However, this was not observed in the current research, since the pre-processing techniques did not result in major gains of model calibration. According to these results, the SGD pre-processing technique is more recommended as an alternative to improve SVM model calibration. In contrast, for the PLSR model, no pre-processing is recommended, since no significant improvement was observed in the statistical parameters.

Table 8.1. Comparison of spectroscopic model accuracy indicated by R^2 and RMSE as affected by pre-processing technique and spectral range using PLSR and SVM methods considering four, three and two potential sources of sediments.

			Four sediment sources (cropland, pasture, unpaved roads, stream bank)				**Three sediment sources** (surface, unpaved roads, stream bank)				**Two sediment sources** (surface, subsurface)			
			PLSR		SVM		PLSR		SVM		PLSR		SVM	
RMSE	**Pre-processing**	RAW	5.26	a	4.83	a	5.29	ab	4.44	a	6.92	a	5.13	a
		SNV	5.62	a	4.27	a	4.66	b	3.96	ab	5.96	a	4.40	a
		DET	5.48	a	4.10	ab	5.32	ab	3.83	ab	6.92	a	4.21	ab
		SGD	6.86	a	3.10	b	6.85	a	2.93	b	7.52	a	3.38	b
	Spectral range	UV	17.77	a	12.4	a	15.89	a	10.04	a	21.27	a	11.8	a
		NIR	2.92	bc	2.56	b	2.29	c	2.58	b	2.39	d	2.88	b
		MIR	4.17	bc	2.74	b	4.48	bc	2.84	b	6.17	bc	3.18	b
		UV+NIR	5.16	b	2.61	b	4.68	bc	2.61	b	3.84	cd	2.77	b
		UV+MIR	5.40	b	2.80	b	6.22	b	2.79	b	7.99	b	3.21	b
		NIR+MIR	1.88	c	2.68	b	1.60	c	2.79	b	1.74	d	3.15	b
		UV+NIR+MIR	3.33	bc	2.70	b	3.55	bc	2.79	b	4.40	cd	3.13	b
	Mean		**5.80**	**Aa**	**4.07**	**Ab**	**5.53**	**Aa**	**3.79**	**Ab**	**6.83**	**Aa**	**4.56**	**Ab**
R^2	**Pre-processing**	RAW	0.94	a	0.94	b	0.95	ab	0.96	b	0.93	a	0.96	b
		SNV	0.94	a	0.96	ab	0.96	a	0.97	ab	0.95	a	0.96	ab
		DET	0.93	a	0.97	ab	0.95	ab	0.98	ab	0.92	a	0.98	ab
		SGD	0.90	a	0.99	a	0.91	b	0.99	a	0.89	a	0.99	a
	Spectral range	UV	0.61	b	0.80	b	0.73	b	0.88	b	0.60	b	0.87	b
		NIR	0.99	a	0.99	a	0.99	a	0.99	a	0.99	a	0.99	a
		MIR	0.98	a	0.99	a	0.98	a	0.99	a	0.96	a	0.99	a
		UV+NIR	0.96	a	0.99	a	0.96	a	0.99	a	0.99	a	0.99	a
		UV+MIR	0.96	a	0.98	a	0.94	a	0.99	a	0.94	a	0.99	a
		NIR+MIR	1.00	a	0.99	a	1.00	a	0.99	a	1.00	a	0.99	a
		UV+NIR+MIR	0.98	a	0.99	a	0.98	a	0.99	a	0.98	a	0.99	a
	Mean		**0.93**	**Ab**	**0.96**	**Aa**	**0.94**	**Ab**	**0.97**	**Aa**	**0.92**	**Ab**	**0.97**	**Aa**

Means followed by the same low case letters in the column, comparing pre-processing techniques and spectral ranges, are not significantly different according to the Tukey test at *p<0.05*. Means followed by the same capital letters in the raw, comparing the number of sediment sources considered, are not significantly different according to the Tukey test at *p<0.05*. Means followed by the same low case letters in the raw, comparing multivariate models, are not significantly different according to the Tukey test at *p<0.05*. Partial Least Square Regression – PLSR; Support Vector Machine – SVM; Ultra-violet-visible – UV; Near Infrared – NIR; MIR – Mid Infrared.

8.3.1.3 Effect of spectral ranges

In all the three approaches, with four, three and two potential sources of sediments, the models calibrated with the UV spectra resulted in higher RMSE and lower R^2 values, regardless of the pre-processing or multivariate model used (Figure A 1 to Figure A 3 and Table 8.2). The other spectral ranges including the UV spectra (especially UV+NIR and UV+MIR) also resulted in models with a low accuracy, mainly when they are combined with the PLSR approach (Table 8.2). The calibration of the SVM model was able to provide better results compared to the PLSR model for UV spectra and also better results than those obtained with most of the other spectral ranges.

Table 8.2. Comparison of the absolute sum of source contributions to individual sediment samples affected by spectral range using PLSR and SVM methods considering four, three and two potential sources of sediments.

	Four sediment sources (cropland, pasture, unpaved roads, stream bank)				**Three sediment sources** (surface, unpaved roads, stream bank)				**Two sediment sources** (surface, subsurface)			
Spectral range	PLSR		SVM		PLSR		SVM		PLSR		SVM	
	---------- % ----------											
UV	284.3	b	528.7	a	285.1	a	536.4	a	230.0	a	486.9	a
NIR	280.4	b	288.1	b	180.3	bc	181.9	b	152.1	b	150.5	b
MIR	228.1	bc	203.5	d	150.0	bc	152.7	b	127.8	b	133.3	b
UV+NIR	294.1	a	318.3	b	184.7	b	204.7	b	149.9	b	172.3	b
UV+MIR	211.7	c	208.7	cd	157.1	bc	158.5	b	146.1	b	129.2	b
NIR+MIR	333.0	a	309.8	b	165.0	bc	190.2	b	161.5	b	150.5	b
UV+NIR+MIR	271.8	abc	279.6	bc	142.1	c	178.5	b	128.0	b	140.7	b

Means followed by the same letters in the column, comparing spectral ranges, are not significantly different according to the Tukey test at $p<0.05$. Partial Least Square Regression – PLSR; Support Vector Machine – SVM; Ultra-violet-visible – UV; Near Infrared – NIR; MIR – Mid Infrared.

With the exception of the UV spectra, the other spectral ranges resulted in R^2 values close to one. For the PLSR, the difference in model performance between the spectral ranges considered were higher, especially when comparing the RMSE values. The best results were observed for the combination of NIR+MIR, which differs statistically in all the approaches from the UV, UV+NIR and UV+MIR spectral ranges. The UV range is highly influenced by the content in iron oxide of soils and sediments (Viscarra Rossel and Behrens, 2010). In the Conceição River catchment, the occurrence of highly weathered and homogeneous soils with the absence of clear composition difference between soil layers and land use sources, had already been, demonstrated with other tracers (geochemical composition, magnetic and colour parameters [Chapter 2]) which

complexifies their discrimination (Ramon et al., 2020; Tiecher et al., 2018). For similar reasons, differences are likely not sufficient between the considered sources are not sufficient to provide discrimination in the UV range.

The absorption features in NIR and MIR wavelengths are mainly related to the content in structural water, clay minerals and organic matter and they can provide a wide range of information about the sample composition (Tiecher et al., 2017a; Viscarra Rossel and Behrens, 2010). Differences in organic matter concentration between surface and subsurface layers may justify the better discrimination obtained in the approach with two sources (surface and subsurface), which presented a lower uncertainty associated with the discrimination of the source (11.9%) and a better percentage of correctly classified source samples (92.8%) compared to the three-source approach (Table 8.5). The NIR and MIR spectra have been widely and successfully used to predict soil organic carbon concentrations (Knox et al., 2015; Moura-Bueno et al., 2019; Ng et al., 2019) and they may provide a good discrimination between sources with different soil organic carbon contents. In addition, the MIR spectra have been proved to be efficient to predict different soil organic carbon fractions (Bellon-Maurel and McBratney, 2011; Reeves III et al., 2006), providing further information about the organic composition of the samples that may improve the discrimination between sources.

Overall, with the exception of the models calibrated with the UV spectra alone, all models were well-calibrated, presenting an R^2 above 0.94 and a RMSE below 7.99%. This results are better than those observed for another small catchment in southern Brazil, where mean validation RMSE values for all pre-processing techniques and spectral ranges exceeded 7.4% for PLSR and SVM models (Tiecher et al., 2021). In the current research, the mean RMSE values remained below 6.83% for the PLSR models and 4.56% for the SVM models (Table 8.1).

Despite the satisfactory statistical values obtained for the model calibrations (Figure 8.3, as an example), the sum of individual source contribution predictions for each sediment sample was not always equal to 100% when using multivariate models. This type of result differs from those of the conventional mixing models that require that the prediction of individual source contributions to fit in a range comprised between 0% and 100%, and that the sum of multiple sources must be equal to 100%. According to the literature, when unconstrained, the closer this sum is to 100%, the better is the performance of the models (Legout et al., 2013; Tiecher et al., 2021). Table 8.2 shows the

average absolute sum for all sediment samples and for each spectral range considered. The results showed that the UV spectra alone provide the least satisfactory results, differing statistically from those obtained with other spectral ranges regardless the number of sources considered and the multivariate models used. Observing the PLSR model calibrated with UV spectra, after the SGD pre-processing, the predicted contribution is underestimated compared to the observed proportions, in particular for the model adjusted for cropland, pasture and unpaved road sources (data not showed). This underestimation led to a lower contribution predicted for each of these sources and, consequently, it led to a lower absolute sum, resulting in values closer to 100%. In addition, a statistical difference between spectral ranges was also observed in the approach with three sources for the PLSR model, where the best quality result was observed for the combination for UV+NIR+MIR (142.1%). This analysis contributed to the identification of the best spectral range to use for source tracing. However, from these results, the unique conclusion that can be drawn is that UV spectra require more caution when they are considered as potential tracers of sediment sources.

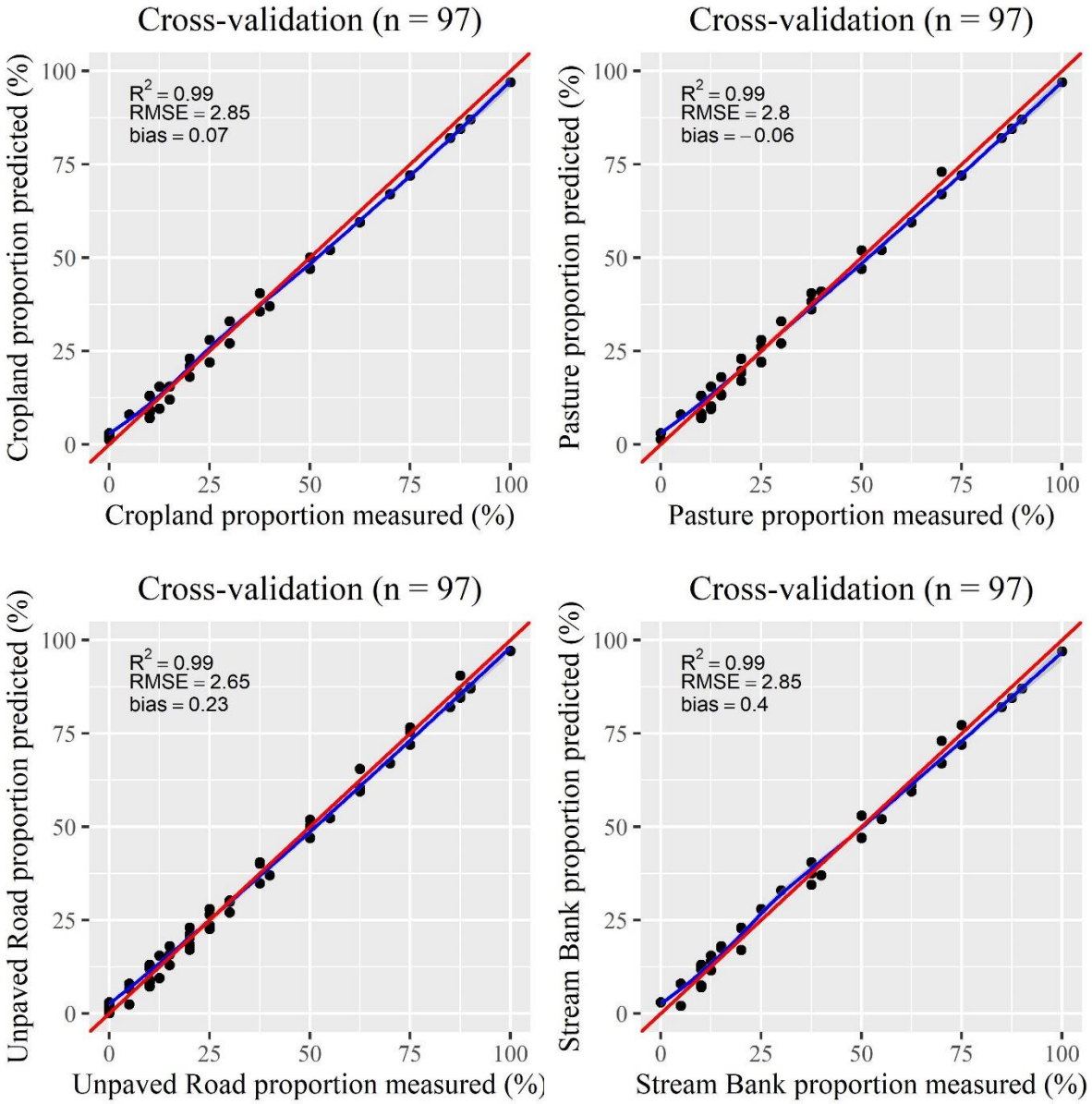

Figure 8.3. Support vector machine model calibration and validation with the MIR spectra after SGD pre-processing.

8.3.1.4 Effect of number of sediment source considered

In Table 8.1, the average statistical values are presented for each multivariate model calibration and each number of sources considered. Figure 8.4 and Figure 8.5 show the Mahalanobis distances between source samples and it illustrates that soil sample properties from cropland and pasture are overlapping. The combination of these two sources in the third approach increased the number of samples for the model calibration, and due to their similarity, this combined approach may result in better statistical results. The opposite situation is observed when combining unpaved roads and stream banks.

Although they both consist of subsurface sources, they are clearly more different from each other compared to the two types of surface sources. The increase in within-source variability when grouping sources together may reduce the quality of model calibration. Previous studies already warned about the uncertainty of the method application in more complex catchments with variations in soil types and land uses (Poulenard et al., 2012).

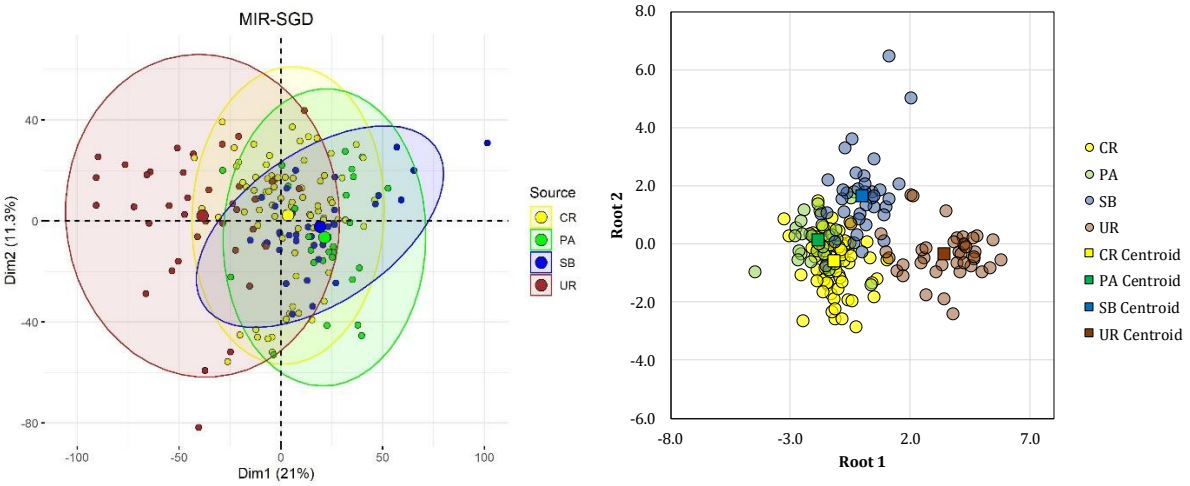

Figure 8.4. Principal component analysis biplots with four sources for the SVM model calibrated with the combination of MIR spectral range and SGD pre-processing technique (left). Two dimensional scatter plot of the first and second functions derived from the DFA (right).

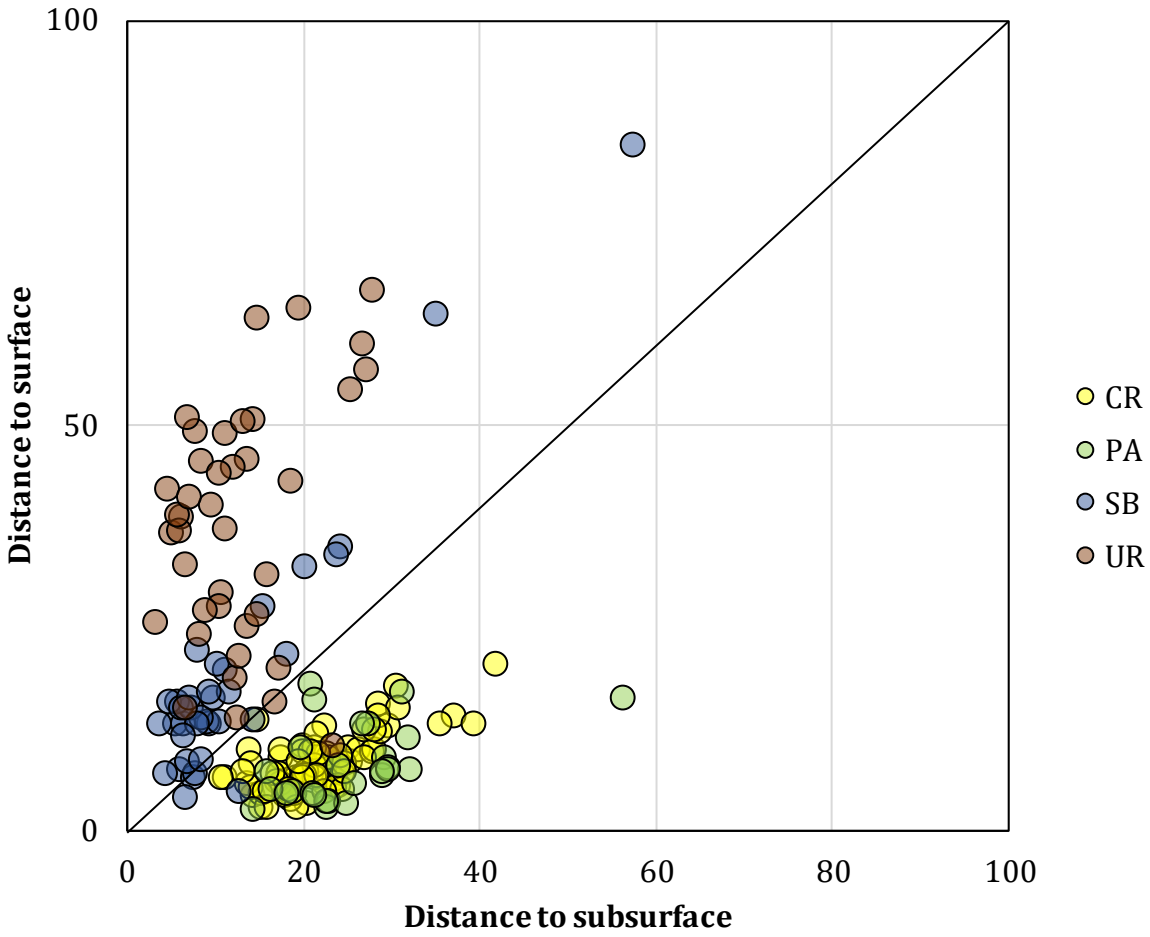

Figure 8.5. Mahalanobis distance from the discriminant analysis to differentiate subsurface samples from surface samples.

When the average statistical values for the three approaches are compared statistically, no significant difference was observed (Table 8.1). However, a higher uncertainty in the model predictions is expected with the increase in the number of sources (Poulenard et al., 2009). Since no significant difference was observed between the tested approaches and a better discrimination is expected when reducing the source number, a principal component analysis (PCA) was applied to the soil data to obtain the natural clustering of each source for the three approaches. Subsequently, a discriminant function analysis (DFA) was applied to the twenty-first PCA components in order to verify the discrimination capability between sources. The DFA was applied to analyse the impact of reducing the number of sources on the discrimination power. The percentage of correctly classified samples by the DFA increased with the reduction in source number,

from 83.4% to 90.6% from four to two sources, respectively (Table 8.3 to Table 8.5). The uncertainty associated with the discrimination of the sources was also reduced, from 28.8% to 15.6%. This analysis shows that the reduction of the source number reduces the uncertainty in the model prediction.

Although the DFA results were obtained from the MIR spectra after SGD pre-processing, it can be seen from the Figure 8.6, Figure 8.7 and Figure 8.8 that the reduction in source numbers decreases the difference between all 56 models with the combination of multivariate models, pre-processing and spectral range in the prediction of the source contributions. In the approach with two sources, for almost all model combinations, there was no significant difference between them (Figure 8.8). Only five models, the SVM model obtained from the UV spectra alone and the PLSR model calibrated with UV spectra after SNV pre-processing differed statistically from all the others. For the approach with three sources, nine models were statistically different and provided lower-quality results than the best set, while for the approach with four sources, sixteen model combinations were found in that situation. The results indicate that as the number of sources is reduced, the mean of absolute sum of individual source contributions becomes closer to 100% and the effect from the pre-processing technique, spectral range and multivariate model is expected to decrease.

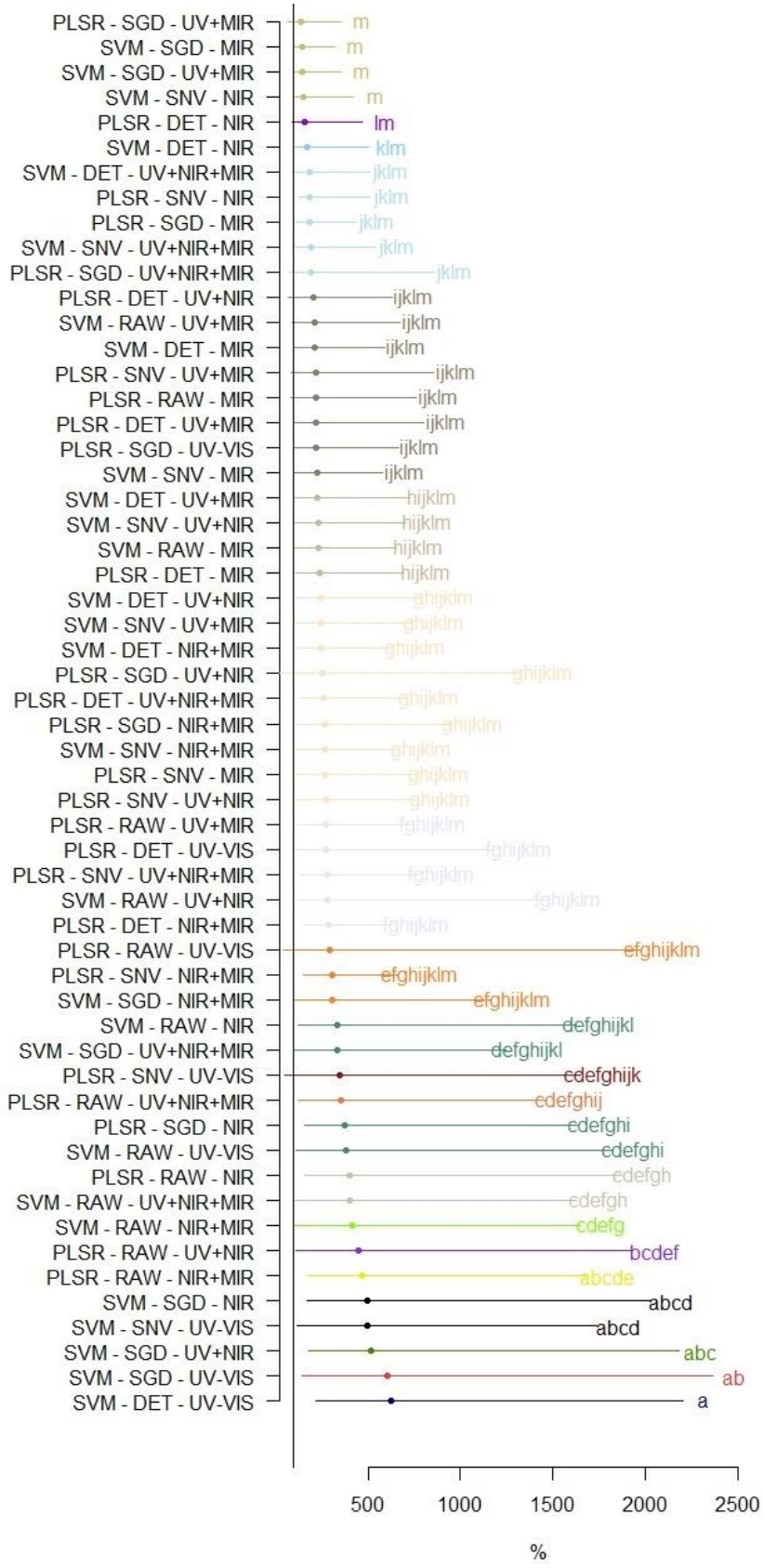

Figure 8.6. Mean test of the source contribution absolute sum average of the sediment samples for the approach with four sources. The vertical black line indicates the 100%. Means followed by the same letters are not significantly different according to the Tukey test at $p<0.05$. Statistically equal means are grouped by colour.

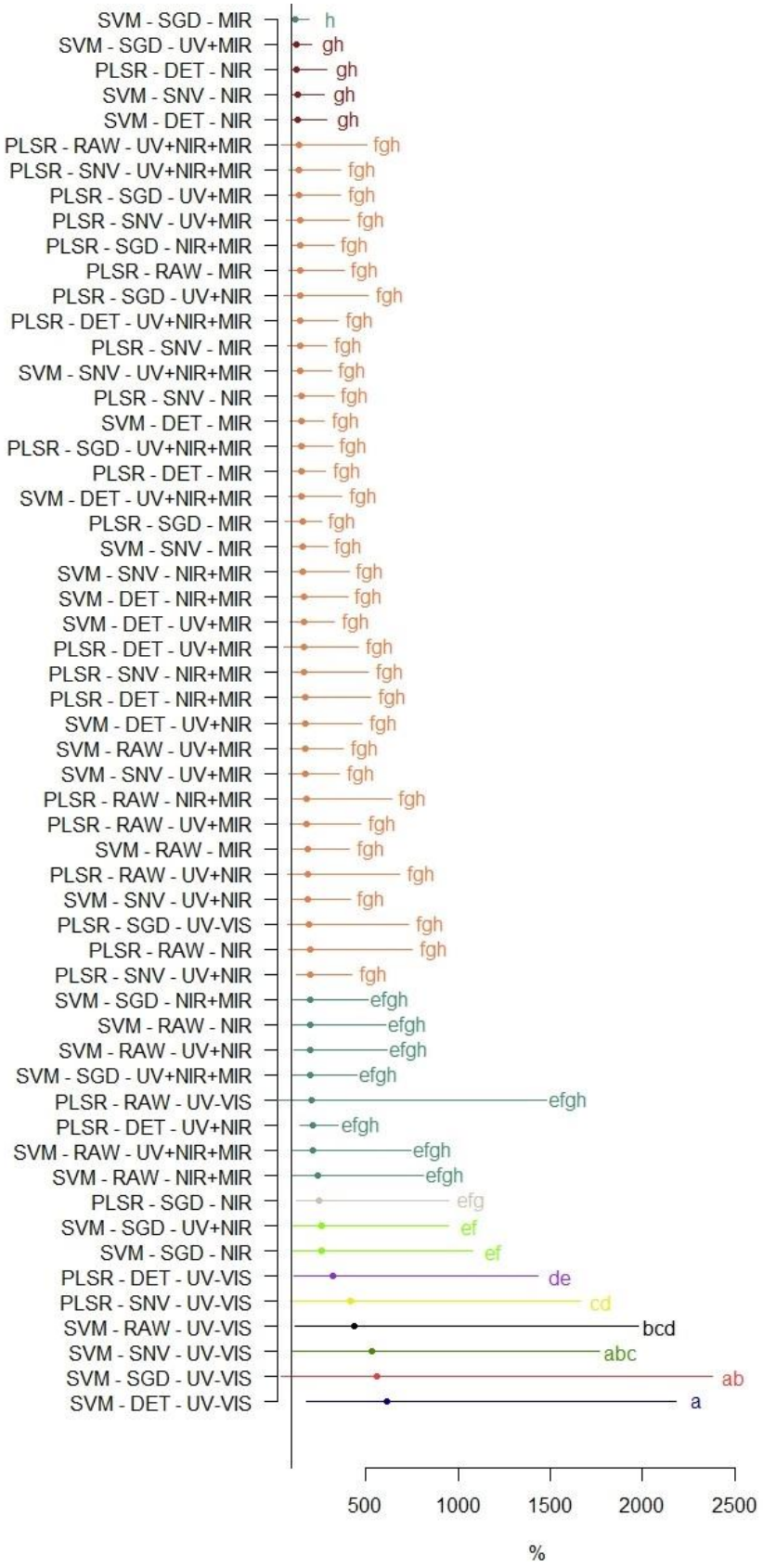

Figure 8.7. Mean test of the source contribution absolute sum average of the sediment samples for the approach with three sources. The vertical black line indicates the 100%. Means followed by the same letters are not significantly different according to the Tukey test at $p<0.05$. Statistically equal means are grouped by colour.

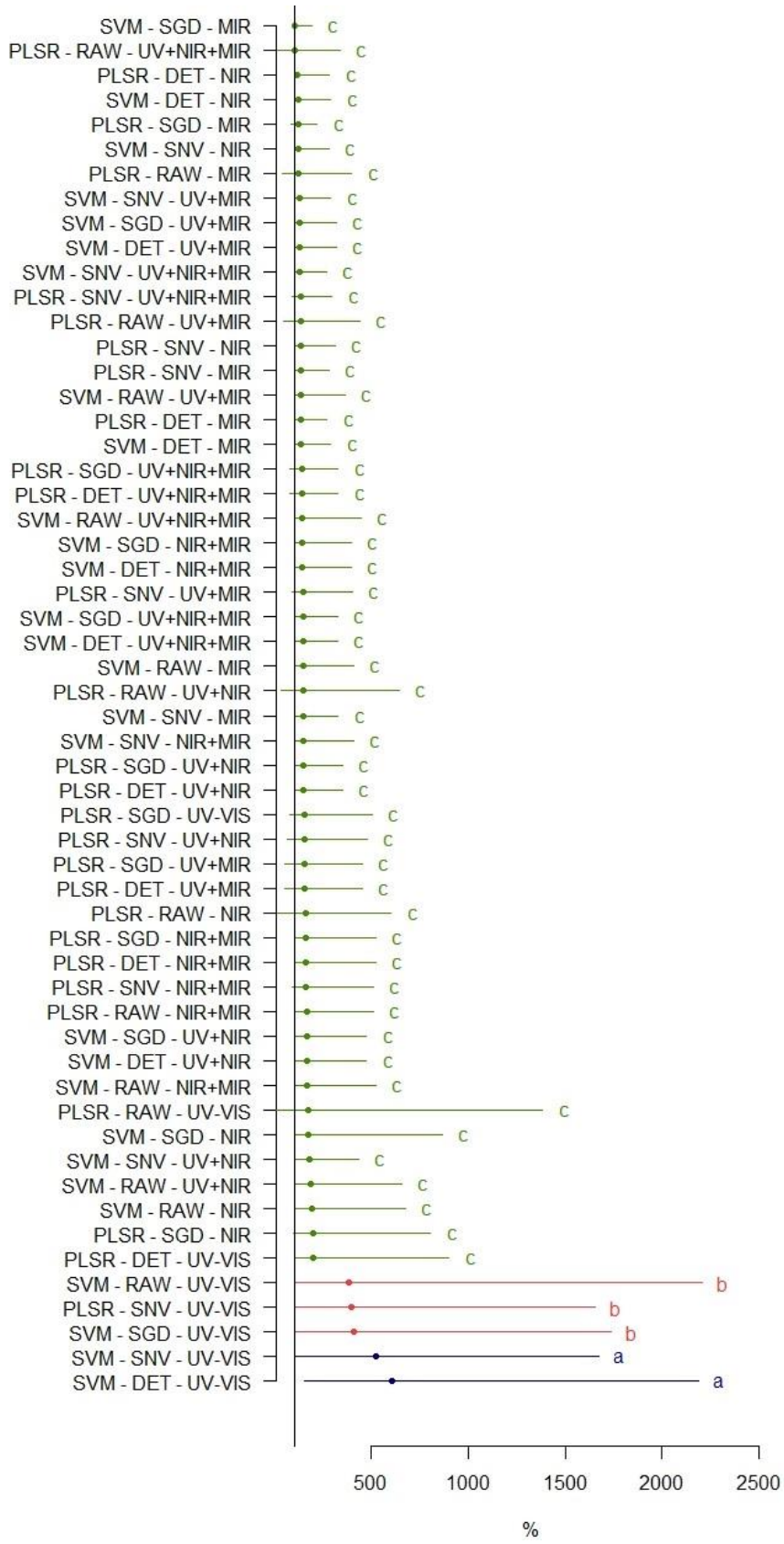

Figure 8.8. Mean test of the source contribution absolute sum average of the sediment samples for the approach with two sources. The vertical black line indicates the 100%. Means followed by the same letters are not significantly different according to the Tukey test at $p<0.05$. Statistically equal means are grouped by colour.

Table 8.3. Discriminant function analysis outputs for the approach with four sources. This analysis was made after the application of the SGD pre-processing technique.

Selected PCA components	1, 15, 3, 4, 5, 6, 7, 14, 9, 10, 19
Wilk's Lambda	0.1068
Variance explained by the variables (%)	89.32
Squared Mahalanobis distances	
Cropland vs Pasture	1.98
Cropland vs Stream Bank	6.41
Cropland vs Unpaved Road	21.40
Pasture vs Stream Bank	6.65
Pasture vs Unpaved Road	28.36
Stream Bank vs Unpaved Road	15.79
Average	13.43
p-levels	
Cropland vs Pasture	<0.001
Cropland vs Stream Bank	<0.001
Cropland vs Unpaved Road	<0.001
Pasture vs Stream Bank	<0.001
Pasture vs Unpaved Road	<0.001
Stream Bank vs Unpaved Road	<0.001
Correctly classified source samples (%)	
Croplands	96.15
Pasture	40.74
Stream Bank	77.78
Unpaved Road	87.5
Average	82.3
Uncertainty associated with the discrimination of the source (%)	
Cropland	21.54
Pasture	55.38
Stream Bank	30.58
Unpaved Road	14.14
Average	30.41

Table 8.4. Discriminant function analysis outputs for the approach with three sources. This analysis was made after the application of the SGD pre-processing technique.

Selected PCA components	1, 14, 3, 4, 5, 6, 7, 19, 9
Wilk's Lambda	0.1369
Variance explained by the variables (%)	86.31
Squared Mahalanobis distances	

Surface vs Stream Bank	5.83
Surface vs Unpaved Road	21.44
Stream Bank vs Unpaved Road	14.30
Average	13.86
p-levels	
Surface vs Stream Bank	<0.001
Surface vs Unpaved Road	<0.001
Stream Bank vs Unpaved Road	<0.001
Correctly classified source samples (%)	
Surface	98.1
Stream Bank	77.78
Unpaved Road	82.5
Average	90.61
Uncertainty associated with the discrimination of the source (%)	
Surface	6.48
Stream Bank	29.42
Unpaved Road	15.64
Average	17.18

Table 8.5. Discriminant function analysis outputs for the approach with two sources. This analysis was made after the application of the SGD pre-processing technique.

Selected PCA components	1, 10, 3, 4, 5, 6, 7, 14, 9
Wilk's Lambda	0.34
Variance explained by the variables (%)	66.27
Squared Mahalanobis distances	
Surface vs Subsurface	7.97
p-levels	
Surface vs Subsurface	<0.001
Correctly classified source samples (%)	
Surface	97.14
Subsurface	86.84
Average	92.82
Uncertainty associated with the discrimination of the source (%)	
Surface	5.64
Subsurface	18.16
Average	11.90

8.3.2 Sediment source contributions

According to the statistical analysis already discussed in the previous section, the combination SVM-SGD-MIR provided the best suite to predict sediment source contributions. Therefore, the sediment source contributions predicted by this combination is presented here for the approaches with different numbers of potential sources. In the first approach with four sources, a higher uncertainty was observed, with source contributions exceeding 100% and including negative contributions predicted for cropland in particular (Figure 8.11). The low discrimination between pasture and cropland samples (Figure 8.4) indicates the occurrence of limited differences in the soil properties for these two superficial sources. As a consequence, the model calibration for these two sources may result in unreliable predictions due to their similar properties, even with the optimum fit of the models for the two sources (Figure 8.3). The results show an underestimation of cropland contribution with negative values, while pastures had higher contributions, especially for Event and TISS samples, where in some cases their contribution exceeded 100% (Figure 8.11).

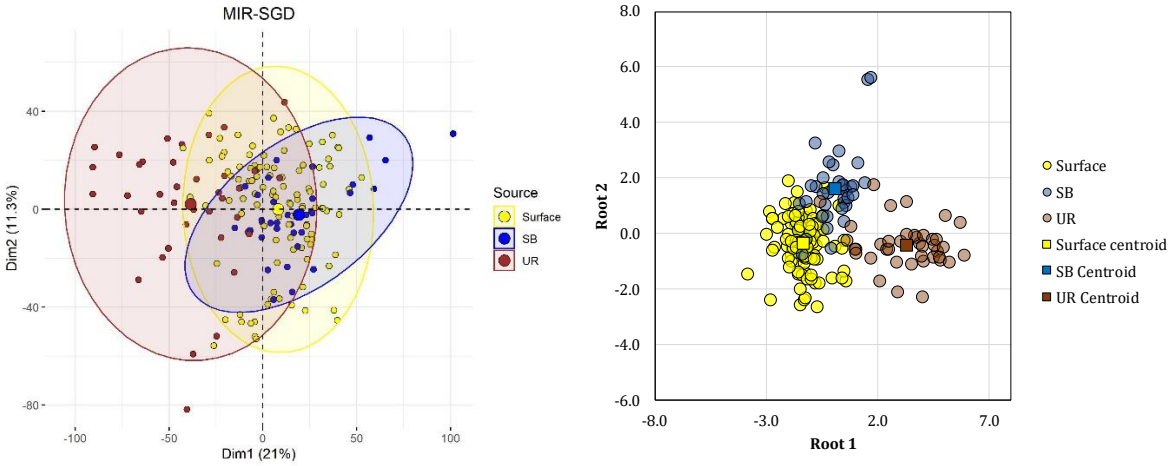

Figure 8.9. Principal component analysis biplots with three sources for the SVM model calibrated with the combination of MIR spectral range and SGD pre-processing technique (left). Two dimensional scatter plot of the first and second functions derived from the DFA (right).

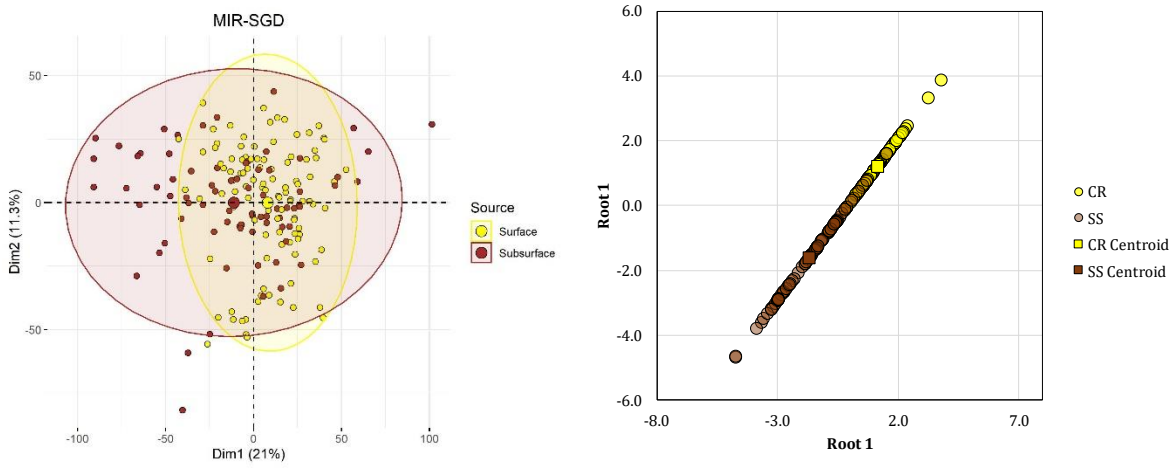

Figure 8.10. Principal component analysis biplots with two sources (a). Two dimensional scatter plot of the first and second functions derived from the DFA (b).

Differences in source contributions were observed according to the types of sediment samples. Pasture provided the main sources of suspended sediment during rainfall events and also for the TISS samples (Figure 8.11). However, considering the low discrimination between cropland and pasture sources, it can be assumed that the main sediment sources for Event and TISS samples are surface sources, as indicated in Figure 8.12. This result is in agreement with those results obtained by previous studies conducted in this catchment (Ramon et al., 2020; Tiecher et al., 2018). In addition, the absence of runoff control, appropriate soil conservation practices and the high erosivity potential of rainfall events in the region, may generate significant transfers of suspended sediment (Didoné et al., 2017). Accordingly, surface sources supplied a greater contribution to sediment samples collected during events as well as for the TISS material. It is important to note that it is usually during the flood events that most of the sediment fluxes take place (Minella et al., 2017a). This indicates that large amounts of sediment and associated nutrients may be transported from agricultural areas and delivered to water bodies, which requires interventions to avoid soil and nutrient losses from the field and contamination of the water bodies. In contrast, the sediment collected on the riverbed shows larger contributions from the stream bank, which is in agreement with the results observed in previous studies conducted in the same catchment (Ramon et al., 2020; Tiecher et al., 2018). The reduction in source number and the combination of similar sources confirm the preliminary observations showing that surface sources provide the main suspended sediment source, for both event-based and TISS samples (Figure 8.12

and Figure 8.13). In contrast, the subsurface sources in general, and stream banks in particular, provide the main source for riverbed sediment samples.

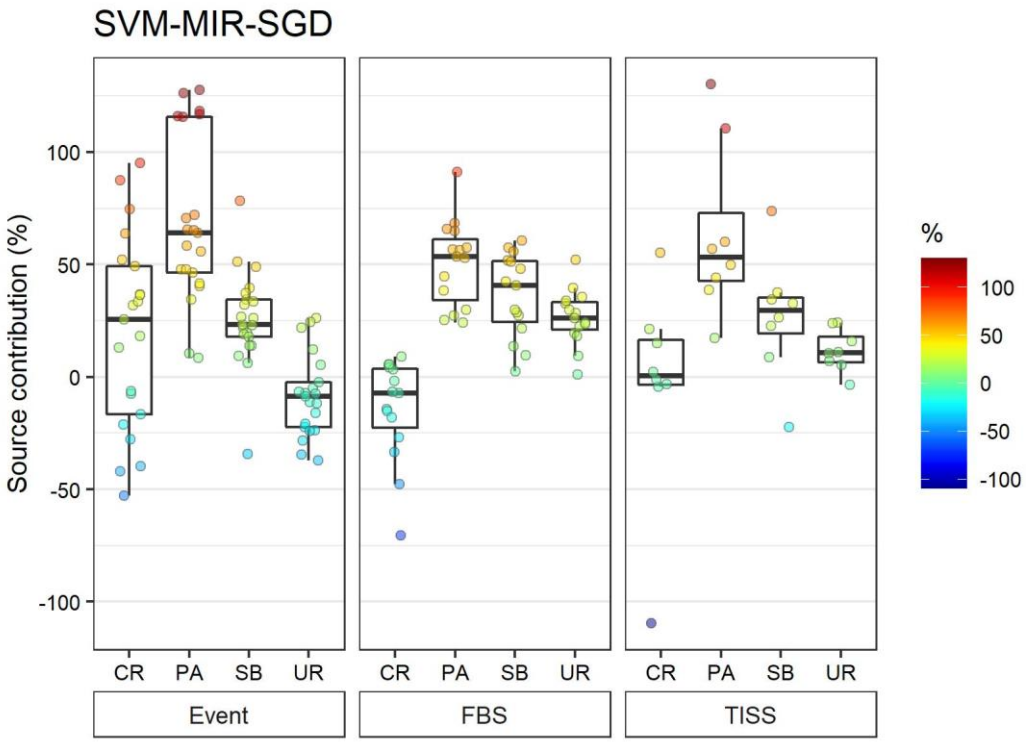

Figure 8.11. Sediment source contributions according to the sampling method predicted from the SVM-SGD-MIR models. Event = Rainfall runoff event; FBS = Fine bed sediment samples; and TISS = Time integrated suspended sediment samples.

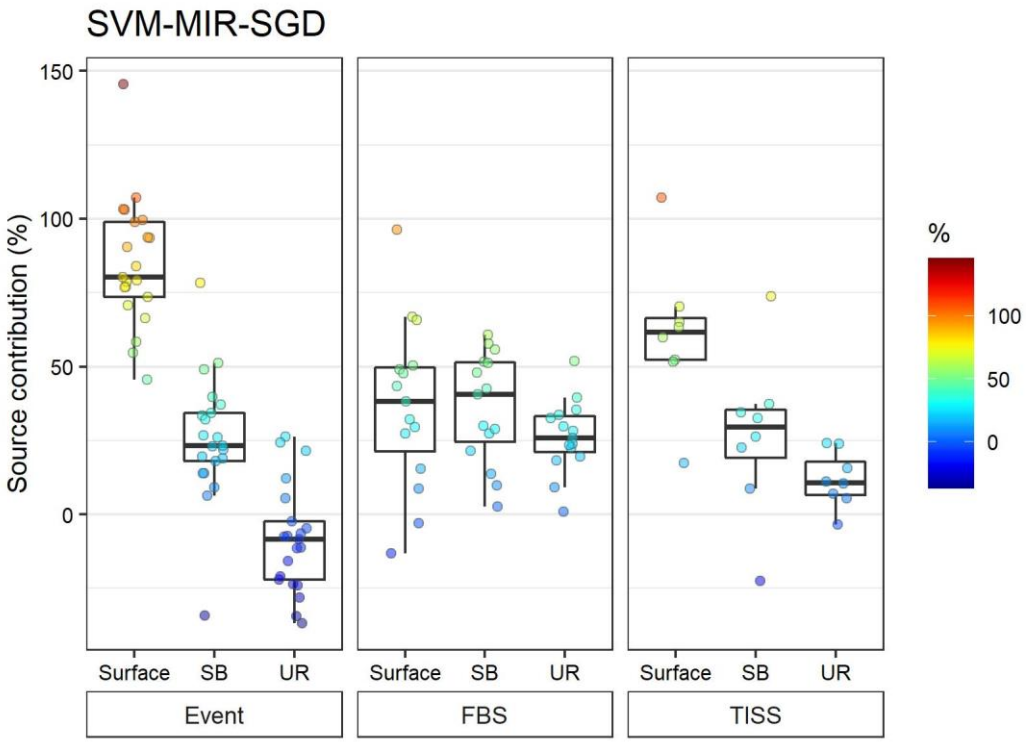

Figure 8.12. Sediment source contributions according to the sampling method predicted from the SVM-SGD-MIR models. Event = Rainfall runoff event; FBS = Fine bed sediment samples; and TISS = Time integrated suspended sediment samples.

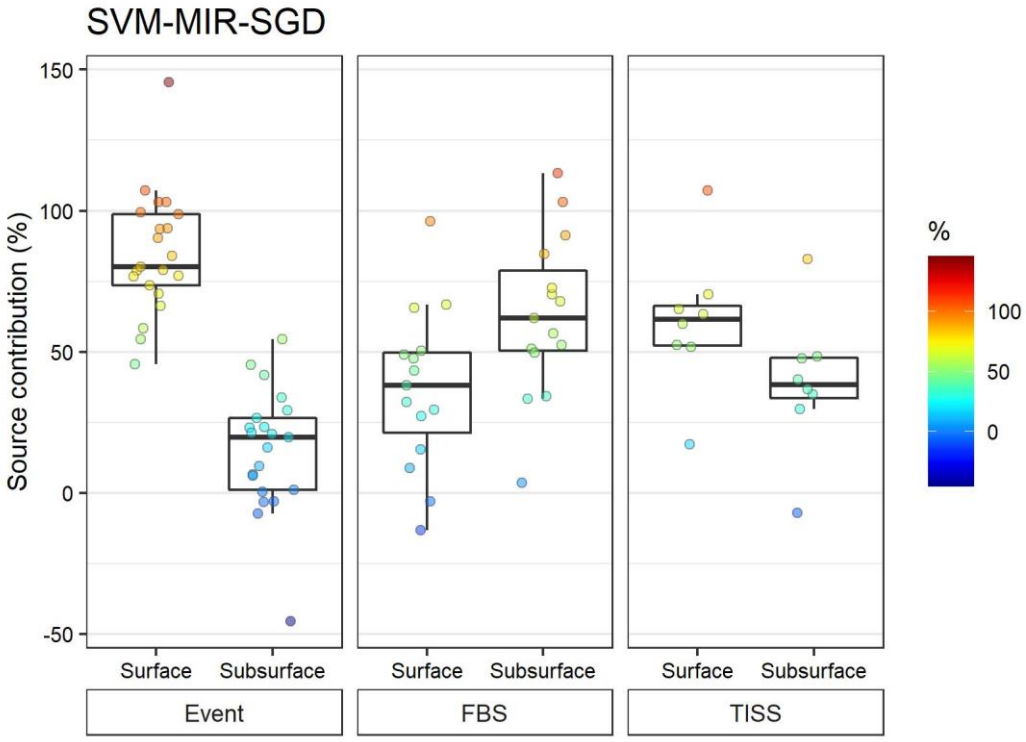

Figure 8.13. Sediment source contributions according to the sampling method predicted from the SVM-SGD-MIR models. Event = Rainfall runoff event; FBS = Fine bed sediment samples; and TISS = Time integrated suspended sediment samples.

The sediment samples analysed in this study was higher than the previous study in the Conceição catchment (Chapter 2), because the sample mass required to perform the spectroscopy analyses were lower (0.2 g) than for geochemical composition and magnetic susceptibility analyses (up to 2 g). For this reason, results for individual samples cannot be compared for all sediment samples. In addition, the sediment sources considered in each study were different and a final comparison between surface and subsurface only can be more reliable. For the TISS samples, the approach based on geochemical composition, magnetic and spectroscopy-derived parameters indicated an average contribution of 73% from surface sources and 27% from subsurface material. In this research, approximately 62% was shown to originate from surface sources and ~38% from subsurface categories. For FBS samples, the previous study indicated an average contribution of 37% from surface and 63% from subsurface sources. The results are very close to those observed in this research, which indicates that different approaches can lead to very similar results as already observe in other studies (Tiecher et al., 2017a). However, we observe that with a larger number of sediment sources, more uncertainty is expected, as observed in the study based on discrete variables with mixing models (Chapter 2), as well as in this research with diffuse reflectance spectroscopy associated to multivariate models.

8.4 Conclusions

Diffuse reflectance spectroscopy was shown to have potential in estimating the contribution of sediment sources from a large and homogeneous subtropical catchment, and may be a more cost-effective method than the more conventional ones. The support vector machine model was found to be the most powerful for estimating sediment source contributions. The ultra-violet-visible spectra were not efficient for tracing the sediment sources in this catchment with homogeneous and highly weathered soils, while near and mid infrared showed good accuracy values. The change in the number of potential sources considered had no significant impact in the model calibration and performance, satisfactory statistical values were obtained for both approaches. However, when a larger number of potential sources is considered, more caution with model calibration is required and testing different models, pre-processing techniques and spectral range is recommended. The approach with four sources indicates that pastures provide the main source for the suspended sediment collected during events and by the time integrated

sampler, however a high uncertainty is associated with this result. Based on the approaches with three and two sources, the model predictions indicate that surface sources provide the main sediment source to suspended sediment samples collected during rainfall events and for time integrated sediment samples, while the stream bank provided the main source to the riverbed sediment samples.

8.5 References

Araújo, S.R., Wetterlind, J., Demattê, J.A.M., Stenberg, B., 2014. Improving the prediction performance of a large tropical vis-NIR spectroscopic soil library from Brazil by clustering into smaller subsets or use of data mining calibration techniques. Eur. J. Soil Sci. 65, 718–729. https://doi.org/10.1111/ejss.12165

Barnes, R.J., Dhanoa, M.S., Lister, S.J., 1989. Standard Normal Variate Transformation and De-Trending of Near-Infrared Diffuse Reflectance Spectra. Appl. Spectrosc. 43, 772–777. https://doi.org/10.1366/0003702894202201

Bellon-Maurel, V., McBratney, A., 2011. Near-infrared (NIR) and mid-infrared (MIR) spectroscopic techniques for assessing the amount of carbon stock in soils – Critical review and research perspectives. Soil Biol. Biochem. 43, 1398–1410. https://doi.org/10.1016/j.soilbio.2011.02.019

Collins, A.L., Pulley, S., Foster, I.D.L., Gellis, A., Porto, P., Horowitz, A.J., 2017. Sediment source fingerprinting as an aid to catchment management: A review of the current state of knowledge and a methodological decision-tree for end-users. J. Environ. Manage. 194, 86–108. https://doi.org/10.1016/j.jenvman.2016.09.075

Didoné, E.J., Minella, J.P.G., Evrard, O., 2017. Measuring and modelling soil erosion and sediment yields in a large cultivated catchment under no-till of Southern Brazil. Soil Tillage Res. 174, 24–33. https://doi.org/10.1016/j.still.2017.05.011

Dotto, A.C., Dalmolin, R.S.D., Caten, A. ten, Gris, D.J., Ruiz, L.F.C., 2019. AlradSpectra: a Quantification Tool for Soil Properties Using Spectroscopic Data in R. Rev. Bras. Ciência do Solo 43, 1–15. https://doi.org/10.1590/18069657rbcs20180263

Farias Amorim, F., Jacques Agra Bezerra da Silva, Yuri, Cabral Nascimento, R., Jacques Agra Bezerra da Silva, Ygor, Tiecher, T., Williams Araújo do Nascimento, C., Paolo Gomes Minella, J., Zhang, Y., Ram Upadhayay, H., Pulley, S., Collins, A.L., 2021. Sediment source apportionment using optical property composite signatures in a rural catchment, Brazil. CATENA 202, 105208.

https://doi.org/10.1016/j.catena.2021.105208

Golosov, V.N., Walling, D.E., 2019. Erosion and sediment problems: global hotspots. Paris, France.

IUSS Working Group WRB, 2015. World reference base for soil resources 2014, update 2015 International soil classification system for naming soils and creating legends for soil maps. World Soil Resources Reports No. 106. FAO, Rome.

Knox, N.M., Grunwald, S., McDowell, M.L., Bruland, G.L., Myers, D.B., Harris, W.G., 2015. Modelling soil carbon fractions with visible near-infrared (VNIR) and mid-infrared (MIR) spectroscopy. Geoderma 239–240, 229–239. https://doi.org/10.1016/j.geoderma.2014.10.019

Laceby, J.P., Evrard, O., Smith, H.G., Blake, W.H., Olley, J.M., Minella, J.P.G., Owens, P.N., 2017. The challenges and opportunities of addressing particle size effects in sediment source fingerprinting: A review. Earth-Science Rev. 169, 85–103. https://doi.org/10.1016/j.earscirev.2017.04.009

Legout, C., Poulenard, J., Nemery, J., Navratil, O., Grangeon, T., Evrard, O., Esteves, M., 2013. Quantifying suspended sediment sources during runoff events in headwater catchments using spectrocolorimetry. J. Soils Sediments 13, 1478–1492. https://doi.org/10.1007/s11368-013-0728-9

Lucà, F., Conforti, M., Castrignanò, A., Matteucci, G., Buttafuoco, G., 2017. Effect of calibration set size on prediction at local scale of soil carbon by Vis-NIR spectroscopy. Geoderma 288, 175–183. https://doi.org/10.1016/j.geoderma.2016.11.015

Melo, D.C.D., Anache, J.A.A., Almeida, C. das N., Coutinho, J. V., Ramos Filho, G.M., Rosalem, L.M.P., Pelinson, N.S., Ferreira, G.L.R.A., Schwamback, D., Calixto, K.G., Siqueira, J.P.G., Duarte-Carvajalino, J.C., Jhunior, H.C.S., Nóbrega, J.D., Morita, A.K.M., Leite, C.M.C., Guedes, A.C.E., Coelho, V.H.R., Wendland, E., 2020. The big picture of field hydrology studies in Brazil. Hydrol. Sci. J. 0, 1. https://doi.org/10.1080/02626667.2020.1747618

Mevik, B.-H., Wehrens, R., Liland, K.H., 2016. Partial Least Squares and Principal Component Regression. Packag. R CRAN.

Meyer, D., Dimitriadou, E., Hornik, K., Weingessel, A., Leisch, F., Chang, C.-C., Lin, C.-C., 2019. Misc Functions of the Department of Statistics, Probability Theory Group (Formerly: E1071), TU Wien. R Packag. version 1.7-3.

Minella, J.P.G., Merten, G.H., Barros, C.A.P. de, Ramon, R., Schlesner, A., Clarke, R.T., Moro, M., Dalbianco, L., 2017. Long-term sediment yield from a small catchment in southern Brazil affected by land use and soil management changes. Hydrol. Process. https://doi.org/10.1002/hyp.11404

Moura-Bueno, J.M., Dalmolin, R.S.D., ten Caten, A., Dotto, A.C., Demattê, J.A.M., 2019. Stratification of a local VIS-NIR-SWIR spectral library by homogeneity criteria yields more accurate soil organic carbon predictions. Geoderma 337, 565–581. https://doi.org/10.1016/j.geoderma.2018.10.015

Ng, W., Minasny, B., Montazerolghaem, M., Padarian, J., Ferguson, R., Bailey, S., McBratney, A.B., 2019. Convolutional neural network for simultaneous prediction of several soil properties using visible/near-infrared, mid-infrared, and their combined spectra. Geoderma 352, 251–267. https://doi.org/10.1016/j.geoderma.2019.06.016

Ni, L.S., Fang, N.F., Shi, Z.H., Tan, W.F., 2019. Mid-infrared spectroscopy tracing of channel erosion in highly erosive catchments on the Chinese Loess Plateau. Sci. Total Environ. https://doi.org/10.1016/j.scitotenv.2019.06.116

Poesen, J., 2017. Soil erosion in the Anthropocene: research needs. Earth Surf. Process. Landforms 84, 64–84. https://doi.org/10.1002/esp.4250

Poulenard, J., Legout, C., Némery, J., Bramorski, J., Navratil, O., Douchin, A., Fanget, B., Perrette, Y., Evrard, O., Esteves, M., 2012. Tracing sediment sources during floods using Diffuse Reflectance Infrared Fourier Transform Spectrometry (DRIFTS): A case study in a highly erosive mountainous catchment (Southern French Alps). J. Hydrol. 414–415, 452–462. https://doi.org/10.1016/j.jhydrol.2011.11.022

Poulenard, J., Perrette, Y., Fanget, B., Quetin, P., Trevisan, D., Dorioz, J.M., 2009. Infrared spectroscopy tracing of sediment sources in a small rural watershed (French Alps). Sci. Total Environ. 407, 2808–2819. https://doi.org/10.1016/j.scitotenv.2008.12.049

Pulley, S., Van der Waal, B., Rowntree, K., Collins, A.L., 2018. Colour as reliable tracer to identify the sources of historically deposited flood bench sediment in the Transkei, South Africa: A comparison with mineral magnetic tracers before and after hydrogen peroxide pre-treatment. CATENA 160, 242–251. https://doi.org/10.1016/j.catena.2017.09.018

R Core Team, 2020. R: A Language and Environment for Statistical Computing [WWW Document]. URL https://www.r-project.org/

Ramon, R., Evrard, O., Laceby, J.P., Caner, L., Inda, A. V., Barros, C.A.P. de, Minella, J.P.G., Tiecher, T., 2020. Combining spectroscopy and magnetism with geochemical tracers to improve the discrimination of sediment sources in a homogeneous subtropical catchment. CATENA 195, 104800. https://doi.org/10.1016/j.catena.2020.104800

Reeves III, J.B., Follett, R.F., McCarty, G.W., Kimble, J.M., Reeves, J.B., Follett, R.F., McCarty, G.W., Kimble, J.M., 2006. Can Near or Mid-Infrared Diffuse Reflectance Spectroscopy Be Used to Determine Soil Carbon Pools? Commun. Soil Sci. Plant Anal. 37, 2307–2325. https://doi.org/10.1080/00103620600819461

Sellier, V., Navratil, O., Laceby, J.P., Legout, C., Allenbach, M., Lefèvre, I., Evrard, O., 2020. Combining colour parameters and geochemical tracers to improve sediment source discrimination in a mining catchment (New Caledonia, South Pacific Islands). SOIL Discuss. in review. https://doi.org/https://doi.org/10.5194/soil-2020-48

Tiecher, T., Caner, L., Minella, J.P.G., Bender, M.A., dos Santos, D.R., 2016. Tracing sediment sources in a subtropical rural catchment of southern Brazil by using geochemical tracers and near-infrared spectroscopy. Soil Tillage Res. 155, 478–491. https://doi.org/10.1016/j.still.2015.03.001

Tiecher, T., Caner, L., Minella, J.P.G., Evrard, O., Mondamert, L., Labanowski, J., Rheinheimer, D. dos S., 2017. Tracing Sediment Sources Using Mid-infrared Spectroscopy in Arvorezinha Catchment, Southern Brazil. L. Degrad. Dev. 28, 1603–1614. https://doi.org/10.1002/ldr.2690

Tiecher, T., Caner, L., Minella, J.P.G., Santos, D.R. dos, 2015. Combining visible-based-color parameters and geochemical tracers to improve sediment source discrimination and apportionment. Sci. Total Environ. 527–528, 135–149. https://doi.org/10.1016/j.scitotenv.2015.04.103

Tiecher, T., Minella, J.P.G., Evrard, O., Caner, L., Merten, G.H., Capoane, V., Didoné, E.J., dos Santos, D.R., 2018. Fingerprinting sediment sources in a large agricultural catchment under no-tillage in Southern Brazil (Conceição River). L. Degrad. Dev. 29, 939–951. https://doi.org/10.1002/ldr.2917

Tiecher, T., Moura-Bueno, J.M., Caner, L., Minella, J.P.G.P.G., Evrard, O., Ramon, R., Naibo, G., Barros, C.A.P. de, Silva, Y.J.A.B., Amorim, F.F., Rheinheimer, D.S., 2021. Improving the quantification of sediment source contributions using different mathematical models and spectral preprocessing techniques for individual or combined spectra of ultraviolet–visible, near- and middle-infrared spectroscopy. Geoderma 384, 114815.

https://doi.org/10.1016/j.geoderma.2020.114815

Viscarra Rossel, R.A., Behrens, T., 2010. Using data mining to model and interpret soil diffuse reflectance spectra. Geoderma 158, 46–54. https://doi.org/10.1016/j.geoderma.2009.12.025

Viscarra Rossel, R.A., Walvoort, D.J.J., McBratney, A.B., Janik, L.J., Skjemstad, J.O., 2006. Visible, near infrared, mid infrared or combined diffuse reflectance spectroscopy for simultaneous assessment of various soil properties. Geoderma 131, 59–75. https://doi.org/10.1016/j.geoderma.2005.03.007

Wijewardane, N.K., Ge, Y., Morgan, C.L.S., 2016. Moisture insensitive prediction of soil properties from VNIR reflectance spectra based on external parameter orthogonalization. Geoderma 267, 92–101. https://doi.org/10.1016/j.geoderma.2015.12.014

Appendices

Table A 1. Source sample proportions in the composite artificial mixtures.

Mixture	Surface		Subsurface		Mixture	Surface		Subsurface	
	Cropland	Pasture	Unpaved Road	Stream banks		Cropland	Pasture	Unpaved Road	Stream banks
	----------%----------					----------%----------			
MIX-1	100	0	0	0	MIX-50	30	30	30	10
MIX-2	0	0	100	0	MIX-51	30	10	30	30
MIX-3	0	0	0	100	MIX-52	40	20	20	20
MIX-4	0	100	0	0	MIX-53	20	20	40	20
MIX-5	25	25	25	25	MIX-54	20	20	20	40
MIX-6	87.5	0	12.5	0	MIX-55	20	40	20	20
MIX-7	75	0	25	0	MIX-56	55	15	15	15
MIX-8	62.5	0	37.5	0	MIX-57	15	15	55	15
MIX-9	50	0	50	0	MIX-58	15	15	15	55
MIX-10	37.5	0	62.5	0	MIX-59	15	55	15	15
MIX-11	25	0	75	0	MIX-60	70	10	10	10
MIX-12	12.5	0	87.5	0	MIX-61	10	10	70	10
MIX-13	0	0	87.5	12.5	MIX-62	10	10	10	70
MIX-14	0	0	75	25	MIX-63	10	70	10	10
MIX-15	0	0	62.5	37.5	MIX-64	85	5	5	5
MIX-16	0	0	50	50	MIX-65	5	5	85	5
MIX-17	0	0	37.5	62.5	MIX-66	5	5	5	85
MIX-18	0	0	25	75	MIX-67	5	85	5	5
MIX-19	0	0	12.5	87.5	MIX-68	70	0	20	10
MIX-20	87.5	0	0	12.5	MIX-69	10	0	70	20
MIX-21	75	0	0	25	MIX-70	20	0	10	70
MIX-22	62.5	0	0	37.5	MIX-71	0	10	70	20
MIX-23	50	0	0	50	MIX-72	0	20	10	70
MIX-24	37.5	0	0	62.5	MIX-73	0	70	20	10
MIX-25	25	0	0	75	MIX-74	70	10	0	20
MIX-26	12.5	0	0	87.5	MIX-75	10	20	0	70
MIX-27	0	87.5	0	12.5	MIX-76	20	70	0	10
MIX-28	0	75	0	25	MIX-77	70	10	20	0
MIX-29	0	62.5	0	37.5	MIX-78	10	20	70	0
MIX-30	0	50	0	50	MIX-79	20	70	10	0
MIX-31	0	37.5	0	62.5	MIX-80	90	0	10	0
MIX-32	0	25	0	75	MIX-81	10	0	90	0
MIX-33	0	12.5	0	87.5	MIX-82	90	0	0	10
MIX-34	0	87.5	12.5	0	MIX-83	10	0	0	90
MIX-35	0	75	25	0	MIX-84	90	10	0	0
MIX-36	0	62.5	37.5	0	MIX-85	10	90	0	0
MIX-37	0	50	50	0	MIX-86	0	0	90	10
MIX-38	0	37.5	62.5	0	MIX-87	0	0	10	90

MIX-39	0	25	75	0	MIX-88	0	10	90	0
MIX-40	0	12.5	87.5	0	MIX-89	0	90	10	0
MIX-41	12.5	87.5	0	0	MIX-90	0	10	0	90
MIX-42	25	75	0	0	MIX-91	0	90	0	10
MIX-43	37.5	62.5	0	0	MIX-92	50	0	50	0
MIX-44	50	50	0	0	MIX-93	50	0	0	50
MIX-45	62.5	37.5	0	0	MIX-94	50	50	0	0
MIX-46	75	25	0	0	MIX-95	0	0	50	50
MIX-47	87.5	12.5	0	0	MIX-96	0	50	50	0
MIX-48	10	30	30	30	MIX-97	0	50	0	50
MIX-49	30	30	10	30					

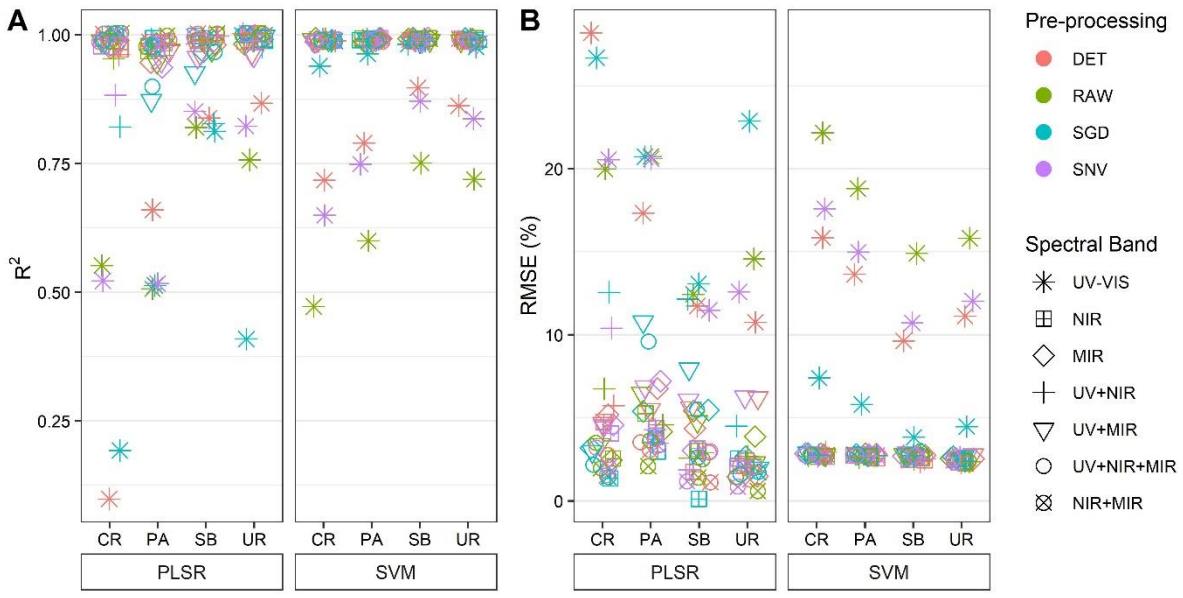

Figure A 1. Statistical analyses of the multivariate model calibration, SVM and PLSR, for the first approach with four sources and different combinations of pre-processing techniques and spectral ranges considering 4 sources.

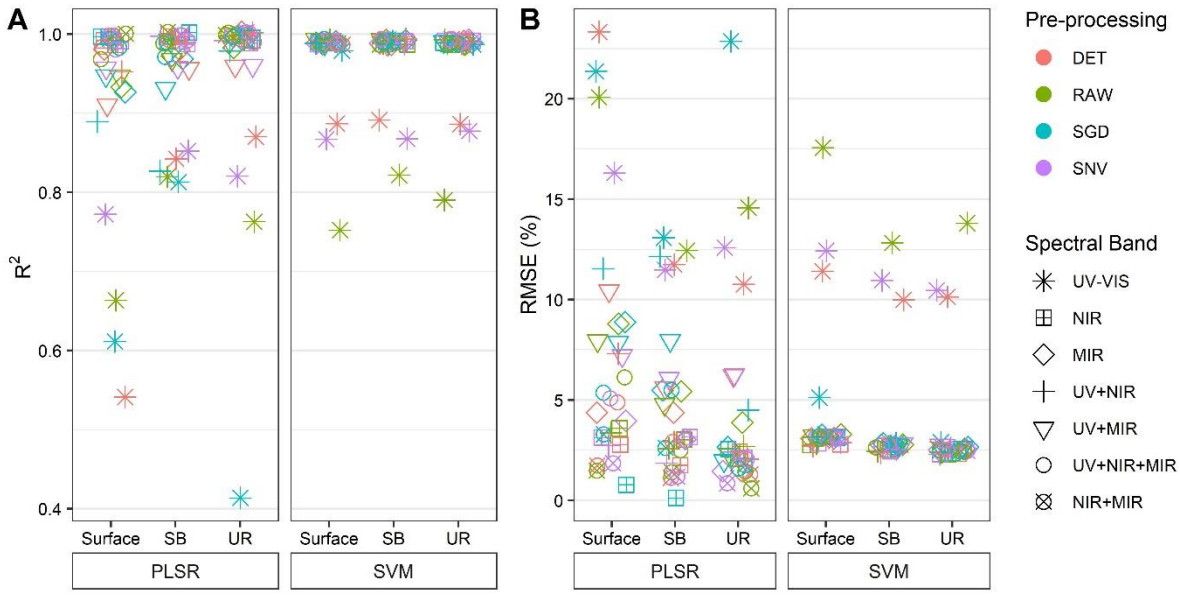

Figure A 2. Statistical analyses of the multivariate models calibration, SVM and PLSR, for two sources with different combinations of pre-processing techniques and spectral ranges considering 3 sources.

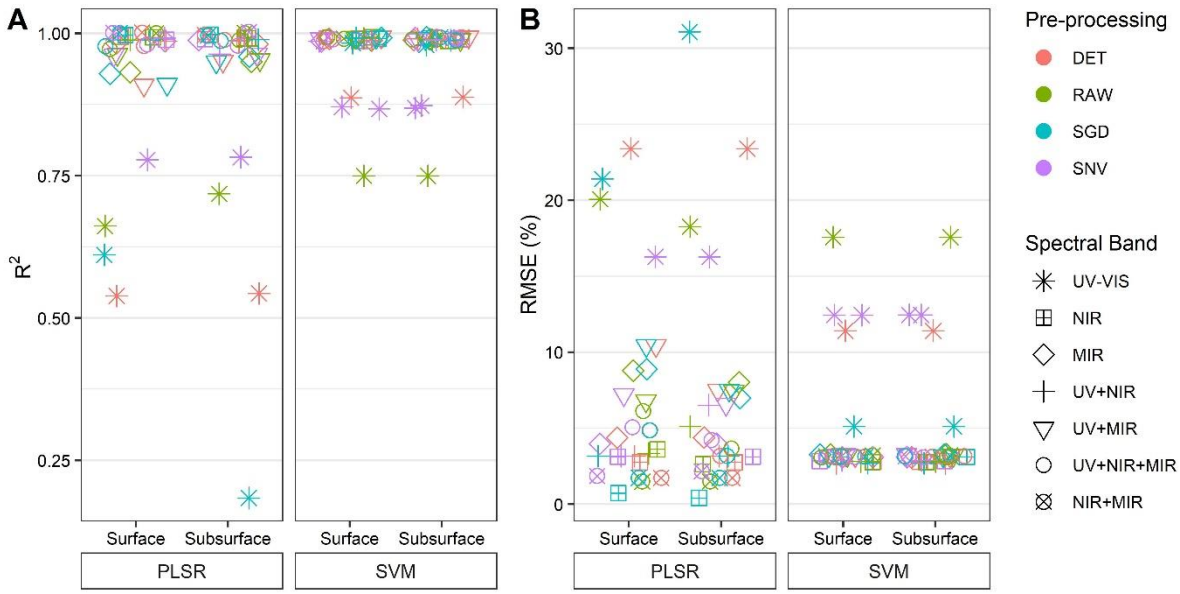

Figure A 3. Statistical analyses of the multivariate models calibration, SVM and PLSR, for two sources with different combinations of pre-processing techniques and spectral ranges considering 2 sources.

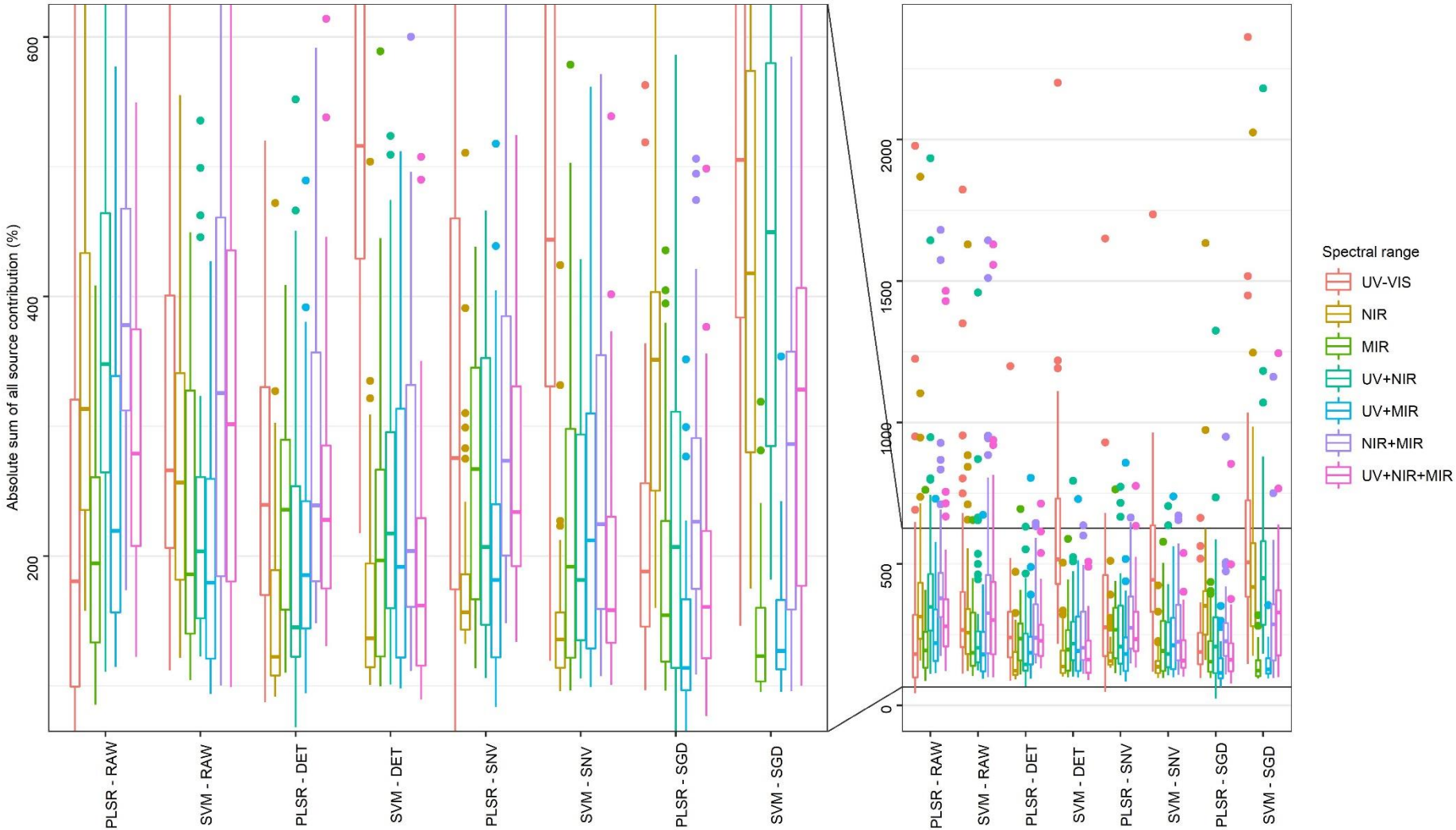

Figure A 4. Absolute sum of source contributions for each individual sample for the approach with four sources.

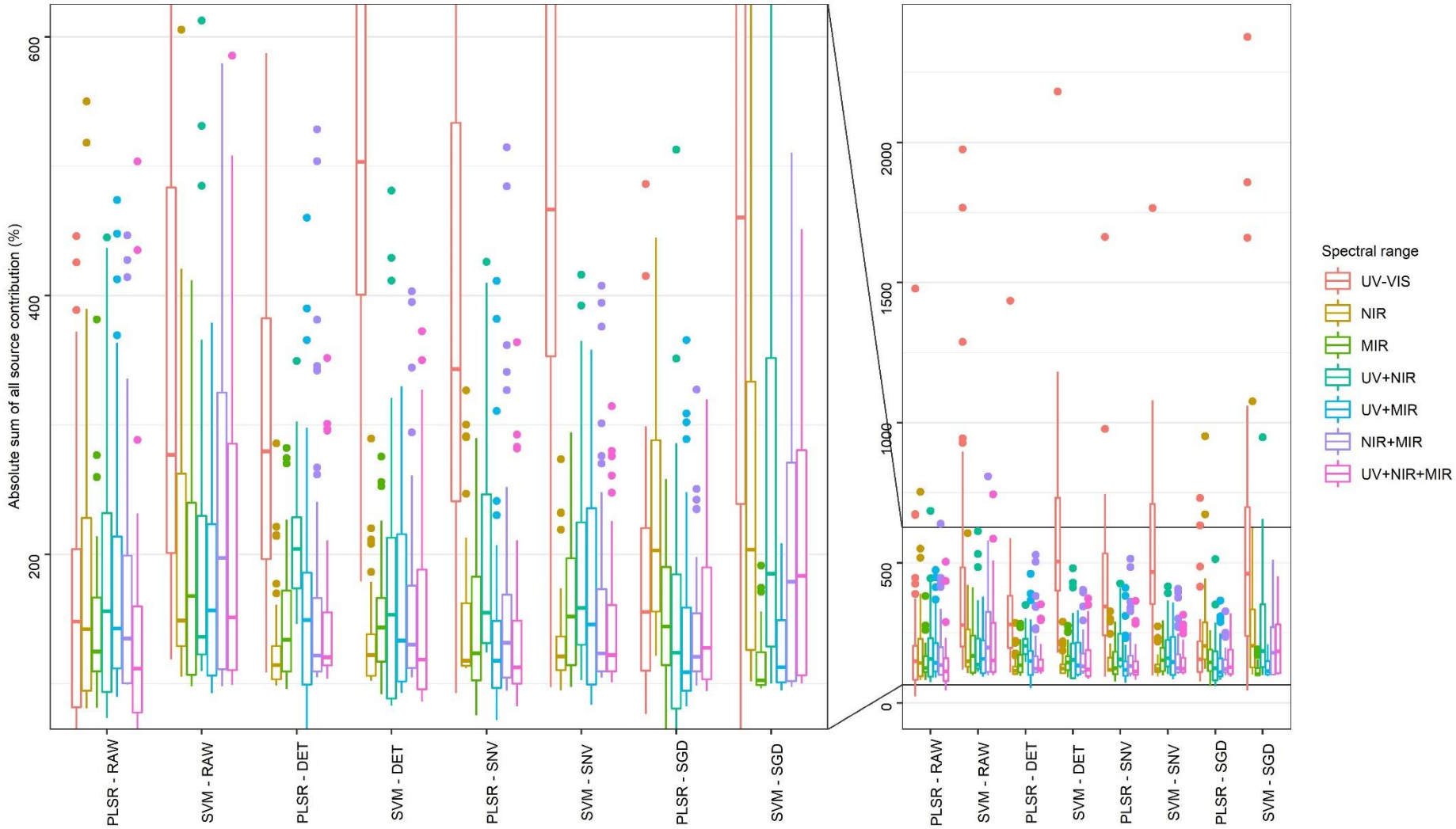

Figure A 5. Absolute sum of source contributions for each individual sample for the approach with three sources.

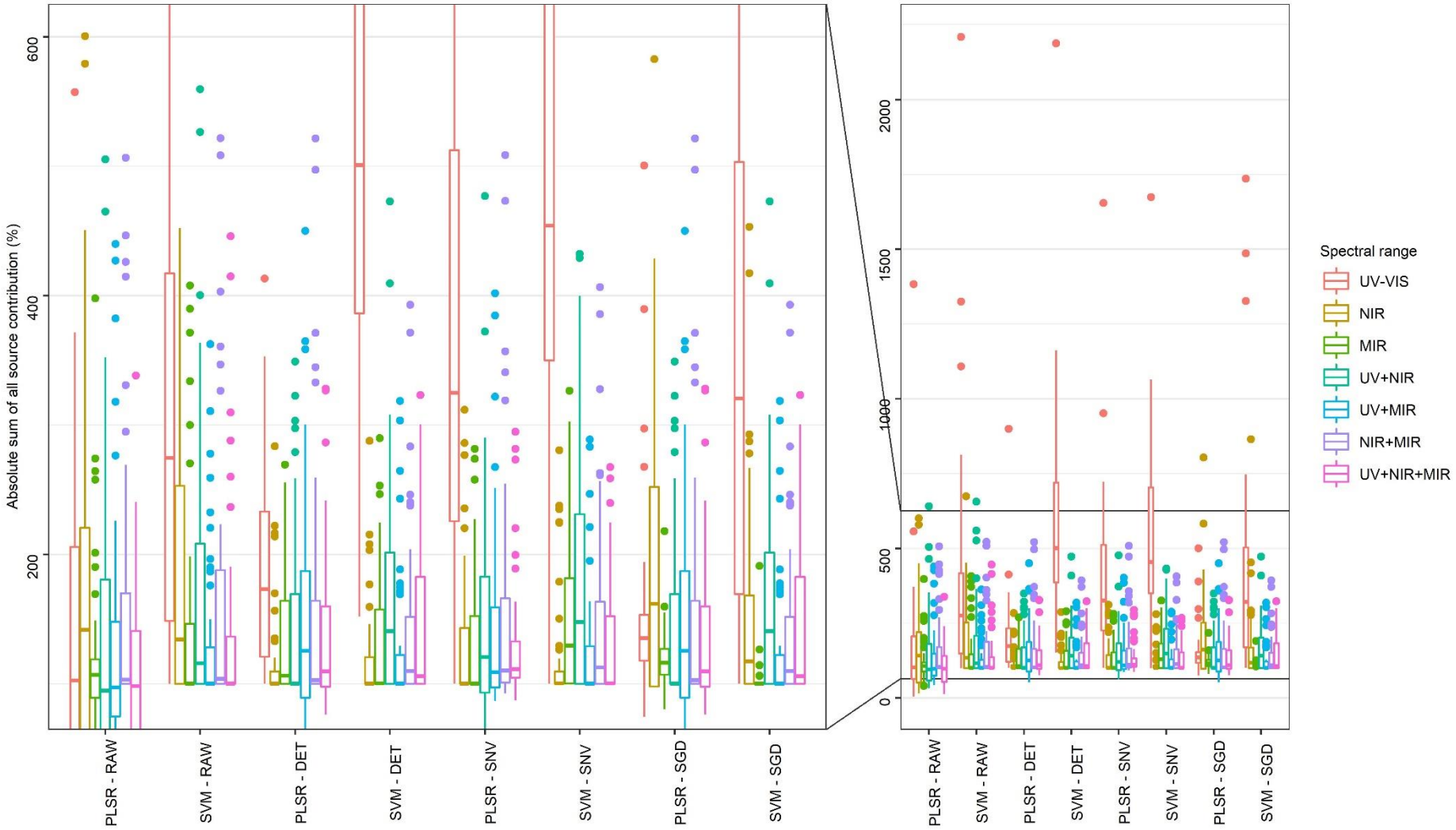

Figure A 6. Absolute sum of source contributions for each individual sample for the approach with two sources.

9 Chapter 4. The conversion of native grassland into cropland in the Pampa biome (Southern Brazil) is increasing suspended sediment supply to river systems

9.1 Introduction

The Pampa biome (Subtropical Grasslands, Savannas and Shrublands) in southern Brazil is a very rich environment in terms of biodiversity. With an area of approximately 178,800 km^2 (2.1% of the Brazilian territory) (Figure 9.1), it is predominantly covered with grassland vegetation (the *Campos Sulinos*), which have often been neglected until recent years in terms of conservation when compared to other biomes in Brazil (Overbeck et al., 2007). The Pampa region is a natural fragile biome, where the climate conditions, with abundant and intense rainfall, occurring on undulated landscapes occupied by soils with low resistance to water and wind erosion (sandy and shallow soils), make the region particularly vulnerable to degradation (Roesch et al., 2009). The profit increases of other agricultural activities during the last twenty years, mainly for soybean production, have economically motivated farmers to convert native grasslands of the Pampa Biome into cropland (Oliveira et al., 2017).

In the state of Rio Grande do Sul, Southern Brazil, the land area under cropland in the Pampa biome has increased by 57%, from 2,691 km^2 under cropland in the summer of 2000/2001 to 4,226 km^2 in the summer of 2014/2015 (Silveira et al., 2017), representing 1.5 and 2.4% of the Brazilian Pampa biome territory respectively (according to the Brazilian Institute of Geography and Statistics - IBGE database). Modernel et al. (2016) observed similar trends in the Pampa region of Argentina and Uruguay, where the conversion of grassland into cropland or degradation by overgrazing increased following the increase in the agricultural commodity prices. As a consequence, the conversion of natural grassland into cropland may increase the soil degradation and threaten the ecosystem services provisions of the Pampa biome. According to a more recent analysis by MAPBIOMAS (2019) derived from satellite images (Supplementary material), the increase in cropland and pasture areas is closely related to the reduction of native grassland.

Figure 9.1. Biomes of Southern Brazil region and the location of the Ibirapuitã River catchment and Uruguay River basin. (Source: ESRI, 2012).

The conversion of natural areas into cropland without adequate land management, can intensify soil erosion processes and consequently increase the sediment delivery to the river systems (Didoné et al., 2015b; Roesch et al., 2009). Accordingly, estimating sediment source contribution is necessary in order to estimate the respective soil degradation and erosion status under different land uses. The sediment fingerprinting technique has been widely used in order to quantify the contribution of sediment sources, providing important information about the areas which require more attention for soil erosion control (Nosrati, 2017; Walling, 2013). This technique can be used with a wide variety of tracers which should have the capacity to discriminate between potential sediment sources in the catchment of interest (Guzmán et al., 2013).

The soils under native grassland in the Pampa biome are naturally rich in soil organic matter and they have a high potential to store carbon. However, this ecosystem shows a large and rapid loss of soil organic carbon when converted into cropland (Pillar et al., 2012). The acceleration of soil degradation under cropland in the Pampa Biome may change the soil organic matter (SOM) composition signature. Growing crops in these soils is expected to increase SOM mineralization and consequently reduce TOC and TN contents compared to soils under natural grassland (JURACEK and ZIEGLER, 2009). Opposite tendencies may be observed for N isotope ratios ($\delta^{15}N$), where the increased N mineralization by soil cultivation and the N enrichment by fertilizer inputs or biological fixation by legumes (soybean mainly), may increase the proportion of the heavy isotope ^{15}N (Amundson et al., 2003). At the same time, the cultivation of C3 plants (soybean and rice) at the expense of natural grassland predominantly composed of C4 plants, may change their C stable isotope ratio ($\delta^{13}C$) signature, providing a potential tracer of the origin of sediment (Stevenson et al., 2005). Therefore, besides being a potential tracer to discriminate between surface and subsurface sources, parameters related to SOM can contribute to discriminate areas under degradation from those that are well-managed, since this variability is directly linked to land use and management (Fox and Papanicolaou, 2007).

The combination of different types of tracers is recommended to improve discrimination between potential sources (Uber et al., 2019). Tracers that already proved as very effective such as fallout radionuclides (^{137}Cs or $^{210}Pb_{xs}$), have high potential to discriminate surface from subsurface sources, where their activities are usually higher in the topsoil (Evrard et al., 2020). However, their application is limited by their costs and the availability of analytical facilities, the relatively high sample mass needed (min. several grams), as well as their limited potential to discriminate between more than two sources. The use of alternative tracers, based on non-destructive, low-cost and rapid analyses, can provide useful information to combine with radionuclides, geochemical or organic composition tracers, improving the discrimination power (Martínez-Carreras et al., 2010a, 2010c). For instance, colour properties have already been used as alternative tracer in multiple study sites and catchment scales (Evrard et al., 2019a; Martínez-Carreras et al., 2010a; Pulley et al., 2018; Ramon et al., 2020; Sellier et al., 2020b). Thus, the objective of this study is to calculate the sediment source contributions, combining organic matter composition, radionuclide and low-cost alternative parameters derived

from UV spectra to evaluate the impact of land use change on soil degradation and sediment delivery to the river systems, in a catchment representative of the Pampa biome in Southern Brazil.

9.2 Methodology

9.2.1 Study site

The Ibirapuitã River catchment is located in the extreme south of Brazil and is representative of the southern grassland region, typical of the Pampa biome. The main outlet of the catchment considered in this study is located next to monitoring point number 76750000 of the Brazilian National Water Agency (ANA, 28°27'22" S, 53°58'24" O) in the county of Alegrete (Figure 9.2), covering a surface area of approximately 5,943 km^2. The altitude ranges between 80 and 370 m a.s.l., and areas >280 meters are located in the headwaters of the catchment, near the border between Brazil and Uruguay and represent less than 15% of the catchment surface. Approximately 90% of the catchment area is characterised by slopes lower than 15%, and slopes decrease in the northern direction, varying from 2 to 5% in the lower Ibirapuitã region. Land use is predominantly native grassland with extensive livestock activity (81%) (Figure 9.3), although as in the whole Pampa region, it tends to be increasingly occupied by soybean cultivation areas.

This study is conducted in three Ibirapuitã River sub-catchments (Figure 9.3). The (i) Ibirapuitã – environmental protection area (EPA) subcatchment, which is an area controlled by the Chico Mendes Institution of Biodiversity Conservation (ICMBio) from the Brazilian National Ministry of the Environment, where native grassland (85%) and natural forests (10%) dominate. Located in the central portion of the Ibirapuitã River catchment, the EPA subcatchment covers an area of 3,196 km^2, where the main soil types are Regosols in the upper half and Acrisols in the lower half, from basalts of the Serra Geral formation (Fácies Alegrete) and sandstones/silts of the Botucatu formation (Fácies Gramado, Caxias and Guará), respectively.

The (ii) Pai-Passo Stream subcatchment (PP) covers a surface area of approximately 1,043 km^2, and it is mainly occupied by native grassland (83%) with extensive livestock on shallow Regosols developed on basalt (Fácies Alegrete), and paddy fields for irrigated rice production (10%) located in the lower and flatter portions of the landscape, where Planosols and Vertisols occur.

The (iii) Caverá Stream subcatchment (CAV) covers approximately 1,455 km^2, and it is the sub-catchment with the higher percentage of cropland with rice and soybean production in the summer and pastures in the winter (15%), as the native grassland (73%) have been converted into cropland on deeper soils, predominantly Acrisols developed on sandstones of the Botucatu formation. In Figure 9.3 and Figure 9.4, the land use, geology and soil classes, of all subcatchments are presented.

In both catchments, features of the landscape such as the ramp length, undulated relief associated to sandy surface soil layers, causes large volumes of runoff concentrated in the hillside causing the formation of gullies. Besides that, the absence of riparian zones and preferential paths caused by animal's circulation close to water bodies, favours the occurrence of stream channel erosion. These erosion processes are widely observed in the catchment, and with less extent, erosion was also observed with unpaved roads during field campaigns.

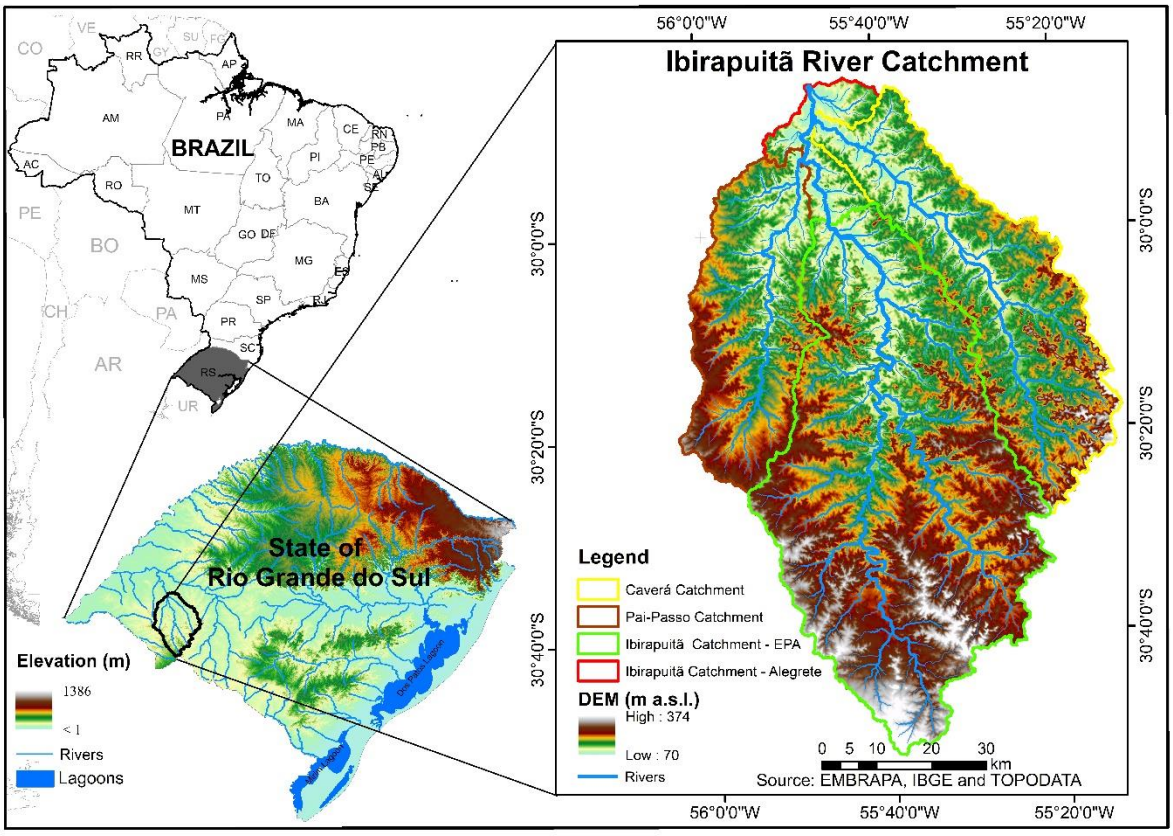

Figure 9.2. Study site location and digital elevation model (DEM).

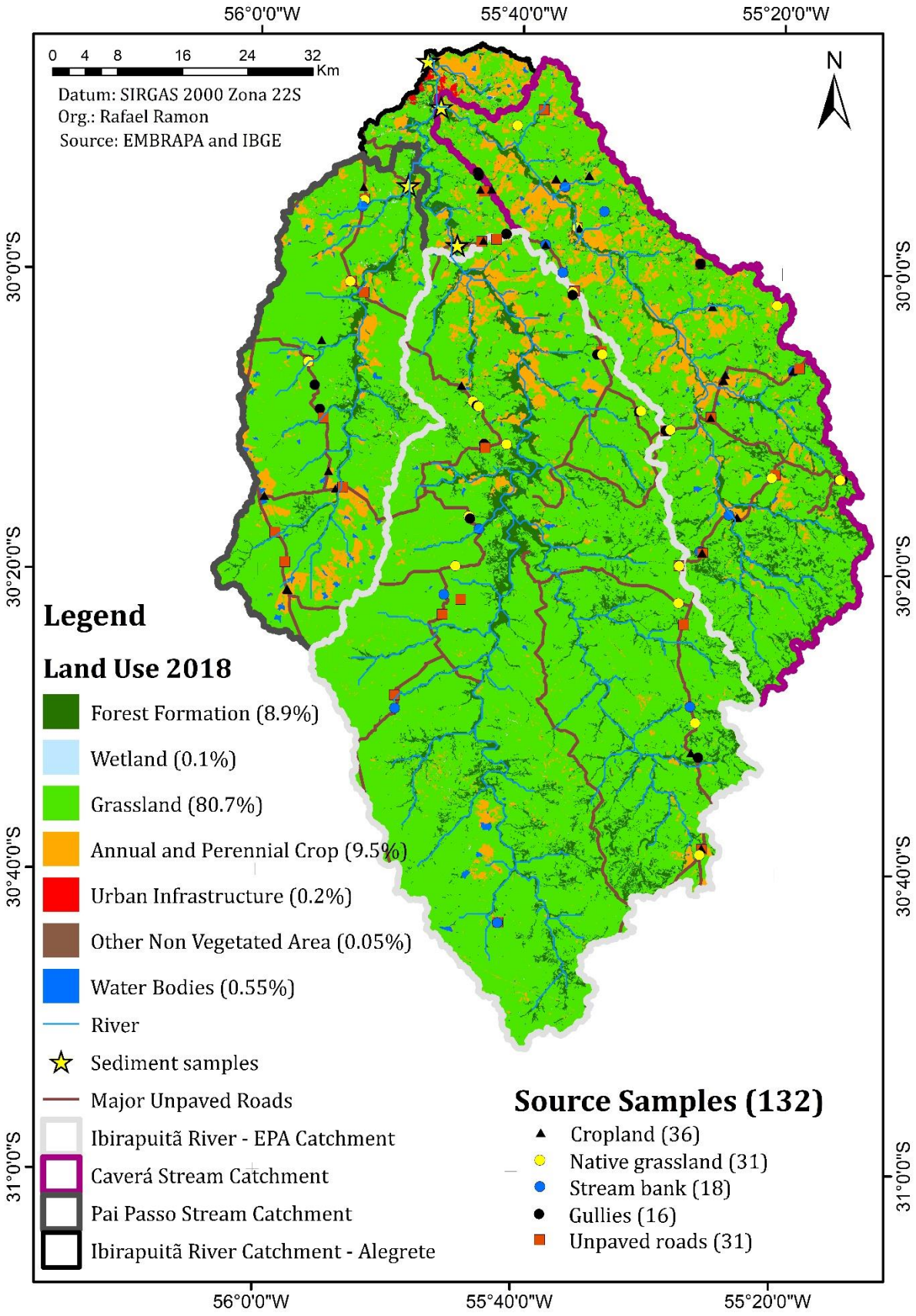

Figure 9.3. Land use and source samples in the Ibirapuitã River catchment.

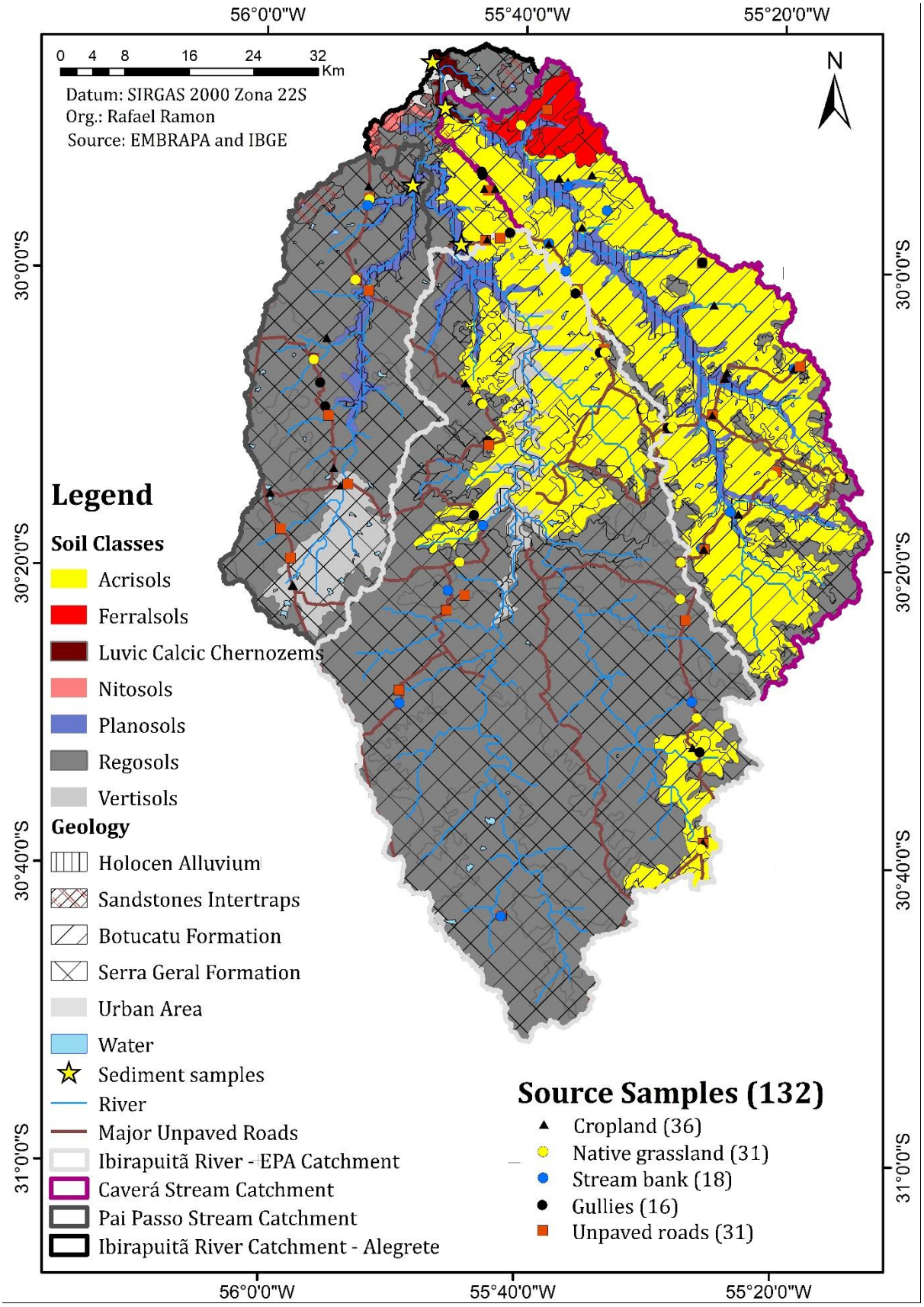

Figure 9.4. Soil types, geology, source and sediment sampling points in the Ibirapuitã River catchment.

9.2.2 Sediment source sampling

To characterize the potential sources, soil composite samples (n=132) were taken in representative areas, including cropland (n=36), native grassland (n=31), unpaved road (n=31), and subsurface sources composed of channel banks (n=18) and gully (n=16) samples (Figure 9.3). In the surface sources (cropland and native grassland), soil from the upper 0-2 cm layer was collected, as this layer is the most likely to be eroded and transported to the waterways. As for the subsurface sources (gully and channel bank) and unpaved roads, samples were collected along the exposed face of the stream channel banks and roads at sites exposed to erosion. For each composite source sample, around 10 sub-samples were collected within a radius of approximately 50 meters, mixed in a bucket and approximately 500 grams of material were stored. Care was taken to avoid sites that have accumulated sediment originating from other sources, to prevent the collection of transient material. The source sampling sites were selected in order to cover all the soil types and the variability in slope positions, as well as the three main tributary catchments.

9.2.3 Sediment sampling

Suspended sediment samples were collected at the Ibirapuitã catchment outlet and at the confluence with its tributaries following two strategies. The first sampling strategy was the deployment of time integrating sediment samplers (TISS) (Figure 9.3). The sampler designed by Phillips et al. (2000) consists in a plastic tube of 75 mm of diameter and 80 cm length, which has a small inlet and outlet tubes (4 mm of diameter) in the extreme edges, which allows the suspended sediment to enter, reducing the flow velocity and allowing the sediment to deposit inside the tube based on the principle of sedimentation. The equipment is submerged for a certain period of time in order to integrate the sediment from different rainfall events, in which the eroded material of the catchment is mobilized under different conditions of transport and energy, and consequently consists of varied physical, chemical and mineralogical characteristics. The sampling interval was not based on a fixed schedule, sampling was performed after a minimum interval of three months and when the river was at a sufficiently low level to have a safe access to the samplers. Finally, the second strategy was to collect samples of lag deposits after a flooding event as the river discharge exceeded its channel's volume causing the river overflow.

9.2.4 Source and sediment analysis

Samples were oven-dried (50° C), gently disaggregated using a pestle and mortar and dry-sieved to 63 μm to avoid particle size effects prior to further analysis (Koiter et al., 2013b; Laceby et al., 2017). Particle size analyses were carried out on the sediment samples with a LS 13 320 laser diffraction particle size analyser (Beckman Coulter) with a Universal Liquid Module after sieving to 2000 μm. Samples were inserted in the liquid module, sonicated while loading until obtaining 8% of obscuration, sonicated for 7 min before, and 5 min while reading, with 73 W.

9.2.4.1 Total organic matter composition

After sieving, the samples were hand-ground with a pestle and mortar to obtain a fine and homogeneous powder. Samples were weighted in tin capsules and a tyrosine laboratory standard was inserted after each four soil or sediment samples to calibrate the measurements (Coplen et al., 1983). Total organic carbon (TOC), total nitrogen (TN), $\delta^{13}C$ and $\delta^{15}N$ isotope ratios were measured using continuous flow isotope ratio mass spectrometry (EA-IRMS). When TN contents were too low, a second run was performed in order to optimize the sample weight for $\delta^{15}N$ measurements. Due to the nature of the soil parental material found in the Ibirapuitã catchment (i.e. clayey and siliceous nature), no carbonate removal was required. A selection of samples was analyzed by X-Ray diffraction, and no carbonated minerals (calcite and dolomite) were found (Brindley and Brown, 1980).

9.2.4.2 Ultra-violet-visible derived parameters

Thirty parameters were derived from the ultra-violet-visible (UV) diffuse reflectance spectra range (200 to 800 nm, with 1 nm step), measured for each powder sample using a Cary 5000 UV-NIR spectrophotometer (Varian, Palo Alto, CA, USA) at room temperature, using $BaSO_4$ as a 100% reflectance standard. Samples were added into the sample port and care was taken to avoid differences in sample packing and surface smoothness. Twenty-two colour parameters were derived from the UV spectra following the colorimetric models described in details by Viscarra Rossel et al. (2006), which are based on the Munsell HVC, RGB, the decorrelation of RGB data, CIELAB and CIELUV Cartesian coordinate systems, three derived from the Hunterlab colour space model (HunterLab, 2015) and two colour indices (Pulley et al., 2018). Finally, 27 colour metric parameters were derived from the spectra of source and sediment samples and used as

potential tracers (L, L*, a, a*, b, b*, C*, h, RI, x, y, z, u*, v*, u', v', Hvc, hVc, hvC, R, G, B, HRGB, IRGB, SRGB, CI and SI). Three additional parameters were calculated from the second derivative curves of remission functions in the visible range of soil and sediment samples, which displayed three major absorption bands at short wavelengths commonly assigned to Fe-oxides (Caner et al., 2011; Fritsch et al., 2005). The first band (A1) corresponds to the single electron transition of goethite (Gt), whereas the two others correspond to the electron pair transition for goethite (A2) and for hematite (Hm) (A3). More details about the calculation of UV derived parameters can be found in Ramon et al. (2020).

9.2.4.3 Fallout radionuclides analysis

Fallout radionuclide activities (^{137}Cs and ^{210}Pb) were measured by gamma spectrometry using low-background high-purity germanium detectors (Canberra/Ortec). Between 10 to 20 grams of samples were weighted into polyethylene containers and sealed airtight and analysed on a detector installed in a lead-protected shield. Measurements were conducted between $80x10^5$ – $130x10^5$ s to optimise counting statistics. The fallout radionuclides ^{210}Pb and ^{137}Cs were obtained from the counts at 46.5 keV and 661.6 keV, respectively. The unsupported or excess lead-210 ($^{210}Pb_{xs}$) was calculated by subtracting the supported activity from the total ^{210}Pb activity using two ^{238}U daughters, i.e. ^{214}Pb (average count at 295.2 and 351.9 keV) and ^{214}Bi (609.3 keV). Radionuclide activities were decay-corrected to the sampling date. For samples with lower ^{137}Cs activities than the detection limits, the half of the detection limit reached for these samples was used instead.

9.2.4.4 Sediment source discrimination and apportionment

Due to the large variability of some parameters within the same source group, samples that presented values for more than three parameters outside of the range defined by the mean ±2 standard deviations of the respective parameter were considered as outliers and removed (Pulley et al., 2020). After this first step, the selection of the discriminant tracers followed the classical three-step procedure: i) a range test; ii) the Kruskal-Wallis *H* test (KW *H* test); and iii) a linear discriminant function analysis (LDA). For passing the range test, mean parameters values for sediment must fall within the range between the maximum and minimum values observed for the sources. The KW *H* test was then performed to test the null hypothesis ($p < 0.05$) that the sources belong to the same population. The variables that provided significant discrimination between sources were analysed with a forward stepwise LDA ($p < 0.1$) in order to reduce the

number of variables to a minimum that maximizes source discrimination (Collins et al., 2010b). The statistical analyses were performed with R software (R Development Core Team, 2017) and more details on the procedure can be found in Batista et al. (2018).

The source contributions were estimated by minimizing the sum of squared residuals (SSR) of the following mass balance un-mixing model:

$$SSR = \sum_{i=1}^{n}\left(\left(C_i - \left(\sum_{s=1}^{m} P_s S_{si}\right)\right)/C_i\right)^2 \quad (3)$$

where n is the number of variables/elements used for modelling, C_i is the value of the parameter i in the target sediment, m is the number of sources, P_s is the optimized relative contribution of source s by SSR minimizing function, and S_{si} is the concentration of element i in the source s. Optimization constraints were set to ensure that source contributions were non-negative and that their sum equalled 1. The un-mixing model was solved by a Monte Carlo simulation with 2500 iterations. More information about model settings and compilation can be found in Batista et al. (2018). Model uncertainties were evaluated based on the interquartile variation range of the predictions from the multiple iterations of Monte Carlo simulation. The median and interquartile range is presented as the source contribution for each of the target sediment samples modelled.

9.3 Results

9.3.1 Monitoring results and suspended sediment characteristics

Discharge and precipitation data measured during the suspended sediment sampling period is presented in Figure 9.5. Rainfall was overall well distributed throughout the year, with the occurrence of a large rainfall event in January, 2019, which resulted in the biggest flood event of the last 60 years according to the national agency records (ANA, 2020). Three sediment samples were collected at the outlet of the Ibirapuitã catchment, two from TISS (TISS.Out 1 and 2), and one from lag deposits (LD.Out). TISS samples were collected in the tributaries as well, two in the Pai-Passo (TISS.PP 1 and 2), two in the Ibirapuitã-EPA (TISS.EPA 1 and 2) and one in the Caverá catchment outlet (TISS.Cav). Some TISS samples were lost because the samplers were either flushed away by the flood or likely removed by local people. For the sediment samples collected at the main outlet, the first TISS sample covers the winter and early spring periods (from May 25 to October 26, 2018). The second TISS sample covers the spring and summer period (from October 26, 2018 to February 19, 2019), which coincide with the summer crop cultivation (Figure 9.5). Two samples from lag deposits were collected, one of them close to the main outlet (LD.Out) and one close to the EPA catchment outlet (LD.EPA), after the main event that occurred in January, 2019. Care was taken to collect only surface sediments deposited in the floodplains to avoid the sampling of local material.

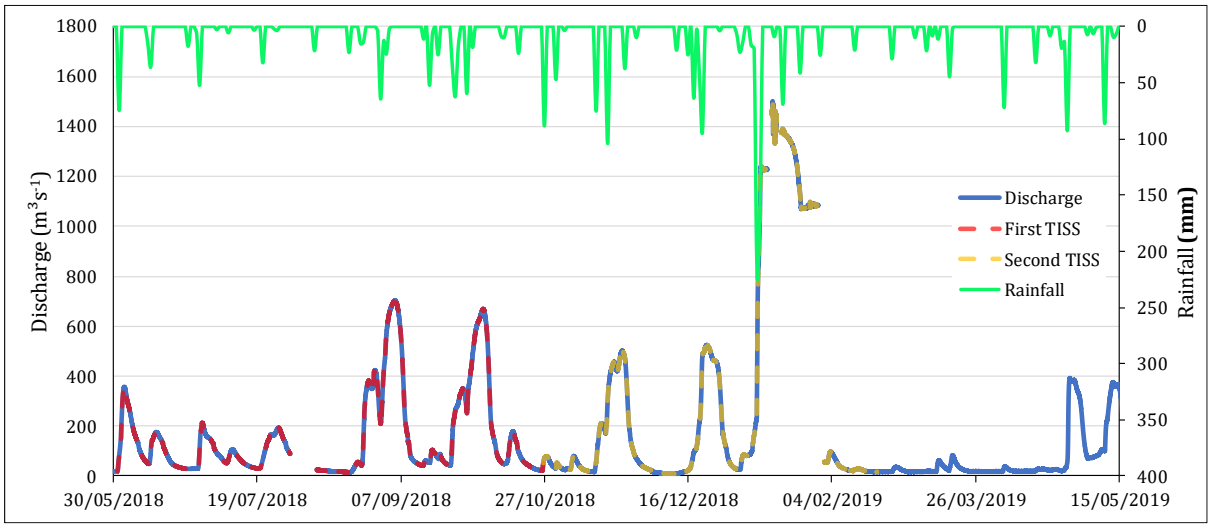

Figure 9.5. Hydrograph and hyetograph during the monitoring period. The background images represent the time integrate sediment sampler on the left, and the deposited sediments after the main event occurred in January of 2019 on the right side.

According to the particle size analyses of suspended sediment samples, more than 80% of the sample volume is composed of particles smaller than 63 μm (Figure 9.6). LD and TISS samples were passed through a 2000 μm mesh sieve to remove the coarsest particles, but all material passed through. In this first sediment fingerprinting approach, the fraction < 63 μm is representative for the suspended sediment samples collected. However, the widespread occurrence of sandy soils in the catchment may result in a high input of coarse sediments in the river system. Due to monitoring difficulties, it was not possible to quantify the bedload sediments, but future studies should consider quantifying this coarser fraction that may be significant in the Ibirapuitã catchment.

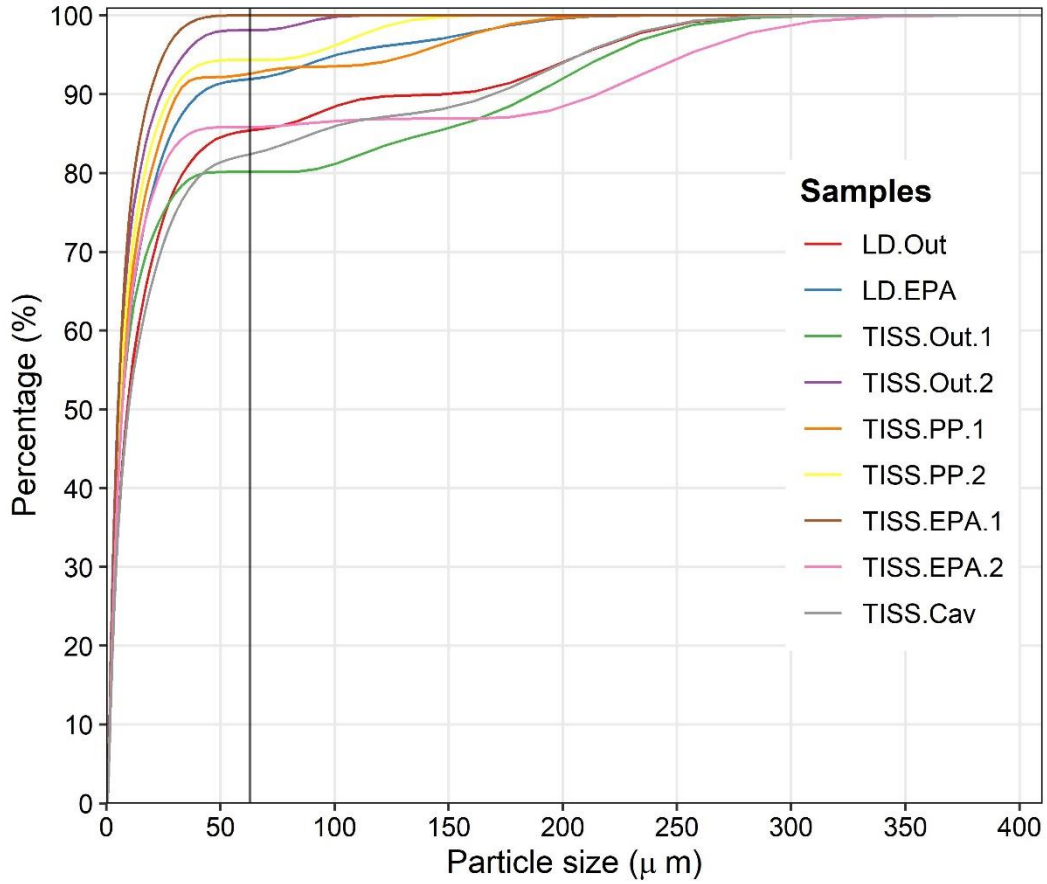

Figure 9.6. Particle size distribution of sediment samples (LD = lag deposit sample; TISS = time integrated suspended sediment sample, Out = main outlet, PP = Pai-Passo catchment, EPA = Environmental Protection Area catchment, Cav = Caverá catchment, 1 = First TISS sampling period, 2 = Second TISS sampling period).

9.3.2 Source and sediment properties

9.3.2.1 Organic matter composition

The four parameters related to the organic matter composition showed a significant difference between at least two sources ($p < 0.05$) (Table 9.2). TOC and TN were highly correlated ($R^2 = 0.97$) with a mean C/N ratio of 10.3 and their concentration in the sources and sediments showed similar patterns. Mean TOC and TN contents were higher in the native grasslands compared to other sources. However, they showed a large SD (46.2 ±16.1 g kg^{-1} and 4.5 ±1.5 g kg^{-1}, respectively) (Figure 9.7). Unpaved roads and subsurface sources had much lower TOC (5.0 ± 1.9 g kg^{-1} and 14.5 ± 7.6 g kg^{-1}, respectively) and TN contents (0.6 ± 0.3 g kg^{-1} and 1.3 ± 0.6 g kg^{-1}, respectively), with lower SDs. Cropland had lower TOC and TN concentrations (32.7 g kg^{-1} and 3.3 g kg^{-1}, respectively) than native grassland, with values closer to those observed in sediment samples (23.5 ± 4.5 g kg^{-1} and 2.2 ± 0.5 g kg^{-1}, respectively).

For sediment fingerprinting, TOC and TN can provide a good discrimination between surface (cropland and native grassland) and subsurface (unpaved road, erosion channel and channel bank) sources (Figure 9.7). Furthermore, the mean percentage of TOC and TN in native grassland is higher than under cropland, and this difference can be useful to quantify the contribution of cropland areas to the sediment collected in the river (Table 9.2). TOC and TN concentration in sediment samples fall within the range of values found in potential sources, taking into account one of the principles of sediment fingerprinting, according to which the potential tracers must be conservative.

The $\delta^{13}C$ and $\delta^{15}N$ values showed contrasting signatures between potential sediment sources, mainly between subsurface sources and cropland. Cropland shown more negative $\delta^{13}C$ mean values with high SD (-19.0 ± 2.0 ‰), while subsurface source shown the less negative mean (-17.2 ± 2.3 ‰) (Table 9.2). The $\delta^{15}N$ presented higher mean values in cropland (8.1 ± 1.0 ‰) and lower values in the native grassland source (7.1 ± 1.3 ‰), while unpaved road and subsurface sources showed intermediate values (7.9 ± 0.9 ‰ and 7.4 ± 0.9 ‰, respectively). For 27 samples including five sediment samples, $\delta^{15}N$ concentration was below the detection limits. Because of the limited data of $\delta^{15}N$ for sediment samples and the deviation of $\delta^{13}C$ values in relation to the sources (Figure 9.7), the isotopes were not included in the sediment fingerprinting approach as potential tracers.

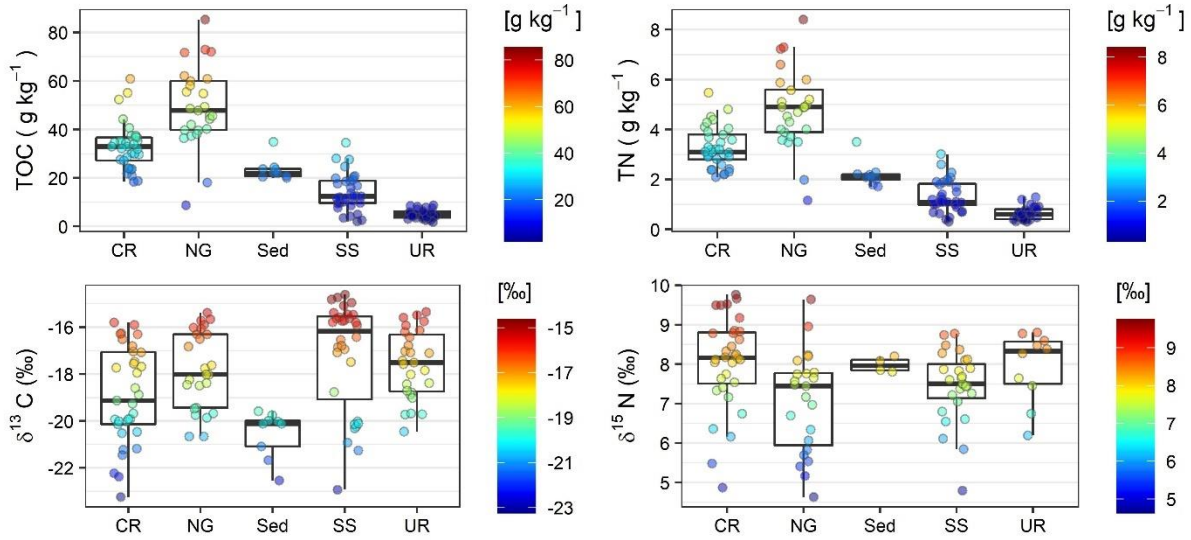

Figure 9.7. Parameters of the organic matter composition and their concentration in in potential sources and sediment samples. (Cropland – CR; Native Grassland – NG; Sediment samples – Sed; Subsurface sources – SS; and Unpaved roads – UR; Total Organic Carbon – TOC; Total Nitrogen – TN).

9.3.2.2 Fallout radionuclide activities

Fallout radionuclides activity was sufficiently higher to be quantified in all the analysed samples. For both, ^{137}Cs and $^{210}Pb_{xs}$, the mean activity was higher in the native grasslands (3.4 ± 1.6 Bq kg^{-1} and 197.7 ± 101.3 Bq kg^{-1}, respectively) than in croplands (2.7 ± 1.2 Bq kg^{-1} and 136.7 ± 63.5 Bq kg^{-1}, respectively) (Figure 9.8). However, the variability within each superficial source was very high, compared to the more uniform results observed in subsurface sources.

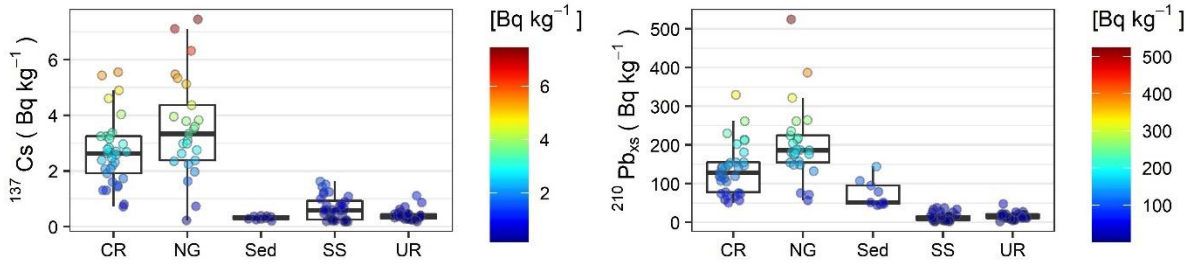

Figure 9.8. Fallout radionuclide activities in potential sources and sediment samples. (Cropland – CR; Native Grassland – NG; Sediment samples – Sed; Subsurface sources – SS; and Unpaved roads – UR).

9.3.2.3 UV derived parameters

Ultra-violet-visible derived parameters showed a large variation within sources, while sediment samples values remained very homogeneous (Figure 9.9). Although many parameters could be extracted from these analyses, only a couple of them turns out to be useful to characterize different sources. Most of the UV derived parameters are highly correlated with each other and are grouped in the same cluster, explaining the same variance observed between groups (Figure 9.10).

Parameters related to the iron oxides, such as A1, A2 and A3, showed no significant differences between surface sources. These tracers are more related to parental material, soil types and genesis. Consequently, values differ mainly between surface and subsurface sources, as it can be observed for A1, with mean values of 0.0008465 and 0.001188, respectively (Figure 9.9). Colour parameters such as chroma and value are influenced by the carbon content and land use type (Wills et al., 2007). Luminosity index (L*), which is related to the dark or light colour of the soil (Hunter Laboratories, 1996), have lower values for native grassland (48.6 ± 5.8) in relation to cropland (52.3 ± 3.2) (where a low number (0-50) indicates dark and a high number (50-100) indicates light). This difference may be attributed to the difference in TOC, that is one of the main responsible for changing soil colours (Viscarra Rossel et al., 2006a). By contrast, RI have

values almost twice higher in the native grassland (0.81 ± 0.6) than in the other three sources (mean of 0.47), and it is one of the parameters that presents the lowest correlation with the other parameters evaluated (Figure 9.10). Significant difference is observed between subsurface source and unpaved road for the hue (h) value of CIE and chroma (hvC) of Munsell chart. Lower chroma values decrease when soil is saturated and chemically reduced, and this lower values can be observed for subsurface sources (gully and channel bank) (Sánchez-Marañón, 2011).

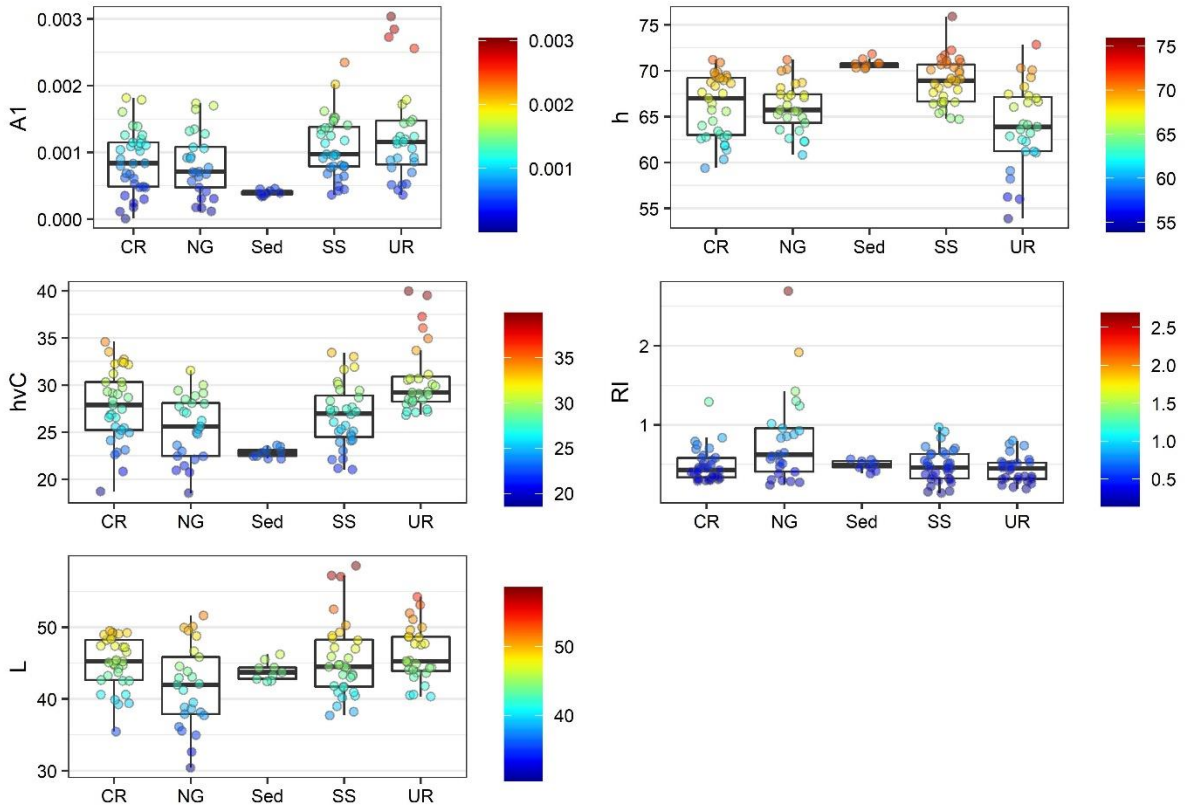

Figure 9.9. Boxplots of UV derived parameters in potential sources and sediment samples. (Cropland – CR; Native Grassland – NG; Sediment samples – Sed; Subsurface sources – SS; and Unpaved roads – UR). This figure only contains five UV derived parameters selected by the LDA from a total of 30 parameters measured.

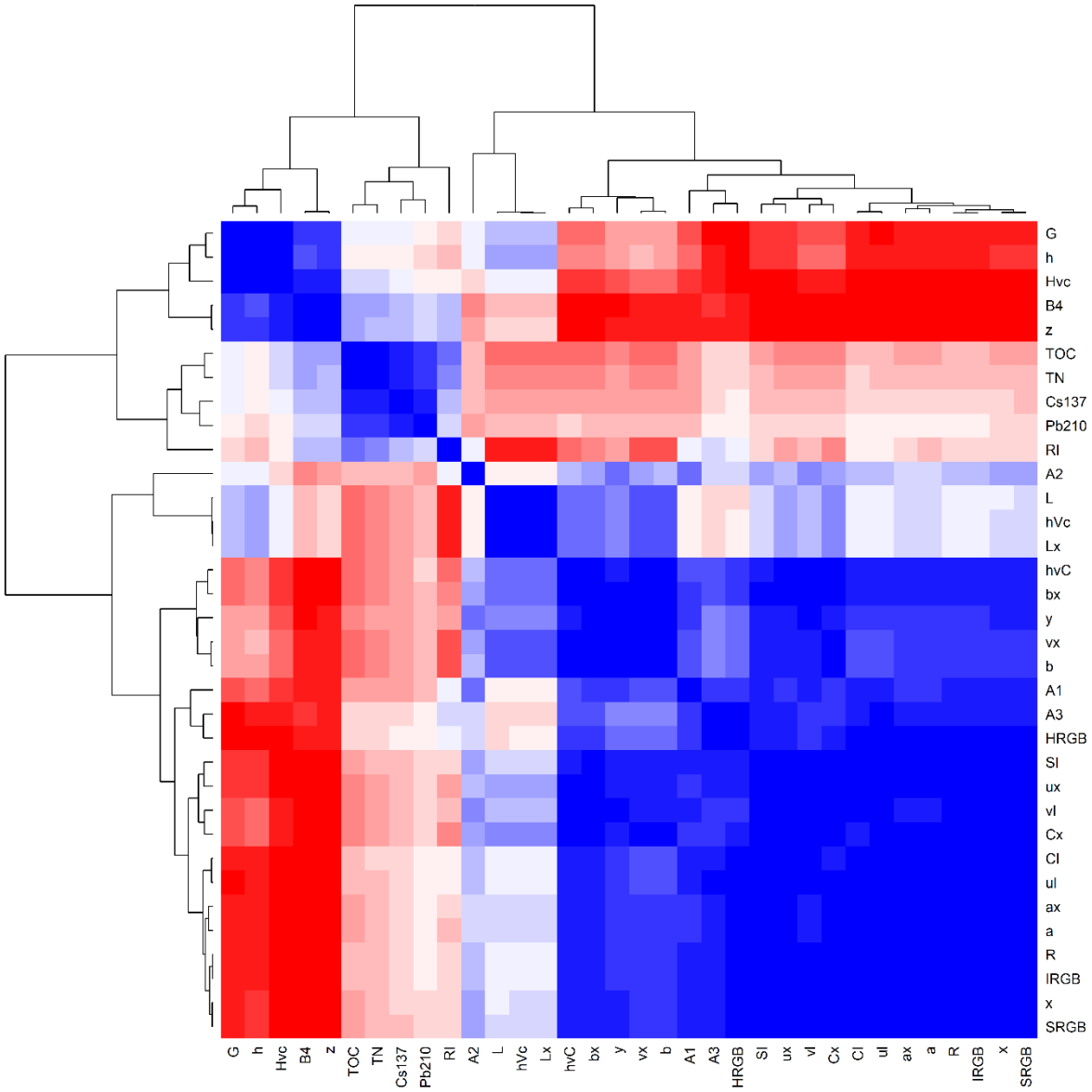

Figure 9.10. Heat map and dendrogram of the variables ordered according to the hierarchical clustering. The representation of the symbols " * " and " ' " used to differentiate the colour parameters, are replaced by the letters "x" and "l" in the figure.

9.3.3 Selection of sediment tracers

In the first step of the data analysis, 15 source samples were removed because more than three parameters fell outside of the range based on the mean of the respective group more or less two standard deviations (SD). Accordingly, only 117 source samples were kept for subsequent analyses. For this study, $\delta^{15}N$ was not used as a tracer, because in some source (n=22) and sediment (n=5) samples, the concentration was below the detection limits, although exhibiting a conservative behaviour and a potential discrimination power between sources. From the 34 parameters considered as potential

tracers, only 14 were conservative, with the sediment values lying between the mean of the sources more or less one SD. According to the KW *H* test, all parameters hold potential to discriminate between at least two sources, allowing all 14 conservative parameters to enter in the LDA.

From the 14 parameters, seven were selected by LDA as the best set of tracers (Table 9.1). TN, h, $^{210}Pb_{xs}$, A1, hvC, RI and L were able to explain 91.1% of the variance between source samples (Table 9.1). The LDA bi-plots presented on Figure 9.11 demonstrate the source reclassification using the best set of tracers from the statistical analysis. Difference between surface and subsurface sources was very clear. The mean Square Mahalanobis distance between surface and subsurface source was 18.5; 11.6 for cropland and 25.5 for native grassland (Table 9.1). The Square Mahalanobis distance between cropland and native grassland was very low, only 4.5, but it was still significant (*p<0.01*). The same was observed between subsurface sources (channel bank and gully) and unpaved roads (only 5.3, *p<0.01*). On average, 83% of the source samples were correctly classified by the LDA.

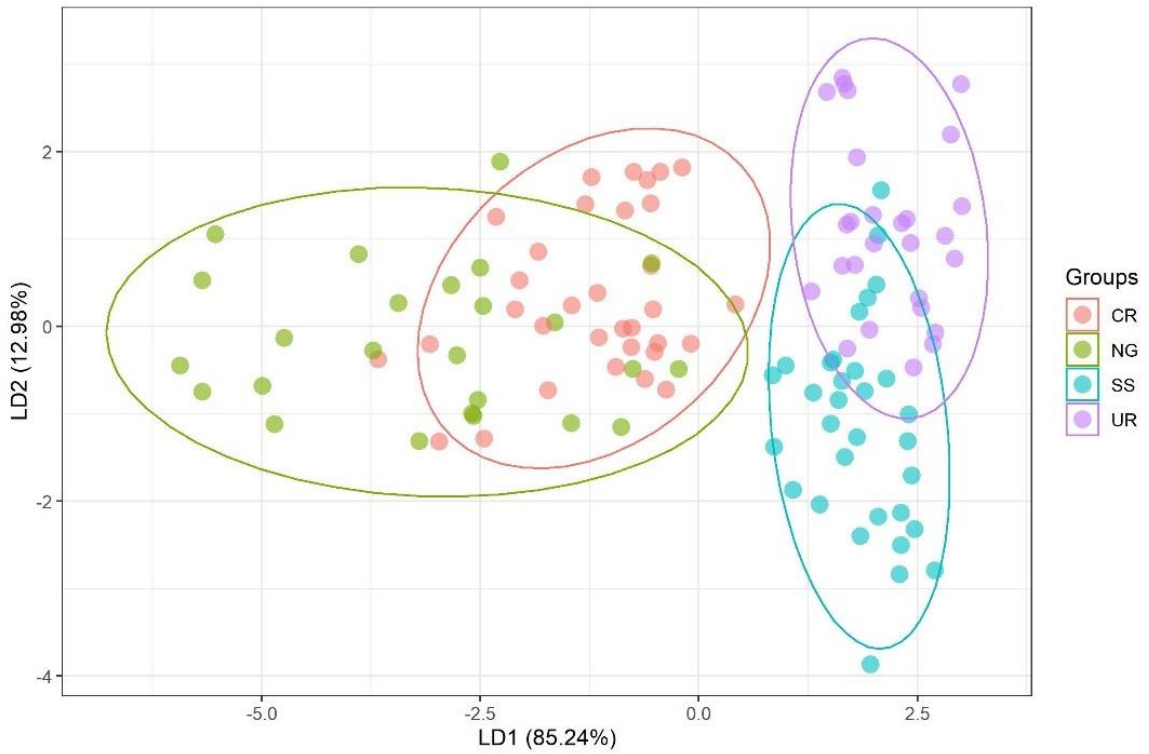

Figure 9.11. Source sample reclassification by the LDA using the selected variables. (Cropland – CR; Native Grassland – NG; Subsurface sources – SS; and Unpaved roads – UR; First linear discrimination function – LD1; second linear discrimination function – LD2).

Table 9.1. Linear discriminant analysis (LDA) parameters.

Selected Tracers	TN, h, $^{210}Pb_{xs}$, A1, hvC3, RI, L
Wilk's Lambda	0.09
Variance explained by the variables (%)	91.1
Squared Mahalanobis distances	
Cropland vs Native Grassland	4.5
Cropland vs Subsurface	11.6
Cropland vs Unpaved Road	12.5
Native Grassland vs Subsurface	25.5
Native Grassland vs Unpaved Road	29.7
Subsurface vs Unpaved Road	5.3
Average	14.8
p-levels	
Cropland vs Native Grassland	<0.001
Cropland vs Subsurface	<0.001
Cropland vs Unpaved Road	<0.001
Native Grassland vs Subsurface	<0.001
Native Grassland vs Unpaved Road	<0.001
Subsurface vs Unpaved Road	<0.001
Source samples correctly classified (%)	
Croplands	84.8
Native Grassland	76.0
Subsurface	84.4
Unpaved Road	85.2
Average	82.9
Uncertainty associated with the discrimination of the source (%)	
Cropland	24.6
Native Grassland	28.4
Subsurface	20.2
Unpaved Road	18.9
Average	23.0

9.3.4 Sediment source apportionment

During the first period of TISS sampling, the mixing model results indicate cropland as the main sediment source for all catchments. Cav and PP catchment have the higher proportion of sediment from cropland (41% and 40%, respectively) compared with the other two catchments (Figure 9.12). The Cav catchment also had the highest contribution of sediment from native grassland (32%), while in the other sites this contribution ranged between 18% and 20%. Subsurface and unpaved roads are the

source which had lower contribution for both catchments in the first period. For the Cav catchment, subsurface and unpaved roads correspond to only 27% of the total sediment supply to the river, while for the EPA, PP and Out they represent 47%, 41% and 41%, respectively (Figure 9.12).

For the second period of TISS sampling, a higher contribution from subsurface and unpaved road was observed, except in the Cav for which the sediment sample was lost. Together, subsurface and unpaved road supplied more than 60% of sediment. Native grassland contribution varied between 9% to 13%, while the mean contribution of cropland was 27% for the three catchments (EPA, PP and Out). The source contribution observed for the second TISS period is very similar to the source contribution observed for the samples of lag deposits (LD). These samples were collected just after the large rainfall event that occurred in January 2019, which could be responsible to a large extent for the sediment transport that occurred during the second period.

The median contribution of cropland and native grassland sources for the TISS samples, considering the 2500 simulations, were close to the mean values (Figure 9.13). However, for subsurface sources, the occurrence of many outliers and extreme values, makes the median differs significantly from the mean, mainly for sediment samples of the first period. The opposite situation was observed for the LD samples, where the median values of surface source contributions differs significantly from the mean, while the subsurface mean and median values were closer (Figure 9.13).

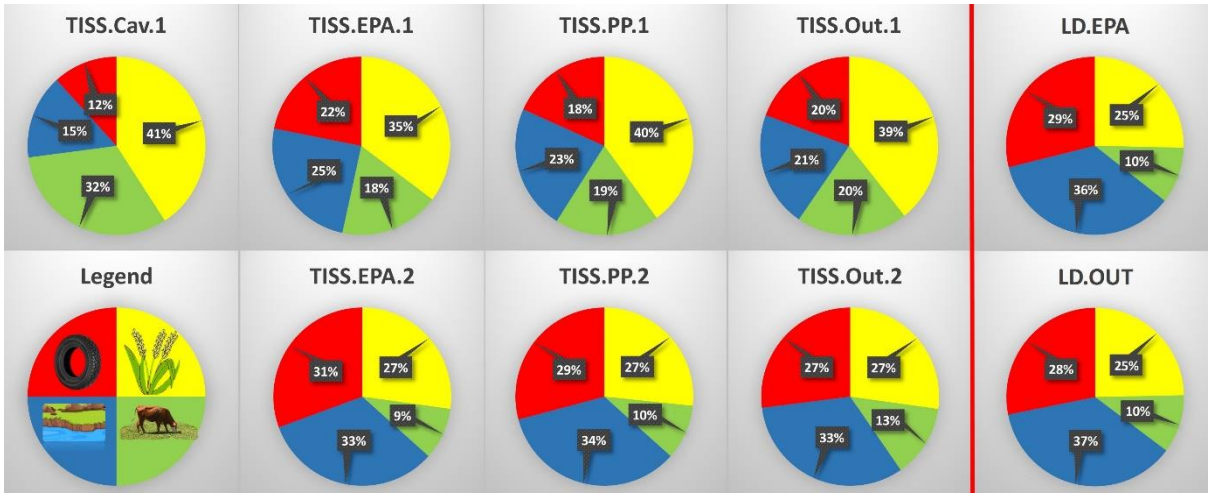

Figure 9.12. Mean sediment source contribution for the individual sediment samples. (LD = lag deposit sample; TISS = time integrated suspended sediment sample; Out = main outlet; PP = Pai-Passo catchment; EPA = Environmental Protection Area catchment; Cav = Caverá catchment; 1 = First TISS sampling period; 2 = Second TISS sampling period).

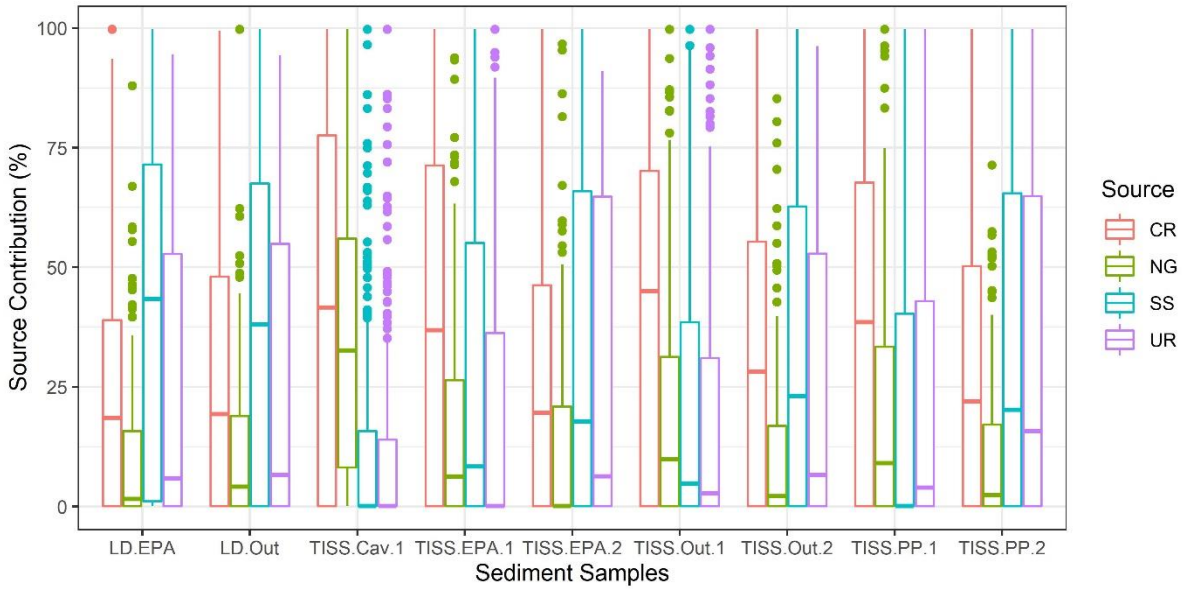

Figure 9.13. Distribution of the sediment source contributions for individual samples considering the 2500 simulations of the mixing model.

9.4 Discussion

9.4.1 Source and sediment samples composition

The Ibirapuitã River catchment shows a high diversity of soil types, mainly due the different geologies and relief variability. In addition, the differences in land use management, may result in this high intra-source variation as that observed for the parameters evaluated in the current research, especially for surface sources. Native grassland was the source showing the greater variability, mainly for parameters related to organic carbon and fallout radionuclides. Overgrazing in fragile areas has likely resulted in native grassland degradation due to soil exposure to water erosion, including formation of gullies (Cordeiro and Hasenack, 2009). Consequently, the high variability of native grasslands management by farmers, can lead to this high intra-source variability.

Grassland represents a significant sink of carbon, and according to the meta-analysis of Guo and Gifford (2002), 59% of the soil organic carbon is lost when grassland is converted into cropland. This can explain the lower TOC and TN content found in cropland compared to grassland in our catchment. The conversion of native grassland into cropland can result in a fast depletion of SOC, as a consequence of a negative balance between C inputs by plant and microorganism's residues and C losses as CO_2 due microbial oxidation of SOC. At the same time, SOC is concentrated in the soil surface

layers, which are the most exposed to soil erosion. When the soil is ploughed for crop cultivation, the soil is further exposed to the impact of rainfall, breaking the aggregates and exposing the physically protected carbon. Thus, the erosion process accelerates the mineralization of C into atmospheric CO_2 and also makes the C associated with sediment to be potentially transported to water courses (Lal, 2003). Beyond the impacts on soil degradation, Booman et al. (2012) observed that grassland area reduction in the Argentinian Pampa may result in a loss of hydrological regulation at the catchment scale, further intensifying the process of soil and water degradation.

The organic carbon more depleted in ^{13}C of cropland samples compared to native grasslands suggests that the introduction of C3 plants may be changing the C signature of the SOC. In the *Campos Sulinos* of the Pampa biome, the C4 grasslands dominate, which suggests that there is a greater accumulation of ^{13}C in natural grasslands (Andrade et al., 2019). The conversion of native grassland into cropland with C3 plants, mainly soybean (*Glycine max*) and rice (*Oriza sativa*) in paddy fields, tends to reduce the proportion of ^{13}C, which result in more negative values of $\delta^{13}C$. During the winter, these areas are usually cultivated with grass pastures, which follow C3 photosynthetic pathways, like ryegrass (*Lolium multiflorum*) and oat (*Avena sativa*).

The higher $\delta^{15}N$ values in cropland and the reduction of TN can be related to the selective mineralization of soil organic matter, leading to TN depletion by leaching or volatilization and ^{15}N enrichment in the residual organic matter pool (Xu et al., 2010). Moreover, plants tend to favour the incorporation of the light nitrogen isotope ^{14}N over ^{15}N. Accordingly, the plant tissues are usually depleted in ^{15}N and the N remaining in the soil is enriched in ^{15}N (Fox and Papanicolaou, 2008). The opposite behaviour is observed in native grassland, once the highest TN content and lower losses of N depleted in ^{15}N by mineralization processes result in lower $\delta^{15}N$. At the same time, the plant residues deposited on the soil surface and depleted in ^{15}N, result in a lower $\delta^{15}N$ in the soil surface compared to the subsurface sources (Huon et al., 2017). The temporal stability of TOC and TN in the fine suspended sediment generated by soil erosion, makes the measurement of these variables an alternative tracer for quantitative information on the sediment source contribution (i.e., using end member mixing models) (Huon et al., 2013).

Ultra-violet-visible derived parameters are mainly controlled by the carbon content and variables related to the pedogenesis process, such as iron oxides and clay content (Bayer et al., 2012). This land use-based approach does not take into account the

soil types variability which is considerably high in the Ibirapuitã catchment. The high variability within sources of these parameters can be explained by this soil types variability. As a consequence, most colour parameters and those related to iron oxides, were not selected as tracers to discriminate between land use based sources.

The variability of radionuclide activities in surface sources can be related to the soil degradation and erosion status of each sampled site (Evrard et al., 2020). The soil degradation status was not taken into account during the sampling campaign, where a wide variability of soil management conditions was covered within each land use. This variability was not observed in subsurface sources, which were sheltered from atmospheric fallout. The lower mean activity of ^{137}Cs and $^{210}Pb_{xs}$ observed for cropland compared to native grassland can be indicative of the higher soil erosion rates under cropland, confirming what was observed for the organic matter composition parameters. As for cropland, some native grassland samples were depleted in ^{137}Cs and also in $^{210}Pb_{xs}$, suggesting that surface soil with higher radionuclide activities was removed by soil erosion.

9.4.2 Sediment source contribution

The mixing model results indicate that land use management can play an important role in the sediment delivery to the river. The combination of soils highly susceptible to erosion, rainfall erosivity (Almagro et al., 2017), slope and land use and management (Roesch et al., 2009) may increase connectivity in different periods (Ares et al., 2020) accelerating the transfer of sediments to the river systems. The first period covered by TISS samples, represents the time after the harvesting of summer crops (rice and soybean mainly) where the soil is exposed without cover crops. During this first period, cropland supplied the main source of suspended sediment. It should be noted that the proportion of the catchment area occupied by cropland remains very low nowadays, covering less than 10% of the total catchment surface. Besides that, samples from the subcatchments which showed higher proportions of croplands, such as Cav and PP, had a slightly higher contribution of sediment coming from cropland. Cropland and pasture have already been reported as the main sediment sources in other tracing studies

developed in southern Brazil (Tiecher et al., 2018, 2017c) where high erosion rates and sediment yields were quantified (Didoné et al., 2014).

For the first sampling period, native grasslands had a greater contribution for the Cav catchment compared to the other catchments. The geology of the Cav catchment, which is mainly sandstone (Figure 9.4), which form sandy soils that are more fragile to erosion (Costa et al., 2018) and consequently more susceptible to degradation due to inappropriate land use. Overgrazing and eventual burning of natural grasslands in these sandy textured soils, followed by erosion and sandification has already been reported as one of the main threats to the Pampa biome (Roesch et al., 2009). The continued expansion of agriculture in the Pampa region may further increase the contribution of sediments and contaminants to river networks due to soil degradation. The region has a high potential of nutrients/contaminants losses due to soil erosion. A global estimation of P losses due to soil erosion, shows that in this region the P losses can be in the order of 1.1 to 20.0 kg ha^{-1} yr^{-1} (Alewell et al., 2020). Appropriate soil conservation practices have to be implemented to avoid the situation where soil degradation can lead to an irreversible status of sandification (Roesch et al., 2009).

The TISS samples which cover the second period showed an increased contribution from subsurface sources. It can be related to the extreme rainfall-runoff event that occurred in January 2019, where the overflow of the river exacerbated erosion in channels and gullies, increasing their contribution to sediment. For the LD samples, similar source contributions were calculated as for the TISS samples of the second period. Previous studies evaluating the sediment source contributions in paired catchments of the Pampa biome, one with two nested forest plantations (Rodrigues et al., 2018) and the other with paired catchments under forest plantation and native grassland (Valente et al., 2020), outlined that stream banks provided the main sediment source through to the collapse of river banks. The absence of riparian vegetation and the occurrence of outcropping deep sandy soil profiles are characteristics observed in the Ibirapuitã catchment that may promote bank erosion. Besides that, overgrazed pastures with full access to stream channels were indicated as accelerating stream bank and gully erosion (Zaimes et al., 2019). In addition, the long and undulating slopes favour the runoff concentration in the convergence zones, leading to the formation of gullies. Valente et al.

(2020) have also shown that grasslands with intensive livestock farming are more susceptible to soil erosion than forest plantations.

Overall, the results of the current research showed that land use change consisting in the conversion of native grassland into cropland may lead to several negative impacts for both the agriculture and the environment. At the same time, better management practices under native grassland have to be considered to reduce overland flow and subsequent gully and stream bank erosion. Grasslands show a high potential to sequester and store soil carbon (Viglizzo et al., 2019) and the grasslands of the Pampa biome provide important ecosystem services that require strategies to improve land management (Modernel et al., 2016). As already pointed out by Oliveira et al. (2017), more studies are needed to give support for policy makers in the definition of strategies for the Pampa biome grasslands conservation.

9.5 Conclusions

This study provides some of the first insights into the impacts of recent land use change on sediment transfers to the water bodies in a representative catchment of the Brazilian Pampa biome. Cropland (32%) and subsurface sources (28%) were shown to supply the main sediment sources in the Ibirapuitã river catchment, followed by unpaved roads (24%). Subsurface sources were the main sources for lag deposit samples while cropland was the main source of suspended sediment samples. Considering the low percentage of the total catchment area currently occupied by cropland (9.5%), these results demonstrate that erosion processes have intensified following the conversion of native grasslands into croplands. The signature differences between cropland and native grassland for organic matter composition and radionuclides activities, also indicate that cropland result in a higher level of soil degradation. Therefore, the conversion of native grasslands into farming areas, in the current condition of soil management, tends to reduce the carbon stock in the soil, reducing its quality, and also increasing the degradation of water resources through the accelerated transfer of sediments and associated contaminants. The soil use according to their respective agricultural suitability and appropriate soil conservation practices are highly recommend for a sustainable agriculture in the region.

Table 9.2. Summary statistics of the parameters analysed and the mean test for each source and sediment samples.

Fingerprint property	Cropland	Native Grassland	Subsurface	Unpaved Road	Sources		Sediments	KW	
	Mean	Mean	Mean	Mean	Max	Min	Mean	p value	H value
n =	33	26	31	27	117		9		
^{137}Cs (Bq kg^{-1})	2.66 ± 1.23	3.35 ± 1.65	0.67 ± 0.44	0.43 ± 0.2	7.45	0.18	0.32 ± 0.06	<0.001	77.8
$^{210}Pb_{xs}$ (Bq kg^{-1})	136.73 ± 63.46	197.67 ± 101.26	14.99 ± 10.58	16.17 ± 9.04	524.56	1.77	74.16 ± 35.32	<0.001	89.5
TN (g kg^{-1})	3.3 ± 0.85	4.47 ± 1.52	1.35 ± 0.63	0.63 ± 0.27	0.73	0.03	2.21 ± 0.52	<0.001	91.3
TOC (g kg^{-1})	32.75 ± 9.12	46.24 ± 16.12	14.52 ± 7.63	5.07 ± 1.95	7.29	0.19	23.54 ± 4.52	<0.001	89.6
CN Ratio	9.89 ± 0.8	10.28 ± 1.08	10.47 ± 2.36	8.15 ± 1.3	16.80	5.30	10.74 ± 0.72	<0.001	35.0
$\delta^{13}C$ (‰)	-19 ± 2.01	-17.79 ± 1.62	-17.2 ± 2.34	-17.59 ± 1.47	-14.61	-23.25	-20.54 ± 1.01	0.002	15.1
$\delta^{15}N$ (‰)	8.11 ± 1.05	7.07 ± 1.3	7.44 ± 0.9	7.94 ± 0.9	9.76	4.63	7.99 ± 0.19	0.048	7.9
A1	0.00086 ± 0.00049	0.00087 ± 0.00045	0.00109 ± 0.00047	0.00129 ± 0.00075	0.00304	0.00001	0.00304 ± 0.00001	0.053	7.7
A2	0.00024 ± 0.00011	0.00029 ± 0.00012	0.00034 ± 0.00019	0.00031 ± 0.00008	0.00077	0.00007	0.00077 ± 0.00007	0.046	8.0
A3	0.00031 ± 0.00024	0.00026 ± 0.00016	0.00022 ± 0.00006	0.00048 ± 0.00042	0.00169	0.00005	0.00169 ± 0.00005	0.015	10.5
Hr	0.29 ± 0.15	0.24 ± 0.07	0.18 ± 0.04	0.25 ± 0.07	0.83	0.11	0.23 ± 0.02	<0.001	27.9
L*	52.35 ± 3.2	48.62 ± 5.85	52.08 ± 4.81	53.38 ± 3.81	63.95	36.48	51.02 ± 1.34	0.010	11.4
a*	9.32 ± 3.17	8.21 ± 2.12	7.68 ± 1.83	11.8 ± 4.32	21.91	4.76	5 ± 0.27	<0.001	21.8
b*	20.55 ± 4.2	18.43 ± 3.48	19.57 ± 3.91	23.39 ± 3.93	32.79	11.69	14.35 ± 0.64	<0.001	18.9
C*	22.6 ± 5.08	20.2 ± 3.95	21.04 ± 4.23	26.29 ± 5.39	39.44	12.82	15.2 ± 0.68	<0.001	19.8
h	66.17 ± 3.43	66.18 ± 2.72	68.64 ± 2.16	63.91 ± 4.66	72.86	53.90	70.78 ± 0.51	<0.001	21.2
x	0.39 ± 0.02	0.39 ± 0.01	0.39 ± 0.01	0.41 ± 0.02	0.46	0.36	0.37 ± 0	0.003	14.3
y	0.38 ± 0.01	0.38 ± 0.01	0.38 ± 0.01	0.38 ± 0	0.39	0.36	0.37 ± 0	0.035	8.6
z	0.23 ± 0.02	0.24 ± 0.02	0.24 ± 0.02	0.21 ± 0.03	0.27	0.16	0.27 ± 0	0.004	13.2
L	45.27 ± 3.16	41.7 ± 5.64	45.04 ± 4.83	46.3 ± 3.82	57.22	30.43	43.92 ± 1.32	0.010	11.4
a	7.66 ± 2.72	6.54 ± 1.8	6.26 ± 1.63	9.81 ± 3.67	18.68	3.67	4 ± 0.22	<0.001	23.4

b	13.14 ± 2.44	11.62 ± 2.29	12.64 ± 2.56	14.7 ± 1.89	18.81	6.89	9.62 ± 0.42	<0.001	20.0
u*	24.12 ± 6.79	21.01 ± 4.85	21.17 ± 4.72	29.32 ± 8.21	49.41	12.40	14.59 ± 0.7	<0.001	22.0
v*	23.42 ± 4.22	20.86 ± 3.97	22.7 ± 4.48	26.01 ± 3.18	32.84	12.58	17.25 ± 0.74	<0.001	19.0
u’	0.23 ± 0.01	0.23 ± 0.01	0.23 ± 0.01	0.24 ± 0.01	0.27	0.22	0.22 ± 0	<0.001	16.2
v’	0.5 ± 0.01	0.5 ± 0	0.5 ± 0	0.51 ± 0	0.52	0.49	0.5 ± 0	0.009	11.7
RI	0.47 ± 0.16	0.8 ± 0.56	0.5 ± 0.21	0.44 ± 0.17	2.69	0.16	0.49 ± 0.06	0.017	10.2
Hvc	198.64 ± 11.24	200.32 ± 8.31	205 ± 6.36	190.56 ± 14.15	215.82	158.24	214.9 ± 1.3	<0.001	20.0
hVc	29.56 ± 1.46	27.86 ± 2.67	29.43 ± 2.19	30.03 ± 1.74	34.85	22.32	28.95 ± 0.61	0.010	11.4
hvC	27.88 ± 3.66	25.58 ± 3.26	26.64 ± 3.32	30.63 ± 3.78	39.99	18.54	22.82 ± 0.53	<0.001	22.9
R	147.86 ± 15.41	144.26 ± 11.46	141.77 ± 9.95	159.41 ± 20.22	205.34	123.20	125.51 ± 1.98	0.002	14.7
G	85.87 ± 2.26	86.14 ± 1.6	87.51 ± 1.18	83.95 ± 4.42	90.14	72.54	88 ± 0.18	<0.001	20.3
B	47.69 ± 6.4	49.35 ± 5.04	49.32 ± 5.08	43.4 ± 6.72	59.94	28.38	57.55 ± 1.11	0.005	12.9
HRGB	5.95 ± 3.36	5.33 ± 2.37	4.02 ± 1.66	8.73 ± 5.6	22.59	1.50	1.76 ± 0.24	<0.001	19.6
IRGB	93.81 ± 2.38	93.25 ± 1.77	92.87 ± 1.54	95.59 ± 3.12	102.66	89.99	90.35 ± 0.31	0.002	14.7
SRGB	50.08 ± 10.88	47.46 ± 8.22	46.23 ± 7.47	58 ± 13.43	88.33	31.63	33.98 ± 1.54	0.003	14.2
CI	0.26 ± 0.06	0.25 ± 0.04	0.24 ± 0.04	0.31 ± 0.07	0.48	0.17	0.18 ± 0.01	<0.001	17.1
SI	0.51 ± 0.09	0.49 ± 0.07	0.48 ± 0.07	0.57 ± 0.09	0.76	0.35	0.37 ± 0.02	0.003	14.0

*SD – Standard Deviation.

9.6 References

Alewell, C., Ringeval, B., Ballabio, C., Robinson, D.A., Panagos, P., Borrelli, P., 2020. Global phosphorus shortage will be aggravated by soil erosion. Nat. Commun. 11. https://doi.org/10.1038/s41467-020-18326-7

Almagro, A., Oliveira, P.T.S., Nearing, M.A., Hagemann, S., 2017. Projected climate change impacts in rainfall erosivity over Brazil. Sci. Rep. 7, 8130. https://doi.org/10.1038/s41598-017-08298-y

Amundson, R., Austin, A.T., Schuur, E.A.G., Yoo, K., Matzek, V., Kendall, C., Uebersax, A., Brenner, D., Baisden, W.T., 2003. Global patterns of the isotopic composition of soil and plant nitrogen. Global Biogeochem. Cycles 17. https://doi.org/10.1029/2002GB001903

ANA, N.W.A., 2020. HidroWeb: hydrologycal information system. [WWW Document]. URL http://www.snirh.gov.br/hidroweb/serieshistoricas (accessed 9.5.20).

Andrade, B.O., Bonilha, C.L., Overbeck, G.E., Vélez-Martin, E., Rolim, R.G., Bordignon, S.A.L., Schneider, A.A., Vogel Ely, C., Lucas, D.B., Garcia, É.N., dos Santos, E.D., Torchelsen, F.P., Vieira, M.S., Silva Filho, P.J.S., Ferreira, P.M.A., Trevisan, R., Hollas, R., Campestrini, S., Pillar, V.D., Boldrini, I.I., 2019. Classification of South Brazilian grasslands: Implications for conservation. Appl. Veg. Sci. 22, 168–184. https://doi.org/10.1111/avsc.12413

Ares, M.G., Varni, M., Chagas, C., 2020. Runoff response of a small agricultural basin in the argentine Pampas considering connectivity aspects. Hydrol. Process. 34, 3102–3119. https://doi.org/10.1002/hyp.13782

Batista, P.V.G., Laceby, J.P., Silva, M.L.N., Tassinari, D., Bispo, D.F.A., Curi, N., Davies, J., Quinton, J.N., 2018. Using pedological knowledge to improve sediment source apportionment in tropical environments. J. Soils Sediments. https://doi.org/10.1007/s11368-018-2199-5

Bayer, A., Bachmann, M., Müller, A., Kaufmann, H., 2012. A Comparison of Feature-Based MLR and PLS Regression Techniques for the Prediction of Three Soil Constituents in a Degraded South African Ecosystem. Appl. Environ. Soil Sci. 2012, 1–20. https://doi.org/10.1155/2012/971252

Booman, G.C., Calandroni, M., Laterra, P., Cabria, F., Iribarne, O., Vázquez, P., 2012. Areal changes of lentic water bodies within an agricultural basin of the Argentinean

Pampas. Disentangling land management from climatic causes. Environ. Manage. 50, 1058–1067. https://doi.org/10.1007/s00267-012-9943-1

Brindley, G.W., Brown, G. (Eds.), 1980. Crystal Structures of Clay Minerals and their X-Ray Identification. Mineralogical Society of Great Britain and Ireland, Colchester and London. https://doi.org/10.1180/mono-5

Caner, L., Petit, S., Joussein, E., Fritsch, E., Herbillon, A.J., 2011. Accumulation of organo-metallic complexes in laterites and the formation of Aluandic Andosols in the Nilgiri Hills (southern India): similarities and differences with Umbric Podzols. Eur. J. Soil Sci. 62, 754–764. https://doi.org/10.1111/j.1365-2389.2011.01389.x

Collins, A.L., Zhang, Y., Walling, D.E., 2010. Apportioning sediment sources in a grassland dominated agricultural catchment in the UK using a new tracing framework. Sediment Dyn. a Chang. Futur. 337, 68–75.

Coplen, T.B., Kendall, C., Hopple, J., 1983. Comparison of stable isotope reference samples. Nature 302, 236–238.

Cordeiro, J.L.P., Hasenack, H., 2009. Cobertura vegetal atual do Rio Grande do Sul, in: Pillar, V.D., Muller, S.C., Castilhos, Z.M. de S., Jacques, A.V.Á. (Eds.), Campos Sulinos - Conservação e Uso Sustentável Da Biodiversidade. MMA, Brasília, pp. 285–299.

Costa, C.W., Lorandi, R., de Lollo, J.A., Imani, M., Dupas, F.A., 2018. Surface runoff and accelerated erosion in a peri-urban wellhead area in southeastern Brazil. Environ. Earth Sci. 77, 1–18. https://doi.org/10.1007/s12665-018-7366-x

Didoné, E.J., Minella, J.P.G., Reichert, J.M., Merten, G.H., Dalbianco, L., de Barrros, C.A.P., Ramon, R., 2014. Impact of no-tillage agricultural systems on sediment yield in two large catchments in Southern Brazil. J. Soils Sediments 14, 1287–1297. https://doi.org/10.1007/s11368-013-0844-6

Didoné, E.J., Paolo, J., Minella, J.P.G., Merten, G.H., 2015. Quantifying soil erosion and sediment yield in a catchment in southern Brazil and implications for land conservation Quantifying soil erosion and sediment yield in a catchment in southern Brazil and implications for land conservation. https://doi.org/10.1007/s11368-015-1160-0

Evrard, O., Chaboche, P.-A., Ramon, R., Foucher, A., Laceby, J.P., 2020. A global review of sediment source fingerprinting research incorporating fallout radiocesium (137Cs). Geomorphology 362, 107103. https://doi.org/10.1016/j.geomorph.2020.107103

Evrard, O., Durand, R., Foucher, A., Tiecher, T., Sellier, V., Onda, Y., Lefèvre, I., Cerdan, O.,

Laceby, J.P., 2019. Using spectrocolourimetry to trace sediment source dynamics in coastal catchments draining the main Fukushima radioactive pollution plume (2011–2017). J. Soils Sediments 19, 3290–3301. https://doi.org/10.1007/s11368-019-02302-w

Fox, J.F., Papanicolaou, A.N., 2008. Application of the spatial distribution of nitrogen stable isotopes for sediment tracing at the watershed scale. J. Hydrol. 358, 46–55. https://doi.org/10.1016/j.jhydrol.2008.05.032

Fox, J.F., Papanicolaou, A.N., 2007. The use of carbon and nitrogen isotopes to study watershed erosion processes. J. Am. Water Resour. Assoc. 43, 1047–1064. https://doi.org/10.1111/j.1752-1688.2007.00087.x

Fritsch, E., Morin, G., Bedidi, A., Bonnin, D., Balan, E., Caquineau, S., Calas, G., 2005. Transformation of haematite and Al-poor goethite to Al-rich goethite and associated yellowing in a ferralitic clay soil profile of the middle Amazon Basin (Manaus, Brazil). Eur. J. Soil Sci. 56, 575–588. https://doi.org/10.1111/j.1365-2389.2005.00693.x

Guo, L.B., Gifford, R.M., 2002. Soil carbon stocks and land use change : a meta analysis. Glob. Chang. Biol. 345–360. https://doi.org/10.1046/j.1354-1013.2002.00486.x

Guzmán, G., Quinton, J.N., Nearing, M.A., Mabit, L., Gómez, J.A., 2013. Sediment tracers in water erosion studies: Current approaches and challenges. J. Soils Sediments 13, 816–833. https://doi.org/10.1007/s11368-013-0659-5

Hunter Laboratories, 1996. Insight on Color: Hunter Lab Color Scale. Appl. Note 8, 1–4.

HunterLab, 2015. The basics of color perception and measurement [WWW Document]. URL https://www.hunterlab.com/basics-of-color-theory.pdf?r=false (accessed 7.9.19).

Huon, S., de Rouw, A., Bonté, P., Robain, H., Valentin, C., Lefèvre, I., Girardin, C., Le Troquer, Y., Podwojewski, P., Sengtaheuanghoung, O., 2013. Long-term soil carbon loss and accumulation in a catchment following the conversion of forest to arable land in northern Laos. Agric. Ecosyst. Environ. 169, 43–57. https://doi.org/10.1016/j.agee.2013.02.007

Huon, S., Evrard, O., Gourdin, E., Lefèvre, I., Bariac, T., Reyss, J., Henry des Tureaux, T., Sengtaheuanghoung, O., Ayrault, S., Ribolzi, O., 2017. Suspended sediment source and propagation during monsoon events across nested sub-catchments with contrasted land uses in Laos. J. Hydrol. Reg. Stud. 9, 69–84. https://doi.org/10.1016/j.ejrh.2016.11.018

JURACEK, K.E., ZIEGLER, A.C., 2009. Estimation of sediment sources using selected chemical tracers in the Perry lake basin, Kansas, USA. Int. J. Sediment Res. 24, 108–125. https://doi.org/10.1016/S1001-6279(09)60020-2

Koiter, A.J., Owens, P.N., Petticrew, E.L., Lobb, D.A., 2013. The behavioural characteristics of sediment properties and their implications for sediment fingerprinting as an approach for identifying sediment sources in river basins. Earth-Science Rev. 125, 24–42. https://doi.org/10.1016/j.earscirev.2013.05.009

Laceby, J.P., Evrard, O., Smith, H.G., Blake, W.H., Olley, J.M., Minella, J.P.G., Owens, P.N., 2017. The challenges and opportunities of addressing particle size effects in sediment source fingerprinting: A review. Earth-Science Rev. 169, 85–103. https://doi.org/10.1016/j.earscirev.2017.04.009

Lal, R., 2003. Soil erosion and the global carbon budget. Environ. Int. 29, 437–450. https://doi.org/10.1016/S0160-4120(02)00192-7

MapBiomas, 2019. Projeto MapBiomas – Coleção v4.0 da Série Anual de Mapas de Cobertura e Uso de Solo do Brasil [WWW Document]. Proj. MapBiomas - é uma Iniciat. multi-institucional para gerar mapas anuais Cober. e uso do solo a partir Process. Classif. automática Apl. a imagens satélite. A descrição Complet. do Proj. encontra-se em http//mapbiomas.o. URL http://mapbiomas.org (accessed 6.2.19).

Martínez-Carreras, N., Krein, A., Gallart, F., Iffly, J.F., Pfister, L., Hoffmann, L., Owens, P.N., 2010a. Assessment of different colour parameters for discriminating potential suspended sediment sources and provenance: A multi-scale study in Luxembourg. Geomorphology 118, 118–129. https://doi.org/10.1016/j.geomorph.2009.12.013

Martínez-Carreras, N., Udelhoven, T., Krein, A., Gallart, F., Iffly, J.F., Ziebel, J., Hoffmann, L., Pfister, L., Walling, D.E., 2010b. The use of sediment colour measured by diffuse reflectance spectrometry to determine sediment sources: Application to the Attert River catchment (Luxembourg). J. Hydrol. 382, 49–63. https://doi.org/10.1016/j.jhydrol.2009.12.017

Modernel, P., Rossing, W.A.H., Corbeels, M., Dogliotti, S., Picasso, V., Tittonell, P., 2016. Land use change and ecosystem service provision in Pampas and Campos grasslands of southern South America. Environ. Res. Lett. 11, 113002. https://doi.org/10.1088/1748-9326/11/11/113002

Nosrati, K., 2017. Ascribing soil erosion of hillslope components to river sediment yield. J. Environ. Manage. 194, 63–72. https://doi.org/10.1016/j.jenvman.2016.10.011

Oliveira, T.E. de, Freitas, D.S. de, Gianezini, M., Ruviaro, C.F., Zago, D., Mércio, T.Z., Dias, E.A., Lampert, V. do N., Barcellos, J.O.J., 2017. Agricultural land use change in the Brazilian Pampa Biome: The reduction of natural grasslands. Land use policy 63, 394–400. https://doi.org/10.1016/j.landusepol.2017.02.010

Overbeck, G.E., Muller, S., Fidelis, A., Pfadenhauer, J., Pillar, V.D., Blanco, C., Boldrini, I.I., Both, R., Forneck, E.D., 2007. Brazil's neglected biome: The South Brazilian Campos. Perspect. Plant Ecol. Evol. Syst. 9, 101–116. https://doi.org/10.1016/j.ppees.2007.07.005

Phillips, J.M., Russell, M.A., Walling, D.E., 2000. Time-integrated sampling of fluvial suspended sediment: A simple methodology for small catchments. Hydrol. Process. 14, 2589–2602. https://doi.org/10.1002/1099-1085(20001015)14:14<2589::AID-HYP94>3.0.CO;2-D

Pillar, V., Tornquist, C., Bayer, C., 2012. The southern Brazilian grassland biome: soil carbon stocks, fluxes of greenhouse gases and some options for mitigation. Brazilian J. Biol. 72, 673–681. https://doi.org/10.1590/S1519-69842012000400006

Pulley, S., Collins, A.L., Laceby, J.P., 2020. The representation of sediment source group tracer distributions in Monte Carlo uncertainty routines for fingerprinting: an analysis of accuracy and precision using data for four contrasting catchments. Hydrol. Process. 1–20. https://doi.org/10.1002/hyp.13736

Pulley, S., Van der Waal, B., Rowntree, K., Collins, A.L., 2018. Colour as reliable tracer to identify the sources of historically deposited flood bench sediment in the Transkei, South Africa: A comparison with mineral magnetic tracers before and after hydrogen peroxide pre-treatment. CATENA 160, 242–251. https://doi.org/10.1016/j.catena.2017.09.018

R Development Core Team, 2017. R: a language and environment for statistical computing.

Ramon, R., Evrard, O., Laceby, J.P., Caner, L., Inda, A. V., Barros, C.A.P. de, Minella, J.P.G., Tiecher, T., 2020. Combining spectroscopy and magnetism with geochemical tracers to improve the discrimination of sediment sources in a homogeneous subtropical catchment. CATENA 195, 104800. https://doi.org/10.1016/j.catena.2020.104800

Rodrigues, M.F., Reichert, J.M., Burrow, R.A., Flores, E.M.M., Minella, J.P.G., Rodrigues, L.A., Oliveira, J.S.S., Cavalcante, R.B.L., 2018. Coarse and fine sediment sources in nested watersheds with eucalyptus forest. L. Degrad. Dev. 29, 2237–2253.

https://doi.org/10.1002/ldr.2977

Roesch, L.F., Vieira, F., Pereira, V., Schünemann, A.L., Teixeira, I., Senna, A.J., Stefenon, V.M., 2009. The Brazilian Pampa: A Fragile Biome. Diversity 1, 182–198. https://doi.org/10.3390/d1020182

Sánchez-Marañón, M., 2011. Color Indices, Relationship with Soil Characteristics, in: Gliński, J., Horabik, J., Lipiec, J. (Eds.), Encyclopedia of Agrophysics. Springer Netherlands, Dordrecht, pp. 141–145. https://doi.org/10.1007/978-90-481-3585-1_237

Sellier, V., Navratil, O., Laceby, J.P., Legout, C., Allenbach, M., Lefèvre, I., Evrard, O., 2020. Combining colour parameters and geochemical tracers to improve sediment source discrimination in a mining catchment (New Caledonia, South Pacific Islands). SOIL Discuss. in review. https://doi.org/https://doi.org/10.5194/soil-2020-48

Silveira, V.C.P., González, J.A., Fonseca, E.L. da, 2017. Land use changes after the period commodities rising price in the Rio Grande do Sul State, Brazil. Ciência Rural 47, 1–7. https://doi.org/10.1590/0103-8478cr20160647

Stevenson, B.A., Kelly, E.F., McDonald, E. V., Busacca, A.J., 2005. The stable carbon isotope composition of soil organic carbon and pedogenic carbonates along a bioclimatic gradient in the Palouse region, Washington State, USA. Geoderma 124, 37–47. https://doi.org/10.1016/j.geoderma.2004.03.006

Tiecher, T., Minella, J.P.G., Caner, L., Evrard, O., Zafar, M., Capoane, V., Le Gall, M., Santos, D.R. dos, 2017. Quantifying land use contributions to suspended sediment in a large cultivated catchment of Southern Brazil (Guaporé River, Rio Grande do Sul). Agric. Ecosyst. Environ. 237, 95–108. https://doi.org/10.1016/j.agee.2016.12.004

Tiecher, T., Minella, J.P.G., Evrard, O., Caner, L., Merten, G.H., Capoane, V., Didoné, E.J., dos Santos, D.R., 2018. Fingerprinting sediment sources in a large agricultural catchment under no-tillage in Southern Brazil (Conceição River). L. Degrad. Dev. 29, 939–951. https://doi.org/10.1002/ldr.2917

Uber, M., Legout, C., Nord, G., Crouzet, C., Demory, F., Poulenard, J., 2019. Comparing alternative tracing measurements and mixing models to fingerprint suspended sediment sources in a mesoscale Mediterranean catchment. J. Soils Sediments 19, 3255–3273. https://doi.org/10.1007/s11368-019-02270-1

Valente, M.L., Reichert, J.M., Legout, C., Tiecher, T., Cavalcante, R.B.L., Evrard, O., 2020. Quantification of sediment source contributions in two paired catchments of the

Brazilian Pampa using conventional and alternative fingerprinting approaches. Hydrol. Process. 34, 2965–2986. https://doi.org/10.1002/hyp.13768

Viglizzo, E.F., Ricard, M.F., Taboada, M.A., Vázquez-Amábile, G., 2019. Reassessing the role of grazing lands in carbon-balance estimations: Meta-analysis and review. Sci. Total Environ. 661, 531–542. https://doi.org/10.1016/j.scitotenv.2019.01.130

Viscarra Rossel, R.A., Minasny, B., Roudier, P., McBratney, A.B.B., 2006. Colour space models for soil science. Geoderma 133, 320–337. https://doi.org/10.1016/j.geoderma.2005.07.017

Walling, D.E., 2013. The evolution of sediment source fingerprinting investigations in fluvial systems. J. Soils Sediments 13, 1658–1675. https://doi.org/10.1007/s11368-013-0767-2

Wills, S.A., Burras, C.L., Sandor, J.A., 2007. Prediction of Soil Organic Carbon Content Using Field and Laboratory Measurements of Soil Color. Soil Sci. Soc. Am. J. 71, 380–388. https://doi.org/10.2136/sssaj2005.0384

Xu, Y., He, J., Cheng, W., Xing, X., Li, L., 2010. Natural 15N abundance in soils and plants in relation to N cycling in a rangeland in Inner Mongolia. J. Plant Ecol. 3, 201–207. https://doi.org/10.1093/jpe/rtq023

Zaimes, G.N., Tufekcioglu, M., Schultz, R.C., 2019. Riparian land-use impacts on stream bank and gully erosion in agricultural watersheds: What we have learned. Water (Switzerland) 11. https://doi.org/10.3390/w11071343

10 Chapter 5. Spectroscopy-based tracing of sediment sources in a large heterogeneous catchment with different geologies of the Pampa Biome (Ibirapuitã River, Southern Brazil)

10.1 Introduction

The increasing demand for foods, fibber and fuel have resulted in an excessive pressure on the natural resources around the world during the last years. The population growth combined with economic convergence resulting from higher per capita incomes can double (+102%) the food demand by 2050 relative to 2009 (Fukase and Martin, 2020). In southern Brazil, the expansion of agriculture in natural areas, such as the native grasslands of the Pampa biome is already observed, which has been particularly driven by the high price of commodities, mainly soybean (Silveira et al., 2017). The Pampa biome region covers an area of approximately 177,000 km^2 in Brazil, and it is mainly occupied by native grasslands used for extensive livestock production. The region presents a high heterogeneity of soil types developed on sedimentary rocks and less weathered volcanic rocks. They are mostly sandy, shallow, and very susceptible to degradation (Roesch et al., 2009). The low productivity of the pastures in the Pampa region associated with inadequate management and overgrazing (Overbeck et al., 2007) has given way to other more profitable activities, such as forests plantations and soybean (Oliveira et al., 2017). As a result, grassland vegetation cover in the Brazilian Pampa decreased 25% in the last 15 years (2576 km^2), being replaced with soybean and cultivated forest (Mengue et al., 2020). For this reason, it is necessary to monitor and estimate the impacts of the land use change in the Brazilian Pampa biome in order to avoid a degradation status that may become difficult to reverse, as it is already likely observed in some punctual areas under sandification process (Roesch et al., 2009).

An increase in soil erosion and soil degradation is expected with land use change, which is also linked to changes in the sediment delivery to the river systems (Walling, 1999). Therefore, the investigation of sediment dynamics at the catchment scale may help to understand the main degradation processes occurring in the landscape (Minella et al., 2009b) and help in guiding the implementation of strategies to prevent soil erosion. The application of conservation practices has already proved to be efficient in the control of soil erosion and reduction of sediment delivery to river network in a small catchment in

Southern Brazil (Minella et al., 2017a). This can be assessed by the quantification of sediment source contributions to the river sediment, helping to direct efforts of soil conservation to the main erosion problem areas in a given catchment (Collins et al., 2017b). Such a method was already tested in the Pampa region, with the objective to quantify the contribution of different land uses in two paired catchments with forest plantation and native grassland (Valente et al., 2020). The results indicated that soil losses under native grassland were larger than in the forest plantation where conservation practices were implemented, showing that extensive livestock over natural grassland requires additional practices to prevent erosion.

Tracing sediment sources relying on the analysis of conventional tracers (e.g. geochemistry, fallout radionuclides) can provide an aiding tool to monitor the impact of the recent land use change in the Pampa biome on sediment delivery to the river system. Besides that, alternative fingerprinting techniques that are less expensive, that require lower sample quantities while remaining quick to analyse, and require less laboratory infrastructures to perform analyses are needed in order to make the method applicable for local managers. To this end, diffuse reflectance spectroscopy can provide an effective alternative to obtain soil and sediment properties and use them as a source tracer (McBratney et al., 2006; Poulenard et al., 2012). Several studies conducted around the world have used diffuse reflectance spectroscopy as a potential sediment tracer according to the review of Tiecher et al. (2021). The method was already successfully applied in a small catchment (1.23 km^2) located in the basaltic plateau of Southern Brazil, where multivariate models calibrated with near and mid infrared data provided comparable results to the conventional method of sediment fingerprinting based on the analysis of geochemical composition (Tiecher et al., 2017a, 2016). A similar approach was tested in two small catchments (0.8 and 1.3 km^2) in the Pampa region (Valente et al., 2020). However, in this last study the method was not as effective as on the basaltic plateau. The multivariate model calibration with ultra-violet-visible spectra did not provide satisfactory results compared to the other methods, showing that even in small catchments there is still a need to improve the technique. A way to achieve this is through the use of different pre-processing techniques that can increase the accuracy of the models to predict sediment source contributions. According to Tiecher et al. (2021), the use of more sophisticated models, such as the non-parametric support vector machine (SVM), can better predict the sediment source contributions. In addition, it is also

possible to improve predictions by combining suitable pre-processing methods. However, although sediment tracing based on diffuse reflectance spectroscopy and multiple spectral pre-processing methods has already been implemented successfully in small catchments, the authors encouraged the community to test different methods and to validate the approach in larger catchments, with different soil and source types.

Therefore, the main objective of this study is to develop a sediment fingerprinting approach based on diffuse reflectance spectroscopy to predict sediment source contributions from agricultural areas in a large – representative – catchment of the Brazilian Pampa biome.

10.2 Methodology

10.2.1 Study site

The study was carried out in a representative catchment of the Brazilian Pampa biome, the Ibirapuitã River catchment. The entire Ibirapuitã catchment covers an area of approximately 7,975 km^2, at its confluence with the Ibicuí River. The monitoring station was located in an upstream portion of the catchment, located next to river gauging station and water quality monitoring station (nº76750000) performed by Brazilian National Water Agency (ANA) (28°27'22"S, 53°58'24"O) in the county of Alegrete (Figure 10.1). This catchment represents 75% of the total area of the Ibirapuitã River catchment, with a drainage area of approximately 5,943 km^2. The slopes in the catchment are mostly flat to undulated, with 90% of the area with slopes lower than 15%. The altitude ranges between 80 and 370 m a.s.l. The climate is classified as of Cfa type according to the Köppen classification, which corresponds to a humid subtropical climate without a defined dry season, with an average precipitation of 1,600 to 1,900 mm per year and an average temperature of 17ºC (Alvares et al., 2013). Native grassland is the main land use in the catchment (81%), followed by cropland, where flooded rice is the main crop, followed by soybean (Figure 10.5). Rice is mainly cultivated in the floodplains where Planosols occurs. Soybean in the summer and pastures in the winter are mainly cultivated in the upper positions of the landscape, where Acrisols and Regosols occurs.

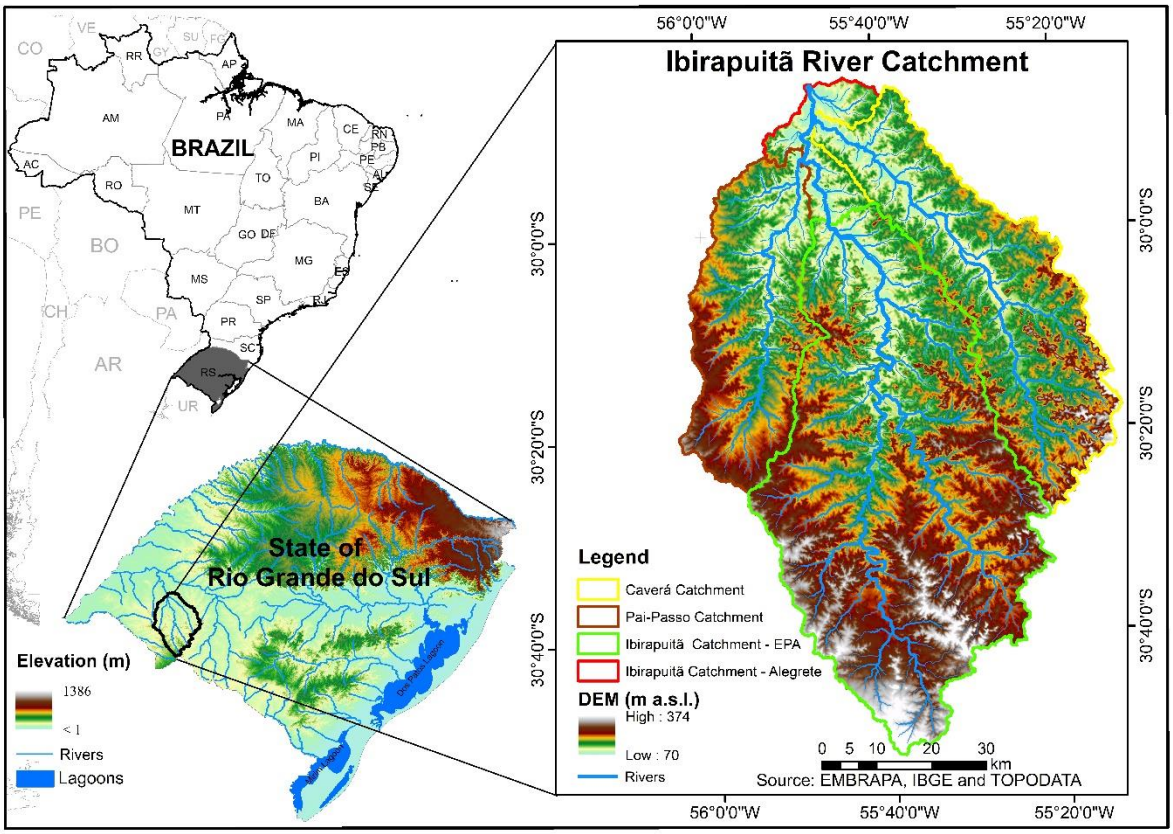

Figure 10.1. Study site location and digital elevation model (DEM).

Sediment samples were collected in three sub-catchments beyond the main catchment outlet (Figure 10.3), which are designed as: (i) Environmental Protection Area catchment (EPA), (ii) Pai-Passo stream, and (iii) Caverá stream. The EPA subcatchment, is an area controlled by the Chico Mendes Institution of Biodiversity Conservation (ICMBio) from the Brazilian National Ministry of the Environment, where native grassland (85%) and natural forests (10%) dominate. Located in the central portion of the Ibirapuitã River catchment, the EPA subcatchment covers an area of 3,196 km^2, where the main soil types are Regosols in the upper half and Acrisols in the lower half, from basalts of the Serra Geral formation (Fácies Alegrete) and sandstones/silts of the Botucatu formation (Fácies Gramado, Caxias and Guará), respectively. The Pai-Passo subcatchment covers an area of approximately 1,043 km^2, and it is mainly occupied by native grassland (83%) with extensive livestock on shallow Regosols developed on basalt (Fácies Alegrete), and paddy fields for irrigated rice production (10%) located in the lower and flatter portions of the landscape, where Planosols and Vertisols occurs. The Caverá subcatchment covers approximately 1,455 km^2, and is the sub-catchment with the higher percentage of cropland with rice and soybean production in the summer and

pastures in the winter (15%). In this catchment, the native grassland, currently covering 73% of the area approximately, have been converted into cropland on deeper soils, predominantly Acrisols developed on sandstones of the Botucatu formation. In Figure 10.2 and Figure 10.3Figure 9.4 is presented the land use, geology and soil classes of all subcatchments.

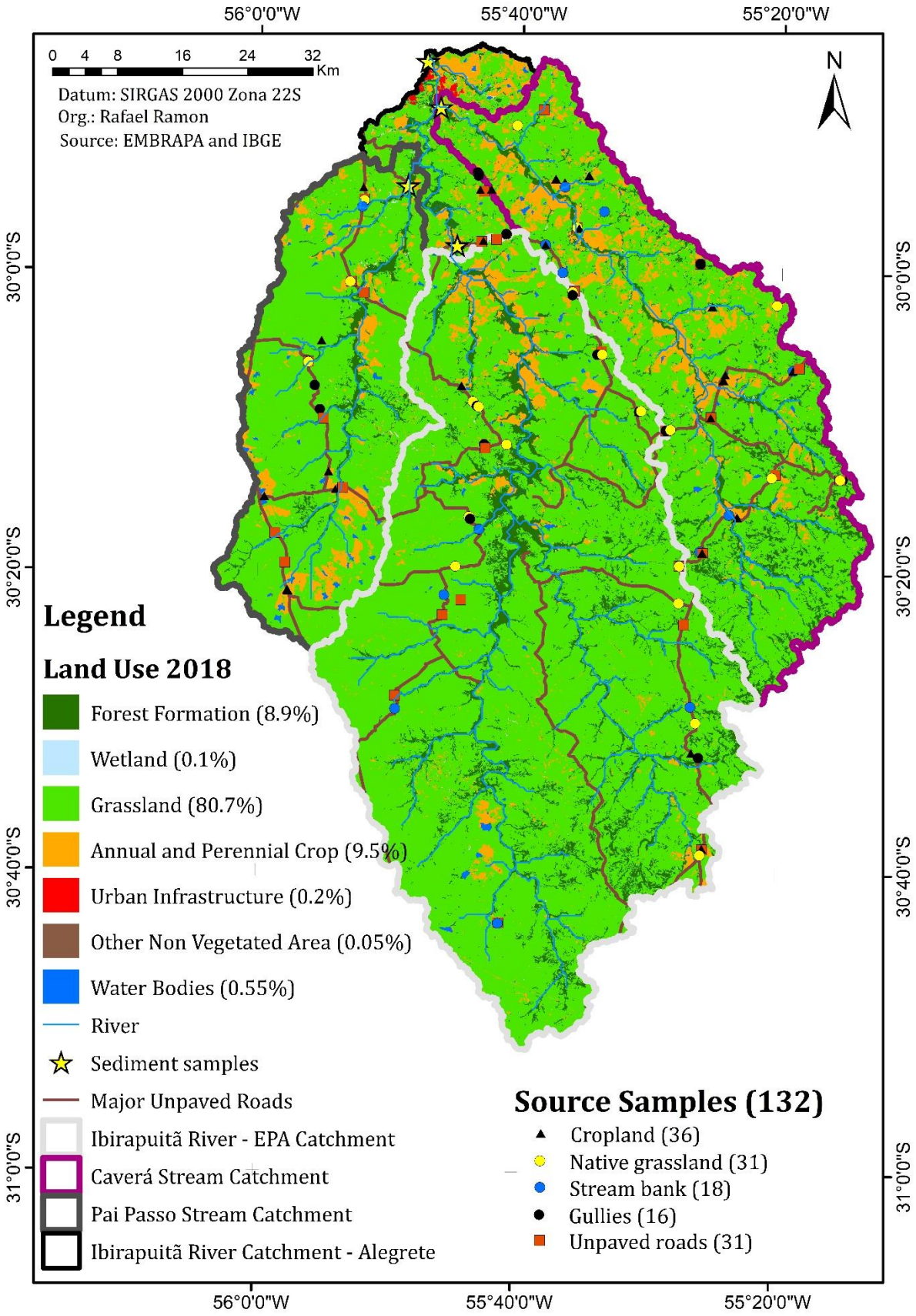

Figure 10.2. Land use and source samples in the Ibirapuitã River catchment.

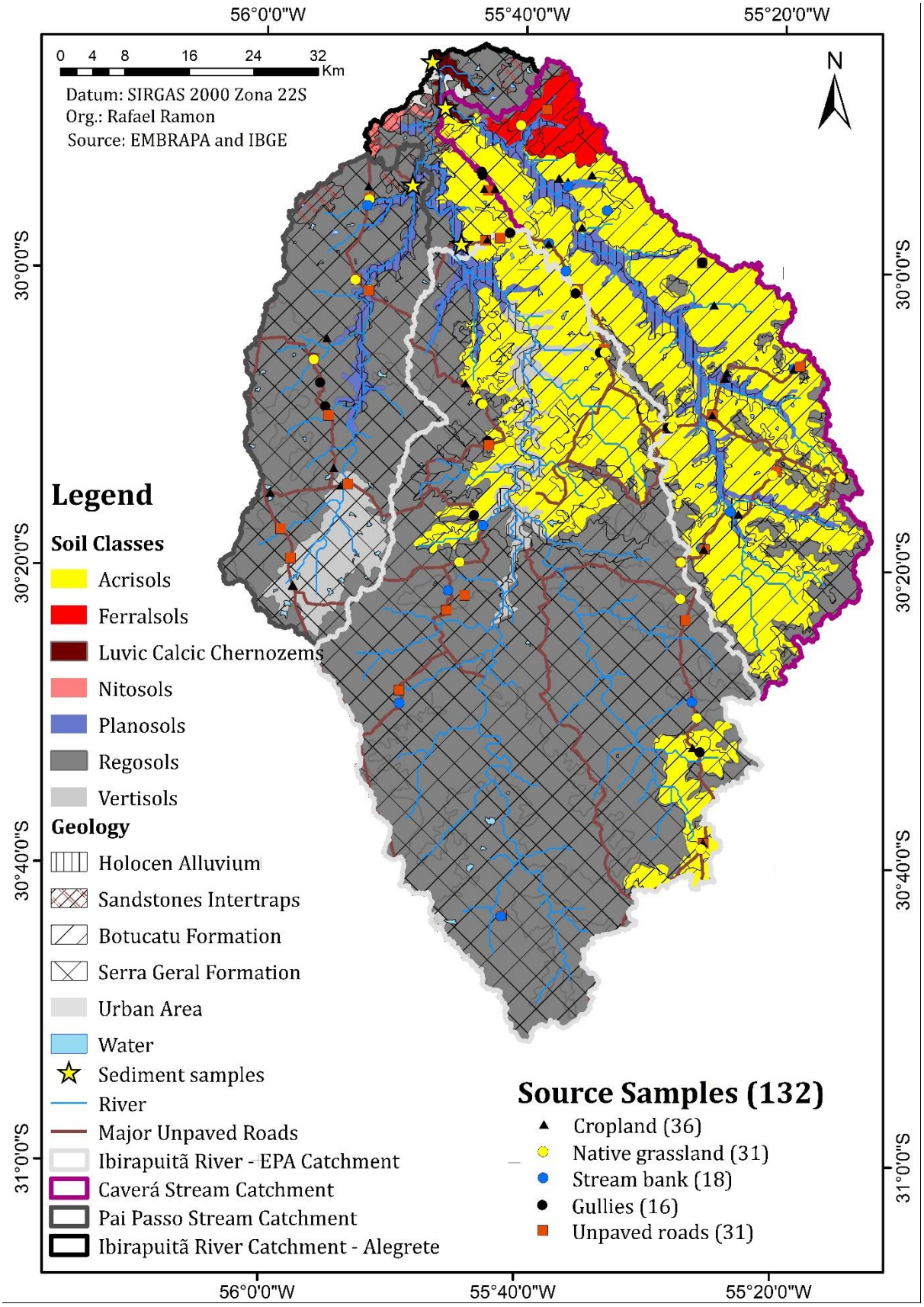

Figure 10.3. Soil types, geology, source and sediment sampling points in the Ibirapuitã River catchment.

In both catchments, features of the landscape such as the ramp length, flat and undulated relief, associated to sandy surface soil layers, causes large volumes of runoff concentrated in the hillside causing the formation of gullies. Besides that, the absence of riparian zones and the occurrence of preferential paths caused by animal circulation close to water bodies, favours the occurrence of concentrated erosion. These erosion processes are widely observed in the catchment, and with a lower extent, erosion was also observed on unpaved roads during field campaigns.

10.2.2 Source and sediment sampling

To characterize the potential sources, soil composite samples (n=132) were taken in representative areas, including cropland (n=36), native grassland (n=31) and subsurface sources composed of channel banks (n=18), gully (n=16) and unpaved road (n=31) samples (Figure 10.2). In the surface sources (cropland and native grassland), soil from the upper 0-2 cm layer was collected, as this layer is the most likely to be eroded and transported to the waterways. For the subsurface sources (channel bank, gully and unpaved road), samples were collected along the exposed face that is exposed to erosion. For each composite source sample, around 10 sub-samples were collected within a radius of approximately 50 meters, mixed in a bucket and approximately 500 grams of material was stored. Care was taken to avoid sites that have accumulated sediment originating from other sources, to prevent sampling of transiting material. The source sampling sites were selected in order to cover all the soil types and the variability in slope positions, as well as the three main tributary catchments. Moreover, all sediment sources were also sampled in areas covered by Botucatu formation and the Serra Geral formation.

Suspended sediment samples were collected at the Ibirapuitã catchment outlet and at the confluence with its tributaries following three strategies (Table 10.1). The first sampling strategy was the deployment of time integrating sediment samplers (TISS) (Figure 10.2). The sampler designed by Phillips et al. (2000) consists in a plastic tube of 75 mm of diameter and 80 cm length, which has a small inlet and outlet tubes (4 mm of diameter) in the extreme edges, which allows the suspended sediment to enter, reducing the flow velocity and allowing the sediment to deposit inside the tube based on the principle of sedimentation. The equipment is submerged for a certain period of time in order to integrate the sediment from different rainfall events, in which the eroded material of the catchment is mobilized under different conditions of transport and

energy, and may consequently show variable physical, chemical and mineralogical characteristics. The sampling interval was not based on a fixed schedule, sampling was performed after a minimum interval of three months and when the river was at a sufficiently low level to have a safe access to the samplers. The second strategy was to collect samples during storm events (Event), where large volume of water (50 to 100 L) was collected with a bucket from a bridge close to the outlet of the main catchment and tributaries. Finally, the third method was to collect samples of lag deposits after a flooding event as the river discharge exceeded its channel's volume causing the river overflow.

Table 10.1. Sediment samples location and date of collection.

Sediment samples			
Id	**Method**	**Location**	**Date/period**
D1	Deposit	Outlet	19/02/2019
D2	Deposit	EPA	19/02/2019
Event-1	Event	Caverá	30/06/2018
Event-2	Event	Outlet	30/06/2018
Event-3	Event	Caverá	27/08/2018
Event-4	Event	EPA	27/08/2018
Event-5	Event	Outlet	28/08/2018
Event-6	Event	Outlet	12/01/2019
Event-7	Event	Outlet	13/01/2019
Event-8	Event	Outlet	14/01/2019
TISS-1	TISS	Pai-Passo	11/07/2018 to 15/10/2018
TISS-2	TISS	Caverá	25/05/2018 to 15/10/2018
TISS-3	TISS	EPA	25/05/2018 to 26/10/2018
TISS-4	TISS	Outlet	25/05/2018 to 26/10/2018
TISS-5	TISS	EPA	26/10/2018 to 20/02/2019
TISS-6	TISS	Pai-Passo	26/10/2018 to 19/02/2019
TISS-7	TISS	Outlet	26/10/2018 to 19/02/2019

10.2.3 Artificial mixtures and sediment analyses

Source and sediment samples were oven-dried at 50°C, gently disaggregated using a pestle and mortar and dry-sieved to 63 μm to minimize the particle size effect (Laceby et al., 2017). Large amounts of coarser sediment were observed on the river bed, however in this study we focused on suspended sediment which is mainly composed of fine particles.

10.2.3.1 Artificial mixtures of sediment sources

The three land use-based sources (namely cropland, native grassland and subsurface) were separated according to the respective type of geological material (sandstone from Botucatu formation (BF) and basalt from the Serra Geral formation (SGF)). The georeferenced samples were classified according to the IBGE geology map (IBGE, 2018). The combination of three land uses and two geologies, resulted in six different sources. Equal proportions of the samples from each sediment source were mixed in the laboratory to prepare a single reference sample for each corresponding source (cropland – CR.BF and CR.SGF, native grassland – NG.BF and NG.SGF and subsurface sources – SS.BF and SS.SGF). Subsequently, these six reference samples were mixed in 120 different proportions from each source (Supplementary material). The Figure 10.4 represents the proportion of each land used-based source when combining geologies according to the land use. These mixtures were then used to calibrate the multivariate mathematical models used to estimate the respective source contributions to the sediment samples.

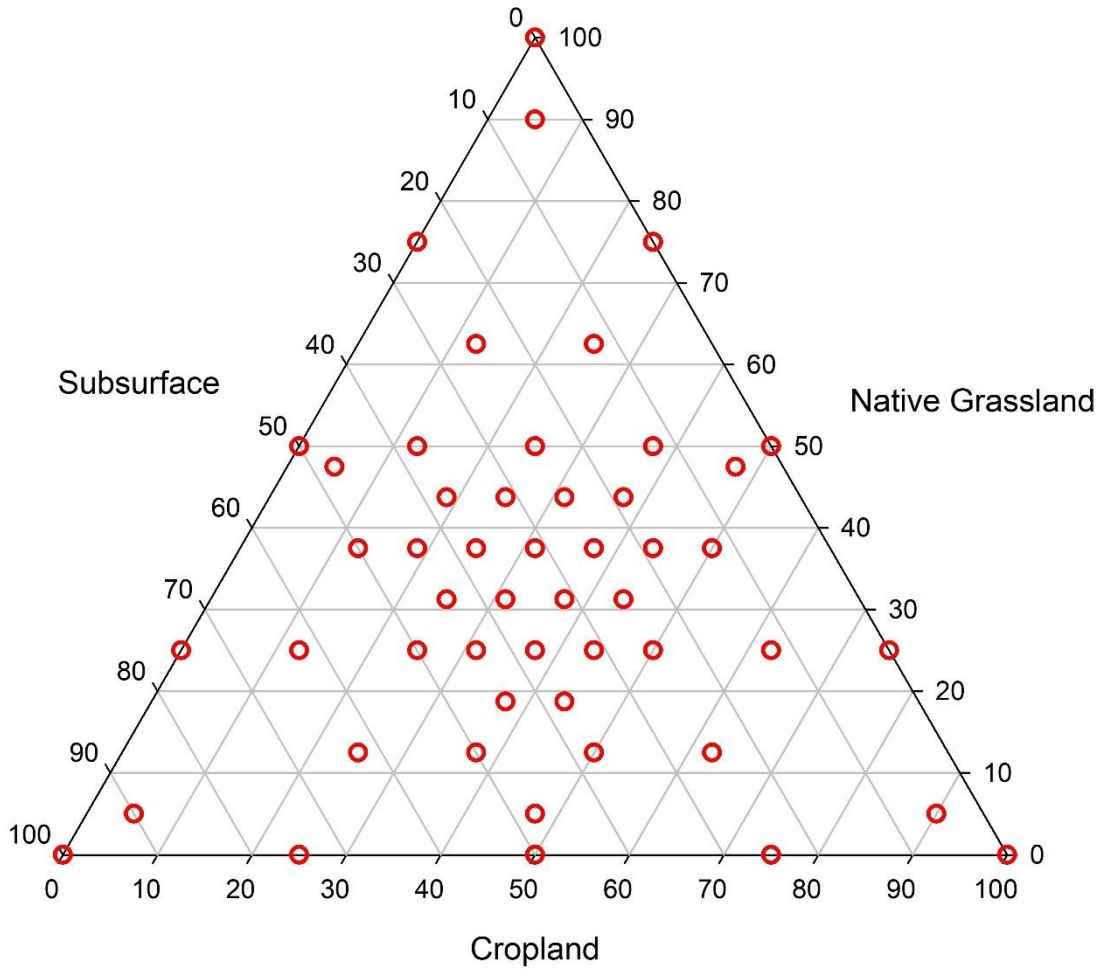

Figure 10.4. Ternary plot with the proportion of each land use based source when combining geologies according to the land use.

10.2.3.2 Spectral analyses

Diffuse reflectance spectral analyses were carried out in the ultraviolet–visible (UV, 200–800 nm with 1 nm step) and near-infrared (NIR, 1000-2500 nm with 1 nm step). UV spectrum were measured for each powdered sample using a Cary 5000 UV-NIR spectrophotometer (Varian, Palo Alto, CA, USA) at room temperature, using $BaSO_4$ as a 100% reflectance standard. NIR spectra was measured using a Nicolet 26,700 FTIR spectrometer (Waltham, Massachusetts, USA) in diffuse reflectance mode with an integrating sphere and a InGaAs detector with 100 readings per spectrum.

10.2.4 Spectral pre-processing techniques and multivariate model calibration and validation

Three different spectral pre-processing techniques were applied to the raw spectrum: i) Standard Normal Variate (SNV), ii) Detrend (DET) and iii) Savitzky-Golay

Derivate (SGD), which were then compared to the raw spectra (RAW). Each pre-processing technique have particular functionalities, aiming to emphasize features of interest and reduce the physical variability due to light dispersion or systematic variations due to environmental and instrumental conditions (Barnes et al., 1989; Dotto et al., 2019). The SNV normalizes the spectral data to correct for light scatter. The DET allows to correct for wavelength-dependent scattering effects, normalizing the spectral data. The SGD reduces the high frequency noise in the signal by smoothing out properties and reducing the low frequency signal by differentiation. The SGD was applied with a first derivative using a first order polynomial and a 11 nm search window, where the search window extent was defined based on prior testing.

Two multivariate models were tested in this research, a parametric multivariate model, the PLSR (method 'pls') (R pls package Mevik et al., 2016), and a non-parametric model, the SVM (method 'svmLinear') (R *e*1071 package Meyer et al., 2019). The PLSR is widely used due to their simplicity, robustness, good performance and easy accessibility. The PLSR converts the spectra into latent variables to reduce the dimensionality and then implement multiple linear regressions between the measured spectra and the variable of interest. The SVM is a bit more powerful, being able to model non-linear relations, which is an advantage for soil analysis, since non-linear relations between spectral variables and organo-mineral components are expected (Tiecher et al., 2021; Viscarra Rossel and Behrens, 2010). The models were calibrated and validated by cross-validation with 10 k-fold, using a random division into segments.

The performance of the models in estimating the contribution from each source to sediment was evaluated by means of the coefficient of determination (R^2) and root mean square error of prediction (RMSE), which are indices of the model accuracy. The models are calibrated for each source individually and the sources contribution sum was not forced to sum up to 100% for each sediment sample. For this purpose, when the sum is not close to 100%, it means that some problem in the fingerprinting approach is occurring. As suggested by Legout et al. (2013) and Tiecher et al. (2021), the closer the total sum of the source contribution in sediment samples is from 100%, the higher is the model performance. All pre-processing and data modelling were performed in R software (R Core Team, 2020). The statistical performance was compared with an ANOVA at a 5% significance level. When significant, the difference between the means of the

multivariate model, the pre-processing technique and the spectral range, were compared using the Tukey test at $p<0.05$.

10.2.5 Building spectroscopy models for different sediment sources

Spectroscopic models were built considering three approaches. First, the models were calibrated for each one of the six potential sources considering the three land uses and two geological material types: i) cropland on the Botucatu Formation (CR-BF) and ii) Serra Geral Formation (CR-SGF), iii) native grassland on the Botucatu Formation (NG-BF) and iv) Serra Geral Formation (NG-SGF) and v) subsurface sources on the Botucatu Formation (SS-BF) and vi) Serra Geral Formation (SS-SGF).

A second approach was developed considering only land use as potential sources in order to reduce complexity and uncertainty in the modelling results. Mixtures samples with the same land use and different geologies were combined to consider only three potential sources.

Finally, a third approach was developed considering only two potential sources (surface (NG + CR) and subsurface sources) without separating the geological formation. The third approach was performed based on previous study conducted in the same catchment, where no significant difference was observed between NG and CR when using radionuclide activity, organic isotopic composition and colour parameters as potential tracers. For this reason, NG and CR were combined to propose an approach that may better reflect the occurrence of two distinct erosion processes observed in the catchment, i.e. surface erosion and channel erosion. The strategy of merging sources with similar characteristics is a method that has already been used with success in other studies to obtain a greater reliability in model prediction (Poulenard et al., 2009).

In total, 24 models were calibrated for each sediment source with the combination of two multivariate models (PLSR, and SVM), three spectra pre-processing techniques (SNV, DET, and SGD) and the raw (RAW) data, and three spectral ranges (UV, NIR, UV+NIR). Altogether, 274 models were built in the present research, considering four (n=144), three (n=78) and two (n=52) potential sources, respectively.

10.3 Results and Discussion

10.3.1 Multivariate model calibration

The multivariate methods provided satisfactory calibrated and validated models with the majority of spectral ranges and pre-processing techniques. A total of 274 multivariate models were adjusted considering the multiple sources, multivariate models, spectral ranges and pre-processing techniques. The average statistical values of each approach are presented in the Table 10.2, which demonstrates the accuracy of the model predictions based on the RMSE and R^2 of cross-validation data. The results are also plotted in Figure 10.5, Figure 10.6 and Figure 10.7 for the approaches with four, three and two sources, respectively. These figures show the statistical values of RMSE and R^2 obtained for each model built. The multivariate models, spectral pre-processing techniques and spectral ranges were compared statistically for each approach (six, three and two sources).

10.3.1.1 Effect of multivariate models

The statistical modelling results were considered satisfactory for both multivariate models, with errors remaining always below 10%, with the exception of the PLSR model adjusted for the CR.SGF source, which presented values slightly above this 10-% threshold (Figure 10.5). Errors below ±10% can be considered as acceptable in sediment tracing studies (Collins et al., 1997), so that most alternatives presented in this research can be applied to trace sediment sources. A significant difference between models was observed for those approaches with two and six sources, where the SVM provided better R^2 (>0.94) and RMSE (<4.85) values compared to the PLSR (R^2 > 0.87 and RMSE < 6.52%) (Table 10.2). For the approach with three sources, SVM also provided better R^2 and RMSE values, although no significant difference was observed (Table 10.2). Similar results were observed in the study developed in the Conceição catchment, where the SVM provided better results compared to PLSR (Chapter 3). The ability of SVM model to handle non-linear relationships between spectrum and soil/sediment properties result in a better fit of the model compared to the PLSR (Viscarra Rossel and Behrens, 2010; Wijewardane et al., 2016). Although the SVM model showed the best results, the gains over the PLSR model can be minimized when using adequate combination of spectral range and pre-processing. For example, combining the NIR spectral range with SNV pre-processing and PLSR model, results in high R^2 and very low RMSE values,

comparable to the best fits obtained by the SVM model, regardless the number of sources considered (Figure 10.5,Figure 10.6 and Figure 10.7). The use of PLSR models for predicting soil properties and also for sediment fingerprinting has been widely used in the literature (Evrard et al., 2013; Ni et al., 2019; Poulenard et al., 2009; Vercruysse and Grabowski, 2018). Tiecher et al. (2017, 2016, 2015) compared the predictions of PLSR model calibrated with UV, NIR and MIR spectra with the predictions obtained with geochemical fingerprints introduced into a mixing model applied to a small headwater catchment (1.23 km^2). The difference between the two methods was below 20% for the approaches with UV and NIR spectra, and for the latter, the differences were minimal. However, the approach with the MIR spectra, resulted in differences of approximately 20%. Uber et al. (2019) also compared the PLSR model with other mixing models based on a mass balance approach and obtained different results with each model. The authors suggested to use more than one model to predict sediment sources when possible to avoid biased results from one type of error. As already stated by other authors, and since there is no consensus in the literature on how to define the best prediction models and the best pre-processing method, conducting preliminary tests considering different models is highly recommended (Tiecher et al., 2021; Uber et al., 2019).

Table 10.2. Comparison of spectroscopic models accuracy indicated by R^2 and RMSE as affected by pre-processing technique and spectral range using PLSR and SVM methods considering four, three and two potential sources of sediments.

Variable	Pre-processing / Spectral range	Six sediment sources (CR.BF, CR.SGF, NG.BF, NG.SGF, SS.BF, SS.SGF)		Three sediment sources (cropland, native grassland, subsurface)		Two sediment sources (surface, subsurface)	
		PLSR	SVM	PLSR	SVM	PLSR	SVM
RMSE	Raw spectra	3.56 a	4.67 a	3.52 a	4.85 a	2.96 a	2.87 a
	Standard normal variate	4.27 a	2.11 b	3.78 a	2.33 b	2.94 a	2.01 b
	Detrend	4.06 a	1.94 b	3.98 a	2.21 b	2.83 a	2.09 b
	Savitzky-Golay Derivate	3.39 a	1.93 b	3.07 a	2.23 b	2.84 a	2.17 b
	Ultra-violet-visible (UV)	6.52 a	3.34 a	6.05 a	3.77 a	4.11 a	2.68 a
	Near-infrared (NIR)	2.25 b	2.22 b	1.55 b	2.42 a	2.22 b	2.19 b
	UV+NIR	2.69 b	2.43 b	3.16 b	2.51 a	2.35 b	2.05 b
	Mean	**3.82 Aa**	**2.66 Ab**	**3.59 Aa**	**2.90 Aa**	**2.89 Aa**	**2.31 Ab**
R^2	Raw spectra	0.96 a	0.94 b	0.97 a	0.95 b	0.99 a	0.99 a
	Standard normal variate	0.94 a	0.99 a	0.96 a	0.99 a	0.99 a	0.99 a
	Detrend	0.94 a	0.99 a	0.96 a	0.99 a	0.98 a	0.99 a
	Savitzky-Golay Derivate	0.95 a	0.99 a	0.98 a	0.99 a	0.99 a	0.99 a
	Ultra-violet-visible (UV)	0.87 b	0.96 b	0.93 b	0.97 a	0.98 b	0.99 b
	Near-infrared (NIR)	0.99 a	0.99 a	0.99 a	0.99 a	0.99 a	0.99 a
	UV+NIR	0.98 a	0.98 a	0.98 a	0.99 a	0.99 a	0.99 a
	Mean	**0.95 Bb**	**0.98 Aa**	**0.97 ABa**	**0.98 Aa**	**0.99 Aa**	**0.99 Aa**

Means followed by the same low case letters in the column, comparing pre-processing techniques and spectral ranges, are not significantly different according to the Tukey test at *p<0.05*. Means followed by the same capital letters in the raw, comparing the number of sediment sources considered, are not significantly different according to the Tukey test at *p<0.05*. Means followed by the same low case letters in the raw, comparing multivariate models, are not significantly different according to the Tukey test at *p<0.05*. Partial Least Square Regression – PLSR; Support Vector Machine – SVM; Ultra-violet-visible – UV; Near Infrared – NIR. Cropland at Botucatu Formation – CR.BF, Cropland at Serra Geral Formation – CR.SGF, Native Grassland at Botucatu Formation – NG.BF, Native Grassland at Serra Geral Formation – NG.SGF, Subsurface source at Botucatu Formation – SS.BF, Subsurface source at Serra Geral Formation – SS.SGF.

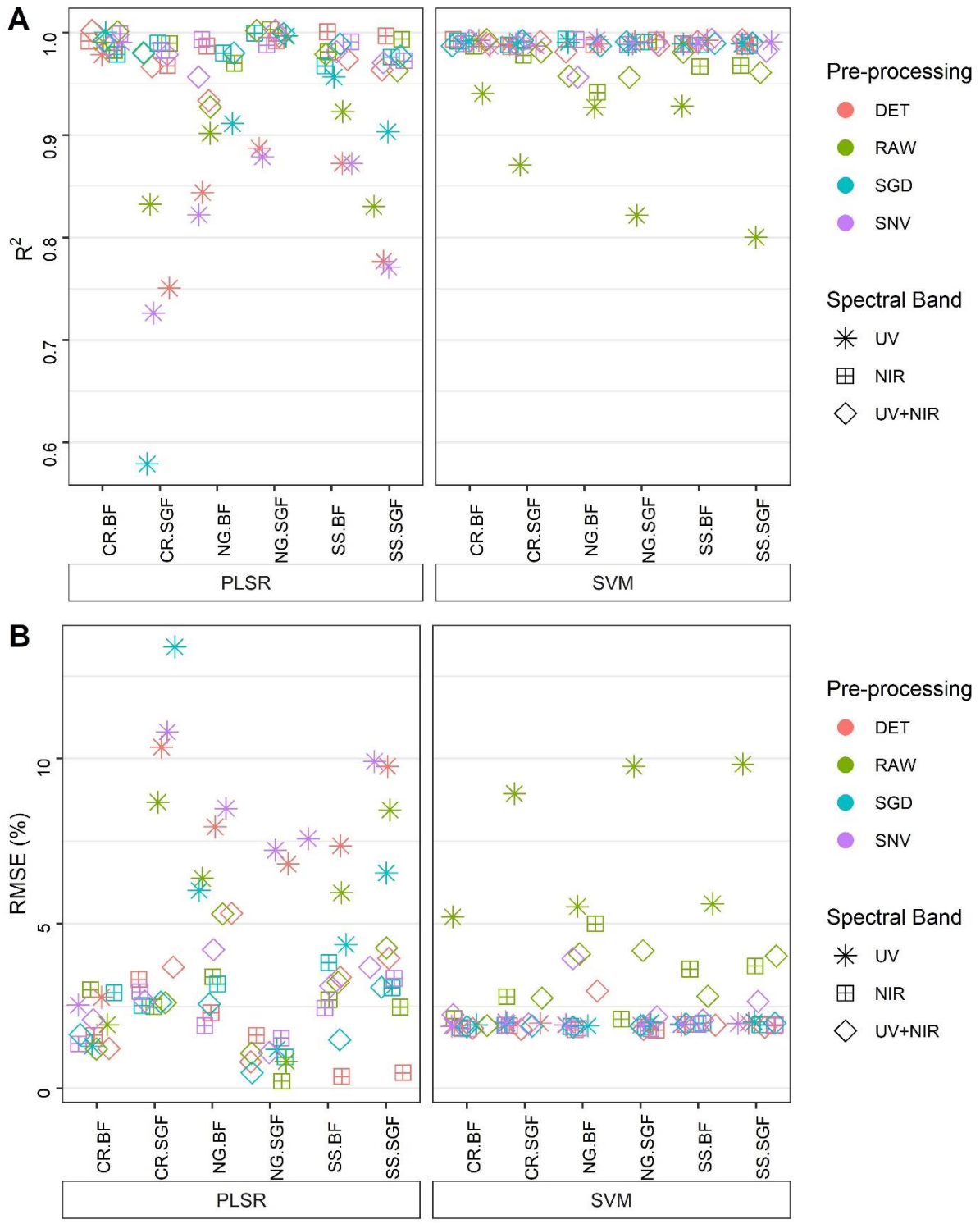

Figure 10.5. Comparison of spectroscopic models accuracy indicated by R^2 and RMSE (root mean square error) as affected by pre-processing technique and spectral range using PLSR and SVM methods for the first approach with six sediment sources and different combinations of pre-processing techniques and spectral ranges.

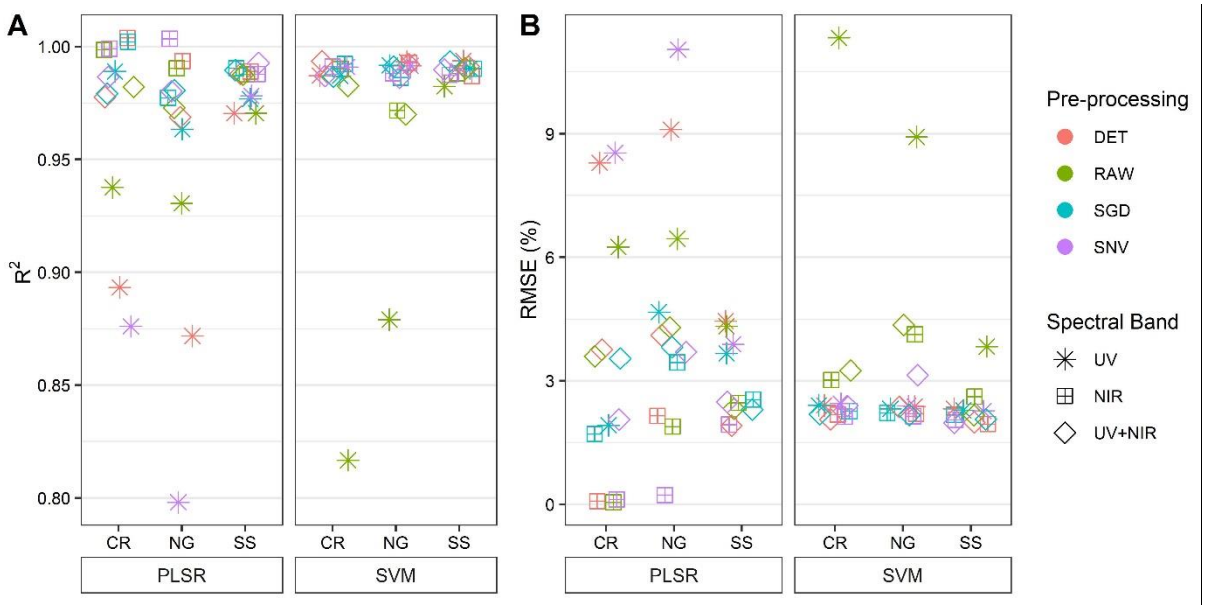

Figure 10.6. Comparison of spectroscopic models accuracy indicated by R^2 and RMSE (root mean square error) as affected by pre-processing technique and spectral range using PLSR and SVM methods for the second approach with three sediment sources and different combinations of pre-processing techniques and spectral ranges.

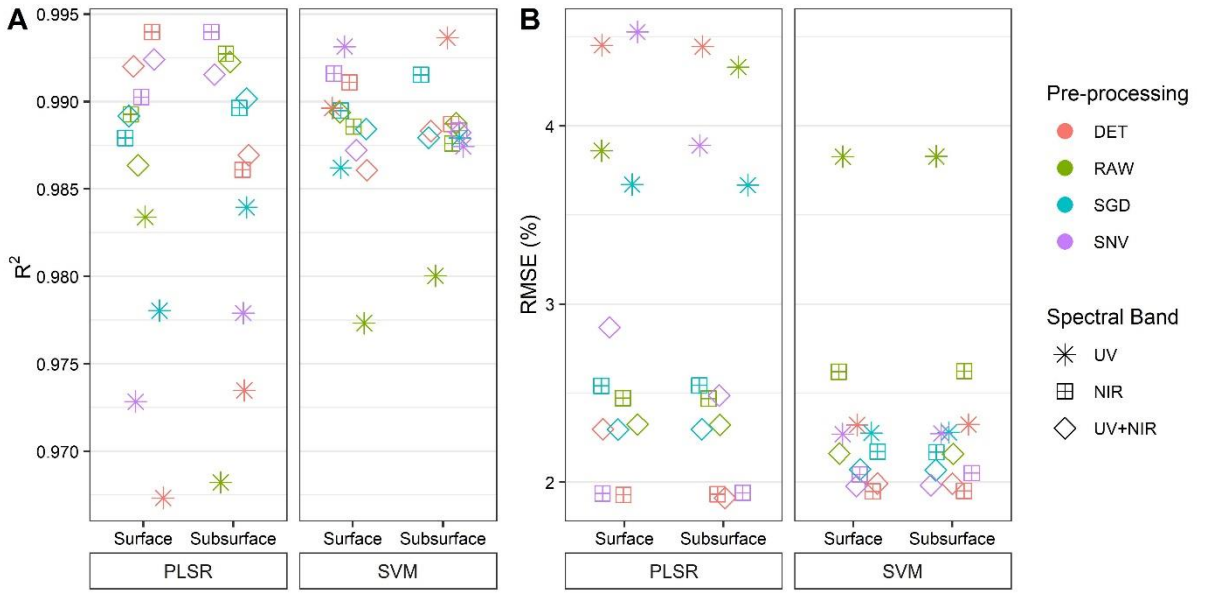

Figure 10.7. Comparison of spectroscopic models accuracy indicated by R^2 and RMSE (root mean square error) as affected by pre-processing technique and spectral range using PLSR and SVM methods for the first approach with two sediment sources and different combinations of pre-processing techniques and spectral ranges.

10.3.1.2 Effect of pre-processing techniques

Three pre-processing techniques of the RAW spectra were tested. For the SVM model, both techniques (SNV, DET and SGD) provided significantly lower RMSE

compared to the RAW spectra (Table 10.2). When using the PLSR model, no significant difference was observed between pre-processing techniques. For the SVM, in the approaches with six and three sources, it was observed an absolute reduction of 2 to 3% in the RMSE, and an increase of 4 to 5% in the R^2 for the three pre-processing techniques in relation to the RAW spectra. For the approach with two sources, besides the significant difference obtained between the RAW spectra and pre-processed ones, the differences between them was less than 1% (min of 2.01 to max of 2.87%). Tiecher et al. (2021) suggests that the variability between sources due to different geologies, soil types and contrasting soil carbon contents would result in a limited improvement of predictive models by the pre-processing technique. This situation is also observed in the Ibirapuitã catchment, where multiple soil types with contrasting characteristics are found, such as Acrisols, Regosols, Planosols, Vertisols and Ferralsols, and also contrasting land uses, such as flooded rice, grassland and soybean cropland. However, a similar impact of the pre-processing methods was also observed for the Conceição catchment which has very homogeneous soil types and land uses (Chapter 3). The minor improvement resulted from the pre-processing techniques in the current research and in that developed in the Conceição catchment, it may be related to the large number of artificial mixtures used to calibrate and validate the model, 97 and 120, respectively. The number of artificial mixtures used in these studies are high compared to those found in previous articles that prepared a lower number of artificial mixtures, such as Tiecher et al. (2017, 2016) with 48, Poulenard et al. (2012) with 45, Evrard et al. (2013) with 20 to 30 and Sellier et al. (2020) with 21. In addition, the low RMSE values and the low improvement achieved with the application of pre-processing techniques may be related to the calibration process. The cross-validation method associated with a large number of samples, may reduce the effect of pre-processing techniques by finding the best adjustment regardless the pre-processing technique.

10.3.1.3 Effect of spectral ranges

Ultra-violet-visible (UV) and near infrared (NIR) spectra were analysed in this study. Both were used individually and combined as tracers in the multivariate models (PLSR and SVM) calibrated with artificial mixtures with known proportions to predict sediment source contributions. The UV spectra alone provided the worst statistical results compared to the NIR and UV+NIR combined. Similar results were observed for the Conceição catchment, where the UV alone provided the least satisfactory results (Chapter

3). A higher RMSE value was also observed by Tiecher et al. (2021) in the Arvorezinha catchment when using UV spectra compared to NIR and MIR, especially for predicting the cropland source contribution. The UV spectral curve is highly influenced by the clay content and that in iron oxides (Viscarra Rossel and Behrens, 2010). However, samples with high variations in organic carbon contents, as observed under cropland and native grassland (Chapter 4), can affect the model calibration, since the organic matter can influence the albedo and the spectral shape resulting in a high RMSE (Tiecher et al., 2021; Viscarra Rossel and Behrens, 2010). The NIR spectral range (1000-2500 nm) can provide more information than the UV spectra (200-800 nm), which is able to detect clay minerals and also organic matter features (Viscarra Rossel and Behrens, 2010). Besides that, in the NIR spectral range, absorption features related to 2:1 clay minerals (e.g. smectite, vermiculite, mica) can be detected, which are very common in soils of the region of interest (Melfi et al., 2004).

10.3.1.4 Effect of number of sediment source considered

There was no effect on the number of sources considered in the model's accuracy as indicated by RMSE, both for the PLSR models and for the SVM models (Table 10.2). However, when considering six and two sources, the SVM models resulted in smaller errors compared to the PLSR models. In addition, according to Legout et al. (2013), a well-fitted model does not mean that it will perform well in predicting the source contributions. Since the models are fitted individually for each source, the contribution of the sources is not forced to sum to 100%. Consequently, the sum of the contributions from each source has also been used as an indication of the quality of the method, with sums very different from 100% indicating the occurrence of a problem in the approach (Poulenard et al., 2012; Tiecher et al., 2021; Uber et al., 2019; Valente et al., 2020). In this study, the sum of the source contributions in the framework of the approach with six sources was higher than 500% for all models and combinations of spectral range and pre-processing treatments (Table 10.3). Several interpretations can be deduced from this result. The first is the fact that considering a greater number of sources, results in the need to sum the uncertainties associated with a greater number of models. Second, in the case of a large and heterogeneous catchment such as the Ibirapuitã River, it allows the sediment characteristics to be very heterogeneous and, potentially, to behave unconservatively. A third possibility is that there is no sufficient discrimination between the samples from the different sources, which has already been observed on the basis of

organic matter composition and colour parameters for cropland and native grassland (Chapter 4). To improve these results, other alternative tracers could help in better discriminating between sources, such as environmental DNA and compound-specific stable isotopes (CSSI), which are theoretically more powerful to discriminate between contrasted land uses (Alewell et al., 2016; Evrard et al., 2019b).

High sums of source contributions were also observed for the three-source approach, despite the lower range amplitudes, which still results in a high uncertainty. In this case, sums over 175% were calculated, exceeding what would be acceptable (Figure 10.8). In contrast, for the approach with two sources, some combinations of multivariate models, spectral ranges and pre-processing techniques, resulted in sums of 100%, exactly (Figure 10.9). This was the case for the approach with PLSR and SVM models combined with UV+NIR spectral range and the RAW spectra and SGD pre-processing. This results suggests that the similarity of cropland and native grassland properties, that were merged in the approach with two sources, may have increased the uncertainty observed in the other approaches where they were considered as individual sources.

Table 10.3. Mean of the absolute sum of source contributions to individual sediment samples predicted by the PLSR and SVM models considering all pre-processing for each spectral range.

Spectral range	**Six sediment sources** (CR.BF, CR.SGF, NG.BF, NG.SGF, SS.BF, SS.SGF)		**Three sediment sources** (cropland, native grassland, subsurface)		**Two sediment sources** (surface, subsurface)	
	PLSR	SVM	PLSR	SVM	PLSR	SVM
	---------- % ----------					
UV	524.3 a	507.6 b	175.9 a	188.2 a	141.6 a	145.4 a
NIR	748.5 a	807.9 a	249.3 a	299.5 a	109.9 a	113.4 a
UV+NIR	622.2 a	627.9 ab	178.3 a	184.2 a	102.9 a	100.1 a

Means followed by the same low case letters in the column, comparing spectral ranges, are not significantly different according to the Tukey test at $p<0.05$. Partial Least Square Regression – PLSR; Support Vector Machine – SVM; Ultra-violet-visible – UV; Near Infrared – NIR. Cropland at Botucatu Formation – CR.BF, Cropland at Serra Geral Formation – CR.SGF, Native Grassland at Botucatu Formation – NG.BF, Native Grassland at Serra Geral Formation – NG.SGF, Subsurface source at Botucatu Formation – SS.BF, Subsurface source at Serra Geral Formation – SS.SGF.

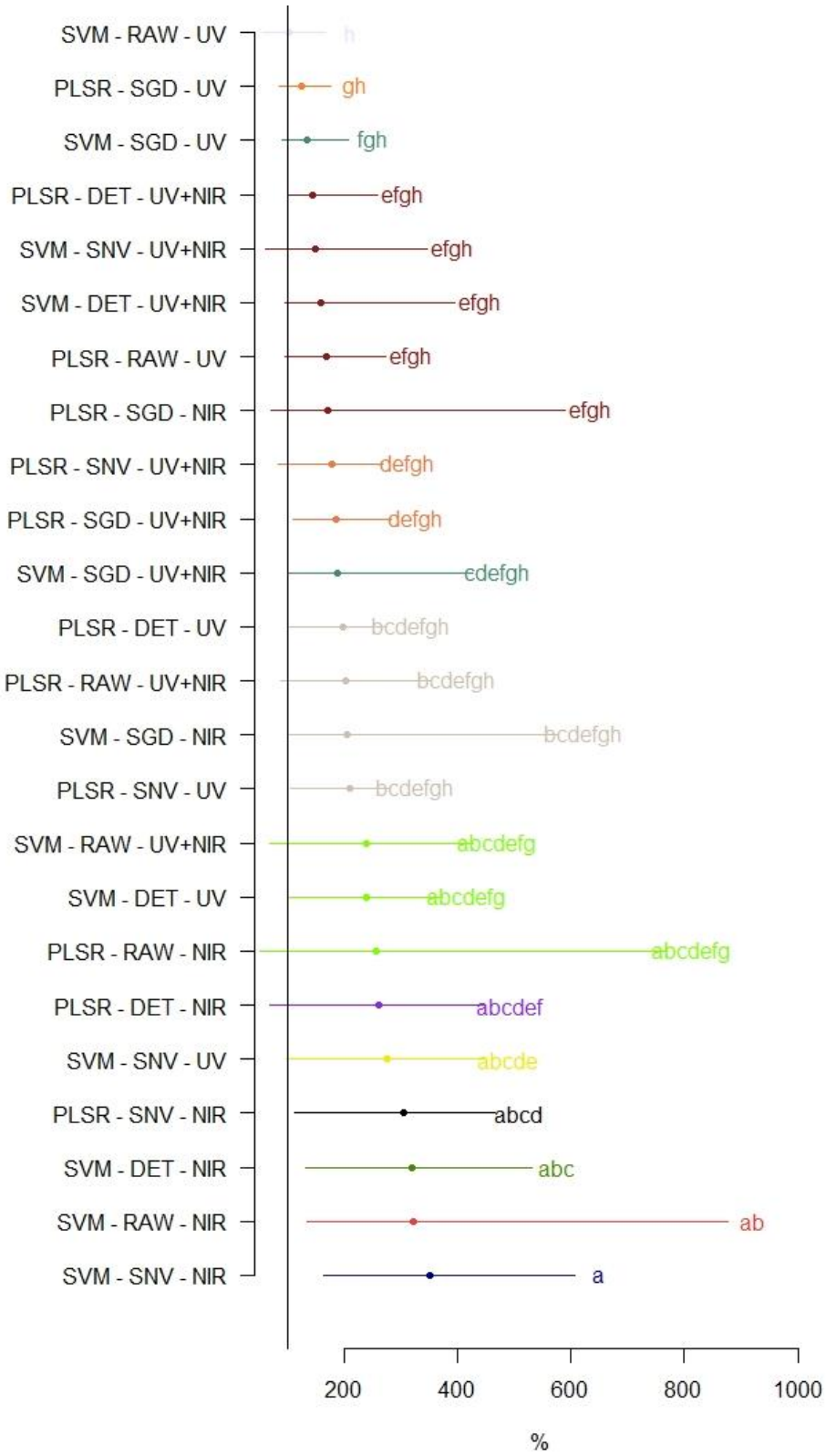

Figure 10.8. Comparison of the absolute sum of sediment source contributions predicted using different combinations of multivariate model, pre-processing technique, and spectral range, considering three potential sediment sources (cropland, native grassland and subsurface). The vertical black line indicates the 100%. Means followed by

the same low case letters are not significantly different by the Tukey test at $p<0.05$. Statistically equal means are grouped by colour.

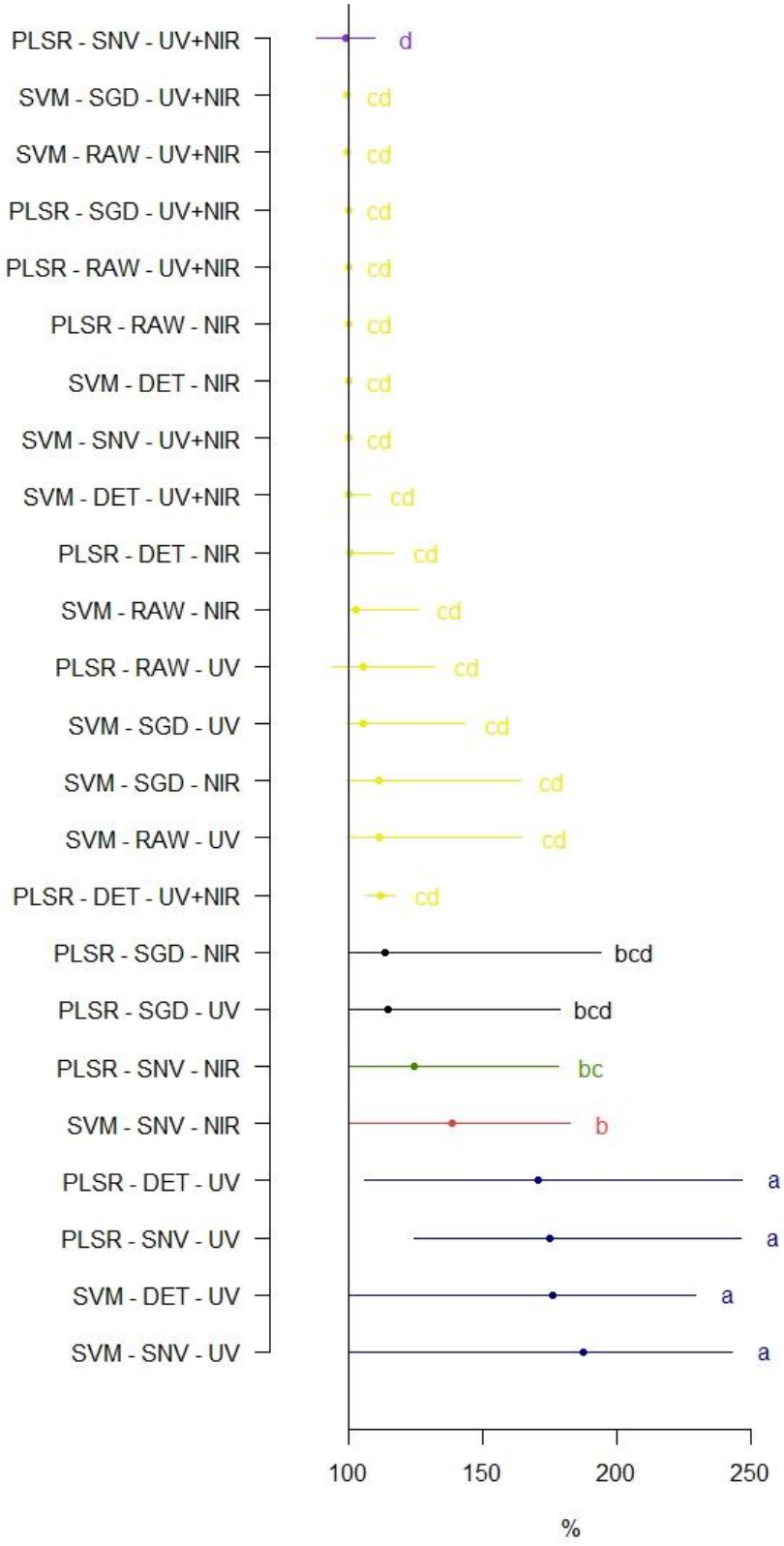

Figure 10.9. Comparison of the absolute sum of sediment source contributions predicted using different combinations of multivariate model, pre-processing technique, and spectral range, considering two potential sediment sources (surface and subsurface).

The vertical black line indicates the 100%. Means followed by the same low case letters are not significantly different by the Tukey test at $p<0.05$. Statistically equal means are grouped by colour.

10.3.2 Sediment source contributions

Due to the high uncertainties observed for the approaches considering six and three sources, the resulting source contributions to the sediment are neither presented nor discussed. For the approach with two sources, more than one combination of multivariate models, spectral ranges and pre-processing techniques provided sum of source contribution close to 100%, indicating good quality and reliability of the models (Legout et al., 2013). Accordingly, Figure 10.10 shows the contributions of surface and subsurface sources to each sediment sample analysed in this study. The SVM and PLSR prediction results for the combination of the UV+NIR spectral range with the RAW spectra and after the SGD pre-processing technique is also shown. The results indicate that both multivariate models (PLSR and SVM) can lead to very similar predictions, which is positive. However, the results show that depending on the pre-processing technique applied (RAW or SGD), there can be a difference in the model predictions, with the need to be even more careful when choosing the method to be used and when interpreting the results.

In the current research, we selected the PLSR model because it was the one that presented a sum of contributions exactly equal to 100%, both for SGD pre-processing and RAW spectrum. Spectrum pre-processing is essential to remove systematic variations, effects of the equipment and analysis conditions, as well as to reduce multicollinearity (Dotto et al., 2017). For this reason, the results obtained by SGD pre-processing were considered to be more appropriate compared to those obtained with the RAW spectrum. Besides that, the SGD was already reported as one of the best pre-processing methods (Knox et al., 2015; Moura-Bueno et al., 2019; Tiecher et al., 2021). Furthermore, the results obtained are also consistent with the results of a previous study conducted in the same catchment (Chapter 4). Figure 10.11 shows the relationships between the source predictions obtained by the spectroscopy method (PLSR-UV+NIR-SGD) against those resulting from the mixing model that made use of the composition of the organic matter, radionuclide activities and colour parameters, as potential tracers of the sediment sources. Although the results are not fully similar, they show a similar trend,

demonstrating that subsurface sources supplied the main sediment source for the samples evaluated.

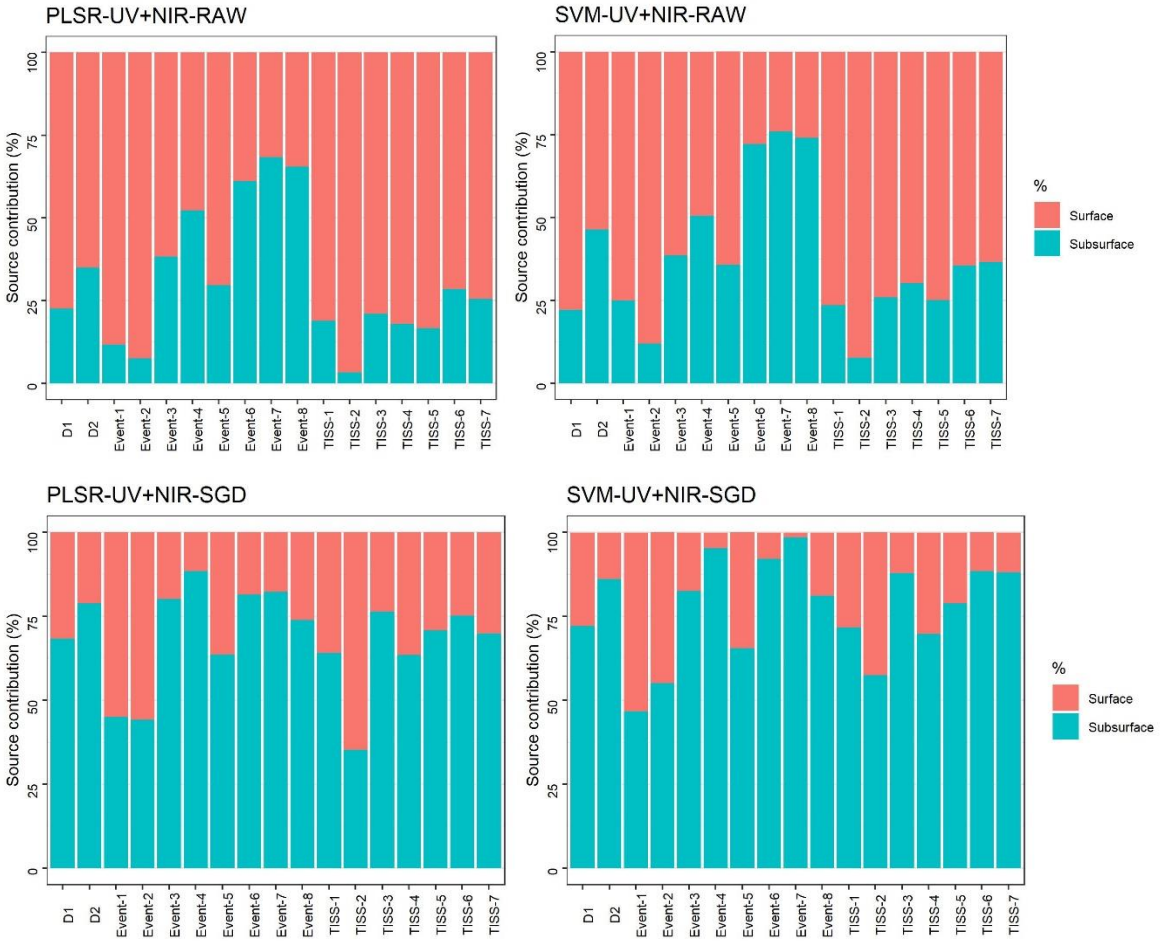

Figure 10.10. Source contributions to sediment for the approaches considering two potential sources using different combinations of multivariate model, spectral pre-processing and spectral range.

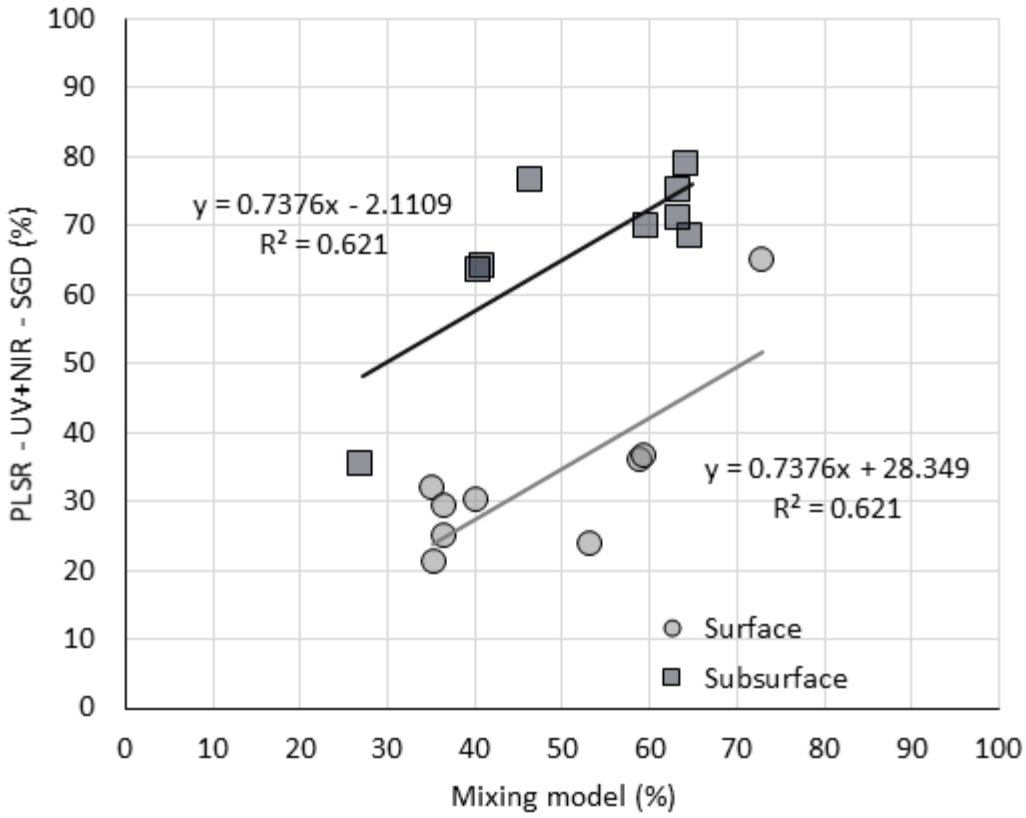

Figure 10.11. Comparison of sediment source contributions predicted by spectroscopy based on PLSR-UV+NIR-SGD model and by the mixing model based on conventional tracing properties (Chapter 4).

When comparing the sediment source contributions from the spectroscopy approach with the previous one based on discrete variables derived from soil composition (Chapter 4) for each individual samples, differences were in their majority below 20% (Figure 10.12b). Both approaches have shown a similar trending about the main sediment source, indicating subsurface source to be more relevant. The mixing model present a wide variation in source contribution between sediment samples when comparted to the spectroscopy approach. Due to the limited number of variables taking into account in the mixing model, it can be more sensitive to some variation in the tracer values.

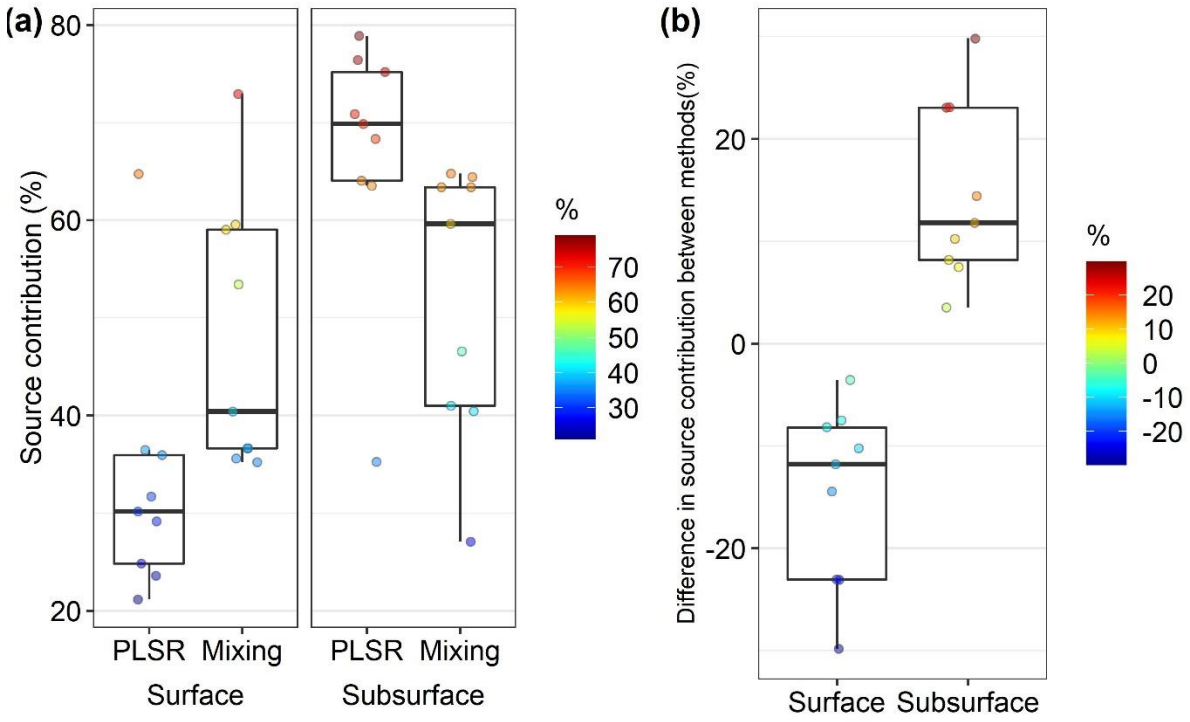

Figure 10.12. Sediment source contributions predicted by spectroscopy based on PLSR-UV+NIR-SGD (PLSR) model and by the mixing model (Mixing) based on conventional tracing properties (Chapter 4) (a). Difference between the prediction of each method for individual sediment samples (b).

The sediment samples were collected during a period of almost one year. The results presented are therefore only representative of the processes that occurred during the monitored period. Collecting samples during a longer period of time would be useful to obtain more robust conclusions regarding the main erosion processes occurring in the catchment. Even though, based on the current results, subsurface is likely to provide the main source, which is a consequence of the widespread erosion occurring in the channels and on the riverbanks, erosion processes that can immediately be observed in the catchment (Figure 10.13).

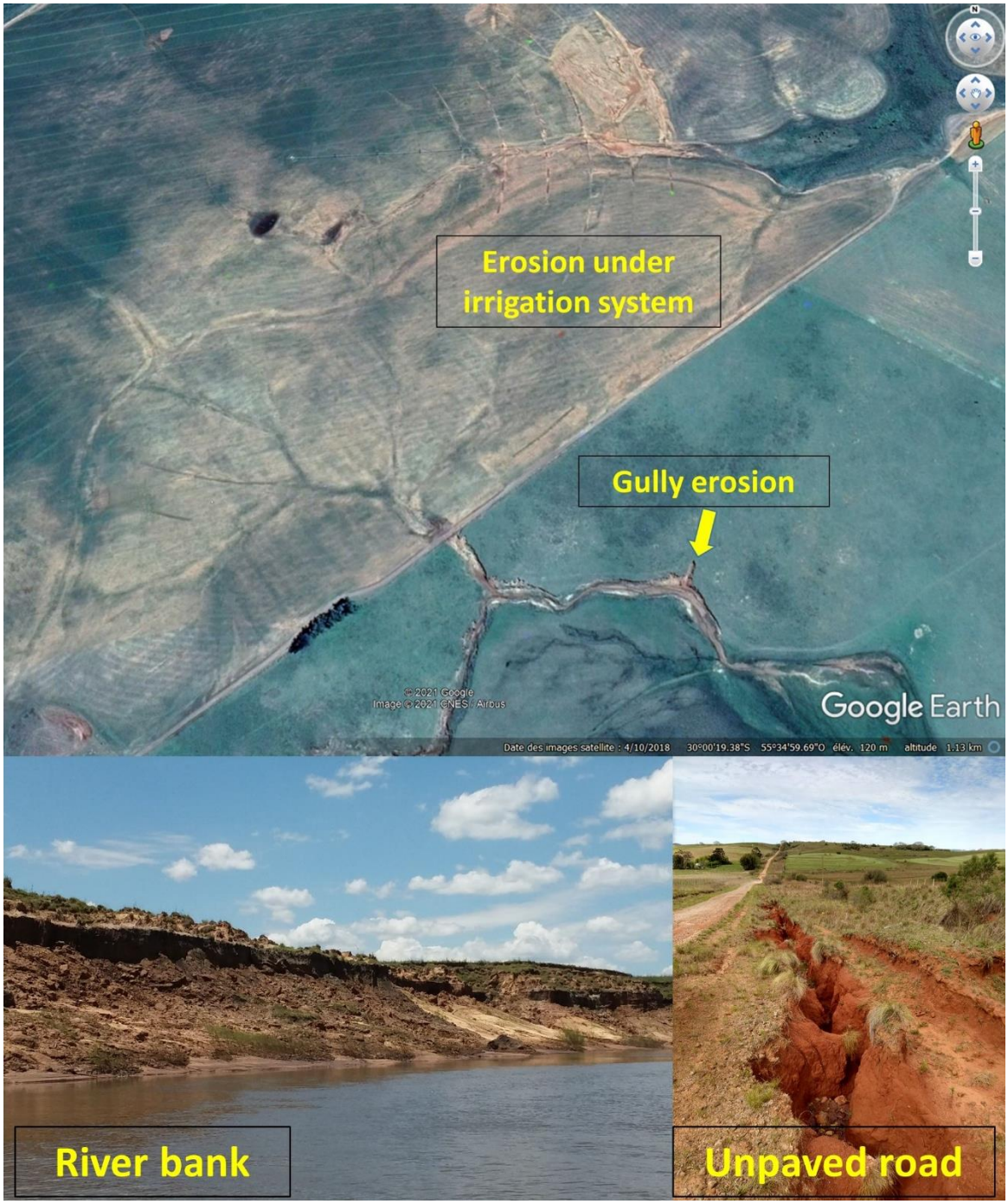

Figure 10.13. Images of erosion hotspots in the catchment, representing the subsurface sources.

Subsurface contribution was higher in almost all samples and at all sediment sampling sites (Figure 10.14), with the exception of the Caverá stream catchment, where for two samples, surface material supplied the main source. The Caverá stream catchment is the tributary with the highest proportion of cropland and where land use change has mainly occurred in the last years. This sub-catchment is also characterised by the occurrence of soils with a high susceptibility to erosion, such as the Acrisols. Although

the current results are not fully conclusive, the degradation of grasslands as well as the increase of soybean production areas, will likely further accelerate soil degradation and erosion, as outlined in the previous study (Chapter 4). In addition, it is possible to verify that there is a slightly greater contribution of surface sources in the outlet (33.3%) and PP sub-catchment (30.4%) compared to the portion of the Ibirapuitã catchment with the lowest cropland area (EPA – 21.4% of contribution from surface). The EPA catchment is mainly covered with native grassland. However, the undulated landscape, the absence of riparian zones, and the formation of cattle preferential paths can favour the concentration of large volumes of surface runoff in channels and subsequent erosion and gully formation. Samples collected at the outlet also mainly originated from subsurface source, whereas surface contribution reached a median value of 33% approximately. Similar findings were observed for the Pai-Passo stream catchment, where surface contribution was around 30%, slightly higher than the EPA catchment, which may be a consequence of the higher proportion of cropland in the Pai-Passo stream catchment. Although the contribution of surface sources is not dominant, care should be taken with soil management and land conservation in areas under native grassland and cropland to increase the sustainable character of production systems and avoid the acceleration of erosion processes further upstream in the near future.

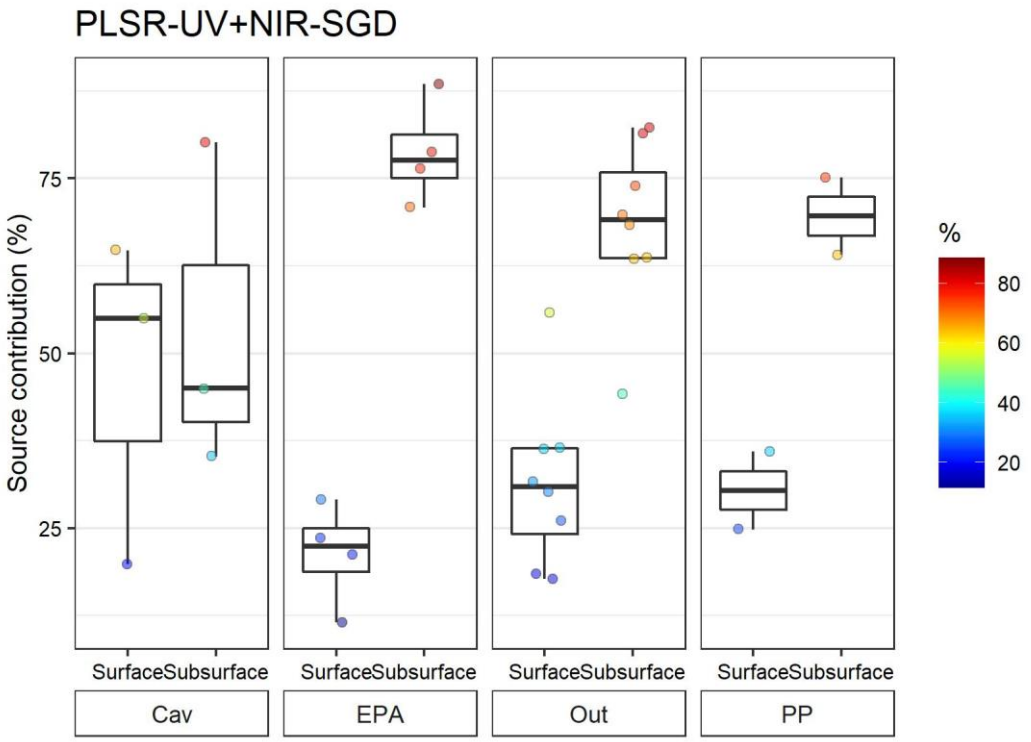

Figure 10.14. Sediment source contributions according to the tributaries, predicted from the PLSR-UV+NIR-SGD models. Cav = Caverá stream catchment; EPA = Environmental Protection Area catchment; Out = Main outlet; and PP = Pai-Passo stream catchment.

Three sediment sampling methods were carried out, including the deployment of TISS, sampling of water during rainfall-runoff events and collection of two flood deposit samples after a major storm that occurred in January 2019. For the three methods, the majority of sediment samples originated from subsurface as the main source (Figure 10.15).

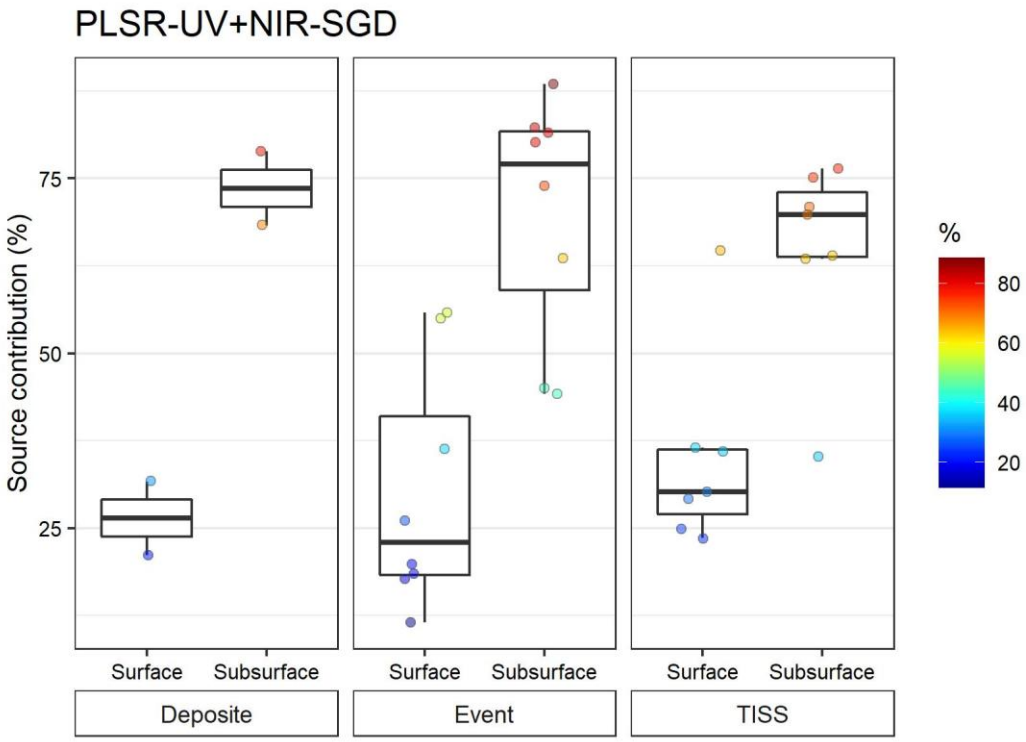

Figure 10.15. Sediment source contributions according to the sampling method predicted from the PLSR-UV+NIR-SGD models. Event = Rainfall runoff event; FBS = Fine bed sediment samples; and TISS = Time integrated suspended sediment samples.

The method implemented in this study illustrates the difficulties of applying the sediment fingerprinting technique in such heterogeneous environments. So far, no tracer nor method has been found to be totally efficient in all cases. When selecting tracers, it is absolutely crucial to take into account those that show a strong physic-chemical basis supporting the discrimination between sources. The use of spectroscopy-based tracing in combination with mathematical and statistical tools through R programming, can facilitate the achievement of multiple tests and models in order to identify the best approach in each situation. Future studies incorporating the analyses of land use-based tracers, such as environmental DNA and CSSI (compound-specific stable isotope), will likely have the potential to increase the discrimination between sources and provide more accurate results in the context of large and heterogeneous agricultural catchment found in subtropical environments.

10.4 Conclusions

The use of diffuse reflectance spectroscopy was not very efficient for predicting sediment source contributions when considering multiple potential origins in a large and heterogeneous catchment, such as the Ibirapuitã River. Reducing the source number

under consideration provided an alternative to reduce uncertainties and obtain robust results regarding the main erosion processes occurring in the catchment. This is the first approach trying to implement this alternative technique in a catchment covering more than a 1000 km^2, and more research is needed at this catchment scale to confirm and further detail the preliminary results obtained in this study. Despite the optimal fit of the multivariate models, their performance in predicting the contribution of sediment sources was limited by the model performance. The Pampa biome is a fragile ecosystem that deserves attention to limit soil degradation. The most recent increase of agricultural commodity prices may lead to an intensive exploitation of the region for agriculture, which requires good soil management practices to avoid irreversible soil degradation and excessive sediment delivery to the river systems. This study provides a solid basis to help local managers implementing more assertive mitigation measures to reduce soil degradation and sediment delivery to the river networks of this fragile area in the future.

10.5 References

Alewell, C., Birkholz, A., Meusburger, K., Schindler Wildhaber, Y., Mabit, L., 2016. Quantitative sediment source attribution with compound-specific isotope analysis in a C3 plant-dominated catchment (central Switzerland). Biogeosciences 13, 1587–1596. https://doi.org/10.5194/bg-13-1587-2016

Alvares, C.A., Stape, J.L., Sentelhas, P.C., de Moraes Gonçalves, J.L., Sparovek, G., 2013. Köppen's climate classification map for Brazil. Meteorol. Zeitschrift 22, 711–728. https://doi.org/10.1127/0941-2948/2013/0507

Barnes, R.J., Dhanoa, M.S., Lister, S.J., 1989. Standard Normal Variate Transformation and De-Trending of Near-Infrared Diffuse Reflectance Spectra. Appl. Spectrosc. 43, 772–777. https://doi.org/10.1366/0003702894202201

Collins, A.L., Pulley, S., Foster, I.D.L., Gellis, A., Porto, P., Horowitz, A.J., 2017. Sediment source fingerprinting as an aid to catchment management: A review of the current state of knowledge and a methodological decision-tree for end-users. J. Environ. Manage. 194, 86–108. https://doi.org/10.1016/j.jenvman.2016.09.075

Collins, A.L., Walling, D.E., Leeks, G.J.L., 1997. Source type ascription for fluvial suspended sediment based on a quantitative composite fingerprinting technique. Catena 29, 1–27. https://doi.org/10.1016/S0341-8162(96)00064-1

Dotto, A.C., Dalmolin, R.S.D., Caten, A. ten, Gris, D.J., Ruiz, L.F.C., 2019. AlradSpectra: a

Quantification Tool for Soil Properties Using Spectroscopic Data in R. Rev. Bras. Ciência do Solo 43, 1–15. https://doi.org/10.1590/18069657rbcs20180263

Dotto, A.C., Dalmolin, R.S.D., Grunwald, S., ten Caten, A., Pereira Filho, W., 2017. Two preprocessing techniques to reduce model covariables in soil property predictions by Vis-NIR spectroscopy. Soil Tillage Res. 172, 59–68. https://doi.org/10.1016/j.still.2017.05.008

Evrard, O., Laceby, J.P., Ficetola, G.F., Gielly, L., Huon, S., Lefèvre, I., Onda, Y., Poulenard, J., 2019. Environmental DNA provides information on sediment sources: A study in catchments affected by Fukushima radioactive fallout. Sci. Total Environ. 665, 873–881. https://doi.org/10.1016/j.scitotenv.2019.02.191

Evrard, O., Poulenard, J., Némery, J., Ayrault, S., Gratiot, N., Duvert, C., Prat, C., Lefèvre, I., Bonté, P., Esteves, M., 2013. Tracing sediment sources in a tropical highland catchment of central Mexico by using conventional and alternative fingerprinting methods. Hydrol. Process. 27, 911–922. https://doi.org/10.1002/hyp.9421

Fukase, E., Martin, W., 2020. Economic growth, convergence, and world food demand and supply. World Dev. 132, 104954. https://doi.org/10.1016/j.worlddev.2020.104954

IBGE, 2018. Mapeamento de Recurso Naturais do Brasil: Escala 1:250.000.

Knox, N.M., Grunwald, S., McDowell, M.L., Bruland, G.L., Myers, D.B., Harris, W.G., 2015. Modelling soil carbon fractions with visible near-infrared (VNIR) and mid-infrared (MIR) spectroscopy. Geoderma 239–240, 229–239. https://doi.org/10.1016/j.geoderma.2014.10.019

Laceby, J.P., Evrard, O., Smith, H.G., Blake, W.H., Olley, J.M., Minella, J.P.G., Owens, P.N., 2017. The challenges and opportunities of addressing particle size effects in sediment source fingerprinting: A review. Earth-Science Rev. 169, 85–103. https://doi.org/10.1016/j.earscirev.2017.04.009

Legout, C., Poulenard, J., Nemery, J., Navratil, O., Grangeon, T., Evrard, O., Esteves, M., 2013. Quantifying suspended sediment sources during runoff events in headwater catchments using spectrocolorimetry. J. Soils Sediments 13, 1478–1492. https://doi.org/10.1007/s11368-013-0728-9

McBratney, A.B., Minasny, B., Viscarra Rossel, R., 2006. Spectral soil analysis and inference systems: A powerful combination for solving the soil data crisis. Geoderma 136, 272–278. https://doi.org/10.1016/j.geoderma.2006.03.051

Melfi, A.J., Montes, C.R., Carvalho, A., Forti, M.C., 2004. Use of pedological maps in the

identification of sensitivity of soils to acidic deposition: Application to Brazilian soils. An. Acad. Bras. Cienc. 76, 139–145. https://doi.org/10.1590/S0001-37652004000100012

Mengue, V.P., Dias de Freitas, M.W., Silva da Silva, T., Fontana, D.C., Scottá, F.C., 2020. LAND-USE and land-cover change processes in Pampa biome and relation with environmental and socioeconomic data. Appl. Geogr. 125. https://doi.org/10.1016/j.apgeog.2020.102342

Mevik, B.-H., Wehrens, R., Liland, K.H., 2016. Partial Least Squares and Principal Component Regression. Packag. R CRAN.

Meyer, D., Dimitriadou, E., Hornik, K., Weingessel, A., Leisch, F., Chang, C.-C., Lin, C.-C., 2019. Misc Functions of the Department of Statistics, Probability Theory Group (Formerly: E1071), TU Wien. R Packag. version 1.7-3.

Minella, J.P.G., Merten, G.H., Barros, C.A.P. de, Ramon, R., Schlesner, A., Clarke, R.T., Moro, M., Dalbianco, L., 2017. Long-term sediment yield from a small catchment in southern Brazil affected by land use and soil management changes. Hydrol. Process. https://doi.org/10.1002/hyp.11404

Minella, J.P.G., Merten, G.H., Walling, D.E., Reichert, J.M., 2009. Changing sediment yield as an indicator of improved soil management practices in southern Brazil. CATENA 79, 228–236. https://doi.org/10.1016/j.catena.2009.02.020

Moura-Bueno, J.M., Dalmolin, R.S.D., ten Caten, A., Dotto, A.C., Demattê, J.A.M., 2019. Stratification of a local VIS-NIR-SWIR spectral library by homogeneity criteria yields more accurate soil organic carbon predictions. Geoderma 337, 565–581. https://doi.org/10.1016/j.geoderma.2018.10.015

Ni, L.S., Fang, N.F., Shi, Z.H., Tan, W.F., 2019. Mid-infrared spectroscopy tracing of channel erosion in highly erosive catchments on the Chinese Loess Plateau. Sci. Total Environ. https://doi.org/10.1016/j.scitotenv.2019.06.116

Oliveira, T.E. de, Freitas, D.S. de, Gianezini, M., Ruviaro, C.F., Zago, D., Mércio, T.Z., Dias, E.A., Lampert, V. do N., Barcellos, J.O.J., 2017. Agricultural land use change in the Brazilian Pampa Biome: The reduction of natural grasslands. Land use policy 63, 394–400. https://doi.org/10.1016/j.landusepol.2017.02.010

Overbeck, G.E., Muller, S., Fidelis, A., Pfadenhauer, J., Pillar, V.D., Blanco, C., Boldrini, I.I., Both, R., Forneck, E.D., 2007. Brazil's neglected biome: The South Brazilian Campos. Perspect. Plant Ecol. Evol. Syst. 9, 101–116.

https://doi.org/10.1016/j.ppees.2007.07.005

Phillips, J.M., Russell, M.A., Walling, D.E., 2000. Time-integrated sampling of fluvial suspended sediment: A simple methodology for small catchments. Hydrol. Process. 14, 2589–2602. https://doi.org/10.1002/1099-1085(20001015)14:14<2589::AID-HYP94>3.0.CO;2-D

Poulenard, J., Legout, C., Némery, J., Bramorski, J., Navratil, O., Douchin, A., Fanget, B., Perrette, Y., Evrard, O., Esteves, M., 2012. Tracing sediment sources during floods using Diffuse Reflectance Infrared Fourier Transform Spectrometry (DRIFTS): A case study in a highly erosive mountainous catchment (Southern French Alps). J. Hydrol. 414–415, 452–462. https://doi.org/10.1016/j.jhydrol.2011.11.022

Poulenard, J., Perrette, Y., Fanget, B., Quetin, P., Trevisan, D., Dorioz, J.M., 2009. Infrared spectroscopy tracing of sediment sources in a small rural watershed (French Alps). Sci. Total Environ. 407, 2808–2819. https://doi.org/10.1016/j.scitotenv.2008.12.049

R Core Team, 2020. R: A Language and Environment for Statistical Computing [WWW Document]. URL https://www.r-project.org/

Roesch, L.F., Vieira, F., Pereira, V., Schünemann, A.L., Teixeira, I., Senna, A.J., Stefenon, V.M., 2009. The Brazilian Pampa: A Fragile Biome. Diversity 1, 182–198. https://doi.org/10.3390/d1020182

Sellier, V., Navratil, O., Laceby, J.P., Legout, C., Allenbach, M., Lefèvre, I., Evrard, O., 2020. Combining colour parameters and geochemical tracers to improve sediment source discrimination in a mining catchment (New Caledonia, South Pacific Islands). SOIL Discuss. in review. https://doi.org/https://doi.org/10.5194/soil-2020-48

Silveira, V.C.P., González, J.A., Fonseca, E.L. da, 2017. Land use changes after the period commodities rising price in the Rio Grande do Sul State, Brazil. Ciência Rural 47, 1–7. https://doi.org/10.1590/0103-8478cr20160647

Tiecher, T., Caner, L., Minella, J.P.G., Bender, M.A., dos Santos, D.R., 2016. Tracing sediment sources in a subtropical rural catchment of southern Brazil by using geochemical tracers and near-infrared spectroscopy. Soil Tillage Res. 155, 478–491. https://doi.org/10.1016/j.still.2015.03.001

Tiecher, T., Caner, L., Minella, J.P.G., Evrard, O., Mondamert, L., Labanowski, J., Rheinheimer, D. dos S., 2017. Tracing Sediment Sources Using Mid-infrared Spectroscopy in Arvorezinha Catchment, Southern Brazil. L. Degrad. Dev. 28, 1603–

1614. https://doi.org/10.1002/ldr.2690

Tiecher, T., Caner, L., Minella, J.P.G., Santos, D.R. dos, 2015. Combining visible-based-color parameters and geochemical tracers to improve sediment source discrimination and apportionment. Sci. Total Environ. 527–528, 135–149. https://doi.org/10.1016/j.scitotenv.2015.04.103

Tiecher, T., Moura-Bueno, J.M., Caner, L., Minella, J.P.G.P.G., Evrard, O., Ramon, R., Naibo, G., Barros, C.A.P. de, Silva, Y.J.A.B., Amorim, F.F., Rheinheimer, D.S., 2021. Improving the quantification of sediment source contributions using different mathematical models and spectral preprocessing techniques for individual or combined spectra of ultraviolet–visible, near- and middle-infrared spectroscopy. Geoderma 384, 114815. https://doi.org/10.1016/j.geoderma.2020.114815

Uber, M., Legout, C., Nord, G., Crouzet, C., Demory, F., Poulenard, J., 2019. Comparing alternative tracing measurements and mixing models to fingerprint suspended sediment sources in a mesoscale Mediterranean catchment. J. Soils Sediments 19, 3255–3273. https://doi.org/10.1007/s11368-019-02270-1

Valente, M.L., Reichert, J.M., Legout, C., Tiecher, T., Cavalcante, R.B.L., Evrard, O., 2020. Quantification of sediment source contributions in two paired catchments of the Brazilian Pampa using conventional and alternative fingerprinting approaches. Hydrol. Process. 34, 2965–2986. https://doi.org/10.1002/hyp.13768

Vercruysse, K., Grabowski, R.C., 2018. Using source-specific models to test the impact of sediment source classification on sediment fingerprinting. Hydrol. Process. 32, 3402–3415. https://doi.org/10.1002/hyp.13269

Viscarra Rossel, R.A., Behrens, T., 2010. Using data mining to model and interpret soil diffuse reflectance spectra. Geoderma 158, 46–54. https://doi.org/10.1016/j.geoderma.2009.12.025

Walling, D.E., 1999. Linking land use, erosion and sediment yields in river basins. Hydrobiologia 410, 223–240. https://doi.org/https://doi.org/10.1023/A:1003825813091

Wijewardane, N.K., Ge, Y., Morgan, C.L.S., 2016. Moisture insensitive prediction of soil properties from VNIR reflectance spectra based on external parameter orthogonalization. Geoderma 267, 92–101. https://doi.org/10.1016/j.geoderma.2015.12.014

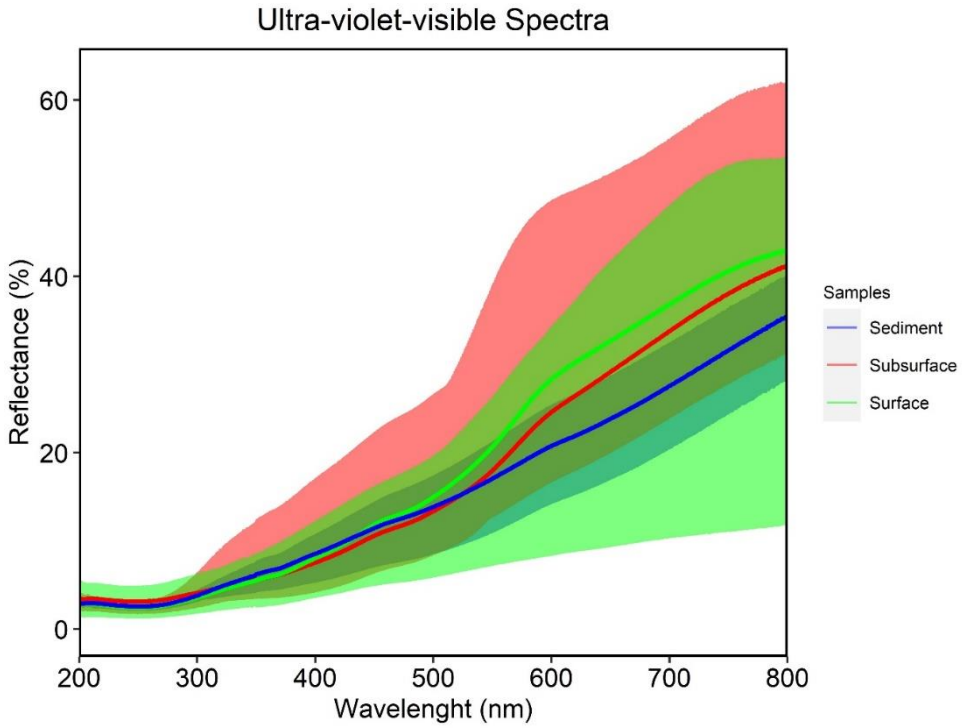

Figure 10.16. Ultra-violet-visible raw spectra for the soil samples from surface and subsurface sources, as well as the sediment samples.

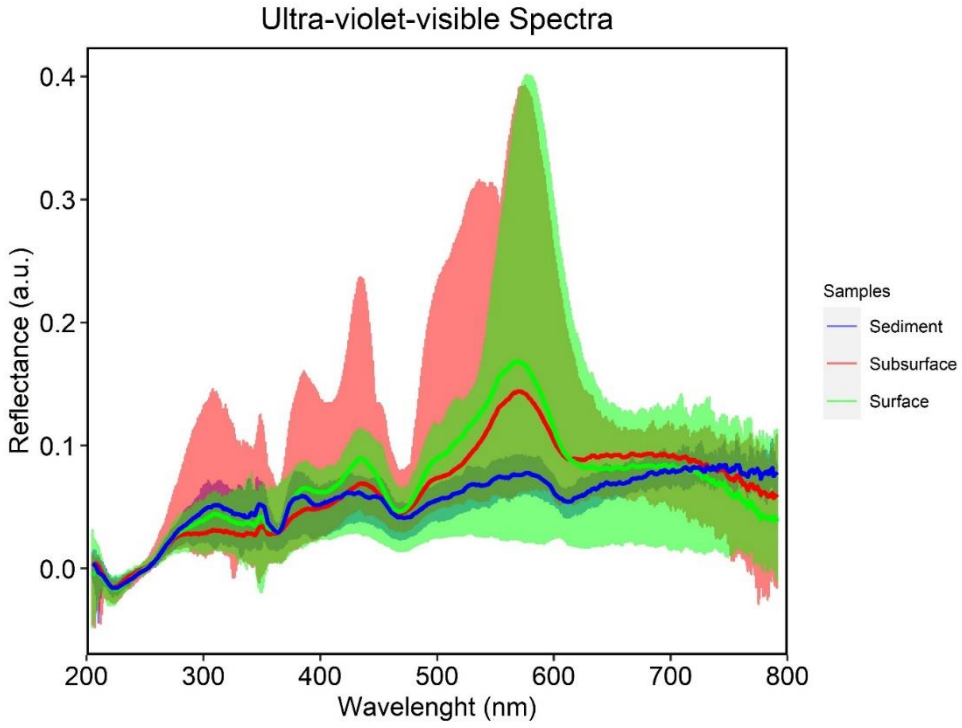

Figure 10.17. Ultra-violet-visible spectra after Savitzky-Golay pre-processing for the soil samples from surface and subsurface sources, as well as the sediment samples.

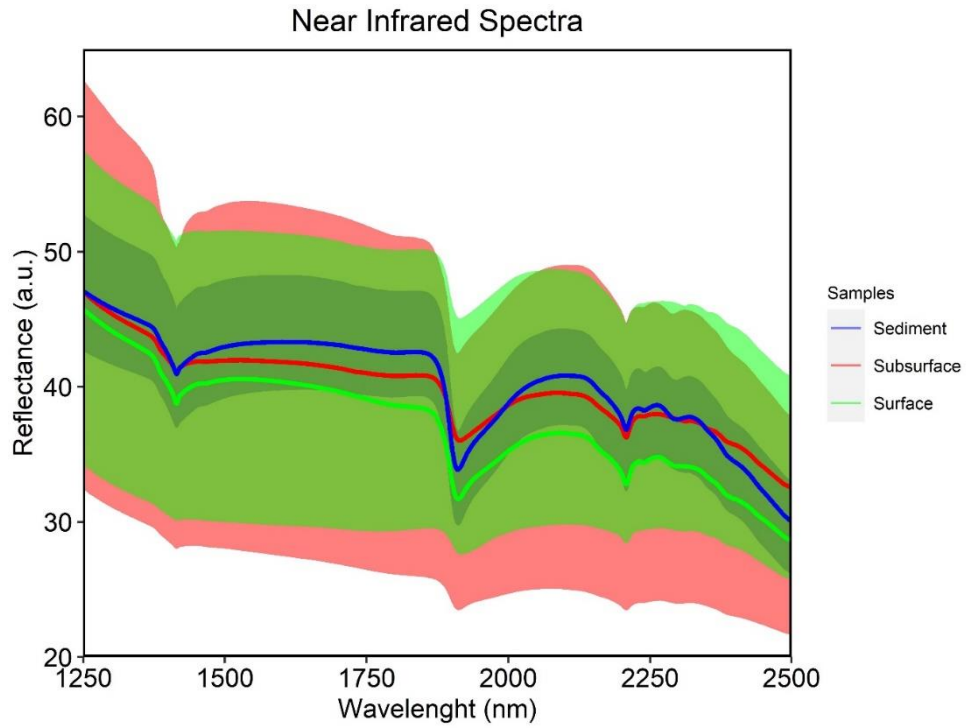

Figure 10.18. Near infrared raw spectra for the soil samples from surface and subsurface sources, as well as the sediment samples.

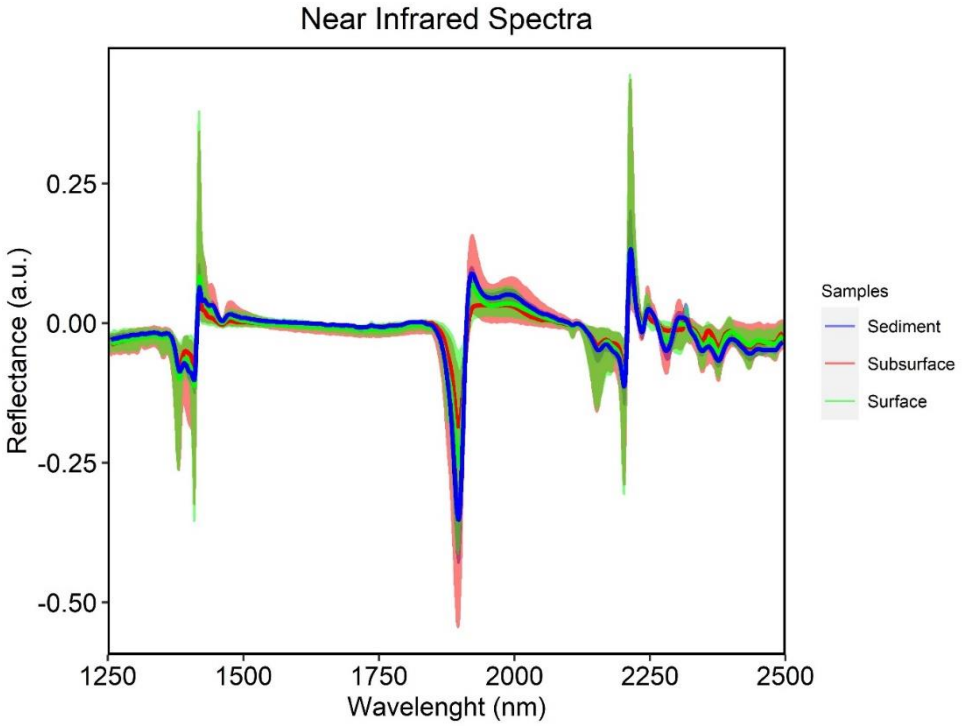

Figure 10.19. Near infrared spectra after Savitzky-Golay pre-processing for the soil samples from surface and subsurface sources, as well as the sediment samples.

Table 10.4. Source sample proportions of the composite artificial mixtures.

Mixtures	Proportions						Mixtures	Proportions					
	CR-SGF	CR-BF	NG-SGF	NG-BF	SS-SGF	SS-BF		CR-SGF	CR-BF	NG-SGF	NG-BF	SS-SGF	SS-BF
M001	50	0	0	50	0	0	M061	100	0	0	0	0	0
M002	37.5	12.5	0	37.5	12.5	0	M062	75	0	25	0	0	0
M003	25	25	0	25	25	0	M063	50	0	50	0	0	0
M004	12.5	37.5	0	12.5	37.5	0	M064	25	0	75	0	0	0
M005	0	50	0	0	50	0	M065	0	0	100	0	0	0
M006	0	37.5	12.5	0	37.5	12.5	M066	0	0	75	0	25	0
M007	0	25	25	0	25	25	M067	0	0	50	0	50	0
M008	0	12.5	37.5	0	12.5	37.5	M068	0	0	25	0	75	0
M009	0	0	50	0	0	50	M069	0	0	0	0	100	0
M010	37.5	0	12.5	37.5	0	12.5	M070	75	0	0	0	25	0
M011	25	0	25	25	0	25	M071	50	0	0	0	50	0
M012	12.5	0	37.5	12.5	0	37.5	M072	25	0	0	0	75	0
M013	31.25	12.5	6.25	31.25	12.5	6.25	M073	62.5	0	25	0	12.5	0
M014	31.25	6.25	12.5	31.25	6.25	12.5	M074	62.5	0	12.5	0	25	0
M015	12.5	31.25	6.25	12.5	31.25	6.25	M075	25	0	62.5	0	12.5	0
M016	6.25	31.25	12.5	6.25	31.25	12.5	M076	12.5	0	62.5	0	25	0
M017	12.5	6.25	31.25	12.5	6.25	31.25	M077	25	0	12.5	0	62.5	0
M018	6.25	12.5	31.25	6.25	12.5	31.25	M078	12.5	0	25	0	62.5	0
M019	25	6.25	18.75	25	6.25	18.75	M079	50	0	12.5	0	37.5	0
M020	25	18.75	6.25	25	18.75	6.25	M080	50	0	37.5	0	12.5	0
M021	18.75	25	6.25	18.75	25	6.25	M081	37.5	0	50	0	12.5	0
M022	6.25	25	18.75	6.25	25	18.75	M082	12.5	0	50	0	37.5	0
M023	6.25	18.75	25	6.25	18.75	25	M083	12.5	0	37.5	0	50	0
M024	18.75	6.25	25	18.75	6.25	25	M084	37.5	0	12.5	0	50	0

M025	18.75	12.5	18.75	18.75	12.5	18.75	M085	37.5	0	25	0	37.5	0
M026	18.75	18.75	12.5	18.75	18.75	12.5	M086	37.5	0	37.5	0	25	0
M027	12.5	18.75	18.75	12.5	18.75	18.75	M087	25	0	37.5	0	37.5	0
M028	45	2.5	2.5	45	2.5	2.5	M088	90	0	5	0	5	0
M029	2.5	45	2.5	2.5	45	2.5	M089	5	0	90	0	5	0
M030	2.5	2.5	45	2.5	2.5	45	M090	5	0	5	0	90	0
M031	50	50	0	0	0	0	M091	0	100	0	0	0	0
M032	37.5	37.5	12.5	12.5	0	0	M092	0	75	0	25	0	0
M033	25	25	25	25	0	0	M093	0	50	0	50	0	0
M034	12.5	12.5	37.5	37.5	0	0	M094	0	25	0	75	0	0
M035	0	0	50	50	0	0	M095	0	0	0	100	0	0
M036	0	0	37.5	37.5	12.5	12.5	M096	-	-	-	-	-	-
M037	0	0	25	25	25	25	M097	0	0	0	50	0	50
M038	0	0	12.5	12.5	37.5	37.5	M098	0	0	0	25	0	75
M039	0	0	0	0	50	50	M099	0	0	0	0	0	100
M040	37.5	37.5	0	0	12.5	12.5	M100	0	75	0	0	0	25
M041	25	25	0	0	25	25	M101	0	50	0	0	0	50
M042	12.5	12.5	0	0	37.5	37.5	M102	0	25	0	0	0	75
M043	31.25	31.25	12.5	12.5	6.25	6.25	M103	0	62.5	0	25	0	12.5
M044	31.25	31.25	6.25	6.25	12.5	12.5	M104	0	62.5	0	12.5	0	25
M045	12.5	12.5	31.25	31.25	6.25	6.25	M105	0	25	0	62.5	0	12.5
M046	6.25	6.25	31.25	31.25	12.5	12.5	M106	0	12.5	0	62.5	0	25
M047	12.5	12.5	6.25	6.25	31.25	31.25	M107	0	25	0	12.5	0	62.5
M048	6.25	6.25	12.5	12.5	31.25	31.25	M108	0	12.5	0	25	0	62.5
M049	25	25	6.25	6.25	18.75	18.75	M109	0	50	0	12.5	0	37.5
M050	25	25	18.75	18.75	6.25	6.25	M110	0	50	0	37.5	0	12.5
M051	18.75	18.75	25	25	6.25	6.25	M111	0	37.5	0	50	0	12.5
M052	6.25	6.25	25	25	18.75	18.75	M112	0	12.5	0	50	0	37.5
M053	6.25	6.25	18.75	18.75	25	25	M113	0	12.5	0	37.5	0	50
M054	18.75	18.75	6.25	6.25	25	25	M114	0	37.5	0	12.5	0	50

M055	18.75	18.75	12.5	12.5	18.75	18.75	M115	0	37.5	0	25	0	37.5
M056	18.75	18.75	18.75	18.75	12.5	12.5	M116	0	37.5	0	37.5	0	25
M057	12.5	12.5	18.75	18.75	18.75	18.75	M117	0	25	0	37.5	0	37.5
M058	45	45	2.5	2.5	2.5	2.5	M118	0	90	0	5	0	5
M059	2.5	2.5	45	45	2.5	2.5	M119	0	5	0	90	0	5
M060	2.5	2.5	2.5	2.5	45	45	M120	0	5	0	5	0	90

* Cropland at Botucatu Formation – CR.BF, Cropland at Serra Geral Formation – CR.SGF, Native Grassland at Botucatu Formation – NG.BF, Native Grassland at Serra Geral Formation – NG.SGF, Subsurface source at Botucatu Formation – SS.BF, Subsurface source at Serra Geral Formation – SS.SGF.

11 Chapter 6. Sediment fingerprinting in the Uruguay River basin – General Discussion

11.1 Introduction

In this last chapter of the thesis, a general discussion on the results obtained in the previous chapters for the two representative tributaries of the Uruguay River basin is provided. In addition, first insights into the sediment characteristics and origin of the main Uruguay river are presented, in order to provide directions for future studies. The objective of this thesis was to quantify the sediment source contributions in two contrasting tributaries of the Uruguay River basin, which differ mainly in terms of soil types and land use. The hypothesis was that land use change in the Pampa biome region and the absence of effective land conservation practices in the Southern Brazilian plateau region, would make agricultural cropland areas the main source of suspended sediments in the Uruguay River basin. The objectives were achieved and the hypothesis was partially confirmed. In the next sections, a general discussion of the results obtained for each individual tributary catchment is provided, and then, a first analysis of the sediment origin of the main Uruguay River is presented and discussed.

11.2 Conceição River catchment

Two studies were developed in the Conceição River catchment with the aim to trace sediment sources in a homogenous catchment in terms of soil types and land uses. The main challenge in this case was to find tracers able to discriminate between five land use-based sources. For the first study, in Chapter 2, an approach considering composite fingerprints was developed to quantify the contribution of five potential sediment sources. Spectroscopy-derived parameters from the ultra-violet-visible wavelength (UV) and magnetic parameters were used in a composite approach with geochemical fingerprints. The results showed a very low discrimination between sources, especially among surface (cropland and pasture) and subsurface sources (unpaved road, stream bank and gully). Due to the highly weathered, deep soil types (e.g. Ferralsols and Nitisols), with a high proportion of clay, the geochemical composition, even between topsoil and subsoil layers, remained homogeneous. The same result was found for colour parameters, with the dominance of red soils, which prevented to obtain significant discrimination among sources.

This was a first attempt to apply a composite sediment fingerprinting approach, relying on tracers related to magnetism, parameters derived from UV and geochemical composition, in a large subtropical catchment with very homogenous soils. The combination of multiple parameters provided the best discrimination between sources, showing that composite fingerprints provide an alternative for sediment tracing in complex sites such as Conceição catchment. Despite the uncertainties associated with the model predictions, the results of the source contributions indicate pastures as the main sediment source for suspended material, which together with cropland, can supply up to more than 50% of the sediment delivered to the river systems (Results from the combination of both alternative tracers, GMUV, in the Figure 11.1). Stream banks also provided an important source, mainly for fine bed sediment, and these results remain in agreement with those obtained in a previous study conducted in the same catchment (Tiecher et al., 2018). The high number of potential sources and the relatively limited quality of the sediment source discrimination impacted the results of the model predictions, requiring further investigations to find more appropriate tracers with the ability to discriminate between these sources. Some crop specific tracers, such as environmental DNA or CSSI, could likely provide an alternative for better understanding soil erosion processes in the Conceição River catchment and other similar homogeneous catchments worldwide.

In the second study, a distinct approach based on the run of multivariate models calibrated with diffuse reflectance spectroscopy data obtained from artificial mixtures with known proportions of each source was tested. Diffuse reflectance spectroscopy in the ultraviolet-visible (UV), near-infrared (NIR) and mid-infrared (MIR) wavelengths can provide a greater amount of information about samples in a more efficient and cost-effective way, which could provide an alternative for these catchments with similar properties between sources. Several combinations considering two multivariate models, spectra pre-processing and spectra wavelength combinations were tested. The support vector machine model (SVM), combined with the mid-infrared spectra after the Savitzky-Golay pre-processing (SGD) was the one that provided the best results. The predictions indicated surface sources as the main source for suspended sediment and subsurface source for the fine bed sediment (Figure 8.13). Since different combination of potential sources and different sediment samples were considered in each approach, it was not possible to provide a direct comparison of their results. However, it is possible to observe

in Figure 11.1 and Figure 11.2 a similar trend in the sediment source contributions according to the sampling method, where surface sources contribute a greater proportion to suspended sediment, whereas subsurface sources supply a greater contribution to FBS.

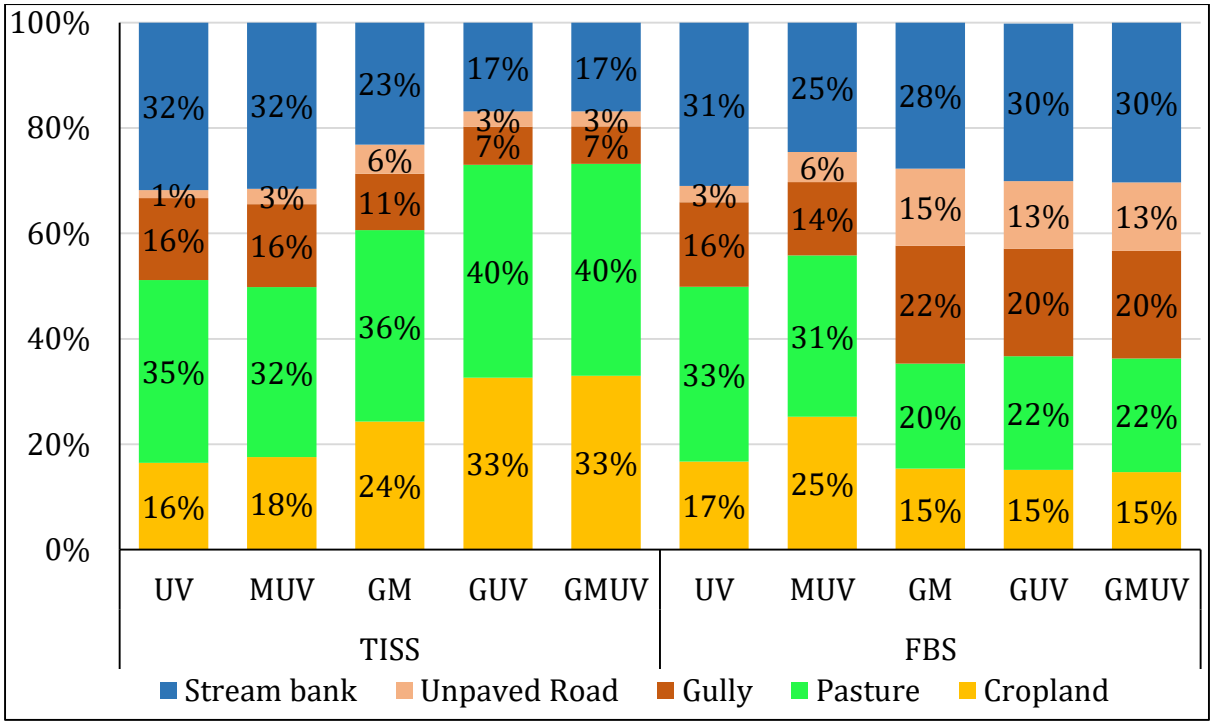

Figure 11.1. Mean contributions of each sediment source for the time-integrated suspended sediment samples (TISS) and for fine bed sediment samples (FBS), following the five approaches relying on different tracer combinations. Ultraviolet-visible derived parameters - UV; magnetic parameters – M; and geochemical composition – G.

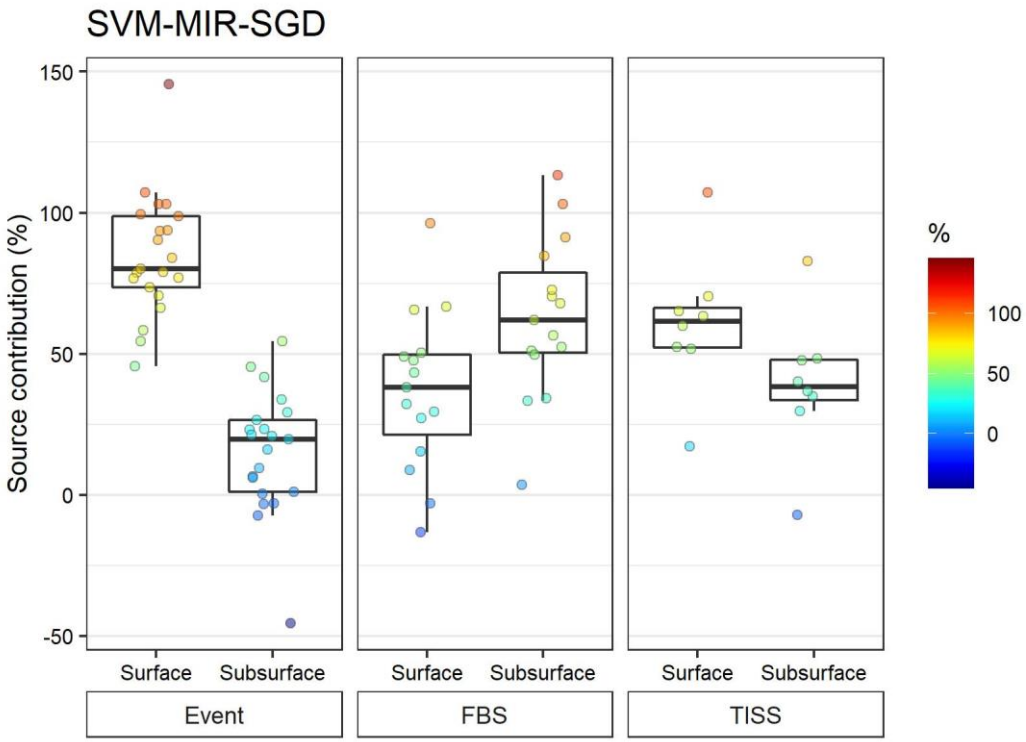

Figure 11.2. Sediment source contributions according to the sampling method predicted from the SVM-SGD-MIR models. Event - Rainfall runoff event; FBS - Fine bed sediment samples; and TISS - Time integrated suspended sediment samples.

11.3 Ibirapuitã River catchment

The Ibirapuitã river catchment shows completely different characteristics compared to the Conceição catchment. Located along the border with Uruguay in the southernmost part of Brazil, the Ibirapuitã catchment is representative of the Pampa biome, where grassland used to be the main land use. Besides that, the geology of the region, i.e. sandstone from the Botucatu Formation mainly and volcanic rocks from the Serra Geral Formation, results in a large variation of soil types. Associated with the pedoclimatic conditions prevailing in the region, sandy and shallow soils are found, and these are highly vulnerable to soil degradation. When not well managed, soils of the region can be driven to an irreversible stat of degradation, such as sandification that already occurs in the region.

Recently, the native grasslands of the Pampa Biome have been converted into cropland areas, mainly soybeans. Therefore, concerned with the impacts of land use change in the region, this study sought to quantify the contribution of the main sources of sediment in the region, in order to assess the potential impact of land use change on sediment inputs into rivers. In addition, testing the sediment fingerprinting technique in

such a heterogeneous catchment, with a greater diversity of soil types and uses, was a challenge contrasting with the situation found in the Conceição catchment, and representative of the second most important region found across the Uruguay River basin. In the Chapter 4, fallout radionuclide activities, organic matter composition and UV-derived parameters were used to quantify the sediment contributions from cropland, native grassland and subsurface sources (including unpaved road, stream bank and gullies). Based on the organic carbon content and radionuclide activities measured in the source samples, it was already possible to observe that cropland had suffered greater soil losses as a consequence of erosion processes or even other degradation processes, since these parameters were more depleted under cropland compared to the soils under native grasslands. By means of the sediment fingerprinting approach, it was demonstrated that source contributions varied according to the sampling period. In the first period (from May 25 to October 26, 2018), surface sources, mainly cropland, supplied the main sources for the sediment reaching the river system. A second sampling period (from October 26, 2018 to February 19, 2019), which included large storms in the catchment, showed higher contributions from subsurface sources compared to the first period. Although surface sources were not the main source during the entire monitoring period, it is important to highlight that the Ibirapuitã catchment has only 9% approximately of the land covered by cropland. Disregarding the uncertainty from the low discrimination between cropland and native grassland, it means that even the lowest contribution from cropland to sediment that reached 25% in the current research is highly significant given the very low proportion covered by this land use in the catchment.

The main objective of this study that was to analyse the impact of land use change was therefore partially achieved. The tracers used in this study were not able to fully discriminate between native grassland and cropland sources. A better discrimination between these two sources would be important to achieve in the future to have greater assertiveness on the real impact of land use change in the region. Furthermore, more monitoring time is necessary to obtain a better representation of the erosion processes occurring in the catchment.

Chapter 5, the second study developed in the Ibirapuitã catchment, followed a similar strategy as that adopted in Chapter 3 for the Conceição catchment. However, in this study, we chose to include the two main geologies as variables for preparing the artificial mixtures used for model calibration/validation. Cropland, native grasslands and

subsurface material were considered as sources, all these classed being divided into two sets corresponding to the two geological formations found in the catchment, Botucatu and Serra Geral Formation, resulting in a total of six potential sources. In contrast with the situation found in the Conceição River catchment, in this study, only those diffuse reflectance spectra in the UV and NIR range were available. As it was also observed in the Conceição River catchment, the spectrum in the UV range did not show sufficient discrimination between sources when used individually. The use of NIR and MIR bands led to better results because they were able to collect more information from the samples, mainly related to the mineralogical composition of their clay and organic matter compounds.

Three approaches were tested, considering six, three and two sources. It was found that the method was not really efficient when considering more than two sources. Although the calibration of the models was satisfactory for all combinations of sources, when evaluating the predictions, a high error was obtained for those approaches considering more than two sources. Only for the approach with two sources the sum of the contributions was close to 100%. For the approaches with three and six sources, the sums exceeded 250%, reaching in some cases up to 900%. For the Ibirapuitã River basin, we were able to evaluate the contribution of each sediment source by the two methods applied, and we verified that, for the majority of the samples, the difference did not exceed 20% (Figure 11.3). Both methods indicate the subsurface sources as the main source, with the spectroscopy method showing less variations between samples.

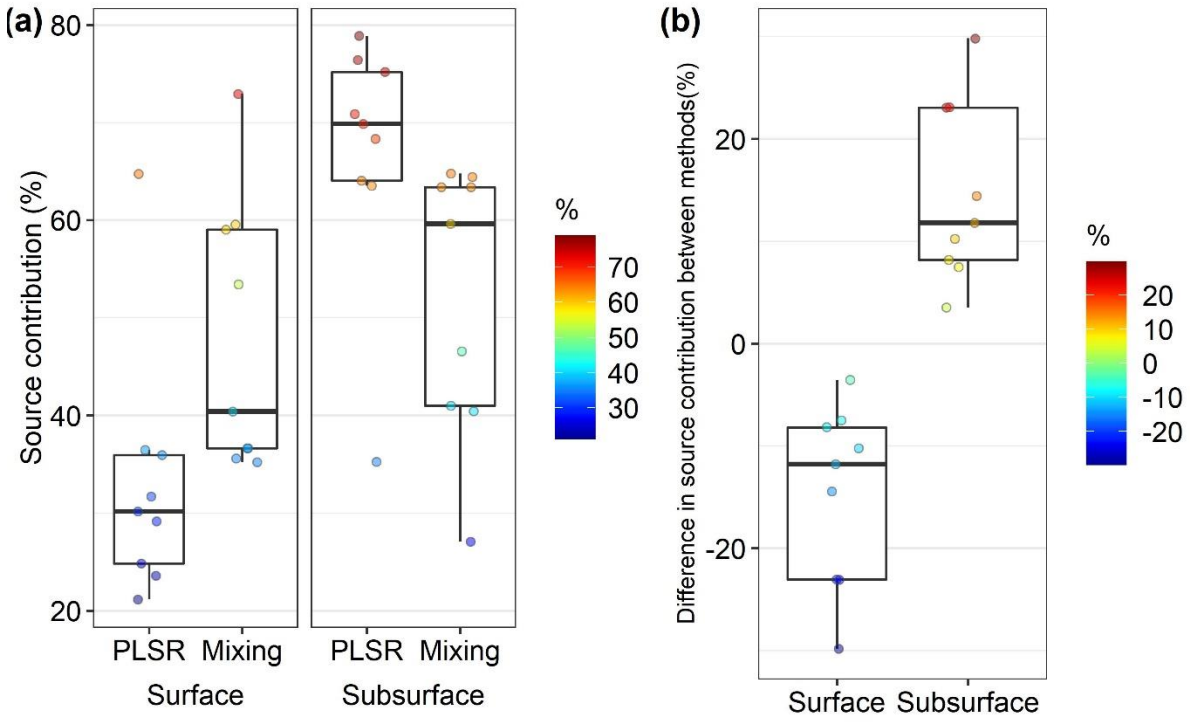

Figure 11.3. Sediment source contributions predicted by spectroscopy based on PLSR-UV+NIR-SGD (PLSR) model and by the mixing model (Mixing) based on conventional tracing properties (Chapter 4) (a). Difference between the prediction of each method for individual sediment samples (b).

11.4 Uruguay River basin

The sediment fingerprinting technique has been widely applied to trace sediment sources in catchments, which can help local managers to direct efforts to mitigate sediment and contaminant delivery to the river systems in a more efficient way. Sediments are responsible for the eutrophication and siltation of water reservoirs. Therefore, identifying the origin of this problem can provide very useful information for better managing situations like that observed in Brazil, Argentina and Uruguay, where hydroelectric power plants are one of the main sources of electric energy. Brazil is equipped with around 1313 hydroelectric power plants in operation, and the most powerful installations are located on the largest rivers, such as the Paraná River, São Francisco River and Tocantins river (Dias et al., 2018). The Uruguay River has several reservoirs along its course in Brazil, but the most downstream reservoir located between Argentina and Uruguay is the largest one. The Salto Grande hydroelectric power plant, which is located downstream of the confluence of the tributaries studied in this thesis (the Conceição and Ibirapuitã river catchments).

However, defining appropriate techniques to trace sources in large basins remains a challenge, as there are multiple potential sources and a high heterogeneity, as observed in the individual Conceição and Ibirapuitã River catchments. Accordingly, based on the knowledge obtained through the application of the technique in its tributaries, we will provide – to the best of our knowledge – the first attempt to trace sediment sources in the Uruguay river basin.

11.4.1 Methodology

In this study, sediment samples collected from the outlet of the Conceição and Ibirapuitã river catchment were considered as potential sources to the sediment collected in the main Uruguay river. The initial aim of the project was to collect sediment samples deposited in the Salto Grande dam. Due to logistical difficulties, it was not possible to collect samples from the dam reservoir and, as an alternative, samples were collected from an island of the river, close to the Uruguaiana county, in the State of Rio Grande do Sul, Brazil (Figure 11.4 and Figure 11.5), in order to provide a first assessment of the properties of sediment transiting in the river at that location. A trench was excavated to allow the collection of sediments in different layers, down to a depth of one meter. Layers with 5-cm increments were collected down to a depth of 50 cm, and then 10-cm layers were taken in the lower part of the profile, between 50 and 100 cm depth (Figure 11.6).

Figure 11.4. Location of the studied catchments, the Salto Grande Dam and the sampling location in the Uruguay river island.

Figure 11.5. Satellite image of the sampling point (yellow marker) on an island in the Uruguay river, close to Uruguaiana, RS (city in the top right of the image). This image was taken four days after the sampling date, on April 24th 2020. Source: Google Earth Pro.

Figure 11.6. Sediment sampling in a deposit within an island of the Uruguay River. Source: the author.

11.4.1.1 Source and sediment analyses

Samples were oven-dried (50° C), gently disaggregated using a pestle and mortar and dry-sieved to 63 μm to limit particle size effects prior to further analysis (Koiter et al., 2013b; Laceby et al., 2017). After sieving, samples were analysed with a spectrophotometer FT-NIR MPA BRUKER OPTIK GmbH to obtain the near infrared spectra (NIR) at wavelengths comprised between 10000 and 4000 cm^{-1}. The analyses were performed in diffuse reflectance mode with an integration sphere and an InGaAs internal detector with a resolution of 2 cm^{-1} and 100 readings per spectrum, the spectra being exported by the equipment software at the nanometre scale.

Derived parameters from the NIR spectra were used as potential tracers in this approach. Some features at spectral wavelengths related to soil properties, such as clay minerals and iron oxides were selected. From these spectral features of interest, some parameters were derived with the R package "hsdar" (Table 11.1), which is a package to create, handle, manipulate, analyse and simulate large hyperspectral datasets (Lehnert et al., 2019). To calculate the features, first a continuum removal transformation with the segmented hull method is applied and the spectra are transformed to band depth (Figure

11.7). The parameters listed in the Table 11.1 are obtained as exemplified in the Figure 11.8.

Table 11.1. Description of the spectrum features parameters calculated.

Variable	Description
area	The feature area is calculated by $$area_{Fi} = \sum_{k=min(\lambda)}^{max(\lambda)} BD\lambda$$ where $area_{Fi}$ is the area of the feature i, min(λ) is the minimum wavelength of the spectrum, max(λ) is the maximum wavelength of the spectrum and BD is the band depth.
max	Maximum value observed in the feature.
maxwl	Wavelength position of the maximum value observed in the feature.
Parameters based on half-max values:	
lo_wlhm	Wavelength position of the lower half-max value.
up_wlhm	Wavelength position of the upper half-max value.
width_wlhm	Difference between wavelength positions of upper and lower half-max values.
gauss_lo	Similarity of the Gauss distribution function and the feature values between the lower half-max and the maximum position. As similarity measurement, the root mean square error is calculated.
gauss_up	Same as above but for feature values between the maximum position and the upper half-max.

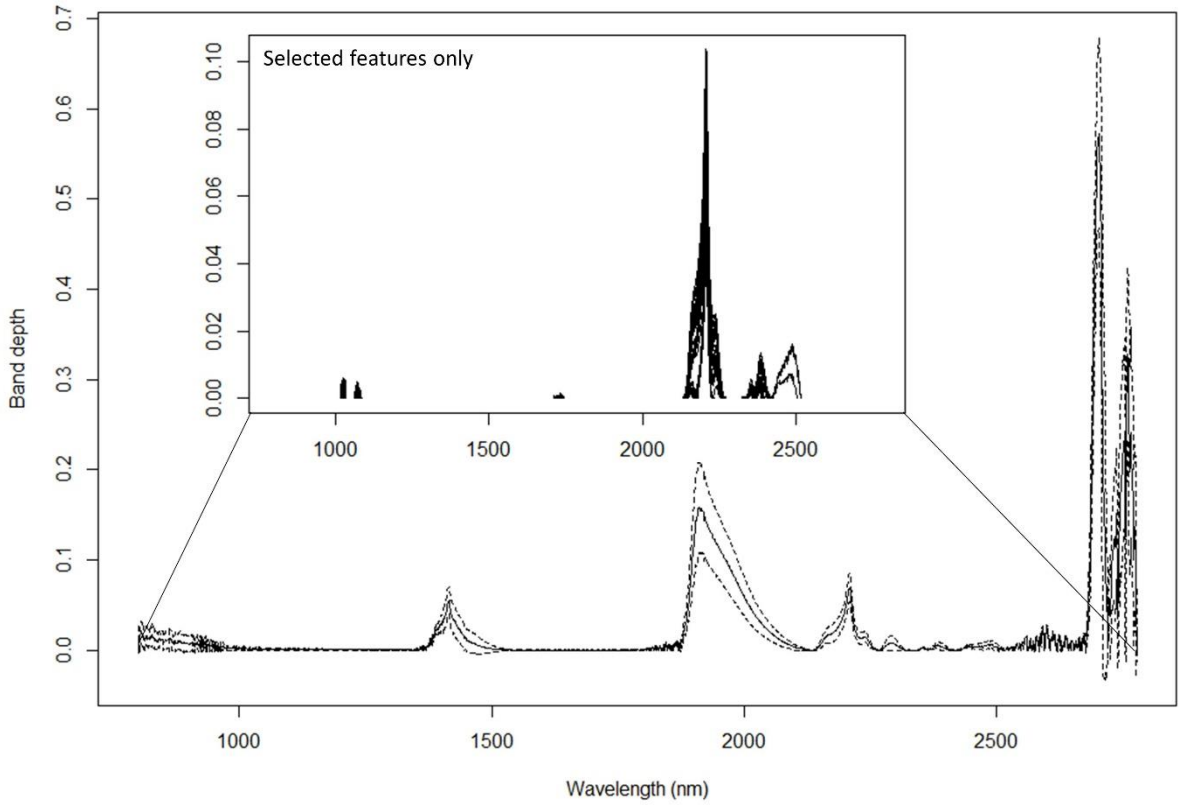

Figure 11.7. Transformation of the spectra to band depth.

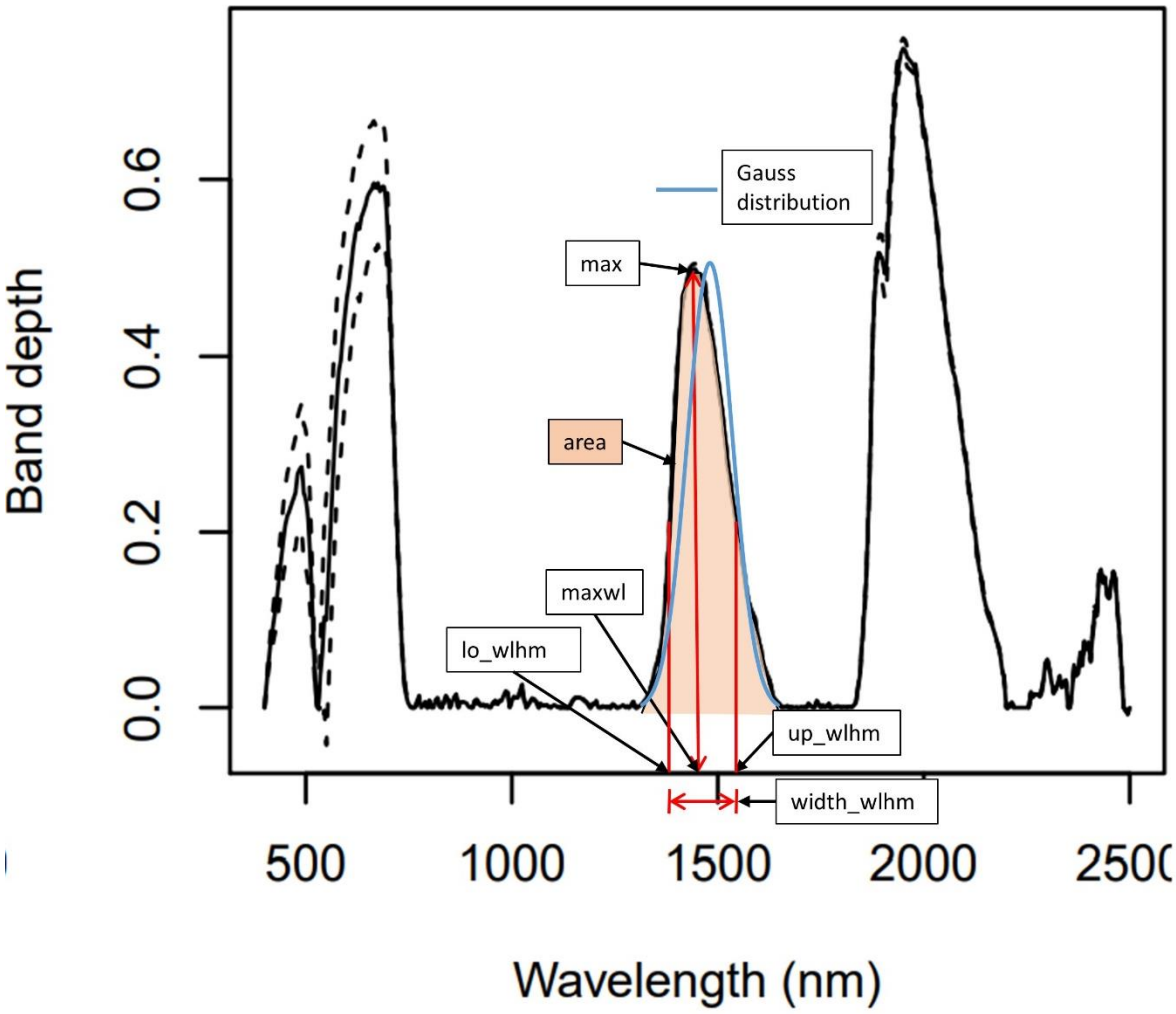

Figure 11.8. Graphical representation of the feature parameters calculated from the spectra. Adapted from Meyer and Lehnert (2020).

11.4.1.2 Magnetic susceptibility

Two grams of each sample were used to measure the magnetic susceptibility in a Bartington MS2B Dual Frequency sensor, with three readings for each sample in high (4.7 kHz) and low frequency (0.47 kHz) modes to obtain the mass specific magnetic susceptibility for high (χ_{HF} – m^3 kg^{-1}) and low frequency (χ_{LF} – m^3 kg^{-1}) (Mullins, 1977). Furthermore, the percentage of frequency-dependent susceptibility (χ_{fd}) was calculated according to the Equation 4 (Dearing et al., 1996), which indicates the presence of viscous grains lying at the stable single domain/superparamagnetic boundary and their delayed response to the magnetizing field (Yu and Oldfield, 1989).

$$\chi_{fd}(\%) = 100 \times \left[\frac{(\chi_{LF} - \chi_{HF})}{\chi_{LF}}\right] \quad (4)$$

11.4.1.3 Sediment source discrimination and apportionment

Two approaches were considered to select the potential tracers. In the first one, the selection followed the classical three-step procedure: i) a range test; ii) the Kruskal-Wallis *H* test (KW *H* test); and iii) a linear discriminant function analysis (LDA). For passing the range test, mean parameters values for sediment must fall within the range between the maximum and minimum values observed for the sources. The KW *H* test was then performed to test the null hypothesis ($p < 0.05$) that the sources belong to the same population. The variables that provided significant discrimination between sources were analysed with a forward stepwise LDA ($p < 0.1$) in order to reduce the number of variables to a minimum while maximizing source discrimination (Collins et al., 2010b).

The second approach was based on the pedological knowledge (Batista et al., 2019) to select the potential tracers. Parameters related to spectral features associated to the occurrence of clay minerals were calculated. Considering that kaolinite is an abundant mineral in soils of the Conceição River catchment, the wavelength corresponding to features reflecting the presence of kaolinite was selected and two parameters related to it were chosen. Similarly, the wavelength related to the features generated by clays with a 2:1 layer structure, which are more abundant in soils from the Ibirapuitã catchment, was selected and from it two parameters were extracted. In addition, a magnetic parameter has been included as there is a difference between the geologies found in the two tributary catchments, and these are associated with different magnetic properties. The parameters manually selected in the second approach were also submitted to the conservative and mean tests, to guarantee that they are conservative and have a good discrimination capacity between sources. The statistical analyses were performed with R software (R Development Core Team, 2017) and more details on the procedure can be found in Batista et al. (2018).

The source contributions were estimated by minimizing the sum of squared residuals (SSR) of the following mass balance un-mixing model:

$$SSR = \sum_{i=1}^{n} \left(\left(C_i - \left(\sum_{s=1}^{m} P_s S_{si} \right) \right) / C_i \right)^2 \quad (5)$$

where n is the number of variables/elements used for modelling, C_i is the value of the parameter i in the target sediment, m is the number of sources, P_s is the optimized relative contribution of source s by SSR minimizing function, and S_{si} is the concentration of element i in the source s. Optimization constraints were set to ensure that source contributions were non-negative and that their sum equalled 1. The un-mixing model was solved by a Monte Carlo simulation with 2500 iterations. More information about model settings and compilation can be found in Batista et al. (2018).

11.4.2 Results and Discussion

The results of the magnetic susceptibility analysis showed that there is a significant difference between sediment originating from the Conceição and Ibirapuitã catchments, which can be attributed to the contrasted soil properties and nature of parent material in both source areas (Pulley and Rowntree, 2016). The magnetic behaviour is closely related to the ferromagnetic properties of the sources and sediment, and the soils of the Conceição catchment show a much higher content in iron oxides, which results in higher tracer values compared to those found in the Ibirapuitã catchment. In the study conducted in the Conceição catchment, which has very homogenous and highly weathered soils, the magnetic parameters did not provide satisfactory discrimination between sources. In the study developed in the Ibirapuitã catchment, magnetic properties were not tested. However, according to the current results, the values found in this catchment are very low, which is related to the soil type characteristics found in the catchment, which are sandy and depleted in iron oxides. Both magnetic parameters show a clear difference between the two sources. The values observed in the Uruguay River sediments are very low, but they remain comprised within the source values, which allows these parameters to be used as tracers (Figure 11.9).

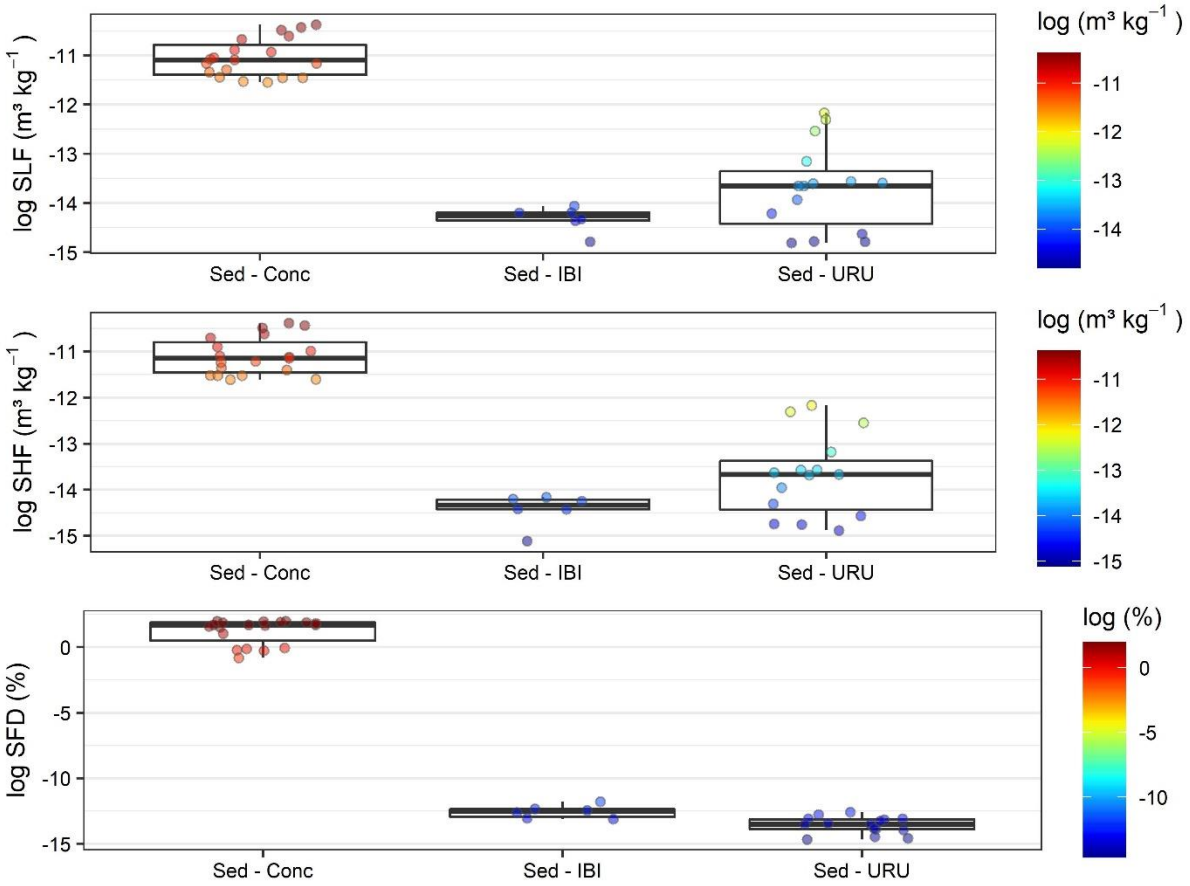

Figure 11.9. Magnetic susceptibility parameters for the sediment samples. SHF, SLF and SFD correspond to the magnetic parameters χ_{HF}, χ_{LF} and χ_{FD}, respectively.

The NIR analyses shows that the sediment properties from the Uruguay River are conservative, i.e., the values were comprised within the range observed for the sources, allowing it to be used as a tracer (Figure 11.10). From the NIR spectra, eight parameters (see Table 11.1) related to each of 10 selected spectral wavelengths (Table 11.2) were extracted, providing a total of 80 parameters. For the first analysis based on the standard three-step selection procedure, ten wavelengths were selected, and these are listed in Table 11.2.

Table 11.2. Spectral features from NIR spectral range selected to extract spectrum features parameters.

Wavelength (nm)	**Assignment**
1025	Electronic transition bands of Fe^{3+}
1075	Electronic transition bands of Fe^{3+}
2160	Fundamental absorption of AlOH band of kaolinite
~2200	Stretch of montmorillonite and illite
2206	combination bands of fundamental and overtone absorptions stretch of montmorillonite and illite
2216	Illite

2230	Fundamental absorption of AlOH band of smectites
2336	Illite
2340	combination bands of fundamental and overtone absorptions of OH stretch of illite
2372	Kaolinite

*Data obtained from Bayer et al. (2012).

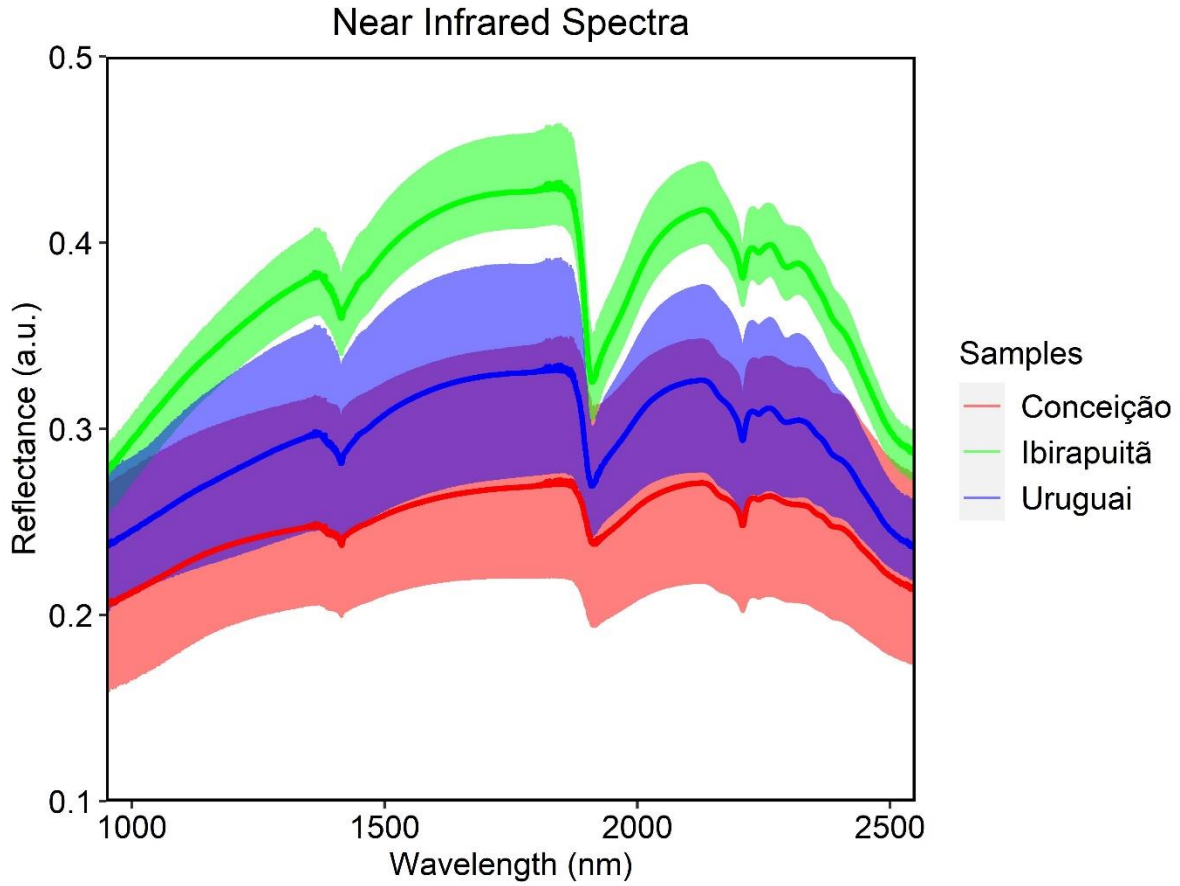

Figure 11.10. Near infrared raw spectra for the sediment samples from the Conceição, Ibirapuitã and Uruguay river catchments. The solid lines represent the spectral average of each source.

From the 80 parameters derived from the NIR spectra, 25 were conservative and showed a discrimination capacity between sources, and they were combined with the three magnetic parameters. The parameters derived from the NIR spectra are highly correlated between most of them, except for those from the spectral range related to the iron oxides (1075) and the χ_{fd}, which is also related to the ferromagnetic properties of the soils (Figure 11.11).

In the approach based on statistical analyses, these tracers were submitted to the DFA, to select the minimum number of tracers that maximized the discrimination between sources. Four tracers were selected in this step, and all of them are related to the wavelength 2372 nm, which is a feature related to the presence of kaolinite, namely

f2372_area, f2372_width_wlhm, f2372_max, f2372_up_wlhm. These parameters were able to correctly classify 100% of the source samples. As it can be seen in the principal component analysis (PCA), the groups are clearly distinguished by the first two components (Figure 11.12).

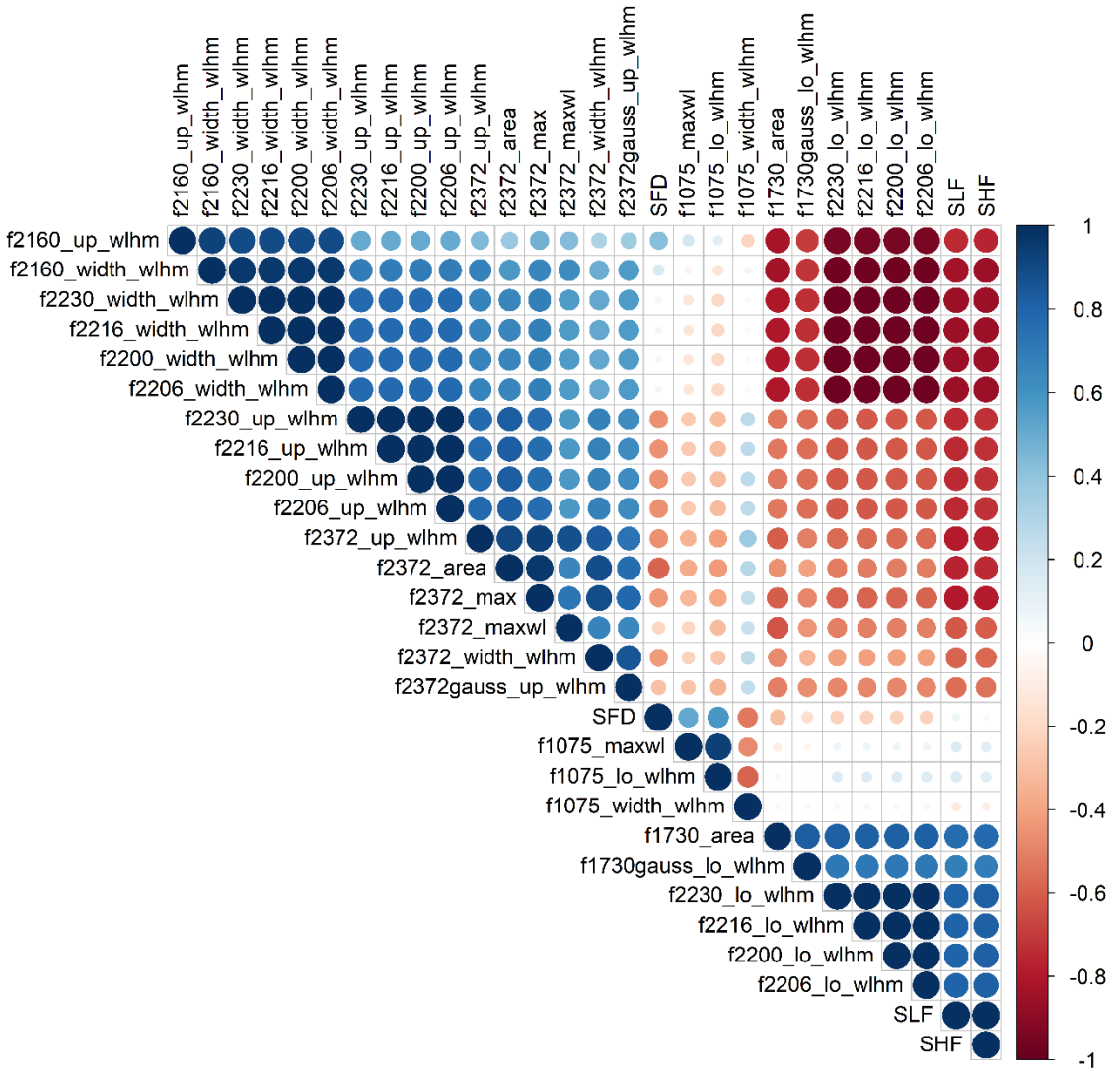

Figure 11.11. Correlation plot between variables that were approved in the conservativeness test and KW H test. SHF, SLF and SFD correspond to the magnetic parameters χ_{HF}, χ_{LF} and χ_{FD}, respectively.

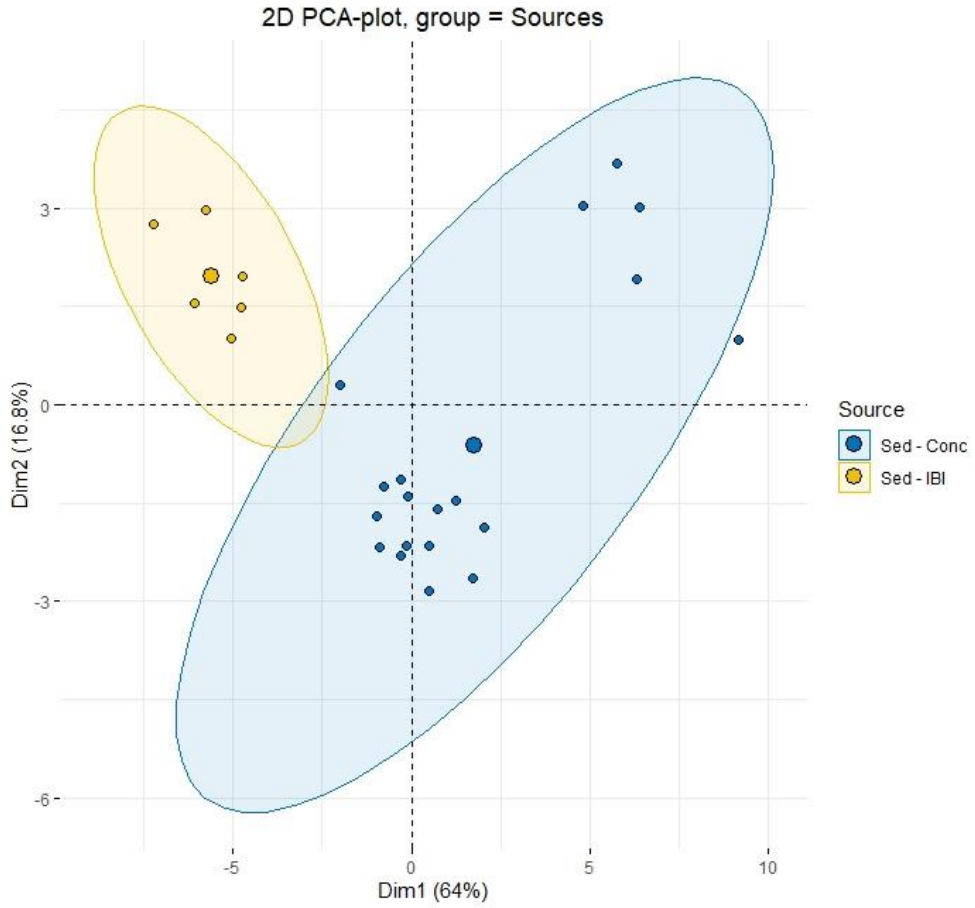

Figure 11.12. Principal component analysis (PCA) based on the parameters selected by the statistical approach.

The mixing model results for the statistical approach showed that in the Uruguay island' sediment upper profile section comprised from zero to 25 cm, the Ibirapuitã sediment is considered as the main source, except for one sample corresponding to the 10-15 cm layer (Figure 11.13). Below 25 cm, the main source is systematically the Conceição sediment, with the exception of the layer corresponding to 70-80 cm, where each tributary contributes with approximately 50%. The background sediment profile picture has been added to support the understanding of the results, showing that there is a clear visual difference between sediment layers accumulated along the profile. The upper layer is made of coarser material, which is similar to that of the sandy soils found in the Ibirapuitã catchment. Below 30 cm approximately, the occurrence of fine sediment increases, and this material is more similar to the sediment originating from the Conceição catchment.

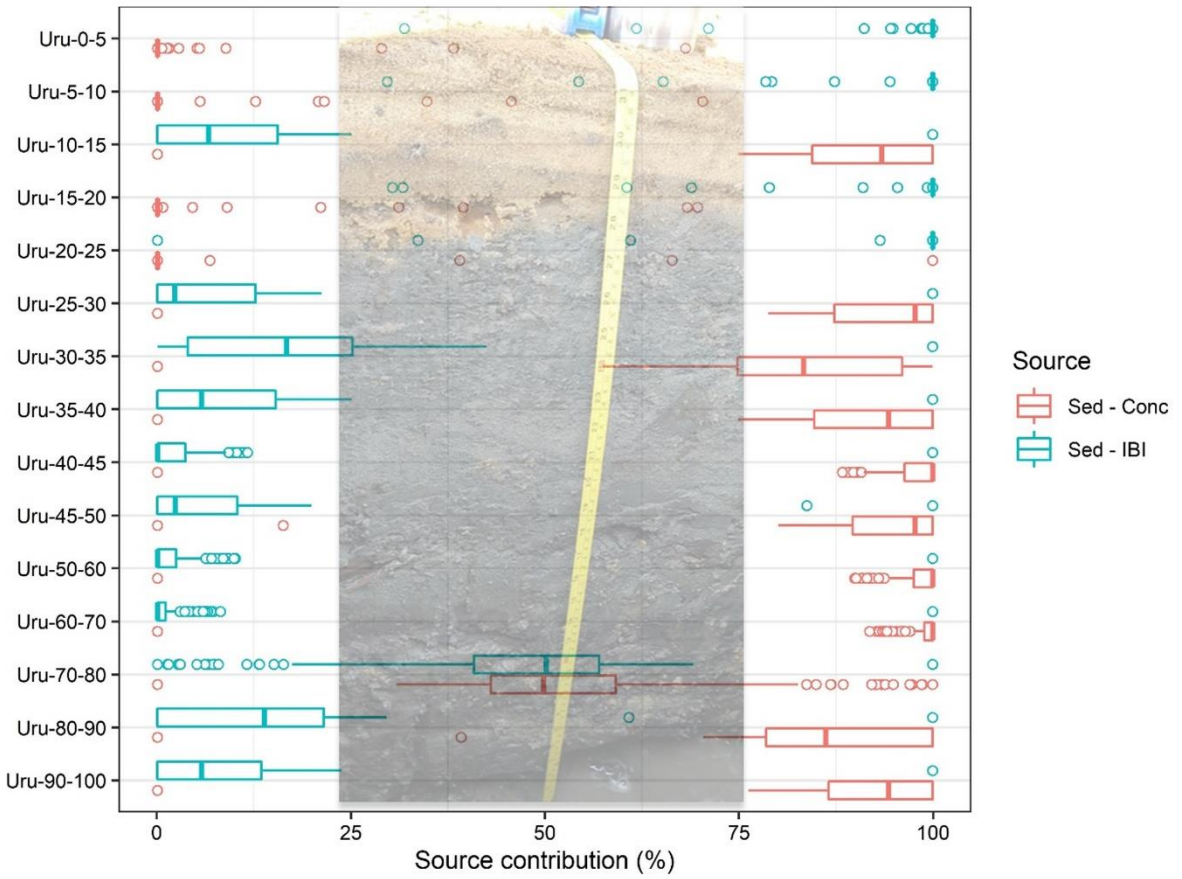

Figure 11.13. Sediment source contribution for the sediment samples of the Uruguay River for the approach based on the statistical selection of the tracers. Conceição – Con, Ibirapuitã – Ibi, Uruguay – Uru.

In the approach based on the pedological knowledge of the study sites, four parameters derived from the NIR spectra and two magnetic properties were considered as potential tracers. The selection of the parameters was based on the knowledge of the mineralogical composition of the soils in the two tributaries. The Ferralsols occurring in the Conceição catchment, are rich in kaolinite. Therefore, two parameters related to the kaolinite were selected, the f2372_width_wlhm and f2372_up_wlhm, which were also selected in the statistical approach. In addition to that, two complementary parameters from the feature wavelength related to the stretch of montmorillonite and illite (2200 nm) were selected, the f2200_width_wlhm and f2200_up_wlhm. Soils containing these 2:1 layer minerals are more common in the Ibirapuitã catchment.

The magnetic parameters were not included in this approach due to the very low values observed in the Ibirapuitã and Uruguay sediment samples (Figure 11.9). Some samples had negative or even null values, and the mixing model does not accept these values. Accordingly, they were not included in this second approach. The results differed

slightly from those obtained with the statistical approach, showing more uncertainty between simulations for this approach, as it can be observed with the larger interval between quartiles (Figure 11.14). The results obtained for the individual samples in this second approach based on pedological knowledge proved to be somewhat more consistent, mainly regarding the sample corresponding to the sediment layer between 10-15 cm. The abrupt transition between layers observed from 25 cm shows that the result of the statistical approach for the 10-15 cm layer may be related to some tracers mismatch at that depth.

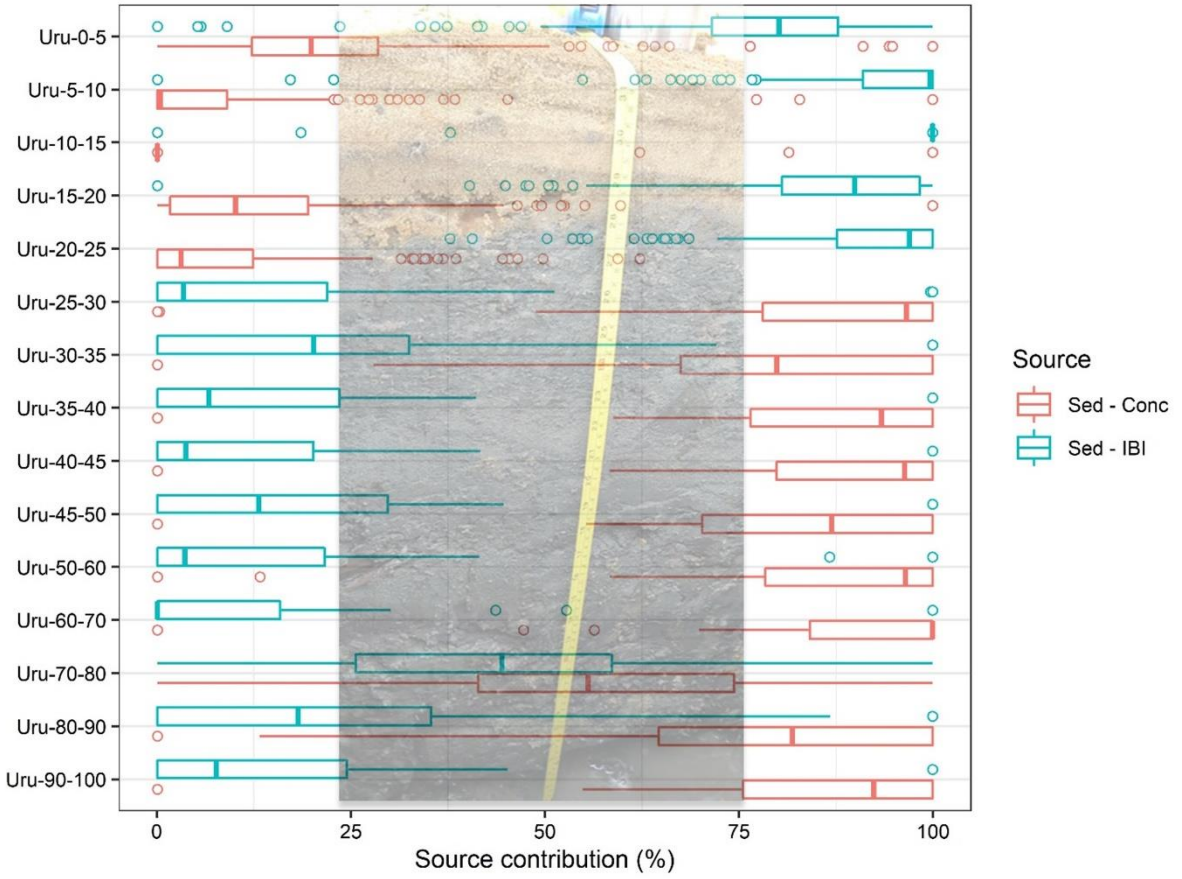

Figure 11.14. Sediment source contributions for the sediment samples of the Uruguay River for the approach based on pedological knowledge. Conceição – Con, Ibirapuitã – Ibi, Uruguay – Uru.

This abrupt transition between the more superficial and subsurface horizons may be related to the occurrence of a large rainfall event that may have caused this distinct deposit of coarser sediments in the superficial layer. An example of this type of storm is the large event that occurred in January 2019, which was monitored in the Ibirapuitã river catchment, which may have contributed a greater amount of material that was deposited there. However, this is only an assumption, and several reasons may have been

involved in the process of deposition of these sediments near the island. Further studies associated with sediment fingerprinting are necessary to further improve our understanding of the processes of sediment transport occurring in a large basin such as the Uruguay River, including the search for representative sediment sampling points. In this case, dating the sediments by means of fallout radionuclide activities may provide a powerful alternative to reconstruct the history of sediment source contributions.

11.5 Final conclusions and perspectives for future studies

The sediment source tracing technique has already proven to be reliable in quantifying the contribution of different sources based on land use and soil types in small catchments across the southern region of Brazil. However, the findings of this thesis, compared to previous studies developed in the region, indicate that as the scale of the study area increases, much more diverse and complex processes of erosion and sediment transfer are introduced and, consequently, their interaction may lead to difficulties to design appropriate techniques of sediment source tracing. These complexity factors may be related to the relief, soil types, connectivity with water bodies, sources of interest, particle size, among others. In this study, two very distinct sets of environmental conditions were analysed, which led to specific difficulties that limited the quality of the results obtained in both contexts.

The perception is that under conditions similar to those found in the Conceição River catchment, where soils are homogeneous and soil horizons are largely undifferentiated, a more targeted approach with tracers specific of the potential land uses should be preferred. The use of environmental DNA and biomarkers such as the CSSI (compound-specific stable isotopes) approach may provide an alternative to differentiate between land uses. When it comes to surface and subsurface sources, the use of tracers that can be added externally, such as fallout radionuclides, elements present in fertilisers and pesticides, among others, should be preferred. It is always better to obtain multiple lines of evidence regarding sediment source contributions, and the advantage of combining these different tracer types is that they all provide complementary information on the sediment origin.

Conditions such as those found in the Ibirapuitã River catchment are even more complex, especially when an approach relying on land uses as potential sources is considered. The great variation in soil types and geologies introduces even more sources

of variability between samples from a given group, which makes it even more difficult to select suitable tracers. In this case, an initial approach that considers tributaries with contrasting multiple characteristics as potential sources, or that is characterized by a specific geology or land use, can provide a powerful alternative to help identifying in a first instance potential tracers to be included in a second time in a more targeted approach. This is a strategy that could have been attempted in this study, but due to difficulties with monitoring and logistics, it was not possible to obtain sufficient sample material in each tributary to allow this type of analysis. However, this is an approach that remains open to be applied in the future in this catchment. A first tentative using spectroscopy parameters as tracers can provide a promising alternative when very different types of soil are considered. In order to obtain a better discrimination between land uses, mainly between native grassland and cropland, the use of environmental DNA and biomarkers such as the CSSI approach may also provide a powerful alternative, although these methods are also associated with limitations and methodological challenges (Capo et al., 2021; Foucher et al., 2020; Hirave et al., 2019; Reiffarth et al., 2019).

When the entire Uruguay River basin was considered, it was found out that it was much easier to identify differences in the properties of sediments that may be linked to regional sources. Based on the results obtained for this first approach in the entire basin of the Uruguay River, we can deduce that there is great potential in the tracing of sediment sources at that scale, considering different sub-basins as potential sources in this region of South America. Considering tributaries with contrasted characteristics that allow for a more targeted analysis of potential tracers can help to achieve greater success in the application of the method. The use of techniques such as diffuse reflectance spectroscopy can be a great ally in preliminary approaches, since the use of potential tracers associated with greater analytical and financial costs, are not always a guarantee of success in the approach.

Finally, considering that both in the Conceição and Ibirapuitã catchments, cropland areas have delivered a major contribution to the sediment supply, it is crucial to monitor the current ongoing period of extensive land use change in the Pampa biome, which tends to be accelerated due to high price of commodities such as soybean. In addition, the absence of conservationist practices in predominantly agricultural areas such as in the northern region of the Uruguay River basin, can provide a major source of

sediment and contaminants to the river network. As demonstrated in the preliminary results obtained in this thesis, the majority of sediments accumulated in the Uruguay River island deposits were found to originate unambiguously from sediments sharing characteristics with those found in the Conceição River.

The validity of the results obtained in this thesis need to be validated over longer time periods which would require more monitoring in the tributary catchments. The analysis of sediment archives would also be useful to offer a longer time perspective on sediment source contributions. Therefore, dating the sediments accumulated in the floodplain, such as those deposits investigated in this thesis, or those accumulated in the reservoir of the Salto Grande Dam would be of large interest. As this dam was built in the 1980s, the sediment deposited can provide a powerful way to reconstruct the erosion processes that took place over the last 40 years, which corresponds to a period of strong transition in agricultural management. Indeed, it coincides with the transition between conventional farming systems and no-tillage systems (including the absence of soil disturbance, crop rotation and permanent soil cover), and the most recent period characterised by a lack of interest in the implementation of conservationist practices (i.e., absence of crop rotation and cover crops in the period between harvests).

Furthermore, other studies considering representative catchments of each region that makes up the Uruguay River basin may provide a good alternative to identify the regions that generate the greatest contribution of sediments and contaminants. Figure 11.15 shows representative catchments of the Uruguay River basin, which could be targeted in future studies. Expanding from the scale of Conceição River, the Ijuí River basin is capable of better representing the entire Rio Grande do Sul plateau, which is the main soybean-producing region in the state. Further to the north, the Chapecó River drains an important region of western Santa Catarina, which is an area with very intensive agricultural production, mainly for pig, poultry and milk production, but also with forestry plantations. Even further upstream from the Uruguay River basin, the Peixe River catchment covers an area with intense industrial activity along its course, but also part of the region of the highland grasslands, which occurs in the two southernmost states of Brazil. These three priority catchments would cover the portion of the Atlantic Rainforest, or Subtropical Moist Broadleaf Forest according to the global nomenclature, that occurs in the basin of the Uruguay River.

For the Pampa Biome region, which comprises the Subtropical and Temperate Grasslands, Savannas and Shrublands, but also the Flooded Grasslands and Savanas that is found in Brazil, Argentina and Uruguay, the Ibicuí river catchment, of which the Ibirapuitã river catchment is also part, would represent more broadly the Pampa biome region which is currently becoming a new agricultural frontier for the production of commodities such as soybeans. Besides this, the Aguapey River and Miriñay River catchments on the Argentinian side have particular characteristics that also deserve to be investigated, although these represent smaller areas within the Uruguay River basin.

It is worth mentioning that the Uruguay River is equipped with several dams along its course and also tributaries in the region of the border between the states of Rio Grande do Sul and Santa Catarina. Therefore, strategies that allow for the evaluation of the impact of these dams on the sediment contribution to the main river should also be taken into account, taking into account the construction periods of these large dams, which may have influenced the sediment dynamics across the river basin.

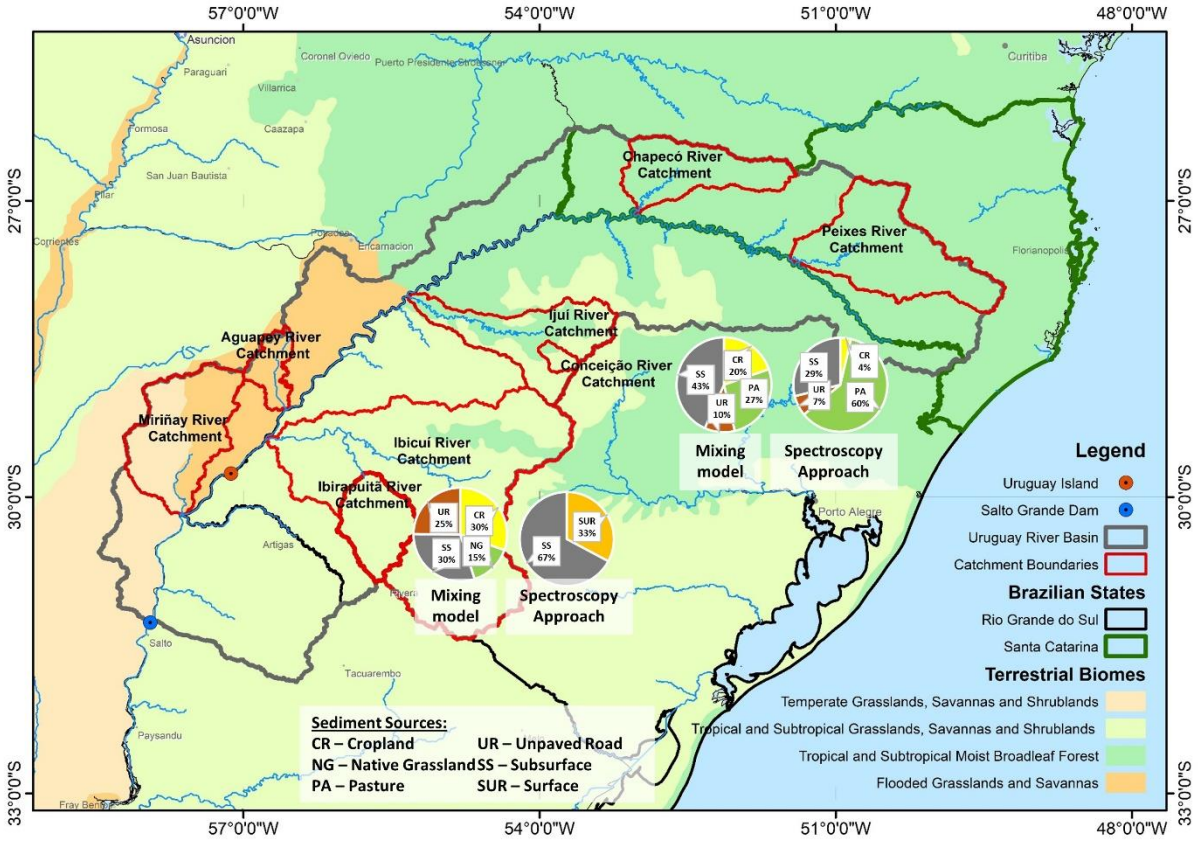

Figure 11.15. Location of the main tributaries of the Uruguay river catchment and average source contribution for the Conceição and Ibirapuitã catchment for the two approaches tested.

11.6 References

Batista, P.V.G., Laceby, J.P., Silva, M.L.N., Tassinari, D., Bispo, D.F.A., Curi, N., Davies, J., Quinton, J.N., 2019. Using pedological knowledge to improve sediment source apportionment in tropical environments. J. Soils Sediments 19, 3274–3289. https://doi.org/10.1007/s11368-018-2199-5

Batista, P.V.G., Laceby, J.P., Silva, M.L.N., Tassinari, D., Bispo, D.F.A., Curi, N., Davies, J., Quinton, J.N., 2018. Using pedological knowledge to improve sediment source apportionment in tropical environments. J. Soils Sediments. https://doi.org/10.1007/s11368-018-2199-5

Bayer, A., Bachmann, M., Müller, A., Kaufmann, H., 2012. A Comparison of Feature-Based MLR and PLS Regression Techniques for the Prediction of Three Soil Constituents in a Degraded South African Ecosystem. Appl. Environ. Soil Sci. 2012, 1–20. https://doi.org/10.1155/2012/971252

Capo, E., Giguet-Covex, C., Rouillard, A., Nota, K., Heintzman, P.D., Vuillemin, A., Ariztegui, D., Arnaud, F., Belle, S., Bertilsson, S., Bigler, C., Bindler, R., Brown, A.G., Clarke, C.L., Crump, S.E., Debroas, D., Englund, G., Ficetola, G.F., Garner, R.E., Gauthier, J., Gregory-Eaves, I., Heinecke, L., Herzschuh, U., Ibrahim, A., Kisand, V., Kjær, K.H., Lammers, Y., Littlefair, J., Messager, E., Monchamp, M.-E., Olajos, F., Orsi, W., Pedersen, M.W., Rijal, D.P., Rydberg, J., Spanbauer, T., Stoof-Leichsenring, K.R., Taberlet, P., Talas, L., Thomas, C., Walsh, D.A., Wang, Y., Willerslev, E., van Woerkom, A., Zimmermann, H.H., Coolen, M.J.L., Epp, L.S., Domaizon, I., G. Alsos, I., Parducci, L., 2021. Lake Sedimentary DNA Research on Past Terrestrial and Aquatic Biodiversity: Overview and Recommendations. Quaternary 4, 6. https://doi.org/10.3390/quat4010006

Collins, A.L., Zhang, Y., Walling, D.E., 2010. Apportioning sediment sources in a grassland dominated agricultural catchment in the UK using a new tracing framework. Sediment Dyn. a Chang. Futur. 337, 68–75.

Dearing, J.A., Dann, R.J.L., Hay, K., Lees, J.A., Loveland, P.J., Maher, B.A., Grady, K.O., Survey, S., Mk, B., 1996. Frequency-dependent susceptibility measurements of environmental materials. Geophys. J. Int. 228–240.

Dias, V. de S., da Luz, M.P., Medero, G.M., Nascimento, D.T.F., 2018. An overview of hydropower reservoirs in Brazil: Current situation, future perspectives and impacts of climate change. Water (Switzerland) 10. https://doi.org/10.3390/w10050592

Foucher, A., Evrard, O., Ficetola, G.F., Gielly, L., Poulain, J., Giguet-Covex, C., Laceby, J.P., Salvador-Blanes, S., Cerdan, O., Poulenard, J., 2020. Persistence of environmental DNA in cultivated soils: implication of this memory effect for reconstructing the dynamics of land use and cover changes. Sci. Rep. 10, 1–12. https://doi.org/10.1038/s41598-020-67452-1

Hirave, P., Wiesenberg, G.L.B., Birkholz, A., Alewell, C., 2019. Understanding the effects of early degradation on isotopic tracers: implications for sediment source attribution using compound-specific isotope analysis (CSIA). Biogeosciences Discuss. 1–18. https://doi.org/10.5194/bg-2019-205

Koiter, A.J., Owens, P.N., Petticrew, E.L., Lobb, D.A., 2013. The behavioural characteristics of sediment properties and their implications for sediment fingerprinting as an approach for identifying sediment sources in river basins. Earth-Science Rev. 125, 24–42. https://doi.org/10.1016/j.earscirev.2013.05.009

Laceby, J.P., Evrard, O., Smith, H.G., Blake, W.H., Olley, J.M., Minella, J.P.G., Owens, P.N., 2017. The challenges and opportunities of addressing particle size effects in sediment source fingerprinting: A review. Earth-Science Rev. 169, 85–103. https://doi.org/10.1016/j.earscirev.2017.04.009

Lehnert, L.W., Meyer, H., Obermeier, W.A., Silva, B., Regeling, B., Bendix, J., 2019. Hyperspectral Data Analysis in R : The hsdar Package. J. Stat. Softw. 89. https://doi.org/10.18637/jss.v089.i12

Meyer, H., Lehnert, L.W., 2020. Introduction to " hsdar ". https://cran.r-project.org/web/packages/hsdar/vignettes/Hsdar-intro.pdf.

Mullins, C.E., 1977. Magnetic Susceptibility of the Soil and Its Significance in Soil Science – a Review. J. Soil Sci. 28, 223–246. https://doi.org/10.1111/j.1365-2389.1977.tb02232.x

Pulley, S., Rowntree, K., 2016. Stages in the life of a magnetic grain: Sediment source discrimination, particle size effects and spatial variability in the South African Karoo. Geoderma 271, 134–143. https://doi.org/10.1016/j.geoderma.2016.02.015

R Development Core Team, 2017. R: a language and environment for statistical computing.

Reiffarth, D.G., Petticrew, E.L., Owens, P.N., Lobb, D.A., 2019. Spatial differentiation of cultivated soils using compound-specific stable isotopes (CSSIs) in a temperate agricultural watershed in Manitoba, Canada. J. Soils Sediments 19, 3411–3426.

https://doi.org/10.1007/s11368-019-02406-3

Tiecher, T., Minella, J.P.G., Evrard, O., Caner, L., Merten, G.H., Capoane, V., Didoné, E.J., dos Santos, D.R., 2018. Fingerprinting sediment sources in a large agricultural catchment under no-tillage in Southern Brazil (Conceição River). L. Degrad. Dev. 29, 939–951. https://doi.org/10.1002/ldr.2917

Yu, L., Oldfield, F., 1989. A multivariate mixing model for identifying sediment source from magnetic measurements. Quat. Res. 32, 168–181. https://doi.org/10.1016/0033-5894(89)90073-2

ÉCOLE DOCTORALE
Sciences mécaniques et énergétiques, matériaux et géosciences (SMEMAG)

Titre : Quantification des sources de sédiments dans des bassins cultivés contrastés (Fleuve Uruguay, sud du Brésil)

Mots clés : érosion des sols, traçage, radionucléides, agriculture, hydrologie

Résumé : Dans cette thèse, nous avons développé des techniques originales de traçage des sources de sédiments dans deux affluents typiques du bassin du fleuve Uruguay présentant des conditions contrastées en termes de géologie, d'utilisation des terres, de gestion et de types de sol. Les résultats indiquent que les sources superficielles (pâturages ou terres cultivées dans le bassin versant de Conceição, et terres cultivées dans le bassin versant d'Ibirapuitã) constituent la principale source de sédiments. Nous concluons que les activités agricoles mises en œuvre sans mesure appropriée de conservation des sols augmentent l'érosion et l'apport de sédiments au système fluvial, entraînant un appauvrissement des sols et une contamination des ressources en eau. Des mesures efficaces de conservation des sols devraient donc être mises en œuvre de toute urgence dans les zones agricoles de cette région afin de réduire l'érosion des sols et l'apport de sédiments aux systèmes fluviaux.

Title: Quantifying sediment source contributions in contrasted agricultural catchments (Uruguay River, Southern Brazil)

Keywords: soil erosion, fingerprinting, fallout radionuclides, agriculture, hydrology

Abstract: In this thesis we developed and applied original sediment source fingerprinting techniques in two tributaries of the Uruguay River catchment with contrasting conditions in terms of geology, land use, management, and soil types. The results indicate surface sources (pasture or cropland in the Conceição catchment, and cropland in the Ibirapuitã catchment) as the main source of suspended sediment. We conclude that agricultural activities implemented without appropriate soil conservation practices increase erosion and sediment delivery to the river system, causing soil impoverishment and contamination of water resources. Appropriate soil conservation practices should therefore be urgently applied in agricultural areas of this region to reduce soil erosion and sediment delivery to the river systems.

Maison du doctorat de l'Université Paris-Saclay, 2ème étage aile ouest, Ecole normale supérieure Paris-Saclay, 4 avenue des Sciences,91190 Gif sur Yvette, France